

**A 'Clip-Cycle' Approach Towards
Enantioselective Synthesis of
Substituted Tetrahydropyrans**

Khadra B. Alomari

Doctor of Philosophy

University of York

Chemistry

October 2022

Abstract

Tetrahydropyrans (THPs) are the fifth most prevalent heterocycle in pharmaceutical molecules, therefore, the development of new methodologies for their asymmetric synthesis can provide access to novel biologically relevant molecules. Despite the popularity of the intramolecular oxa-Michael reaction for the synthesis of substituted THPs, the control of enantioselectivity usually focus on intermolecular reactions, with only a few intramolecular variations reported.

An asymmetric 'clip-cycle' reaction has been developed toward the synthesis of 2,2'- and 3,3'-spirocyclic THPs with high enantioselectivity (up to 99%). The cyclisation precursors were initially prepared by 'clipping' together the alcohol fragment and an aryl thioacrylate (*via* catalytic olefin metathesis), which was then followed by intramolecular oxa-Michael cyclization catalyzed by chiral phosphoric acids (CPA) to yield the tetrahydropyran products. The α , β -unsaturated thioesters sit in the 'Goldilocks zone' of the reactivity and enantioselectivity. They can be easily converted into a wide variety of different functional groups. The absolute stereochemistry of cyclization was determined experimentally as (*S*).

To reduce the uncatalyzed background reaction, the reaction conditions of the 3,3'-sipro THP substrate were changed, either by lowering the temperature or increasing the catalyst concentration. Lowering the reaction temperature to 20 °C resulted in an inversion of the product's absolute configuration. On the other hand, a change in the catalyst loadings at 20 °C caused the reaction outcomes to be enantio-inverted whereas the change in the catalyst concentrations at 50 °C gave the same absolute configuration in all cases. Kinetic studies were conducted to explain the observed enantio-inversion in all regimes.

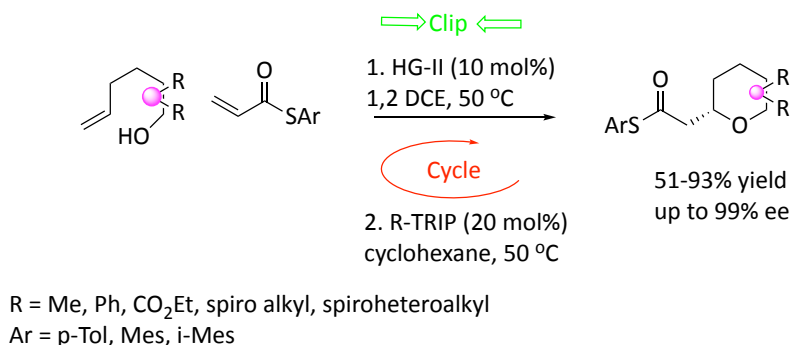


Table of Contents

1	Introduction	16
1.1	THPs in Natural Products	16
1.2	THPs in Pharmaceuticals	17
1.3	Oxocarbenium Ion Cyclization-Prins Cyclization	19
1.4	Hetero-Diels-Alder Reaction	29
1.5	Modified Maitland-Japp Reaction	36
1.6	Oxa-Michael Reaction.....	42
1.6.1	Racemic cyclization.....	43
1.6.2	Asymmetric cyclization	47
1.7	Spiro-tetrahydropyrans	52
2	Results and Discussions	56
2.1	Asymmetric Synthesis of Substituted Tetrahydropyrans	56
2.1.1	Previous work within Clarke group.....	56
2.1.2	Synthesis of the Cyclization Precursors	61
2.1.3	Brønsted Acid Catalysed Cyclization.....	67
2.1.4	Optimization of the Reaction Conditions.....	73
2.2	Substrate Scope of 'Clip-Cycle' Reaction	81
2.2.1	Scope of the reaction for 2,2'-disubstitution.....	81
2.2.2	Synthesis of an unsubstituted tetrahydropyran	86
2.3	Computational Studies and Determination of Absolute Configuration and the Enantioselective Determining Step	90
2.3.1	Computational studies and kinetic isotope effect (KIE).....	90
2.3.2	Predicted and experimental Kinetic isotope effect (KIE)	91
2.3.3	Determination of the absolute stereochemistry	94
2.4	Scope of the reaction for 3,3'-disubstitution and One Pot Reaction	96
2.4.1	Scope of the reaction for 3,3'-disubstitution.....	96
2.4.2	One pot reaction.....	101
2.4.3	Summary of results.....	103

2.5	The enantio-inversion Observation of Spiro-THP Substrate.....	105
2.5.1	The enantio-inversion observation.....	105
2.5.2	NMR- spectroscopic investigation of the catalyst species.....	111
2.5.3	Non-linear effect of the catalyst (NLE)	116
2.5.4	Catalyst orders and aggregation.....	120
2.5.5	Computational studies and kinetic isotope effect (KIE).....	126
2.5.6	Determination of ΔH and ΔS	127
2.5.7	Summary of results.....	131
3	Conclusion.....	133
4	Future Work.....	134
5	Experimental.....	136
5.1	General Experimental.....	136
5.2	Experimental Details for the ‘Clip-Cycle’ Reactions	137
5.2.1	Synthesis of ‘Clip-Cycle’ Precursors	137
5.2.2	2,2-Disubstituted alcohols	164
5.2.3	3,3-Disubstituted alcohols	169
5.3	Synthesis of Thioesters	177
5.4	Determination of the Absolute Stereochemistry.....	180
5.5	Kinetic Isotope Studies	181
5.6	HPLC Data.....	183
5.6.1	The enantio-inversion of 3,3'-spiro THP	201
6	Abbreviations.....	211
7	References	216

List of Figures

Figure 1. Tetrahydropyran-containing natural products	16
Figure 2. Pharmaceuticals containing tetrahydropyran	18
Figure 3. Normal-demand and inverse-electron-demand all-carbon and hetero Diels-Alder reaction.....	30
Figure 4. <i>cis</i> -Ti and <i>trans</i> -Ti chelated systems	40
Figure 5. Asymmetric cycloetherification <i>via</i> intramolecular oxy- Michael addition reaction mediated by bifunctional organocatalyst	48
Figure 6. Possible transition state of the reaction.....	50
Figure 7. PMI plot of the ZINC 'lead-like' database.	53
Figure 8. Computational transition states adopts for the stereodivergent oxa-Michael cyclization	57
Figure 9. ¹ H NMR of 196 shows the signals of the α and β-protons in the alkene region. ...	66
Figure 10. ¹ H NMR of 197	68
Figure 11. HMQC spectrum showing C-8 and C-9 with respective protons in 197	69
Figure 12. COSY spectrum showing correlation between H-8, H-8', and H-9 in 197	69
Figure 13. HPLC chromatogram of the synthesised THP 197 with rac-CSA	70
Figure 14. Crude ¹ H NMR of the asymmetric reaction of 198 using (<i>R</i>)-TRIP	71
Figure 15. HPLC chromatogram of the synthesised THP 198 with (<i>R</i>)-TRIP	72
Figure 16. Structure of chiral phosphoric acid catalysts used in reaction screening.....	74
Figure 17. The effect of the nature of the thioester on the enantioselectivity of the reaction.....	77
Figure 18. HPLC chromatogram of the synthesised THP 215 with rac-CSA	79
Figure 19. HPLC chromatogram of the synthesised THP 216 with (<i>R</i>)-TRIP.....	80
Figure 20. ketones selected to test 2,2'-substituted scope.....	82
Figure 21. Thorpe-Ingold effect	87
Figure 22. Reactive-rotamer effect on cyclization, Thorpe-Ingold effect.....	88
Figure 23. Reactive rotamer effect and the energy diagram for the cyclization ⁸²	88

Figure 24. Experimental KIE of 251_{H/D}	93
Figure 25. Esters selected to test 3,3'-disubstituted scope	96
Figure 26. HPLC chromatogram of the synthesised racemic 3,3'-spiroTHP product 290 with rac-(CSA)	100
Figure 27. HPLC chromatogram of the synthesised 3,3'-spiroTHP product 290 with (<i>R</i>)-TRIP at 50 °C.....	100
Figure 28. HPLC chromatogram of the synthesised 3,3'-spiroTHP product 290 with (<i>R</i>)-TRIP at room temperature	101
Figure 29. HPLC chromatogram of the synthesised 3,3'-spiroTHP product 298 with (<i>R</i>)-TRIP at 50 °C (A), and 20 °C (B)	107
Figure 30. ³¹ P NMR of 20 mol% (<i>R</i>)-TRIP at 20 °C	112
Figure 31. ³¹ P NMR of 20 mol% (<i>R</i>)-TRIP with different catalyst loadings at different temperatures	113
Figure 32. Asymmetric amplification in the Biginelli reaction catalyzed by phosphoric acid A: non-linear effect in toluene, B: linear effect in chloroform	116
Figure 33. The relation between the enantioselectivity of the product and the enantiopurity of the catalyst	117
Figure 34. Non-linear effect of (<i>R</i>)-TRIP at 50 °C	118
Figure 35. Non-linear effect of (<i>R</i>)-TRIP at 50 °C	119
Figure 36. ³¹ P NMR of (<i>R</i>)-TRIP with 50% ee.....	120
Figure 37. Bures' analysis to determine the order in catalyst	121
Figure 38. Catalyst order determination at 20 °C: initial rates (A), normalized initial rates with different power values (B, C, D).....	122
Figure 39. Catalyst order determination: low cat. loadings at 20 °C (A), high cat. loadings at 20 °C (B), Low cat. loadings at 50 °C (C), high cat. loadings at 50 °C (D).....	124
Figure 40. Possible fraction of the catalyst as a monomeric species (f_{mono}) and fraction of the starting material consumed by the monomeric species (Y_{mono}) for different orders of catalyst.....	125
Figure 41. Predicted KIE of the CPA-catalysed oxa-Michael reaction mechanism	126

Figure 42. Rate of reaction under various temperature conditions	128
Figure 43. Eyring plot at low temperature reactions.....	129
Figure 44. A:Rate of reaction under various temperature conditions.....	130
Figure 45. Experimental KIE of 251_{H/D}	181
Figure 46. Experimental KIE of 251 at room temperature.....	182

List of Schemes

Scheme 1. General mechanism of Prins reaction	19
Scheme 2. Hanschke reactin to synthesis THP ring	19
Scheme 3. General stereochemical outcome of the Prins cyclization.....	20
Scheme 4. List and co-workers' iDP Brønsted acid-promoted asymmetric Prins cyclization strategy.....	21
Scheme 5. Mechanism of Chiral Brønsted acid catalyzed asymmetric Prins cyclization	23
Scheme 6. List and co-workers' iIDP Brønsted acid-promoted asymmetric Prins cyclization strategy.....	24
Scheme 7. The synthesis 2,6-disubstituted-4-acetamido-tetrahydropyran derivatives.....	25
Scheme 8. Prins-Ritter general mechanism.....	25
Scheme 9. Oxonia-Cope rearrangement	26
Scheme 10. Mechanism of the oxonia-Cope reaction in the Prins cyclization	27
Scheme 11. Cyclization of enantioenriched alcohol (S)- 46	27
Scheme 12. Cyclization of electron-deficient enantioenriched alcohol (S)- 55	28
Scheme 13. Partial racemization through 2-oxonia-Cope allyl transfer	28
Scheme 14. Partial racemization by reversible 2-oxonia-Cope rearrangement	29
Scheme 15. Synthesis of B ring 74 of Lasanolide A.....	31
Scheme 16. Synthesis of the THP ring of the macrolactone core of (+)- Neopeltolide	31
Scheme 17. Chen's asymmetric synthesis of THP derivatives <i>via</i> IEDHDAR.....	33
Scheme 18. Bifunctional-catalyzed enantioselective synthesis of tetrahydropyran derivatives <i>via</i> IEDHDAR	34
Scheme 19. Imidodiphosphoric acids catalyzed asymmetric synthesis of THP derivatives <i>via</i> IEDHDAR.....	35
Scheme 20. The Maitland and Japp reaction.....	36
Scheme 21. The Cornubert and Robinet reaction	37
Scheme 22. Updating the Maitland and Japp reaction	37
Scheme 23. Updating the Maitland and Japp reaction to synthesise substituted THPs	38

Scheme 24. The revised one-pot Maitland and Japp reaction	39
Scheme 25. Synthesis of centrolobine 122 <i>via</i> Maitland and Japp reaction	40
Scheme 26. Asymmetric synthesis of substituted THPs <i>via</i> diketene.....	41
Scheme 27. Synthesis of the C1-C19 bis-pyran unit of the phorboxazoles	42
Scheme 28. Stereodivergent strategy employed in the synthesis of aspergillide A and B ..	43
Scheme 29. Synthesis of aspergillides B 138	44
Scheme 30. Synthesis of (\pm)-centrolobine 144	44
Scheme 31. Proposed biosynthetic pathway of the synthesis of polyketide tetrahydropyrans	45
Scheme 32. Biomimetic synthesis of 2,6- <i>cis</i> tetrahydropyrans of ester surrogate	45
Scheme 33. Intramolecular oxa-Michael cyclisation of α,β -unsaturated thioester	46
Scheme 34. Enantioselective cycloetherification promoted by thiourea.....	47
Scheme 35. Asymmetric synthesis of 2-substituted THPs mediated by bifunctional organocatalyst	48
Scheme 36. Asymmetric synthesis of substituted THPs catalysed by primary-secondary dienamines	49
Scheme 37. Synthesis of tri-substituted THPS.....	50
Scheme 38. Proposed mechanism for the formation of 168	51
Scheme 39. Asymmetric synthesis of spiro-THPs	54
Scheme 40. The iodocyclization step into spiro-THPs	54
Scheme 41. Stereodivergent synthesis of the C20-C32 tetrahydropyran core of phorboxazole	56
Scheme 42. Preliminary computational work into the chiral acid catalyzed oxa-Michael cyclisation	58
Scheme 43. Asymmetric Michael reaction for the synthesis of THPs.....	59
Scheme 44. Preliminary computational work and DFT calculation of the chiral acid catalyzed oxa-Michael cyclisation.....	60
Scheme 45. Synthesis of 2,2'-dimethyl alcohol	61
Scheme 46. Synthesis of mesityl thioacrylate 192	62

Scheme 47. Lipshtuz's cross metathesis reaction in the presence of CuI	64
Scheme 48. Cross-metathesis reaction for the cyclization precursor 196	64
Scheme 49. Mechanism of olefin metathesis initiation	65
Scheme 50. The catalytic cycle of olefin metathesis	65
Scheme 51. Racemic cyclization of 2,2'-dimethyl substrate.....	67
Scheme 52. Cyclization of 2,2'-dimethyl substrate with (<i>R</i>)-TRIP.....	71
Scheme 53. Asymmetric Michael reaction for the synthesis of THPs.....	75
Scheme 54. Asymmetric Michael reaction for the synthesis of THPs	76
Scheme 55. Synthesis of triisopropyl thioacrylate 213	78
Scheme 56. Cross-metathesis reaction for the cyclization precursor 214	78
Scheme 57. Racemic cyclization of 2,2'-dimethyl THP 215	79
Scheme 58. Cyclization of 2,2'-dimethyl THP 216 with (<i>R</i>)-TRIP.....	80
Scheme 59. Synthesis of 2,2'-substituted precursors.....	83
Scheme 60. Asymmetric cyclisation to form 2,2'- substituted tetrahydropyrans	84
Scheme 61. Asymmetric synthesis of 2,2'-spirocyclohexyl THP 243	85
Scheme 62. Synthesis of the unsubstituted tetrahydropyran 249	86
Scheme 63. Synthesis of the unsubstituted tetrahydropyran 249	89
Scheme 64. Computational exploration of the CPA-catalysed oxa-Michael reaction mechanism.....	90
Scheme 65. Predicted KIE of the CPA-catalysed oxa-Michael reaction mechanism.....	91
Scheme 66. Cyclization of H/D KIE reaction	92
Scheme 67. Transesterification using silver triflate and methanol	94
Scheme 68. Synthesis of (<i>R</i>)-2,2'-dimethyl tetrahydropyran acetic acid ester 255	95
Scheme 69. Synthesis of 3,3'-substituted precursors.....	97
Scheme 70. Asymmetric cyclisation to form 3,3'- substituted tetrahydropyrans	98
Scheme 71. Background cyclization of 3,3'-substituted tetrahydropyrans	98
Scheme 72. Asymmetric cyclisation to form 3,3'- substituted tetrahydropyrans at rt	99
Scheme 73. Asymmetric "Clip-Cycle" synthesis of substituted tetrahydropyrans in a one- pot reaction	103

Scheme 74. Asymmetric synthesis of spiro-THP 298	105
Scheme 75. Asymmetric synthesis of spiro-THP 298 at different temperatures.....	106
Scheme 76. The enantioselective Henry reaction under various temperature conditions	108
Scheme 77. Asymmetric synthesis of spiro-THP 298 with different catalyst loading of (<i>R</i>)- TRIP at 50 °C	109
Scheme 78. Asymmetric synthesis of spiro-THP 298 with different catalyst loading of (<i>R</i>)- TRIP at 20 °C	110
Scheme 79. Chiral sterically demanding phosphoric acids: inhibited homodimerization and novel heterodimeric activation.....	114
Scheme 80. <i>Asymmetric amplification in the Biginelli reaction catalyzed by phosphoric acid</i>	115
Scheme 82. Asymmetric synthesis of spiro-THP 309 with different enantiopurity of (<i>R</i>)- TRIP	117
Scheme 83. Asymmetric synthesis of spiro-THP 309 with different enantiopurity of (<i>R</i>)- TRIP	119
Scheme 84. Possible conditions to derivatise THP 308	134
Scheme 85. potential application of use of α,β -unsaturated thioester as a Michael acceptor for the synthesis of THF	135

List of Tables

Table 1. Asymmetric Michael reaction for the synthesis of THPs.....	60
Table 2. Olefins categories for selective cross metathesis	63
Table 3. Conditions screening for the synthesis of THPs	75
Table 4. Conditions screening for the synthesis of THPs	76
Table 5. Catalyst screening for the synthesis of 2,2'-spirocyclohexyl THP 243	85
Table 6. Conditions screen for the unsubstituted tetrahydropyran 249	89
Table 7. Conversion of 251_{H/D} over the time at 50 °C.....	93
Table 8. Synthesis of spiro-THP 298	105
Table 9. Asymmetric synthesis of spiro-THP 298 at different temperatures	106
Table 10. The enantioselective Henry reaction under various temperature conditions ...	108
Table 11. Asymmetric synthesis of spiro-THP 298 with different catalyst loading of (<i>R</i>)-TRIP at 50 °C.....	109
Table 12. Asymmetric synthesis of spiro-THP 298 with different catalyst loading of (<i>R</i>)-TRIP at 20 °C.....	110
Table 13. Asymmetric synthesis of spiro-THP 309 with different enantiopurity of (<i>R</i>)-TRIP	118
Table 14. Asymmetric synthesis of spiro-THP 309 with different enantiopurity of (<i>R</i>)-TRIP	119
Table 15. Calculated KIE of the CPA-catalysed oxa-Michael reaction mechanism at different regimes	127
Table 16. The calculated activation parameters for both regimes	131
Table 17. Conversion of 250_{H/D} over the time at 50 °C.....	181
Table 18. Conversion of 251_{H/D} over the time at room temperature.....	182
Table 19. Conversion of 251 over the time at room temperature with (<i>R</i>)-TRIP _{H/D}	182

Acknowledgements

First and foremost, I'd like to thank my supervisor, Prof. Paul Clarke, for the opportunity to work on this fascinating and challenging project. His guidance, motivation, and faith in me have been invaluable over the last four years. I'd also like to thank Paul for always being available to offer advice and guidance on my project, even during the difficult time caused by the COVID-19 pandemic, and for all of the thesis proofreading he's done and returning corrections so quickly that I had to keep up with his pace!

My PhD would not be possible without the financial support of Jazan University. I'd also like to thank Dr. Anne Routledge, my IPM, for her invaluable advice and suggestions during TAP meetings, as well as her encouragement and support throughout my PhD. My thanks also go to the University of York's analytical services, particularly Heather Fish and Karl Hale for their assistance in acquiring data, both of whom were always happy to answer any queries I had.

Without the people to do it with, research would be half the fun, so a big thanks to all the Clarke group members past and present for making the lab such a friendly and welcoming place. Even when things don't seem to be going your way or the stresses pile up, having a group as brilliant as the Clarke group helps. Chris deserves special recognition for his assistance and patience in answering my numerous questions. To Saikiran, thank you for sharing helpful hints for making the most of my time and for our chats over lunch or cake. To Gift, for being so encouraging and friendly, especially during my lows. Selin, thank you for teaching me the most useful Turkish words.

Last but not least, I'd like to express my gratitude to the people in my life who have always been supportive of everything I've done. Thank you so much to my mum, my husband Atiah, and my children Dalya, Mourad, and Asmahan for always being there for me, believing in me, and making my dream come true!

Declaration

I hereby declare that the substance of this thesis has not been submitted, nor is currently being submitted, in candidature for any other degree.

I also declare that the work embodied in this thesis is the result of my own investigations and in the event the work of others has been used this has been fully acknowledged in the text.

Some of the research outlined in thesis has been published in the following paper:

Enantioselective “Clip-Cycle” Synthesis of Di-, Tri- and Spiro-substituted Tetrahydropyrans.

K. Alomari, N. Sai Pavan Chakravarthy, B. Duchadeau, K. Ermanis and P. A. Clarke

Org. Biomol. Chem. 2022, 20, 1181.

1 Introduction

1.1 THPs in Natural Products

Tetrahydropyrans (THPs) are important structural motifs found in many natural products as well as biologically active compounds.¹ They range in structure and complexity from simple tri-substituted tetrahydropyran core units like diospongin A **1** and B **2**^{2,3} which are promising candidates for treating osteoporosis, a skeletal disease, to multi-substituted tetrahydropyran core units like phorboxazole A **3**, B **4** and psymberin **5**.^{4,5} Phorboxazole A **3** and B **4** have potent activity against *C. albicans* as well as the entire range of 60 cancer cell lines held by the National Cancer Institute (NCI), with exceptional inhibition of cell growth (GI_{50} 's $< 7.9 \times 10^{-10}$ M) with analogues reaching the picomolar range for cytotoxicity. Psymberin is a sea slug-derived cytotoxin that has been found to be highly bioactive, with LC50s at nanomolar concentrations against various types of tumors (Figure 1).⁶

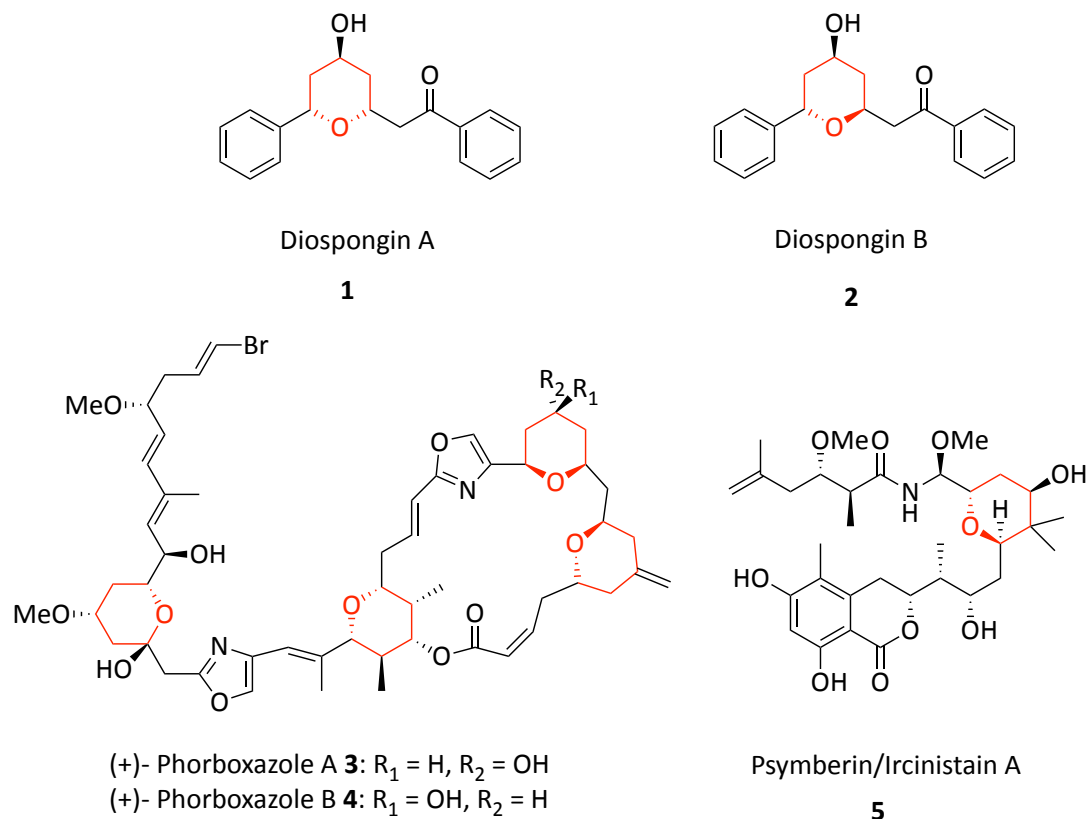


Figure 1. Tetrahydropyran-containing natural products

1.2 THPs in Pharmaceuticals

Natural products have grown in popularity as a starting point for the discovery and development of novel pharmacological compounds. This is mostly because of their structural and chemical diversity, as well as their abundance in nature, as new natural compounds are discovered on a regular basis.⁷ Oxygen heterocycles are the second most frequently encountered heterocycles in FDA approved pharmaceuticals.⁸ A recent report on the ring systems, and frameworks of drugs as described by the FDA showed that the tetrahydropyran ring system is the fifth most prevalent heterocycle in pharmaceutical molecules.⁷ Their significance is clear because they serve as exciting medicinal leads.⁹ A variety of diseases are treated by these drugs (Figure 2). For example, rapamycin (sirolimus **6**) and its derivatives, everolimus **7** and temsirolimus **8** are immunosuppressive agents and have oncological applications such as in the treatment of advanced renal cell carcinoma (RCC), mantle cell lymphoma (MCL) as well as hormone receptor-positive, human epidermal growth factor receptor 2 (HER2)-negative breast cancer.¹⁰ Teniposide **9** and artemether **10** are chemotherapeutic and anti-parasite agents, respectively, while spectinomycin **11** is an antibiotic.⁸

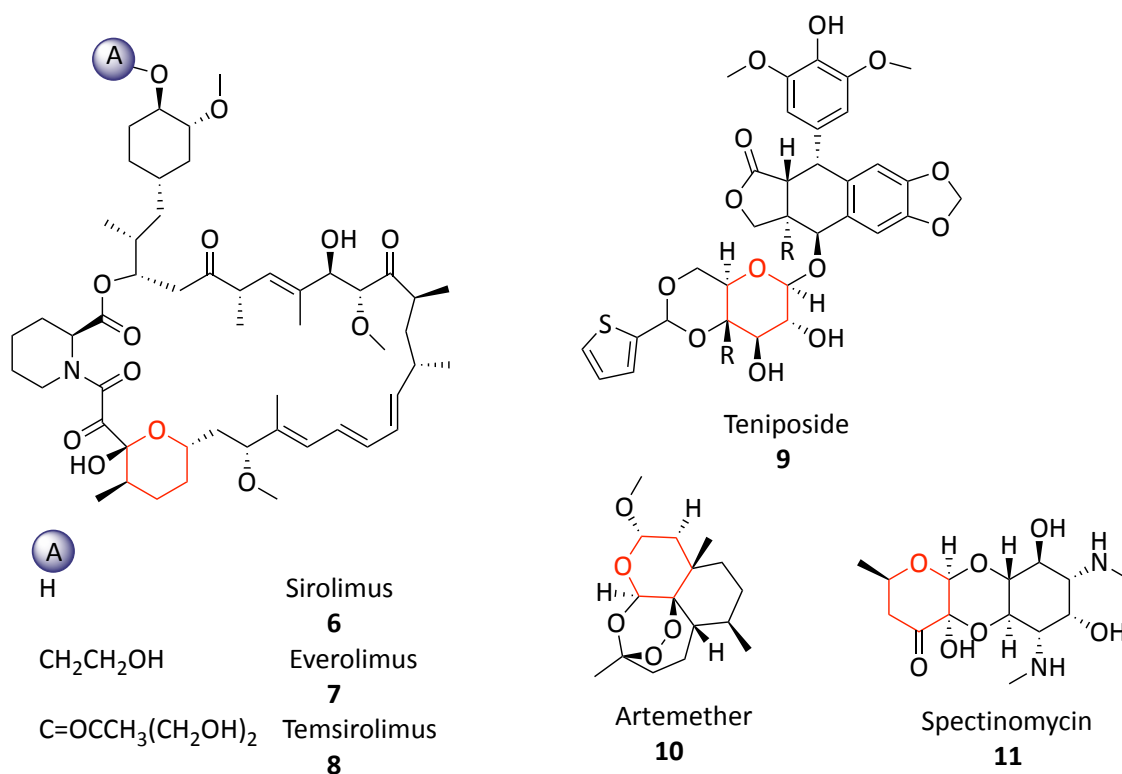
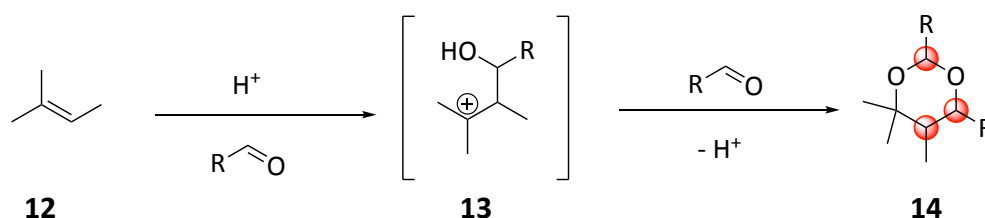


Figure 2. Pharmaceuticals containing tetrahydropyran

The presence of at least one or more stereocenters on the tetrahydropyran ring is a critical feature of all structures illustrated in both Figures 1 and 2. This coupled with the increase in single enantiomer drug candidates, makes synthesising chiral compounds highly desirable. Due to their ubiquity in natural products and pharmaceuticals, the synthesis of various chiral tetrahydropyran skeletons has attained great interest. Numerous strategies for the efficient and stereo-controlled production of THPs have been developed for several years. A selection of these approaches is shown here to illustrate the breadth of available literature-based reactions.

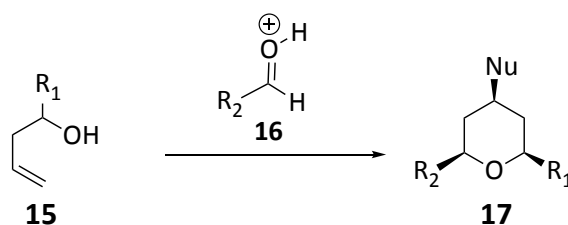
1.3 Oxocarbenium Ion Cyclization-Prins Cyclization

The Prins reaction has proven to be a powerful technique for the stereoselective synthesis of the THP scaffold and its application in natural product total synthesis.¹¹ The Prins reaction was discovered and described for the first time by Hendrik Jacobus Prins in 1919.¹² It involves the acid-catalyzed electrophilic addition of olefins **12** to aldehydes, which ultimately results in the generation of carbenium ions (**13**, Scheme 1). A nucleophile, such as a second equivalent of an aldehyde, can intercept this intermediate **13** to form 1,3-dioxanes **14**.



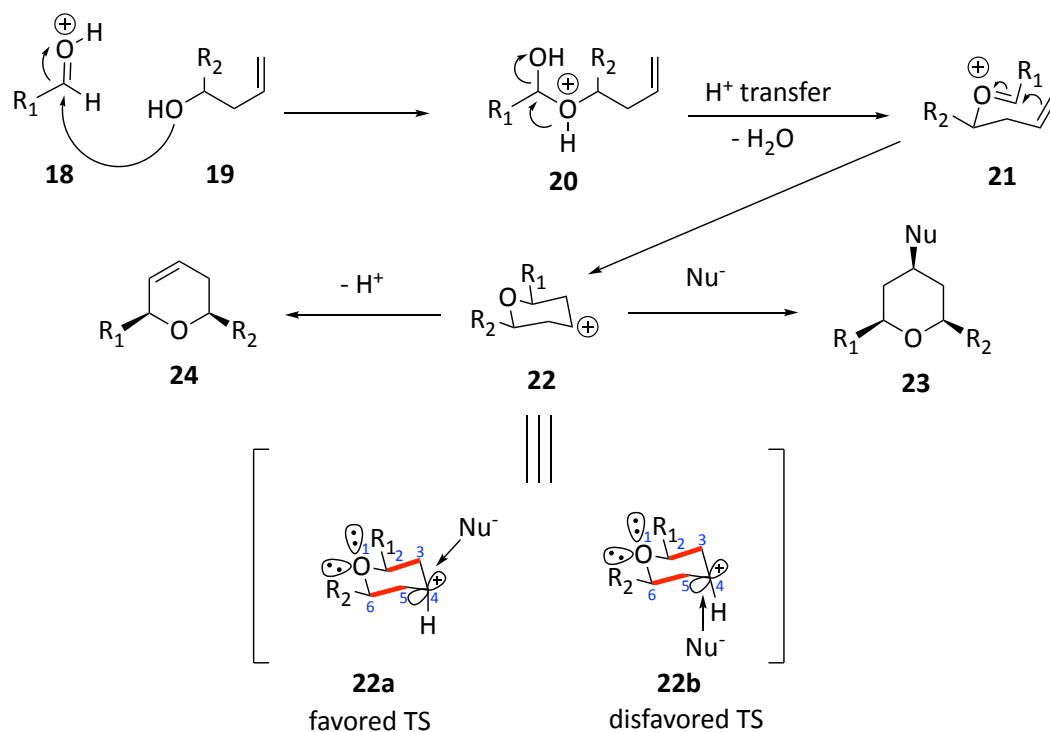
Scheme 1. General mechanism of Prins reaction

In 1955, Hanschke made a significant discovery regarding this reaction. He reported that the tetrahydropyran ring could be selectively constructed through a Prins reaction by using 3-buten-1-ol and a number of different aldehydes or ketones in the presence of acid (Scheme 2).¹³



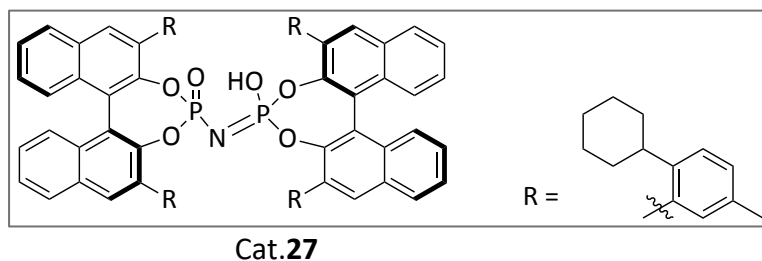
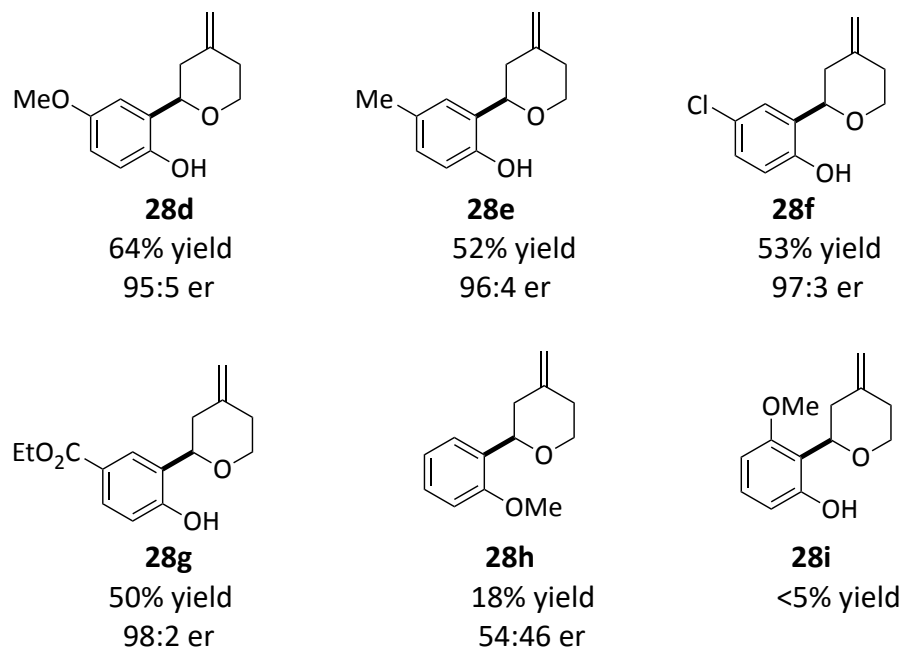
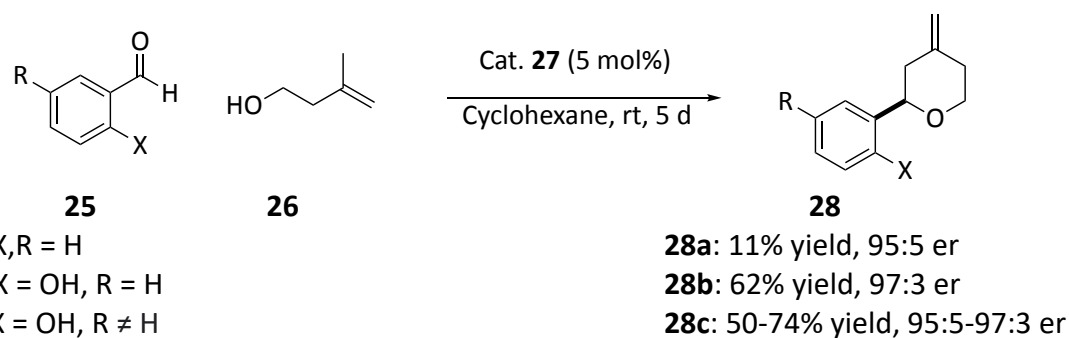
Scheme 2. Hanschke reaction to synthesise THP ring

The mechanism of this reaction was described as proceeding through an oxocarbenium ion intermediate captured by a π -nucleophile, followed by the addition of an external nucleophile, resulting in the formation of products **23** (Scheme 3). On the other hand, the formation of the 2,6-disubstituted dihydropyran **24** resulted from successive proton loss in the absence of an external nucleophile.



Scheme 3. General stereochemical outcome of the Prins cyclization

The result of the Prins cyclization's exclusive *cis*-stereoselectivity could be attributed to the most favourable conformation adopted by **22** with equatorial orientation of the 2,6-substituents (R_1 and R_2). Alder used density functional theory (DFT) to explain the formation of all-*cis*-2,4,6-trisubstituted THPs and stated that in the presence of an external nucleophile, the stabilisation of the carbocation intermediate was favoured through stereoelectronic effects.¹⁴ In an equatorial attack, the vacant *p*-orbital of C4 in TS **22a** overlapped efficiently with the HOMO of the incoming nucleophile. Furthermore, the pseudoaxial C4 hydrogen atom in TS **22a** resulted in an optimal overlap between σ and σ^* of C2-C3 and C5-C6 with the oxygen atom's coplanar equatorial lone pair and the empty *p*-orbital at C4. These orbital stabilisation, combined with the incoming nucleophile's lack of 1,3-diaxial interaction (mostly halide), resulted in a preferential equatorial attack over an axial attack by the nucleophile (Scheme 3), yielding all-*cis*-2,4,6-trisubstituted THPs.

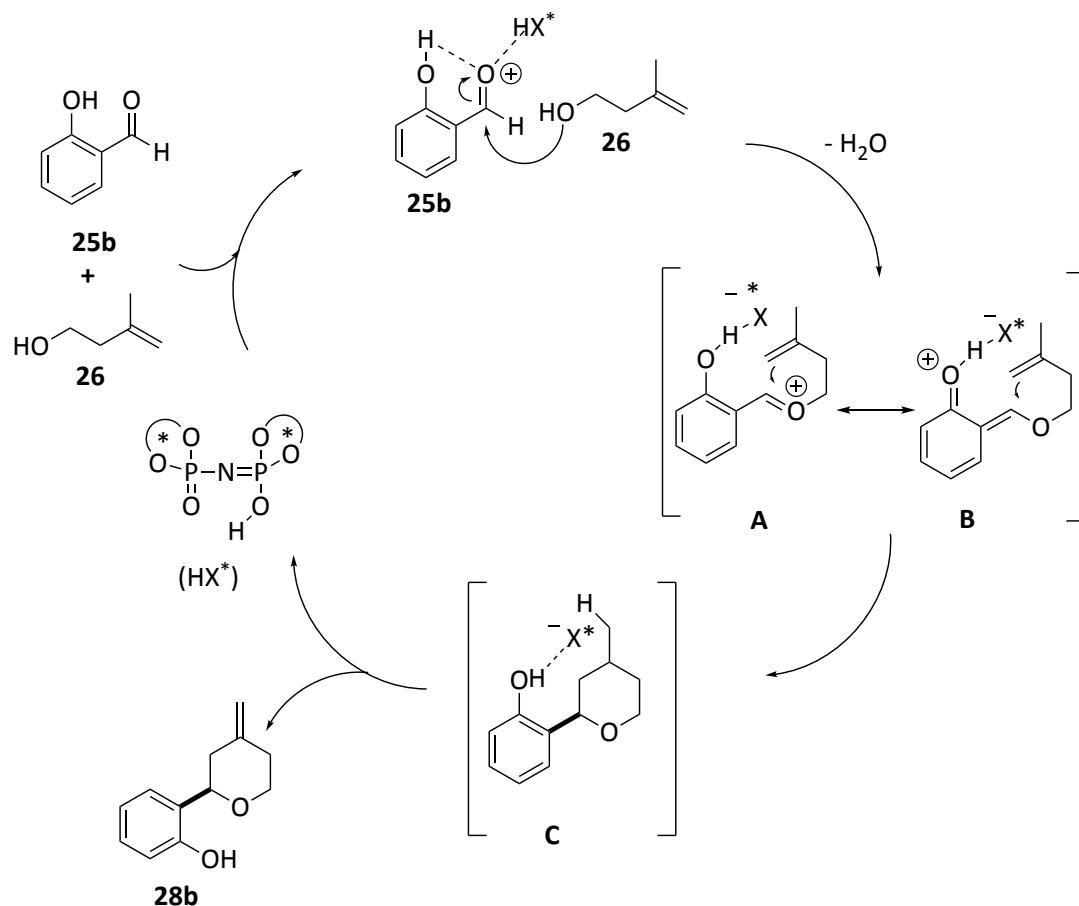


Scheme 4. List and co-workers' iDP Brønsted acid-promoted asymmetric Prins cyclization strategy

In 2015, List *et al.* reported an asymmetric Prins cyclization with aromatic aldehyde **25** and 3-methylbut-3-en-1-ol **26** catalysed by chiral imidodiphosphoric acid (iDPA) **27** to yield substituted tetrahydropyran with high enantioselectivity (Scheme 4).¹⁵ A chiral bis-

BINOL-based imidophosphoric acid **27** was effective in this reaction, and the extreme bulkiness of this catalyst was critical to the transformation's success. The initial investigation was conducted with benzaldehyde **25a** and 3-methyl-3-buten-1-ol **26**. Several chiral Brønsted acids were tested, including phosphoric acids, disulfonimides, and imidodiphosphates, and all showed either a poor yield and/or low enantioselectivity. Surprisingly, salicylaldehyde **25b** produced a significantly improved reaction profile, with a yield of 62% and an excellent e.r. of 97:3. The use of cyclohexane as the solvent with 5 Å molecular sieves at room temperature provided the best combination of yield and enantioselectivity. At the 5-position of the aromatic ring, a variety of commercially available salicylaldehyde derivatives **25c** containing electron-rich, electron-poor, sterically demanding, and halogen substituents were tolerated. A substrate with a 6-position substitution did not yield the corresponding product **28i**. Using 2-methoxybenzaldehyde resulted in a low yield and poor enantioselectivity for product **28h**.

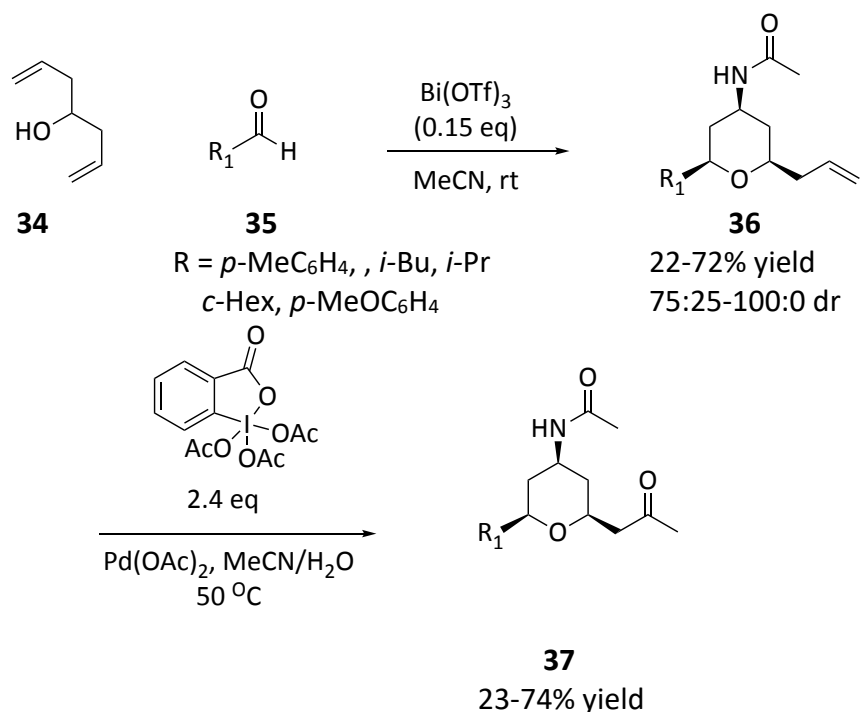
The results obtained by substituting a methyl ether for the salicylaldehyde gave product **28h**, demonstrating that the *ortho* hydroxy group of the aldehyde was critical for reactivity and enantioselectivity.¹⁶ Internal activation *via* intramolecular hydrogen bonding between the hydroxy and carbonyl groups can explain the increased reactivity. Furthermore, it was known that the bifunctional catalyst can form intermolecular hydrogen bonds with both the hydroxyl and carbonyl/imino groups in transition states, thereby activating the aldehyde.



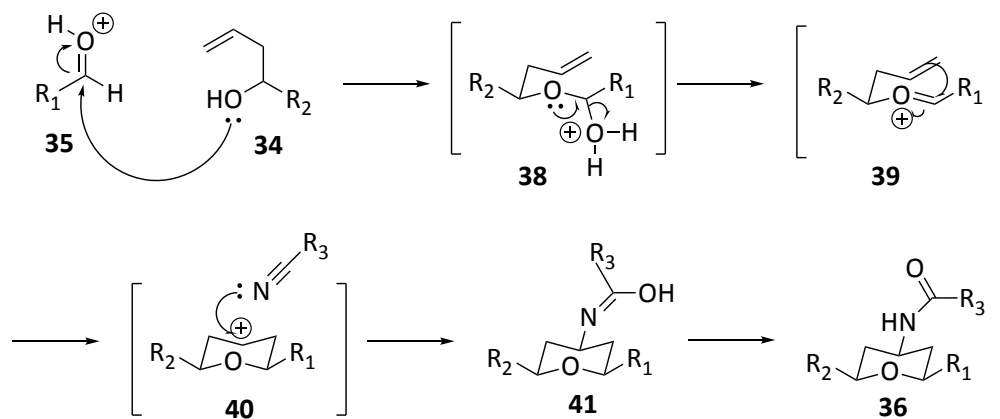
Scheme 5. Mechanism of chiral Brønsted acid catalyzed asymmetric Prins cyclization

In Scheme 5, a plausible mechanism suggested that the initial condensation of aldehyde **25b** and alcohol **26** produced the oxocarbenium ion in **A**, which also contained the chiral imidodiphosphate counteranion. Ion pair **A** can also be described as the resonance structure of a protonated *ortho*-quinone methide in **B**. The essential enantiodifferentiating C-C bond formation gave THP **C** a new chiral centre and a tertiary carbocation. In the final deprotonation step, the sterically encumbered imidodiphosphate anion favoured the kinetic removal of a proton from the primary position in order to afford selectively the exocyclic alkene product **28b**.

7). The presence of unsaturation on the lateral chain of **36** could lead to new compound libraries. In this context, the Wacker oxidation of the terminal double bond into methyl ketones using Pd(OAc)₂ as the catalyst and Dess-Martin periodinane as the oxidant. When the conditions were applied to THP derivatives **36**, the reaction produced the expected methyl ketones **37** in convenient yields (Scheme 7). The general mechanism for producing the product could be explained as hemi-acetal formation **38** followed by Prins cyclization **39** and Ritter amidation **40** (Scheme 8).¹⁹

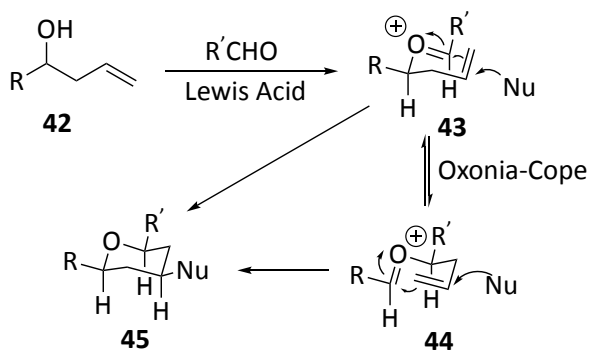


Scheme 7. The synthesis 2,6-disubstituted-4-acetamido-tetrahydropyran derivatives



Scheme 8. Prins-Ritter general mechanism

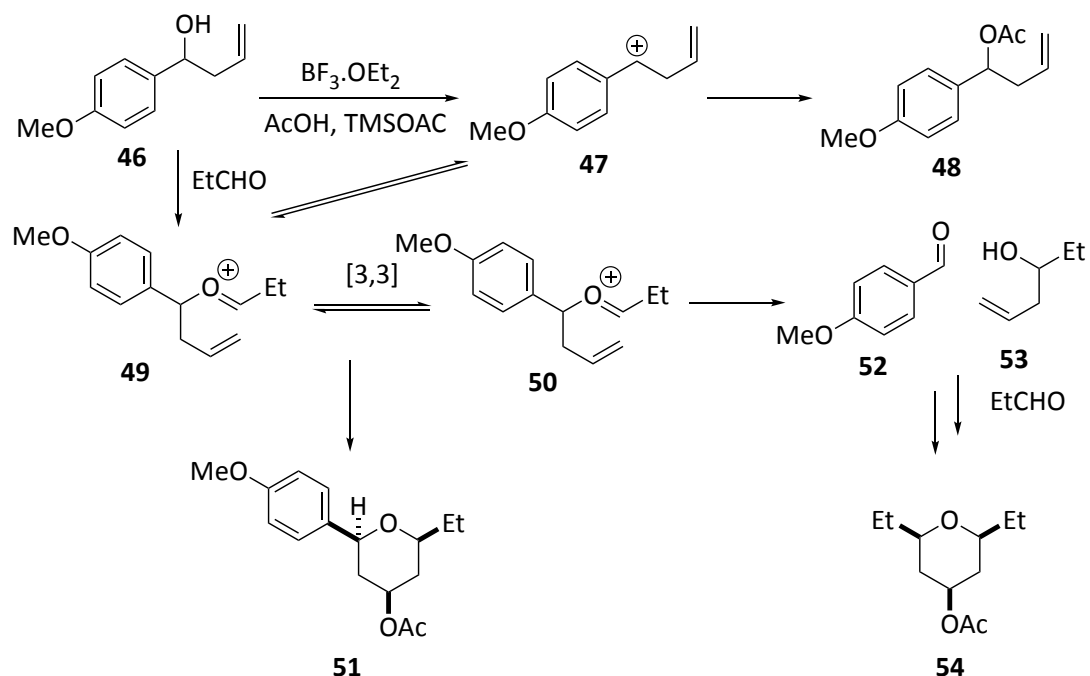
Although the Prins cyclization is a powerful tool for the synthesis of 2,6-disubstituted THPs, it has some limitations that limit its wide applicability.¹¹ The racemization caused by competing oxonia-Cope rearrangement and side-chain exchange are the major drawbacks of Prins cyclization (Scheme 9).²⁰



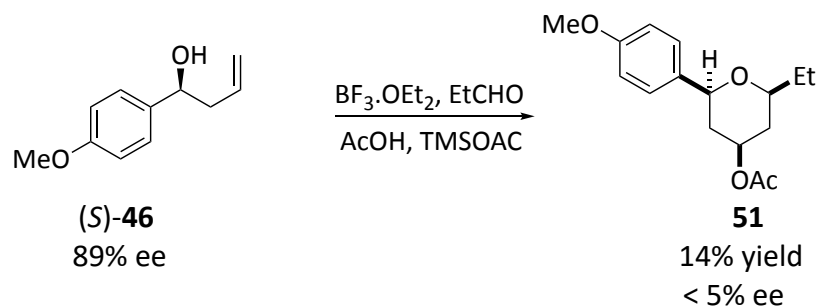
Scheme 9. Oxonia-Cope rearrangement

Willis and co-workers investigated the reactivity of various aryl group-substituted homoallylic alcohols **46** with propanal in the presence of a Lewis acid, yielding the expected tetrahydropyran **51** as a single diastereomer *via* an oxocarbenium intermediate (Scheme 10).^{20,21} The nature of the aromatic ring, which played a critical role in product formation, influenced the reaction. Homoallylic alcohols with an electron-rich substituent at the arene ring produced predominantly symmetric THP product **54** instead of the desired trisubstituted heterocycle **51**.

The mechanism of the reaction was further investigated using enantioenriched homoallylic alcohol (*S*)-**46** with 89% ee, which favoured 2-oxonia-Cope rearrangement to yield THP **51** in 14% yield and 5% ee (Scheme 11). The lack of enantioselectivity in product **51** indicated that racemization occurred during the reaction. The loss of optical purity was explained as the result of the formation of a benzylic cation, which was stabilised by the electron-rich aromatic substituent.

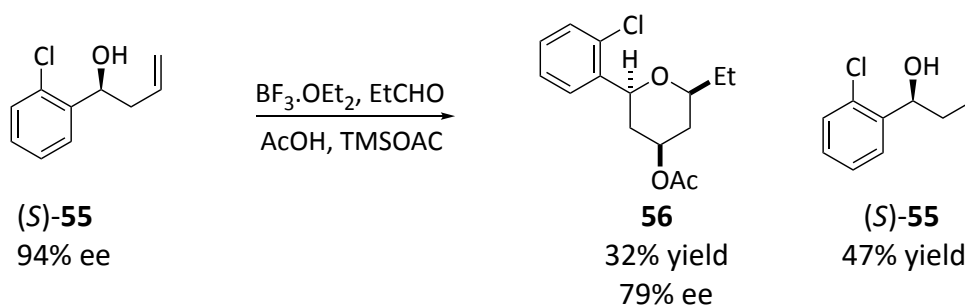


Scheme 10. Mechanism of the oxonia-Cope reaction in the Prins cyclization



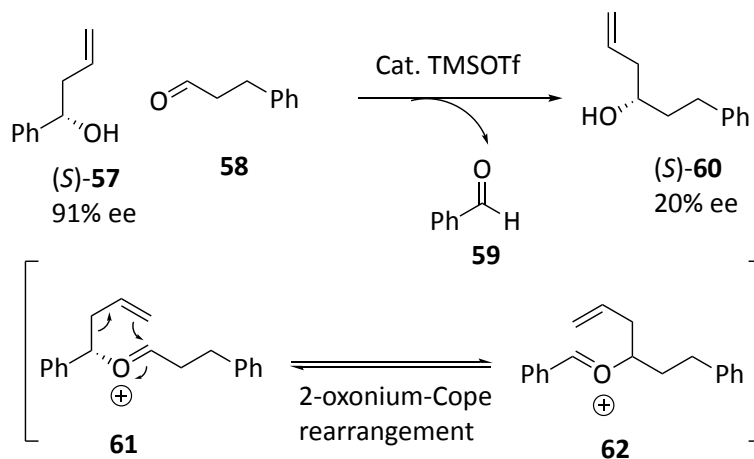
Scheme 11. Cyclization of enantioenriched alcohol (*S*)-46

On the other hand, the reaction with aromatic alcohol containing the electron-deficient substituent produced the desired trisubstituted THP **56** as well as the recovered starting material (*S*)-**55**. As shown in Scheme 12, the enantioenriched homoallylic alcohol **55** (94% ee) with an electron-deficient substituent was investigated with propanal, which proceeded with high selectivity to give the corresponding THP **56** (79% ee, 32% yield) along with some recovered starting material (*S*)-**55** (47%).



Scheme 12. Cyclization of electron-deficient enantioenriched alcohol (S)-55

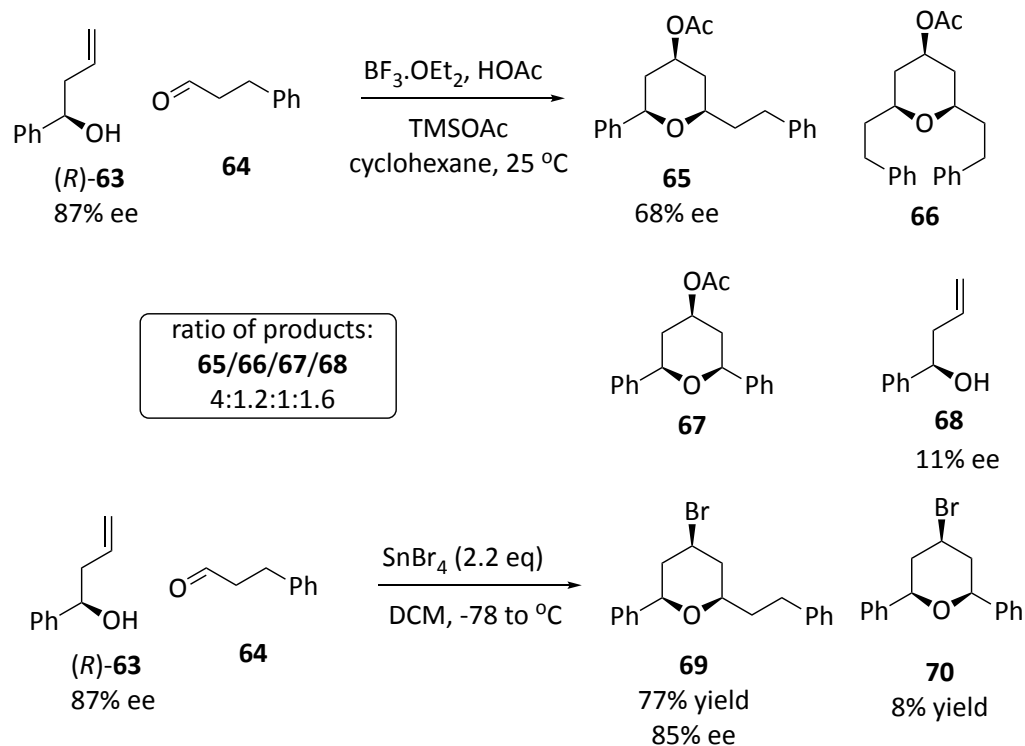
At the same time, partial racemization was reported, by Rychnovsky, *via* reversible 2-oxonia-Cope rearrangement and side-chain exchange.^{22,23} As shown in Scheme 13, racemization occurred during allyl transfer as a result of 2-oxonia-Cope rearrangement *via* a 3,3-sigmatropic shift, which played an important role in the reaction.



Scheme 13. Partial racemization through 2-oxonia-Cope allyl transfer

The Prins cyclization of alcohol (R)-63 and aldehyde 64 was studied under various Lewis acid conditions, as illustrated in Scheme 14.²³ The partial racemization of the desired product 65 (from 87% ee to 68% ee) caused by $\text{BF}_3 \cdot \text{OEt}_2$ /HOAc cyclization resulted in the formation of side-chain exchange products 66 and 67, symmetric tetrahydropyran. This

observation supported the intervention of a 2-oxonia-Cope-mediated side-chain exchange reaction and was entirely consistent with the result obtained by Willis and co-workers²⁰, which led to the partial racemization observed in the desired product formation. On the other hand, SnBr₄ was found to be more efficient than BF₃.OEt₂/HOAc in terms of enantiopurity retention in major product **69** during cyclization (from 87% ee to 85% ee, Scheme 14). This was most likely due to faster cyclization with SnBr₄, which suppressed the competing 2-oxonia-Cope process.



Scheme 14. Partial racemization by reversible 2-oxonia-Cope rearrangement

1.4 Hetero-Diels-Alder Reaction

The Hetero-Diels-Alder (HDA) reaction is an additional method that can be utilised in the synthesis of natural products to construct THP rings. Depending on the conditions,

the HDA reaction can exhibit high levels of regioselectivity as well as endo-stereoselectivity.^{24,25}

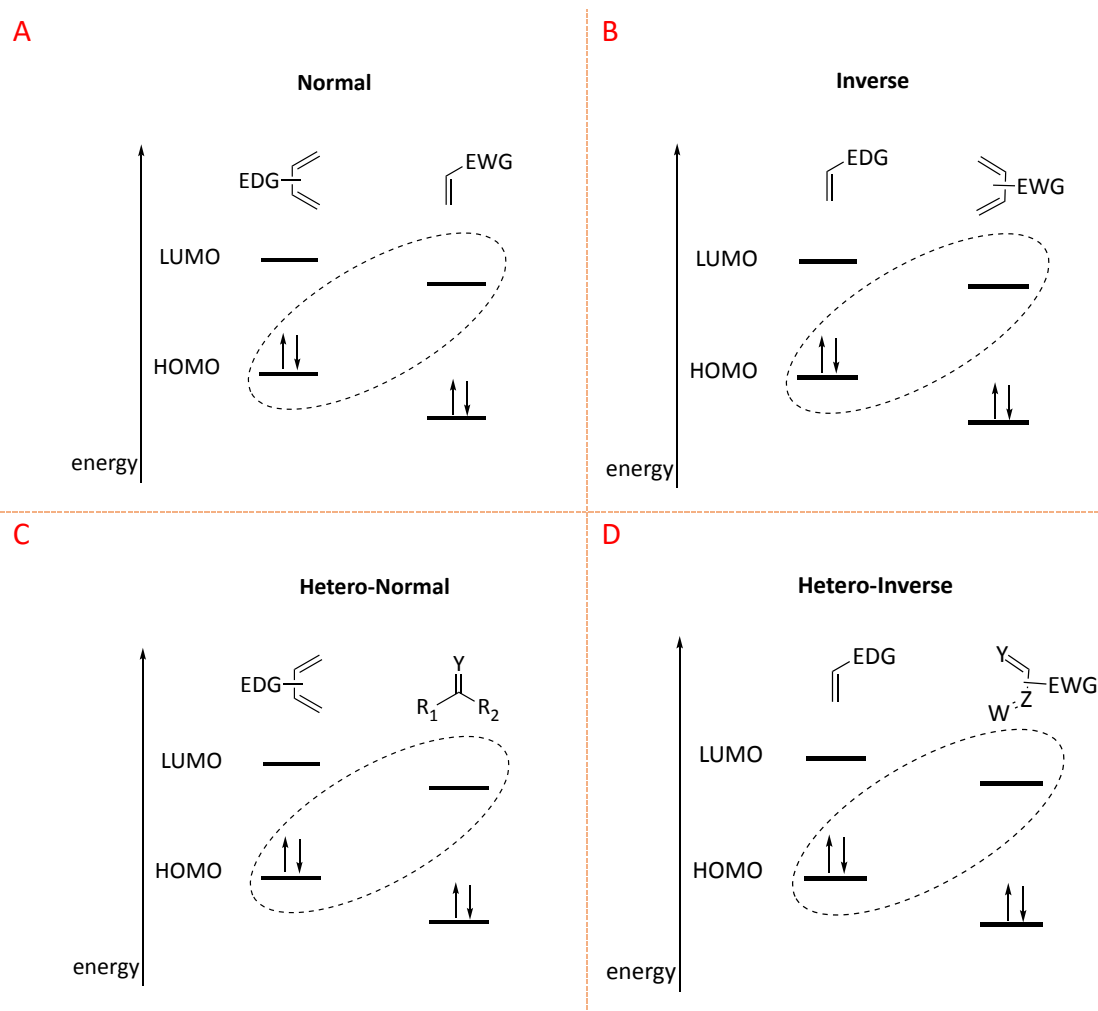
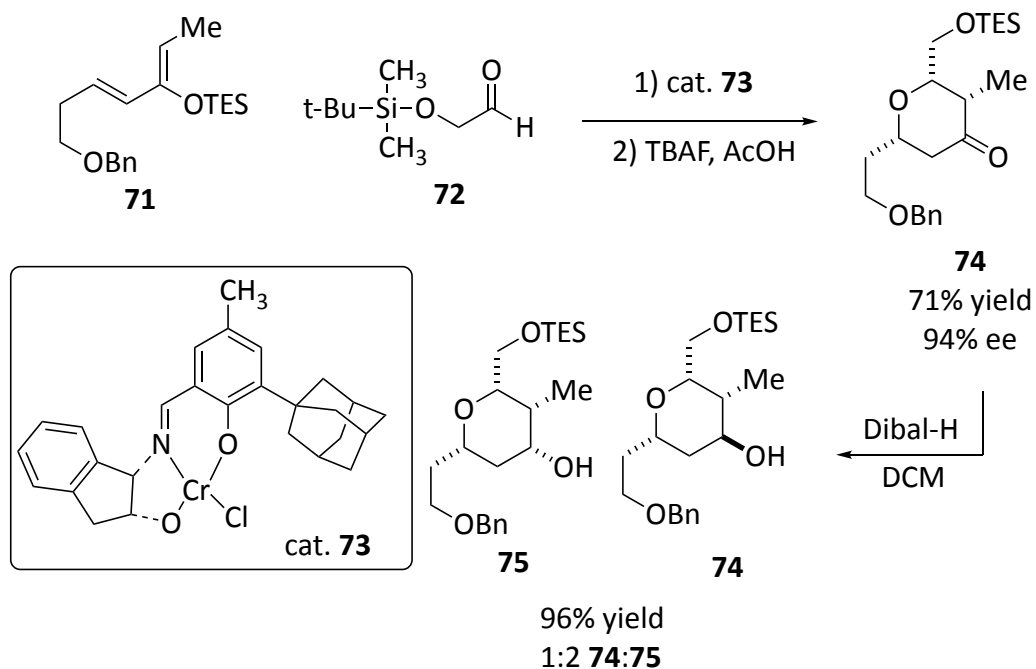


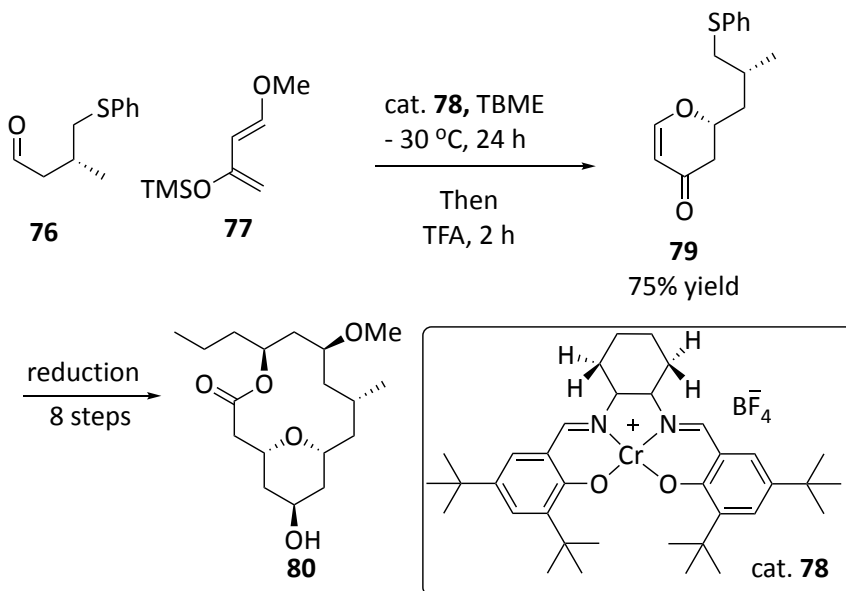
Figure 3. Normal-demand and inverse-electron-demand all-carbon and hetero Diels-Alder reaction

Ghosh reported an asymmetric HDA reaction in the key step in the synthesis of B ring **74** of lasanotide A.²⁶ Jacobsen and co-workers' chiral tridentate Schiff base chromium(III) complex (1*S*,2*R*) **73**²⁷ was used as the catalyst (10 mol %) in the asymmetric hetero-Diels-Alder reaction between diene **71** and **72**. In the same reaction flask, the resulting dihydropyran silyl enol ether was treated with TBAF/AcOH to remove the TES group and give the corresponding ketone **74** in 71 % yield and with 94 % ee. Ketone

reduction with Dibal-H gave the THP of the B ring in 96% combined yield of axial alcohol **74** and equatorial alcohol **75** as a 1: 2 separable mixture (Scheme 15).



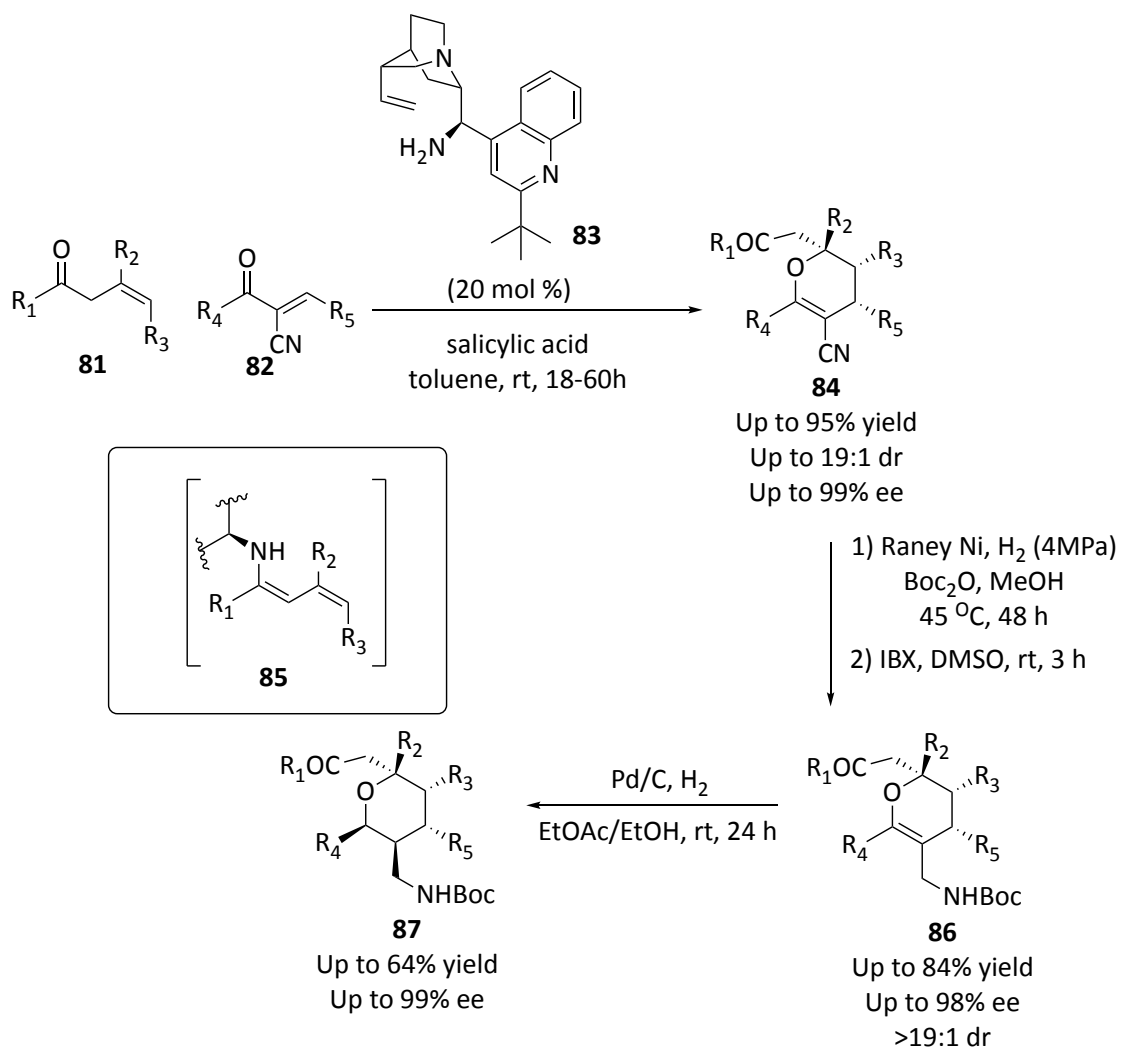
Scheme 15. Synthesis of B ring **74** of lasanotide A



Scheme 16. Synthesis of the THP ring of the macrolactone core of (+)- neopeltolide

The Raghavan group used the same method, an HDA reaction, to synthesise the THP ring of the macrolactone core of (+)-neopeltolide **80**.²⁸ The THP ring was formed by Jacobsen's catalyst ((S,S)-Cr(III)-salen-BF₄⁺) **78**, which was promoted by aldehyde **76** and siloxy diene **77**. After 8 more steps, **80** was formed in 60% yield (Scheme 16).

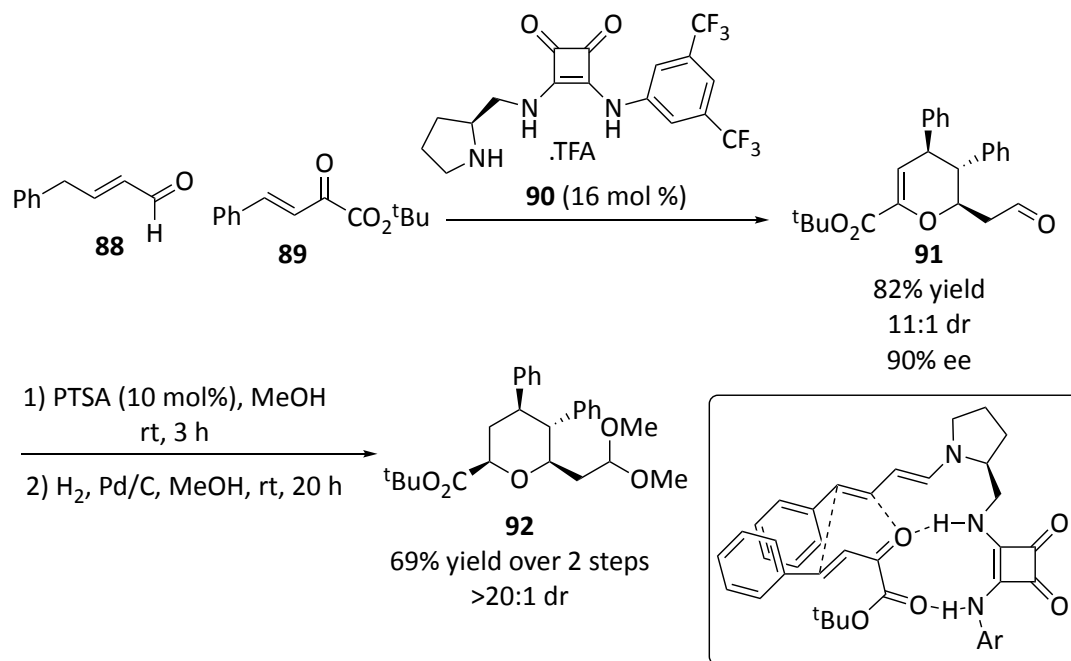
The activation of different dienophiles' HOMO has been widely used as an organocatalytic strategy, allowing the development of new inversion-electron-demand hetero Diels-Alder (IEDHDA) systems. Amine-based (enamine and dienamine) catalysis has been the preferred system because it can covalently generate the dienophile *in situ*, increasing the energy of the HOMO of different aldehydes through the formation of transient chiral (di)enamines or enolates, which allow the corresponding cycloaddition with excellent enantiocontrol. In this context, Chen described the asymmetric inverse-electron-demand oxa-Diels-Alder reaction using β,γ -unsaturated ketones **81** (Scheme 17).²⁹ In the presence of a cinchona-derived primary amine as a catalyst **83**, the reaction occurred with excellent yields, high diastereoselectivities, and excellent enantioselectivities. The ketone-derived **81** *in situ* formed dienamine evolves **85** *via* the usual β,γ -regioselectivity, allowing the synthesis of the corresponding highly substituted dihydropyran derivatives **84**. Then, in the presence of Raney Ni and (Boc)₂O, the cyano group was smoothly hydrogenated and then protected as an N-Boc derivative. Due to the ketone's reduction to alcohol with low diastereoselectivity, reoxidation of the intermediate with IBX yielded compound **86** as a ketone form in a moderate yield. Furthermore, the alkene moiety of **86** was chemoselectively hydrogenated under the mild catalytic conditions of Pd/C and H₂, resulting in a high yield of the pure tetrahydropyran derivative **87** with four stereogenic centres.



Scheme 17. Chen's asymmetric synthesis of THP derivatives via IEDHDAR

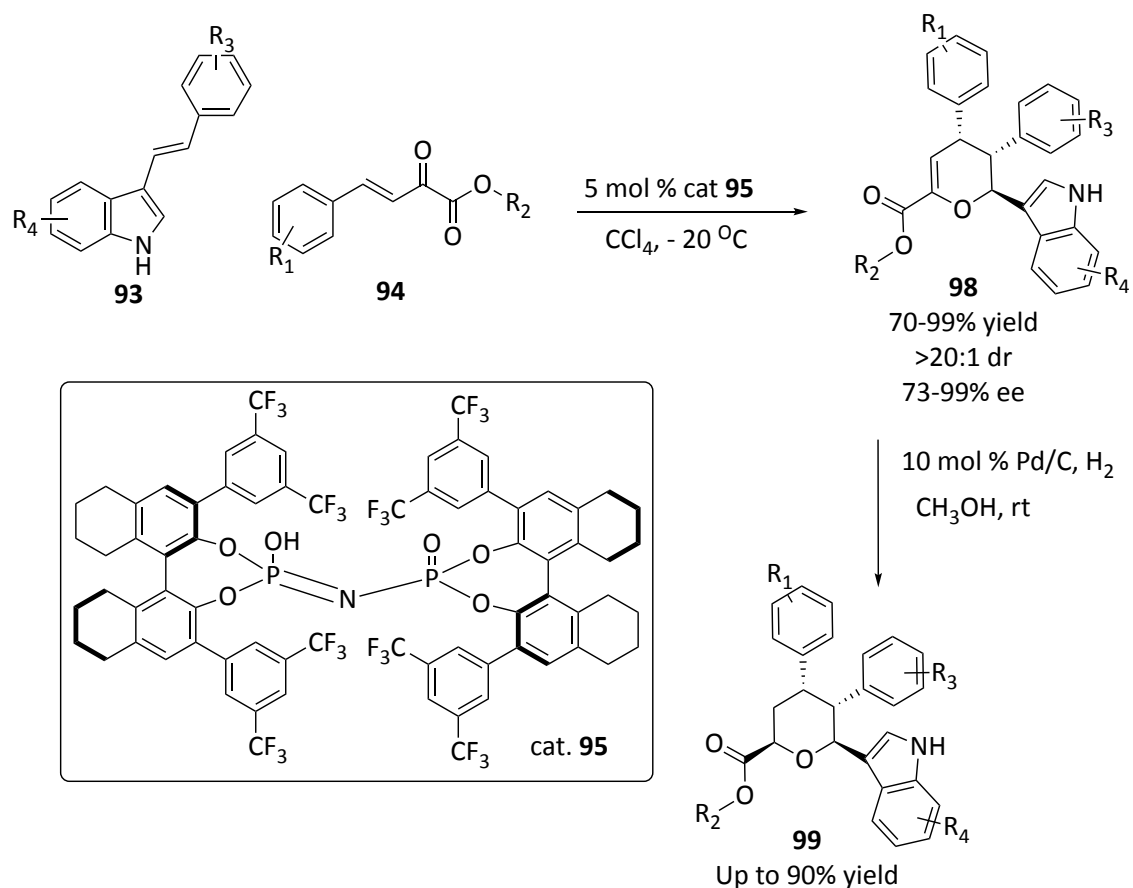
Bifunctional catalysts have been of great interest in the organocatalytic field and have made substantial contributions to the field of asymmetric synthesis.²⁵ Utilizing their ability to perform simultaneous activation of the electrophile and nucleophile, these catalysts have also been used to synergistically facilitate the HOMO-raising and the LUMO-lowering activation of both reaction partners, thereby initiating the asymmetric inversion-electron-demand hetero Diels-Alder reaction (IEDHDAR).^{30,31} This has made this strategy an extremely useful method for the synthesis of compounds that are difficult to obtain through other methods. In this way, the combination of amine catalysis with a hydrogen bond donor core in the same bifunctional organocatalyst has enabled the exploitation of this strategy

via the *in situ* formation of the corresponding (di)enamine or iminium ion, which acts as a dienophile, and the simultaneous activation of the diene via hydrogen bonding interactions.



Scheme 18. Bifunctional-catalyzed enantioselective synthesis of tetrahydropyran derivatives via IEDHDAR

In this context, Jørgensen reported the enantioselective synthesis of dihydropyran derivatives with three contiguous stereogenic centres in excellent yields, high diastereoselectivities, and excellent enantioselectivities (Scheme 18).³² The method used a squaramide-based organocatalyst with a pyrrolidine moiety **90** that was involved in the dienamine generation *in situ* (dienophile). The reaction occurred via the expected β,γ -regioselectivity, and the authors reported that the reaction occurred via a coordinated mechanism. The hydrogenation of the double bond in **91** was successful when Pd/C was used as the catalyst. However, prior to hydrogenation, the aldehyde moiety had to be protected as its corresponding dimethyl acetal. Fortunately, both reactions could be performed in a single pot, increasing the approach's operational simplicity.



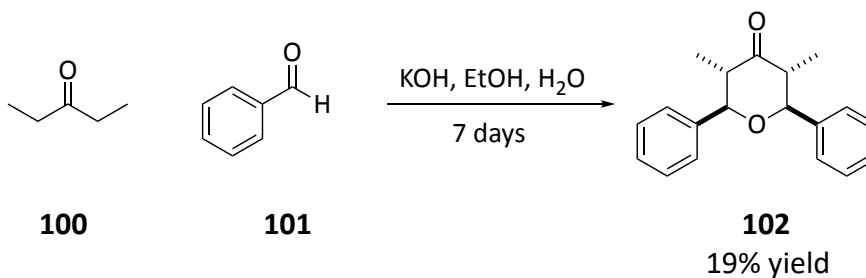
Scheme 19. Imidodiphosphoric acids catalyzed asymmetric synthesis of THP derivatives via IEDHDAR

In 2019, Zhang and co-workers described an enantioselective inverse-electron-demand oxa-Diels–Alder reaction of β,γ -unsaturated α -ketoesters **94** using 3-vinylindoles **93** as dienophiles and catalysed by imidodiphosphoric acids **95** (Scheme 19).³³ Excellent yields (70–99%), diastereoselectivities (>20:1 d.r.), and enantioselectivities (73–99% ee) were achieved in the synthesis of a series of optically active 3,4-dihydro-2H-pyran derivatives **98**, with three contiguous stereogenic centres (Scheme 19). Simple hydrogenation reduction can convert the resulting indole containing 3,4-dihydro-2H-pyran **98** to tetrahydropyran derivatives **99**, which were found in several biologically active compounds. Initially, the catalyst **95** captured two reactants through the formation of double H-bonds. Meanwhile, the 3,5-bis(trifluoromethyl)-phenyl groups at the 3,3' position

of catalyst **95** shield the *Si* face of the of β,γ -unsaturated α -ketoesters **94**. Consequently, a predominant *Re* face attack of 3-vinylindole **93** yielded the product **98**.

1.5 Modified Maitland-Japp Reaction

The Clarke group has spent the last twenty years expanding the scope of the Maitland-Japp reaction, which produced a functionalised THP **102** from the simple starting materials 3-pentanone **100** and benzaldehyde **101**.³⁴ Japp and Maitland's 1904 publication described the experimental details of a reaction observed eight years earlier by Vorländer;³⁵ the THP **102** was formed with a moderate 19% yield in a condensation reaction promoted by potassium hydroxide (Scheme 20).

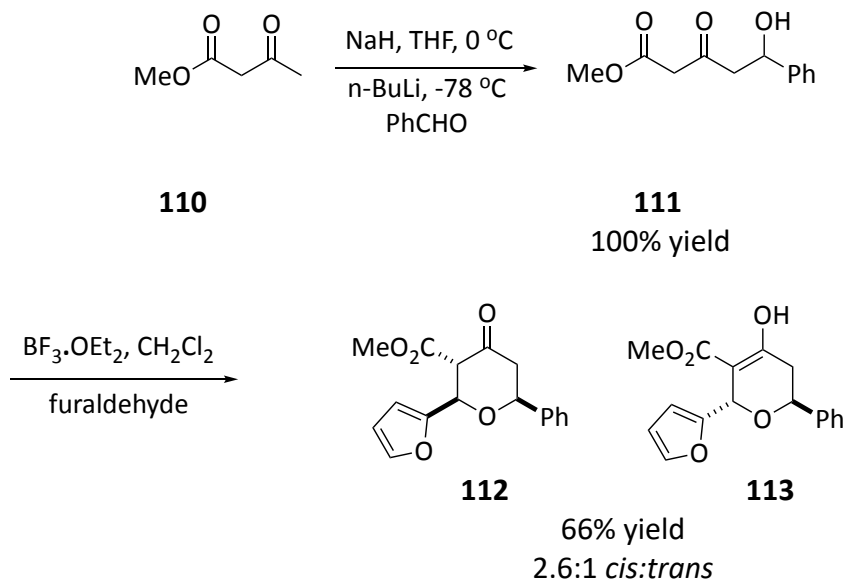


Scheme 20. The Maitland-Japp reaction

In 1968, Whiting and Baxter demonstrated that the THP **102** had an all-equatorial 2,6-*cis* isomer.³⁶ Although the reaction to form it was an interesting method of forming THPs, there were several issues with its widespread application for THP synthesis. Aside from the long reaction time and low to moderate yield, the product was symmetrical; alternative aldehydes would result in a mixture of symmetrical and unsymmetrical THPs.

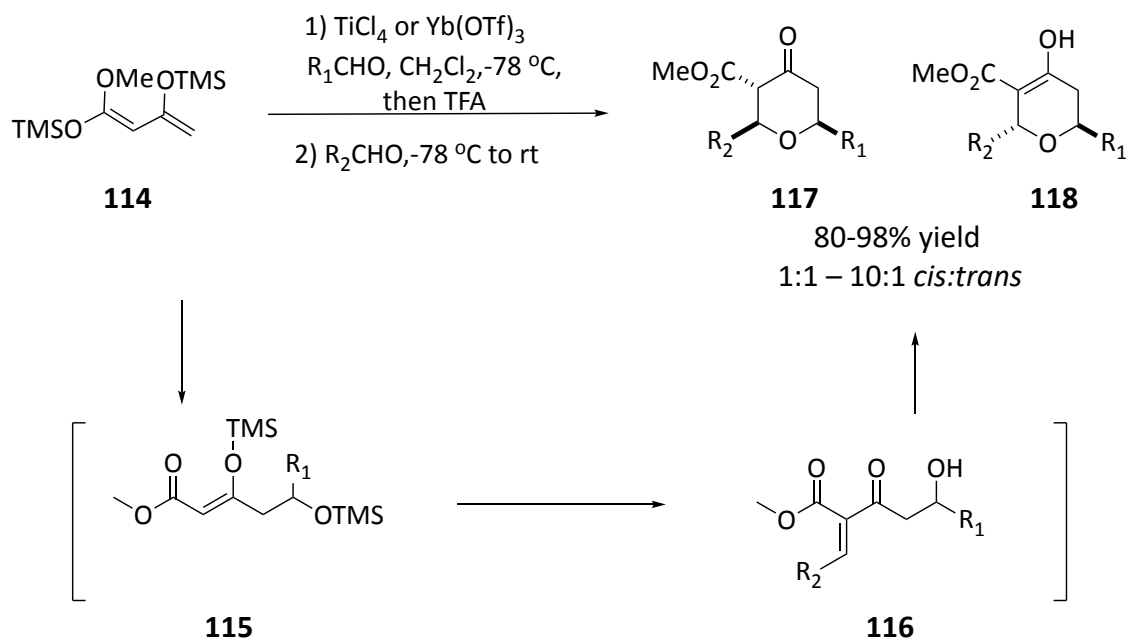
In 1934, Cornubert and Robinet demonstrated that a similar THP synthesis could be accomplished under acidic conditions (Scheme 21).³⁷ The 2,6-*cis* THP **105** with a remarkable diastereomeric excess was obtained by mediating the reaction between acetonedicarboxylic acid **103** and benzaldehyde **104** with HCl where the cyclization proceeded with concomitant decarboxylation.

Michael step were required to form the THP ring. Thus, boron trifluoride diethyl etherate was an appropriate Lewis acid for both steps, allowing the formation of 2,6-disubstituted THPs as a mixture of the 2,6-*cis* ketone **112** and 2,6-*trans* enol **113** diastereomers (Scheme 23).



Scheme 23. Updating the Maitland-Japp reaction to synthesise substituted THPs

A Lewis acid common to the aldol and cyclisation steps was required to carry out the reaction in a one-pot, sequential fashion. The bis-silyl dienolate of methylacetoacetate (Chan's diene⁴⁰) **114** was used because of its ease of use and higher reactivity, and both TiCl_4 and $\text{Yb}(\text{OTf})_3$ promoted the addition of the Chan's diene **114** to a variety of aldehydes. The addition of TFA was required to deprotect the intermediate silyl enolate formed after the aldol reaction in order to promote the Knoevenagel condensation and subsequent oxa-Michael reaction, which produced THPs as a mixture of 2,6-*cis* ketone **117** and 2,6-*trans* enol **118** diastereomers in excellent yields (Scheme 24).^{41,42}



Scheme 24. The revised one-pot Maitland and Japp reaction

The 2,6-*cis* keto products **117** were produced predominantly by $\text{Yb}(\text{OTf})_3$, whereas TiCl_4 produced predominantly 2,6-*trans* enol products **118**. This selectivity was attributed to chelation of the developing THP to the Lewis acid. TiCl_4 dissolved more easily in the reaction solvent and can form a 6-membered co-ordinate system with the C-4 enolate anion and the C-3 ester group. This system flattened the ring, reducing the unfavourable interaction of a pseudo-axial substituent in the forming 2,6-*trans* product (Figure 4). In contrast, the developing 2,6-*cis* product's equatorial substituent would form steric clash between the C2 and C3 substitutions, thus it would be twisted into a more axial position, making it less energetically favourable. Meanwhile, because the Lewis acid, $\text{Yb}(\text{OTf})_3$, is less soluble, this chelation did not occur, and the more energetically favourable bis-equatorial 2,6-*cis* product was formed preferentially.

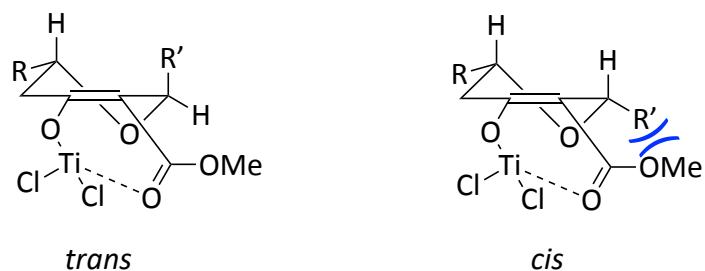
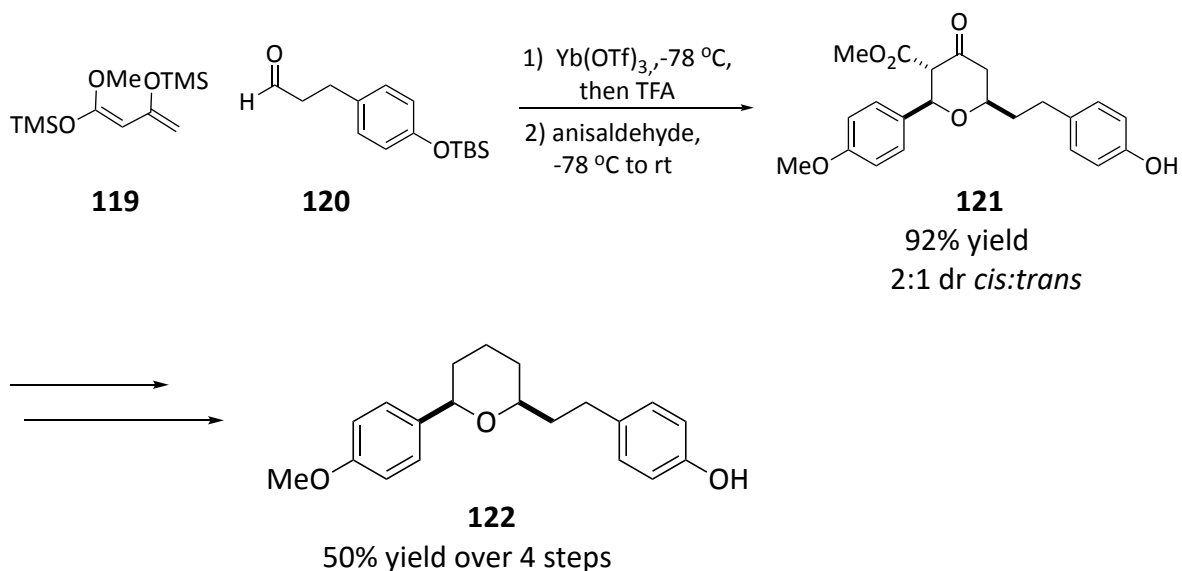


Figure 4. *cis-Ti* and *trans-Ti* chelated systems

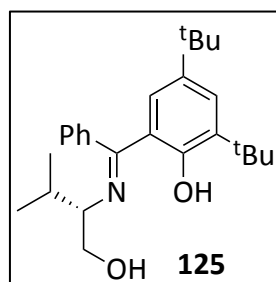
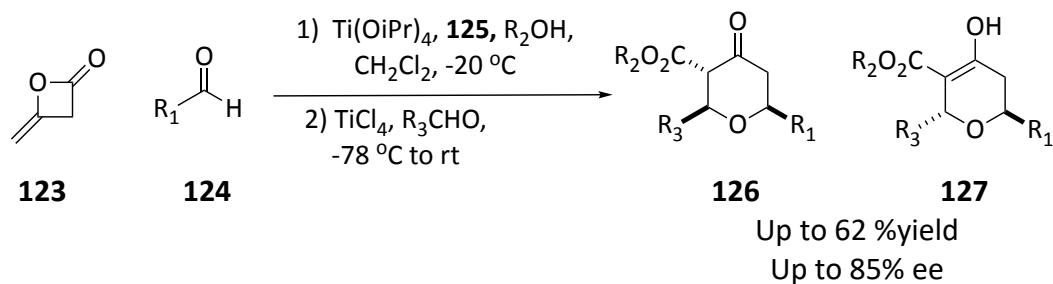
This method was used in the synthesis of centrolobine (Scheme 25).^{43,44} To create the 2,6-*cis* THP **121**, Yb(OTf)₃ was used as the Lewis acid, resulting in a 2:1 diastereomeric ratio in favour of the desired isomer. The THP **121** was decarboxylated with lithium hydroxide and hydrogen peroxide followed by removal of the ketone *via* a dithiolane using Raney nickel yielded centrolobine **122** in 50% yield over the four synthetic steps.



Scheme 25. Synthesis of centrolobine **122** via Maitland-Japp reaction

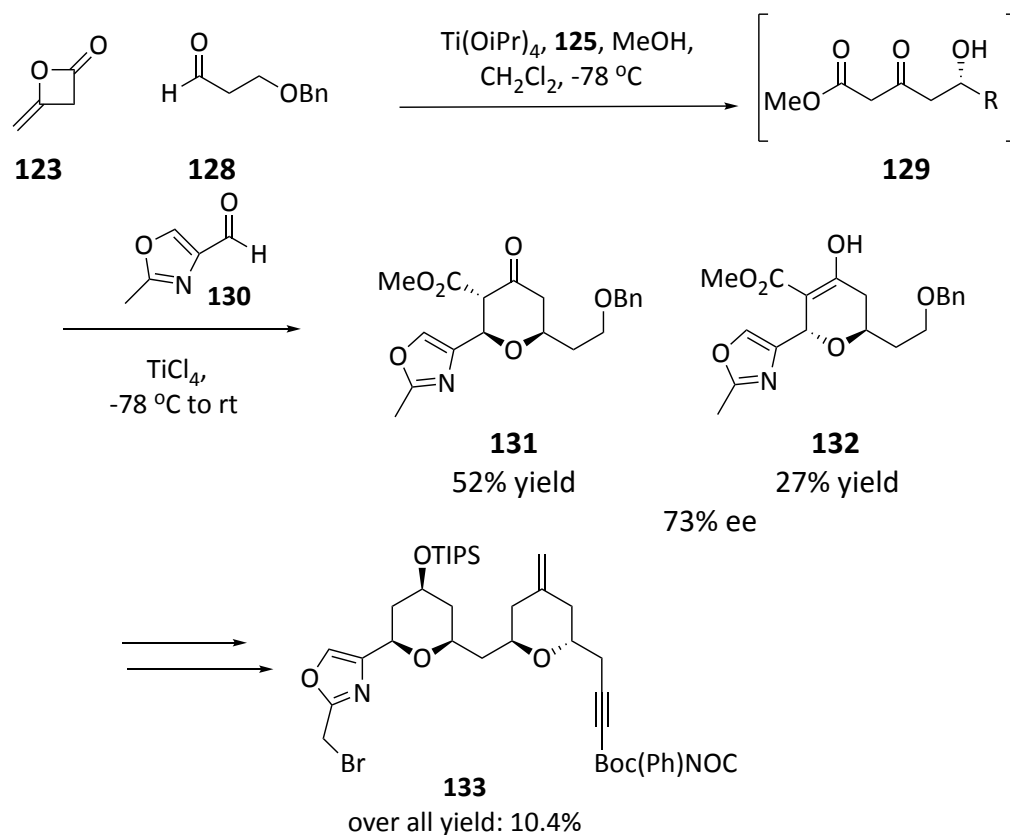
Attempts were made to make the reaction more atom economical by replacing Chan's diene, which requires two steps to synthesise, with commercially available diketene **123**.⁴⁵ In the diketene Maitland-Japp reaction, the mono- γ -titanium enolate of a β -ketoester

was formed by nucleophilic ring-opening of diketene *via* ligand transfer from the activating Lewis acid (TiCl₄ or Ti(iOPr)₄). The addition of methanol or isopropanol as a nucleophile would produce methyl or isopropyl δ -hydroxy- β -ketoesters. This reaction's asymmetric variant was then developed.⁴⁶ Using Ti(OiPr)₄ as the Lewis acid and a Schiff's base ligand **125**, the aldol reaction produced δ -hydroxy- β -ketoesters in good to high enantiomeric excess (Scheme 26). The Knoevenagel/oxy-Michael cyclisation was completed without stereochemistry erosion, yielding asymmetric THPs **126** and **127** in up to 85% ee.



Scheme 26. Asymmetric synthesis of substituted THPs via diketene

Due to the successful development of an asymmetric Maitland-Japp reaction, Clarke decided to attempt this method for the synthesis of the C1-C19 *bis*-pyran unit of the phorboxazoles.⁴⁷ The synthesis began with an asymmetric Maitland-Japp reaction between diketene **123** and aldehyde, 3-benzyloxypropanal, **128** to produce δ -hydroxy- β -ketoester, which was then cyclized with oxazole aldehyde **130** to generate a mixture of THP rings **131** and **132** in 52% and 27%, respectively with 73% ee (Scheme 27). After additional steps, the C1-C19 *bis*-pyran unit of the phorboxazoles was formed with overall yield 10.4%.



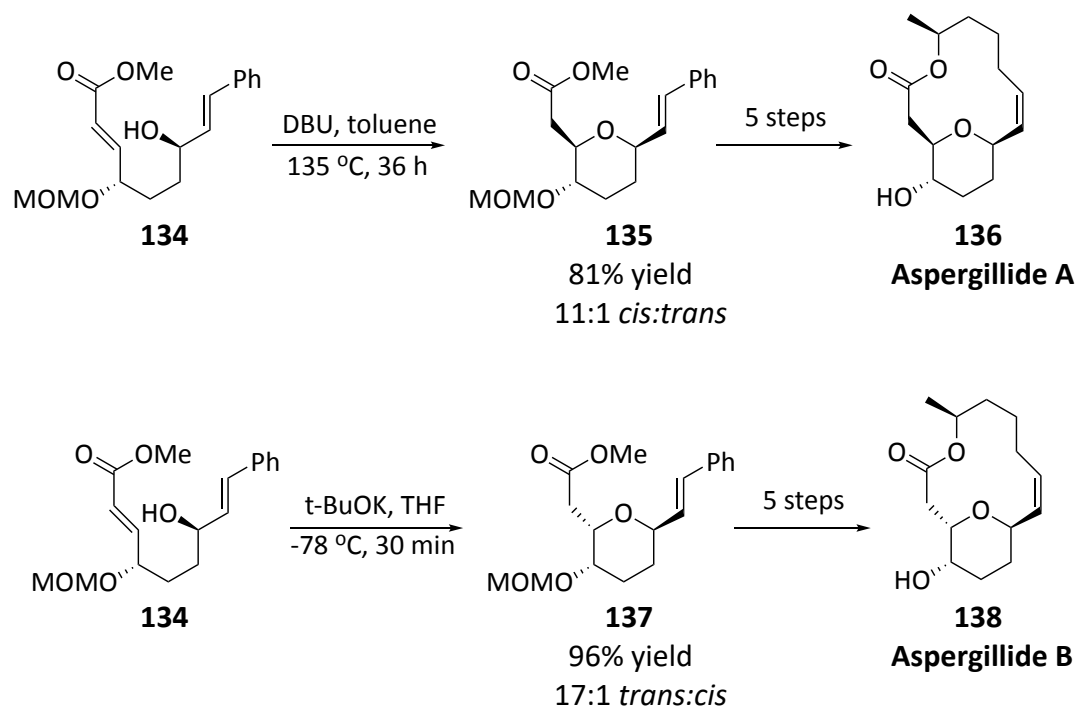
Scheme 27. Synthesis of the C1-C19 bis-pyran unit of the phorboxazoles

1.6 Oxa-Michael Reaction

Michael reactions are widely used in organic synthesis.⁴⁸ There are several hetero-Michael reactions, including aza-Michael, sulfa-Michael, phospho-Michael, and oxa-Michael (oxo- or oxy-Michael). In 1878, Loydl published the oxa-Michael reaction, which involved the addition of oxygen nucleophiles (primarily alcohols) to an acceptor conjugated system to form an intermediate enolate, which on protonation gives rise to β -ether compounds.⁴⁹ Furthermore, oxa-Michael reactions can be an efficient method for the construction of oxygen-containing heterocycles like tetrahydropyrans.⁵⁰

1.6.1 Racemic cyclization

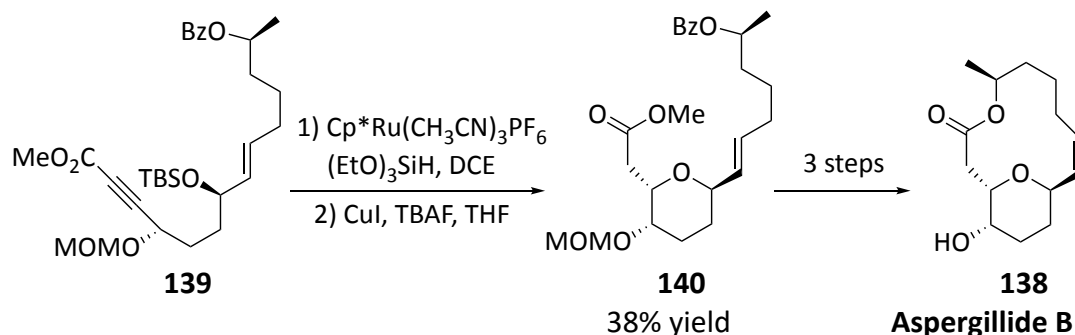
Fuwa *et al.* used a stereodivergent strategy to obtain aspergillide A **136** and aspergillide B **138** by subjecting the cyclization precursor **134** to a variety of conditions.⁵¹ Under basic conditions at a low temperature, the *trans* isomer **137** was synthesised with 96% yield and selectivity (dr = 17:1), resulting in the synthesis of aspergillide B **138** in five steps. However, a switch in selectivity was observed at a higher temperature, leading to the synthesis of aspergillide A **136** by generating the *cis* isomer **135** with 81% yield and selectivity (dr = 11:1). This variation in selectivity was due to the transition from kinetic control at lower temperatures to thermodynamic control at higher temperatures (Scheme 28).



Scheme 28. Stereodivergent strategy employed in the synthesis of aspergillide A and B

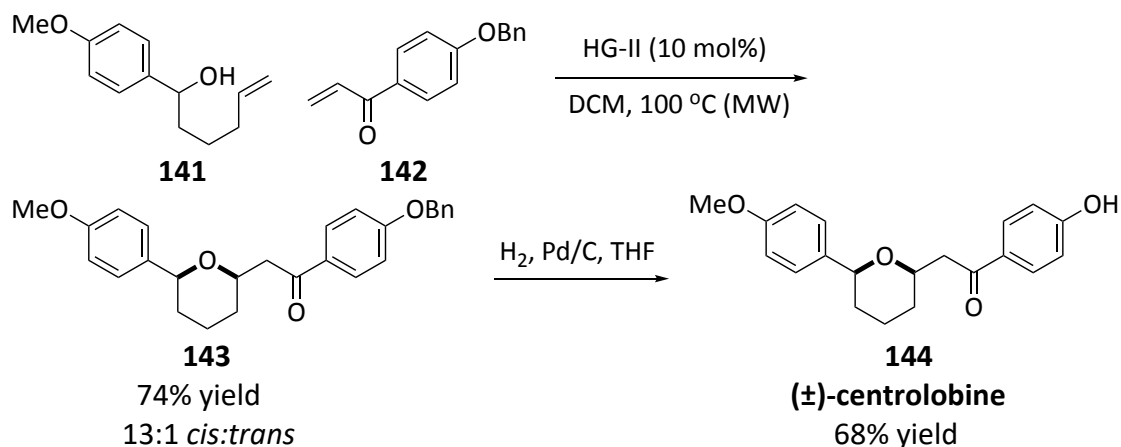
Conversely, the Trost group used ruthenium-catalyzed *trans*-hydrosilylation to synthesise the THP ring of aspergillides B **138**.⁵² The hydrosilylation/protodesilylation reaction was used to chemoselectively reduce the alkyne **139** and form an *E*-double bond,

followed by deprotection/oxy-Michael reaction to yield 2,6-*trans* THP **140** in 38% yield. THP **140** was then converted into aspergillides B **138** in three steps (Scheme 29).



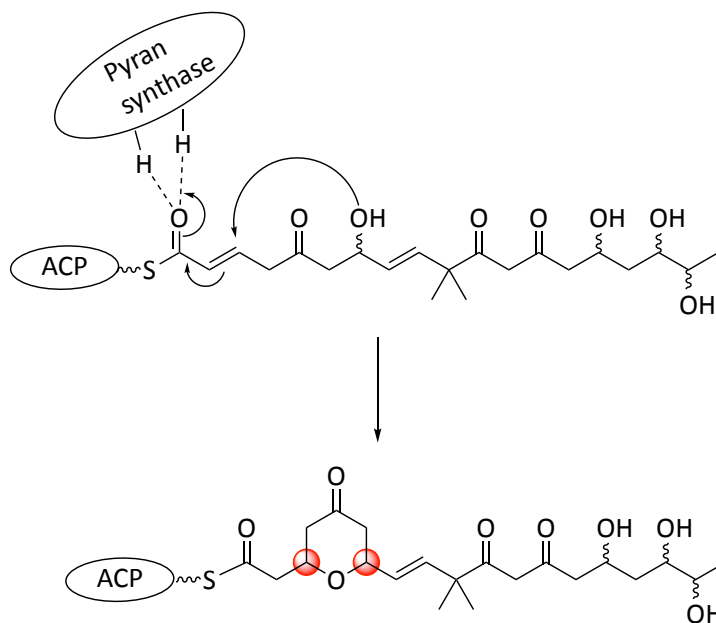
Scheme 29. Synthesis of aspergillides B **138**

Fuwa synthesised (\pm)-centrolobine **144** using the tandem metathesis/oxa-Michael reaction method.⁵³ The cross metathesis of the hydroxyl alkene **141** and an α,β -unsaturated ketone **142**, derived from readily available *p*-benzyloxybenzaldehyde, resulted in a crude mixture containing the desired 2,6-*cis* disubstituted tetrahydropyran **143** in a 13:1 ratio with respect to the *trans* isomer. The desired isomer **143** was isolated with a 74% yield after separation. Deprotection of the benzyl ether group by hydrogenolysis resulted in 68% yield of (\pm)-centrolobine **144**. Starting with commercially available *p*-benzyloxybenzaldehyde, a domino cross metathesis/oxa-Michael addition strategy yielded (\pm)-centrolobine in just four linear steps, demonstrating the efficiency and utility of this strategy (Scheme 30).



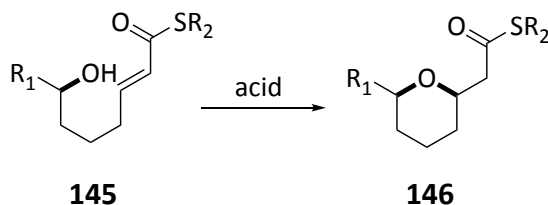
Scheme 30. Synthesis of (\pm)-centrolobine **144**

Several studies on the biosynthesis of polyketide-containing tetrahydropyrans suggested that tetrahydropyrans are formed *via* an intramolecular oxa-Michael cyclisation of α,β -unsaturated thioesters catalysed by pyran synthase and activated by hydrogen bonding (Scheme 31).^{54 55}

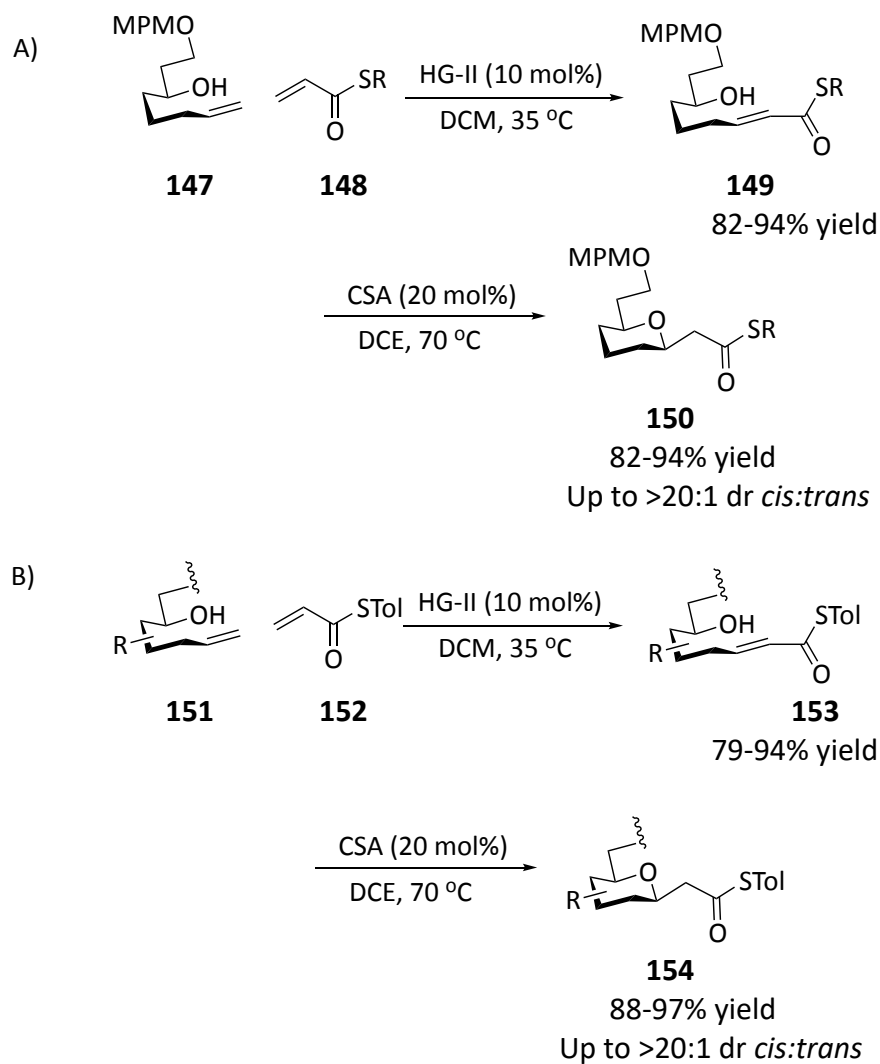


Scheme 31. Proposed biosynthetic pathway of the synthesis of polyketide tetrahydropyrans

Inspired by the biosynthesis, Fuwa proposed a biomimetic synthesis of 2,6-*cis* tetrahydropyrans **146** *via* intramolecular oxa-Michael cyclisation of α,β -unsaturated ester surrogates **145** catalysed by Brønsted acid (Scheme 32).⁵⁵



Scheme 32. Biomimetic synthesis of 2,6-*cis* tetrahydropyrans of ester surrogate



Scheme 33. Intramolecular oxa-Michael cyclisation of α,β -unsaturated thioester

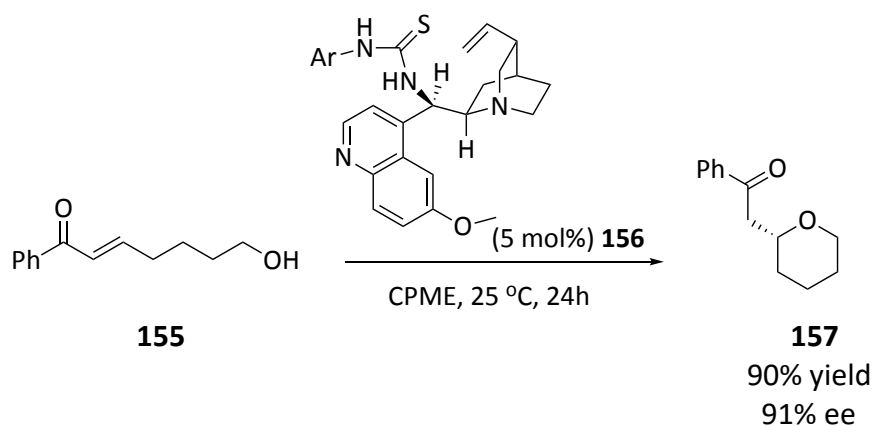
Based on the proposed synthesis,⁵⁵ hydroxy olefin **147** was subjected to the metathesis conditions with various α,β -unsaturated thioesters **148** catalyzed by Hoveyda Grubbs-II catalyst (HG-II) to form the cyclization precursors **149**. The precursors **149** were then cyclized using camphor sulfonic acid (CSA) in a Brønsted acid catalysed oxa-Michael reaction. With a yield of 72% and a dr >20:1, 2,6-*cis* tetrahydropyran **150** was obtained using a tolyl thioester **152** (Scheme 33-A). A substrate scope was carried out using various hydroxyl alkenes **151** and the tolyl thioester **152** to obtain excellent yields (88-97%) and diastereoselectivities (>20:1) for a variety of tetrahydropyrans **154** (Scheme 33-B).

This methodology is particularly appealing due to the versatility of using thioesters as Michael acceptors by derivatizing them into different functional groups under mild conditions with excellent yields.⁹

1.6.2 Asymmetric cyclization

For many decades, small organic molecules capable of catalysing reactions have been known, resulting in asymmetric organocatalysis becoming a hot field of research. Furthermore, due to the high efficiency, selectivity, low cost, environmental friendliness, and other properties of organocatalytic catalysts, an increasing number of research groups are developing organocatalytic asymmetric reactions to obtain the corresponding enantio-enriched products.

Matsubara *et al.* developed an amine-thiourea **156** catalysed cycloetherification reaction involving an intramolecular oxa-Michael reaction (Scheme 34).⁵⁶ The authors concentrated their efforts on optimising a procedure for synthesising various tetrahydrofurans (THF) starting from ϵ -hydroxy- α,β -unsaturated ketones. Nonetheless, they reported one case in which they obtained the tetrahydropyran-based product **157** with high yield and enantioselectivity (90% yield, 91% ee).



Scheme 34. Enantioselective cycloetherification promoted by thiourea

The catalyst's role in this intramolecular transformation was to increase the electrophilicity of α,β -unsaturated ketone **155** by forming an H-bond with the thiourea moiety **156**. Meanwhile, the quinuclidine scaffold can partially deprotonate the hydroxyl group, resulting in an intramolecular nucleophilic attack (Figure 5).

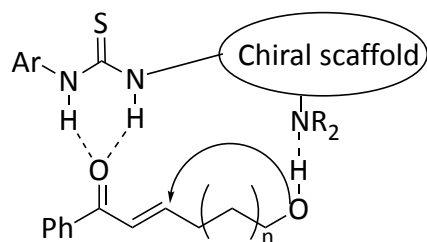
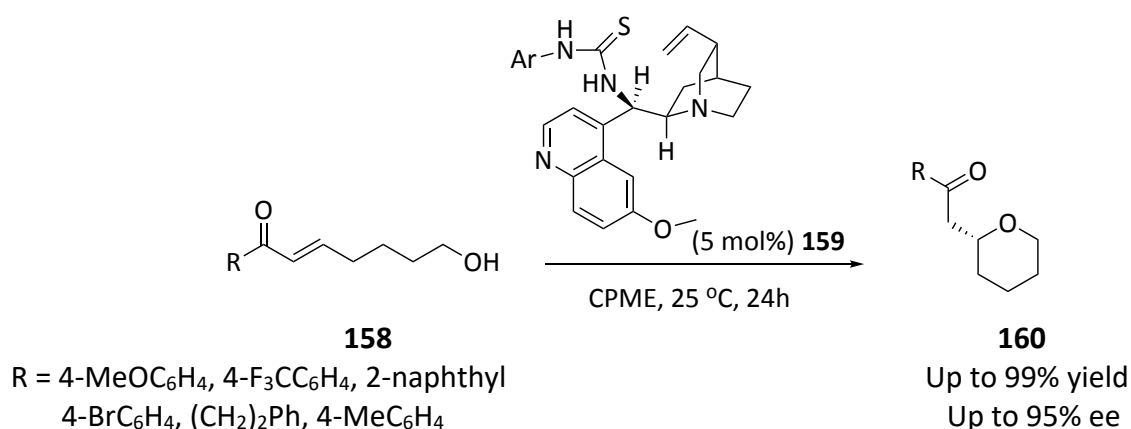


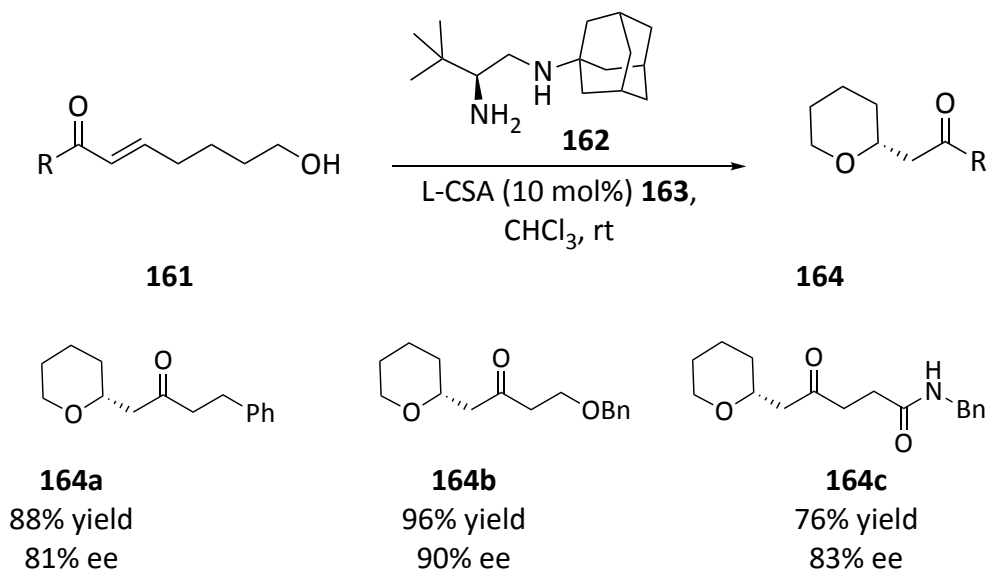
Figure 5. Asymmetric cycloetherification via intramolecular oxy- Michael addition reaction mediated by bifunctional organocatalyst

A few years later, Matsubara *et al.* investigated the scope of this reaction using various substrates **158** with both electron withdrawing and electron donating groups.⁵⁷ It was found that the electronic and steric properties of the substituents have no effect on the outcome of the reaction and the substituted THPs **160** obtained with high yields and enantioselectivity (Scheme 35).



Scheme 35. Asymmetric synthesis of 2-substituted THPs mediated by bifunctional organocatalyst

Similarly, Zhao and co-workers reported an asymmetric intramolecular oxa-Michael reaction of α,β -unsaturated ketone **161** catalysed by primary-secondary dienamines **162** in the same year.⁵⁸ The 2-substituted tetrahydropyrans **164** were obtained with good to excellent yields and enantioselectivity (Scheme 36).



Scheme 36. Asymmetric synthesis of substituted THPs catalysed by primary-secondary dienamines

To explain the observed stereochemical results, a bifunctional iminium mechanism could be invoked (Figure 6). The primary amine moiety of the catalyst **162** was thought to activate enone **161** by forming an iminium ion, whereas the secondary amine was thought to activate the nucleophilic hydroxyl group. The bulky groups on both sides of the catalyst shield the *si*-face of the enone in this transition state **I**, causing the alcohol oxygen atom to attack the *re*-face of the enone **161**. Acid additives were discovered to play a significant role in the catalytic efficiency of these amino acid-derived diamine catalysts. The acid additive may facilitate the formation of the iminium ion and promote intramolecular nucleophilic ring closure by protonating the catalyst amine and generating a suitable leaving group.

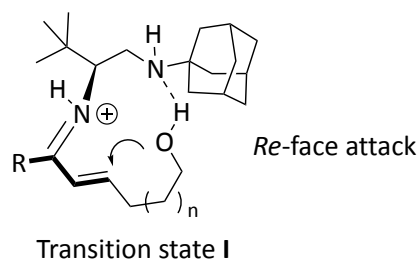
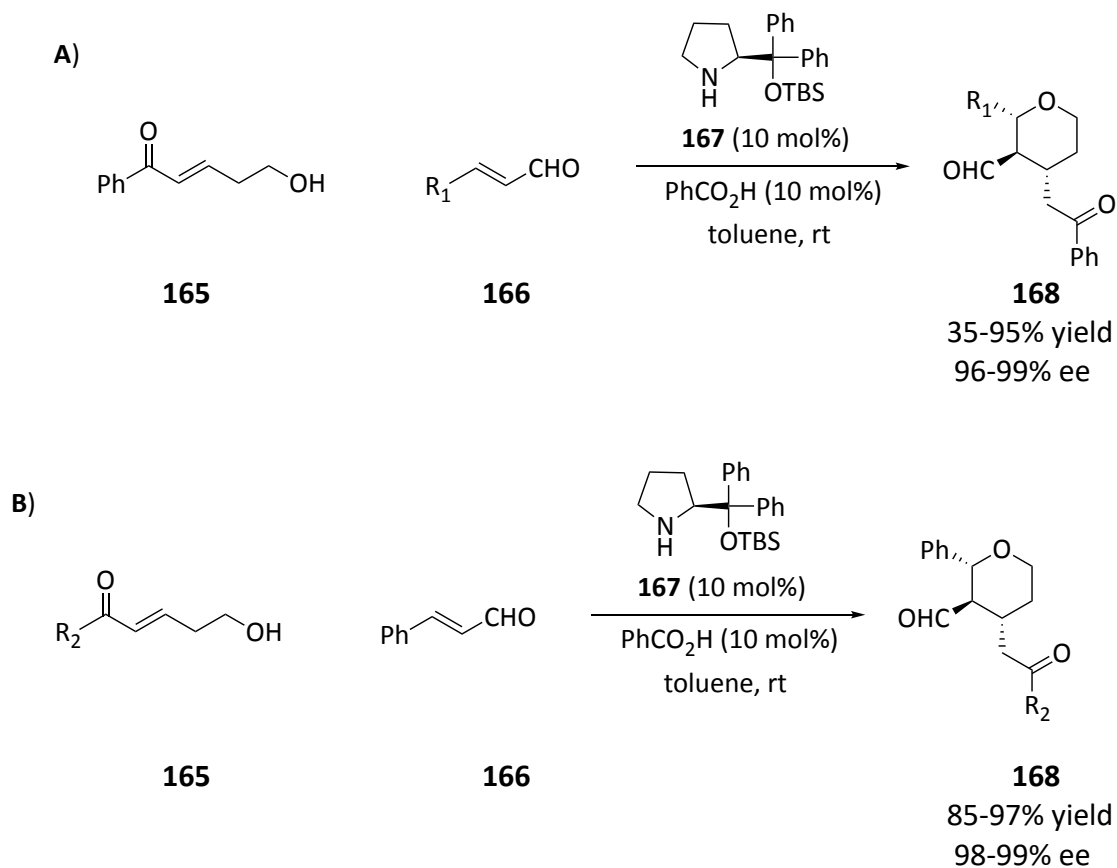


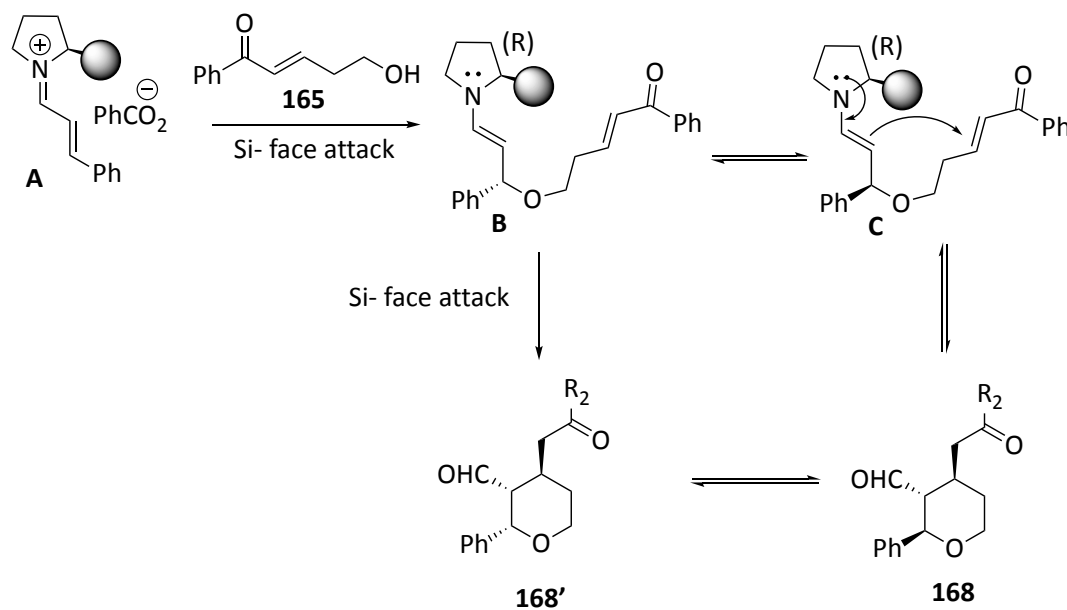
Figure 6. Possible transition state of the reaction

In 2018, Pan and co-worker used tandem iminium-enamine catalysis to develop an asymmetric synthesis of 2,3,4-trisubstituted THPs **168**.⁵⁹ A double Michael addition reaction between γ/δ -hydroxy- α,β -unsaturated carbonyls **165** and enals **166** was used in the process to obtain the substituted THPs **168** in high enantio- and diastereoselectivities (Scheme 37).



Scheme 37. Synthesis of tri-substituted THPS

Initially, (*E*)-5-hydroxy-1-phenylpent-2-en-1-one **165** and cinnamaldehyde **166** were reacted in chloroform with catalyst **167** in the presence of benzoic acid. The desired tetrahydropyran **168** was formed in good yield as a single diastereomer, but the enantiomeric excess was only 78%. After some experimentation, it was discovered that using toluene as a solvent improved both enantioselectivity (>99%) and yield (90%). Following the establishment of the proper conditions, a screening of a variety of enals **166** for the reaction was carried out (Scheme 37-A). The reaction was demonstrated to be applicable to both aromatic and aliphatic enals **166**. The enantiomeric excess was excellent irrespective of the nature and position of the functional groups in the phenyl ring (Scheme 37-A). The focus then shifted to investigating the role of δ -hydroxyenones **165** in the reaction (Scheme 37-B). As a result, various *para*-substituted δ -hydroxyenones **165** were prepared and tested in the reaction. The reactions proceeded smoothly, and excellent enantioselectivities were obtained in all cases.



Scheme 38. Proposed mechanism for the formation of **168**

Scheme 38 depicts a plausible mechanism for the formation of **168**. Iminium ion **A** was first created by combining enal **166** and a catalyst **167**. Then, the attack of enone **165**

on **A**'s *Si* face provided enamine **B**. Enamine **B** then cyclized to form diastereomeric tetrahydropyran **168'**, which underwent reversible oxa-Michael transformation into more stable all equatorial **168**. Alternatively, enamine **B** can be converted to enamine **C** *via* a reversible oxa-Michael reaction, which produced **168** on further cyclization.

1.7 Spiro-tetrahydropyrans

For a long time, saturated monocyclic units - cyclohexane, cyclopentane, piperidine, and so on - dominated chemistry and drug discovery.⁶⁰ The situation began to change at the turn of the century. Lovering introduced the concept of "escape from flatland" in 2009, and it has already changed the way medicinal chemists think.^{61,62}

The analysis of principal moments of inertia (PMI) is a method for depicting the three-dimensional shape of a molecule on a two-dimensional plot (Figure 7).⁶³ The plot is ternary and depicts the three molecular shape extremes. The plot's top left vertex represents an acetylene equivalent, a species that is sp hybridised and has a 'rod-like' shape. The plot's bottom vertex represents a benzene equivalent, a species that is sp^2 hybridised and has a planar shape. The plot's top right vertex represents an adamantane equivalent, a species with sp^3 hybridization and a cage or sphere-like structure. As a result, depending on how well a compound represents the three classes of morphology, it will fall somewhere between the three vertices.⁶⁴

With relative ease, PMI analysis can be used to profile the three-dimensionality of a large library of compounds. The library was made up of 35,270 randomly chosen molecules from the respective ZINC subset that were deemed 'lead-like.' plotted onto a PMI plot, which is represented by the blue dots (Figure 7). The plot clearly shows that the area of space represented by three-dimensional molecules or sp^3 hybridised molecules is sparsely populated, whereas the area of space represented by two-dimensional structures is densely

populated. Approximately 75% of the molecules lie to the left of this line demonstrating the obvious disparity.

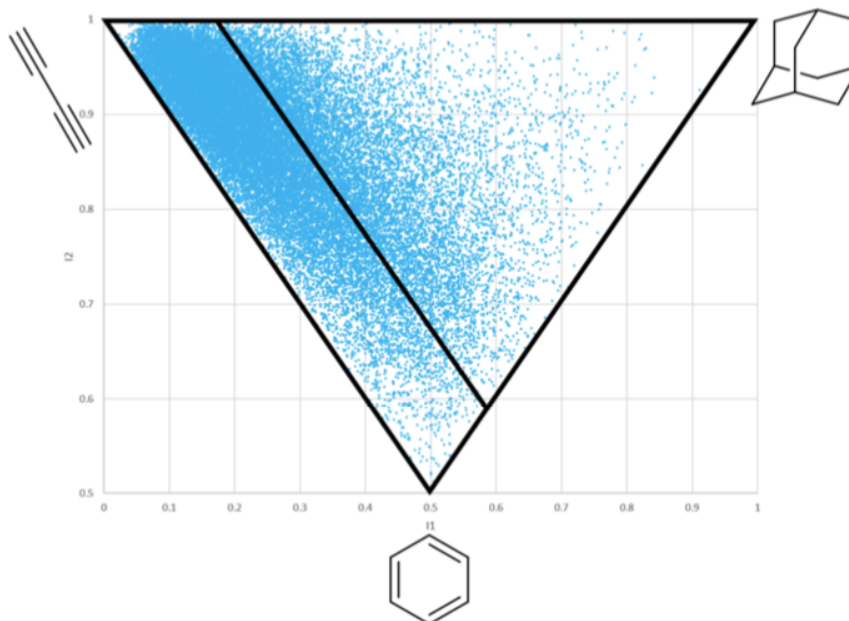
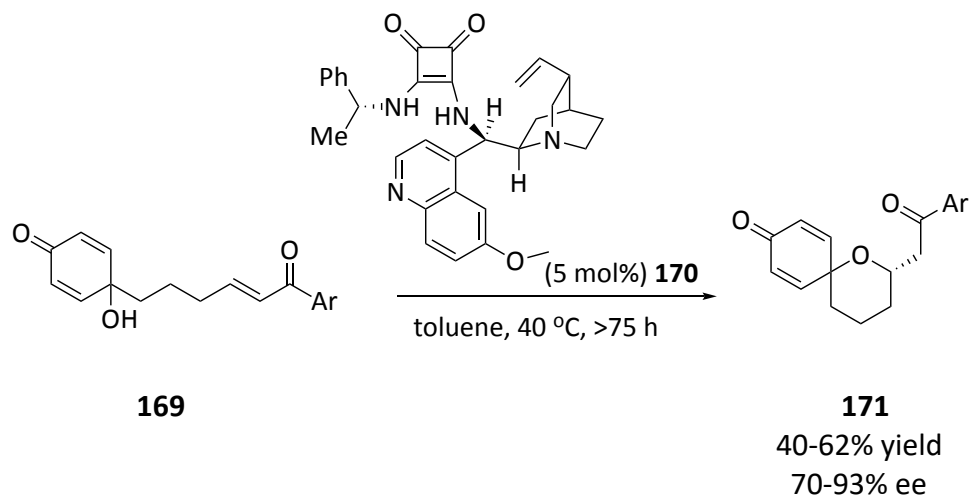


Figure 7. PMI plot of the ZINC 'lead-like' database

There is a growing consensus that spirocyclic molecules have a privileged position among all the sp³-rich structural types because they are conformationally well defined, allowing the functionality of the spirocycles to be elaborated in well-defined directions, which increases interaction with the target molecule, giving it a greater chance of having pharmaceutical importance. Also, because these molecules are in an area of sp³ chemical space that hasn't been fully explored yet, they have new intellectual property.

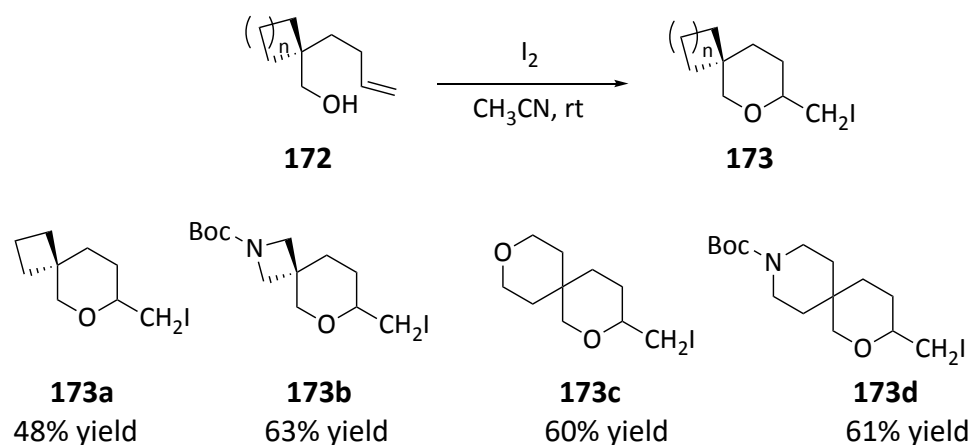
While spiro carbocyclic substituents are extremely common in chemistry, their corresponding oxa-spirocyclic counterparts are virtually unknown.⁵⁹ There had previously been some interest in oxa-spirocycles, but examples reported in the literature were rare and non-systematic, particularly for spiro THPs.

In 2016, Ghorai and co-workers reported an asymmetric oxa-Michael reaction of α -tertiary alcohols **169** using cinchona-alkaloid-based chiral bifunctional squaramide catalyst **170**.⁶⁵ Even though the reaction required long time (> 75 hours), the spiro-THPs **171** were obtained in good yields with good to high enantioselectivities (Scheme 39).



Scheme 39. Asymmetric synthesis of spiro-THPs

In 2021, Mykhailiuk *et al.* reported a gram scale racemic cyclization of spiro-THPs in which the key synthetic step was iodocyclization (Scheme 40).⁶⁰ Various six-membered oxaspirocyclic iodides **173** were prepared in 48-64% yield. The low yields of the products was due to incomplete conversion of the reactions.



Scheme 40. The iodocyclization step into spiro-THPs

Even though there was some interest in oxa-spirocycles, the examples that were reported in the literature were non-asymmetric, and the asymmetric version has not been investigated, which could be an appealing feature for the drug discovery process. Enantiopure compounds are essential for the study of biological molecules; therefore, it is imperative to synthesise spiro-THP as a single enantiomer. In light of this knowledge, the literature precedent left a number of unanswered questions. The following sections aim to answer these questions while achieving the end results.

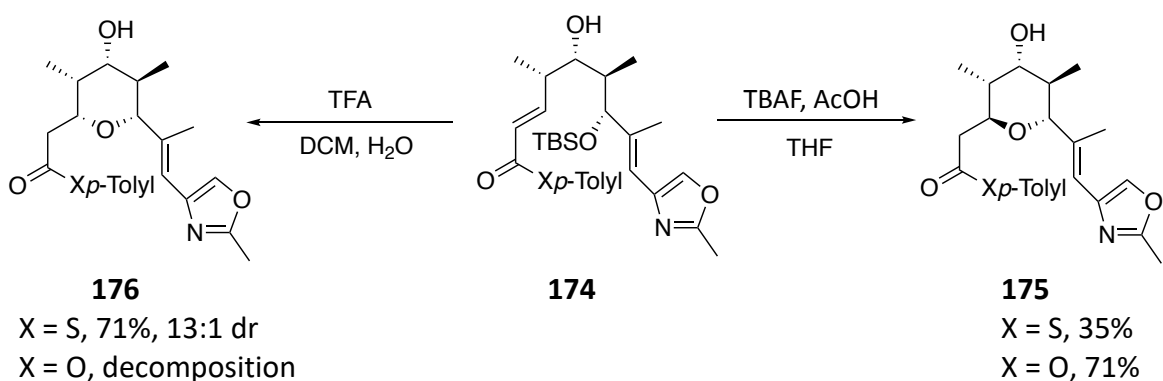
2 Results and Discussions

2.1 Asymmetric Synthesis of Substituted Tetrahydropyrans

2.1.1 Previous work within Clarke group

The stereoselective synthesis of heterocycles has been a key part of the Clarke group's research, and the methods developed have enabled the synthesis of natural products.^{1,2,66,67} Since heterocyclic rings, particularly chiral ring systems, are prevalent in natural products and pharmaceuticals, there has been a lot of interest within the group to develop new strategies to facilitate the synthesis of these heterocycles asymmetrically.

The Clarke group developed a stereodivergent oxa-Michael cyclization for the stereoselective synthesis of the tetrahydropyran in the C20-C32 core of phorboxazole.⁶⁸ In the cyclization of the precursor **174** under basic conditions (buffered TBAF), both the oxa- and the thioester led to the production of the 2,6-*trans*-tetrahydropyran **175**. On the other hand, when the acidic conditions (CSA or TFA) were applied, the 2,6-*cis*-tetrahydropyran **176** thioester was formed with high selectivity over the *trans* product with a 13:1 dr while the oxoester decomposed (Scheme 41).



Scheme 41. Stereodivergent synthesis of the C20-C32 tetrahydropyran core of phorboxazole

In order to explain these interesting results, the mechanism of both reactions was then explored through experimental and computational studies.⁶⁸ These studies indicated that the 4-hydroxyl group was crucial for the stereodivergence that was observed during the reaction. Under the conditions of buffered TBAF, the 4-hydroxyl group was involved in stabilization of the transition state and took part in hydrogen bonding with cyclizing alkoxide *via* a boat-like transition state **177**, which resulted in the formation of the 2,6-*trans*-tetrahydropyran (Figure 8). In contrast, investigation of the acid mediated cyclization revealed that the molecule adopted a chair-like transition state **178** with *cis* product favoured supporting the results seen in the synthetic studies (Figure 8). Also, it worth noting that the 4-hydroxyl group did not participate in the *cis* selective cyclization.

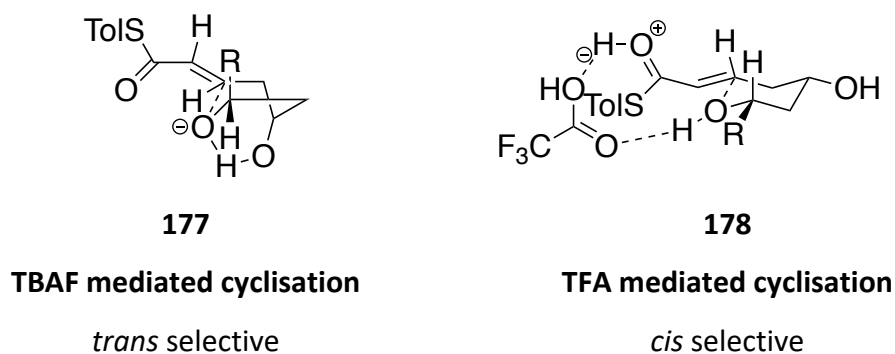
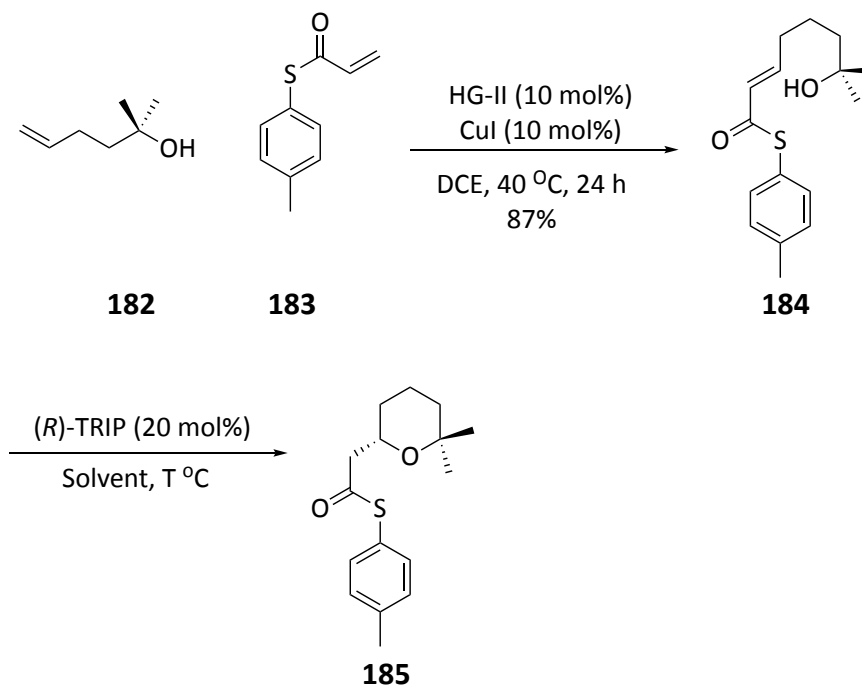


Figure 8. Computational transition states adopts for the stereodivergent oxa-Michael cyclization

In the *cis*-selective reaction, the trifluoroacetic acid served as proton shuttle. While the electrophilicity of the Michael acceptor increased as a result of protonation of the thioester, the nucleophilicity of the alcohol increased as a result of simultaneous deprotonation of the alcohol. Intriguingly, the oxaester's transition state energy was 7.6 kcal mol⁻¹ higher than that of the thioester, causing the oxaester's rate of cyclization to be significantly slower. This would then allow for a competing decomposition process to occur, resulting in the selection of the thioester over the oxaester with the acidic mediated cyclisation.

The synthesis of 2,2'-dimethyl alcohol **184** and its cyclization using (*R*)-TRIP as the chiral catalyst to form tetrahydropyran **185** was examined (Scheme 43). As the preliminary computational studies predicted the *S*-enantiomer, this was assumed to be the product stereochemistry until it was determined. The initial attempt of the cyclization of 2,2'-dimethyl alcohol was carried out at room temperature in DCM with (*R*)-TRIP resulted in a low conversion of 9% and almost racemic product with 3% ee (Table 1, entry 1). The cyclization was then attempted in less polar solvents like toluene and cyclohexane. The cyclization in toluene gave a very low conversion of 6% and racemic product (entry 2). Upon raising the temperature of the reaction to 50 °C and carrying the reaction in toluene, there was a marked improvement in both the conversion and ee which reached 30% and 13% respectively (entry 3). When toluene was replaced with cyclohexane, the conversion improved to 77%, however there was only a marginal improvement in the ee to 18% (entry 4).

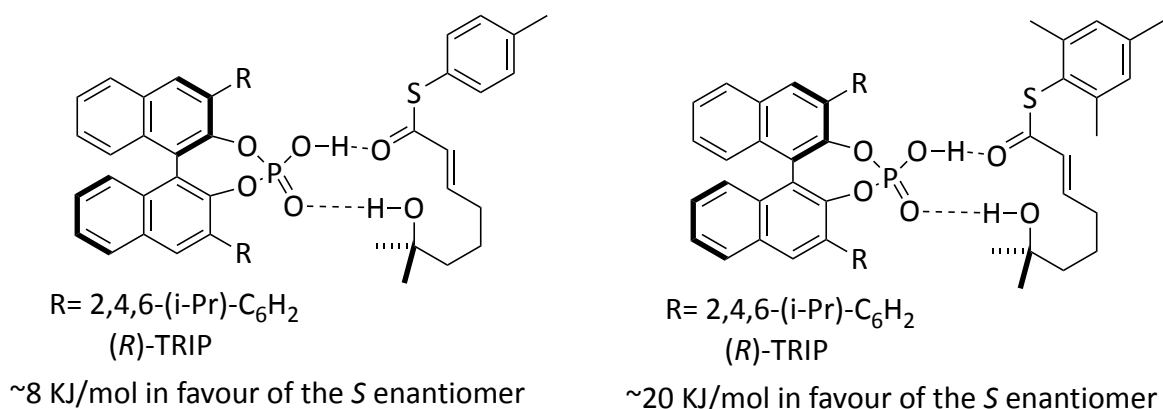


Scheme 43. Asymmetric Michael reaction for the synthesis of THPs

Entry	Solvent	T °C	Conversion %	ee %
1	DCM	rt	9	3
2	toluene	rt	6	-
3	toluene	50	30	13
4	cyclohexane	50	77	18

Table 1. Asymmetric Michael reaction for the synthesis of THPs

Preliminary computational work and DFT calculation of the chiral acid catalyzed oxa-Michael cyclisation showed that increasing the steric bulk of the substitution on the thioester increased the energy barrier between enantiomers from 8 KJ/mol to more than 20 KJ/mol favouring the *S* enantiomer, hence predicting an increase in the enantioselectivity of the product (Scheme 44).



Scheme 44. Preliminary computational work and DFT calculation of the chiral acid catalyzed oxa-Michael cyclisation

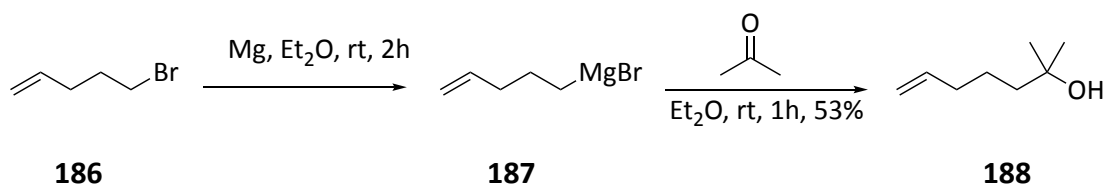
As a result of this earlier work, we can see that there is a correlation between substitution, the thioester and the enantioselectivity of the reaction. In light of this knowledge, together with the literature precedent left quite a few unanswered questions which we hoped to answer within our research project.

2.1.2 Synthesis of the Cyclization Precursors

To evaluate the asymmetric oxa-Michael reaction and validate its viability for the asymmetric synthesis of functionalized tetrahydropyrans, a number of questions needed to be addressed:

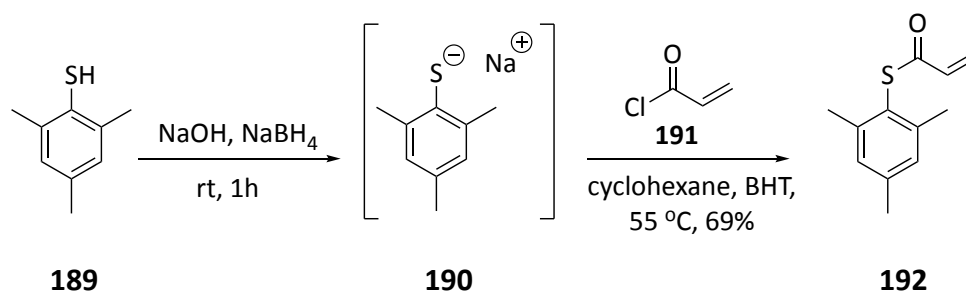
1. Does altering the reaction conditions such as, the catalyst, solvent, and temperature, have an impact on the yield or the selectivity of the reaction?
2. Does the presence of substitutions on the thioester confer any benefits during the course of the intramolecular oxa-Michael reaction in order to generate enantioenriched tetrahydropyrans?
3. What substrates and scopes can be utilised to test the scope and limitations of the reaction, and what kind of functionality can be incorporated into the products?

In order to get answers to these questions, the first step that needed to be achieved was to synthesise the 2,2'-dimethyl precursor that would make it possible to optimise the conditions of the reaction. The synthetic route to the cyclization precursor began with the synthesis of 2,2'-dimethyl alcohol which was adapted from literature procedure (Scheme 45).⁶⁹ The synthesis involved the initial generation of the Grignard reagent **187** by a metalation of a 4-bromobut-1-ene **186**, followed by the addition of acetone in anaerobic conditions to give the 2,2'-dimethyl alcohol **188** (Scheme 45). The reaction was quenched with a saturated NH₄Cl solution to protonate the alkoxide ion and the tertiary alcohol **188** was obtained in 53% yield (Scheme 45).



Scheme 45. Synthesis of 2,2-dimethyl alcohol

The subsequent precursor compound required to be synthesised was the thioacrylate which would function as intramolecular Michael acceptor. The synthesis of the mesityl thioacrylate, which showed the highest selectivity in preliminary computational work, was attempted using the procedure adopted by Fuwa (Scheme 46).⁹ The synthesis began with the deprotonation of thiol **189** in a solution of NaOH(aq)\NaBH₄ to generate the thiolate anion **190**, which makes it a harder nucleophile and less prone to react at the soft β position of the acryloyl chloride. To this, a solution of acryloyl chloride **191** in cyclohexane, containing the additive butylated hydroxytoluene (BHT), was added to react with the thiolate in a nucleophilic addition reaction. The addition of both NaBH₄ and BHT was to reduce any disulfide formed in the starting material and to prevent radical polymerisation of both acryloyl chloride and the product respectively. Upon column chromatography, **192** was afforded in 69% yield (Scheme 46).



Scheme 46. Synthesis of mesityl thioacrylate **192**

Following the acquisition of the alcohol **188** and thioacrylate **192**, the subsequent step involved the formation of the Michael acceptor required for cyclization *via* cross metathesis. The group has previously been successful in performing cross metathesis with the relevant thioacrylate⁷⁰; nevertheless, the use of acrylates in metathesis reaction can lead to a number of complications. This is because if both cross metathesis candidates are of similar reactivity and used in similar amounts, in a purely statistical mixture of products can be expected. This can be alleviated by the use of multiple equivalents of the more accessible olefin. According to a report by Grubbs, olefins can be classified depending on the levels of homodimerization that are observed and the reactivity of the homodimer

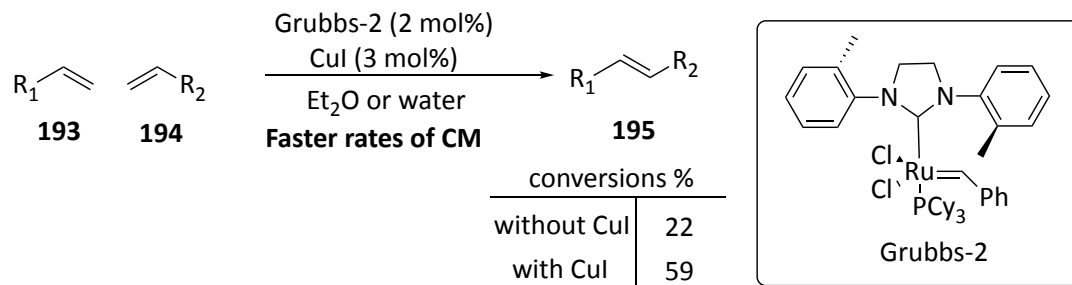
when they are subjected to a variety of metathesis catalysts (Table 2).⁷¹ Acrylates are classified as a Type II olefin, which indicates that their homodimerization proceeds more slowly when they are exposed to a second generation Grubbs catalyst. Even though the homodimerization of the alcohol containing alkene happens very quickly, the homodimer itself is still a candidate for metathesis. This is because it can then undergo a subsequent reaction with the acrylate, which reacts more slowly, to generate the desired cross metathesis product.

Olefin Type	Example
Type I (fast homodimerization)	Terminal olefins, allylic alcohols, esters, allyl boronate esters, allyl halides, styrenes (no large ortho substit.), allyl silanes, protected allyl amines
Type II (slow homodimerization)	styrenes (large ortho substit.), acrylates, acrylamides, acrylic acid, acrolein, vinyl ketones
Type III (no homodimerization)	1,1-disubstituted olefins, non-bulky tri-sub. olefins, vinyl phosphonates

Table 2. Olefins categories for selective cross metathesis

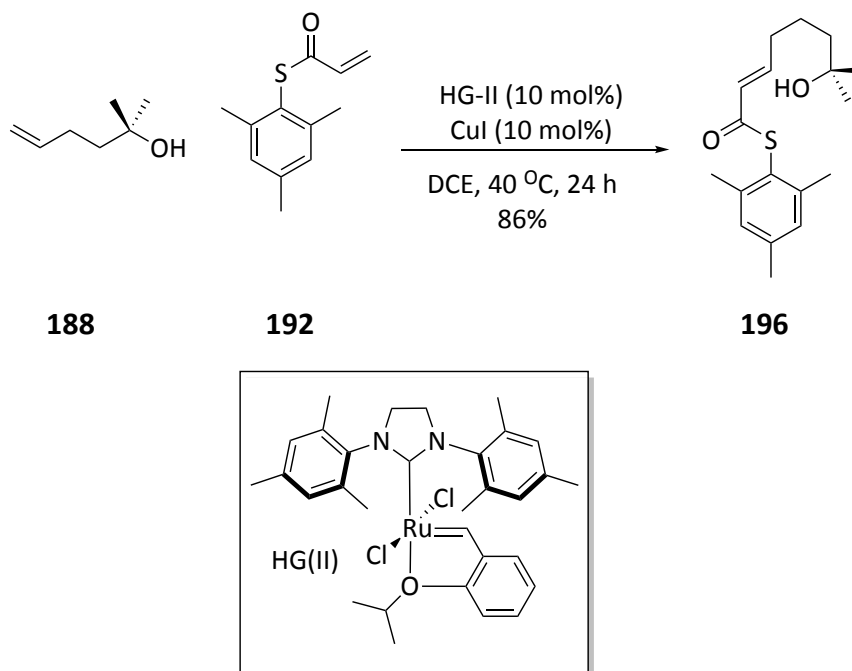
Quantification of the reagents and conditions established within the Clarke group serve as the foundation of the standard approach for our cross metathesis reaction utilising a Ru-based phosphine free Hoveyda-Grubbs 2nd Generation catalyst that was initially synthesised by Hoveyda and co-workers.^{67,72} This involved the use of 3.0 equivalent of thioester **192**, low Ru-catalyst loading (10 mol%) and CuI (10 mol%) as co-catalyst for the ‘Copper-Iodide Effect’.⁷³ This effect as first reported by Lipshtuz, who demonstrated that the addition of copper iodide in conjunction with Grubbs catalyst led to an increase in the coupling rate of acrylates with other olefins (Scheme 47).⁷³ The stabilizing impact of the

iodide ion on the catalyst was cited as the cause as it increased the catalyst's overall reactivity.

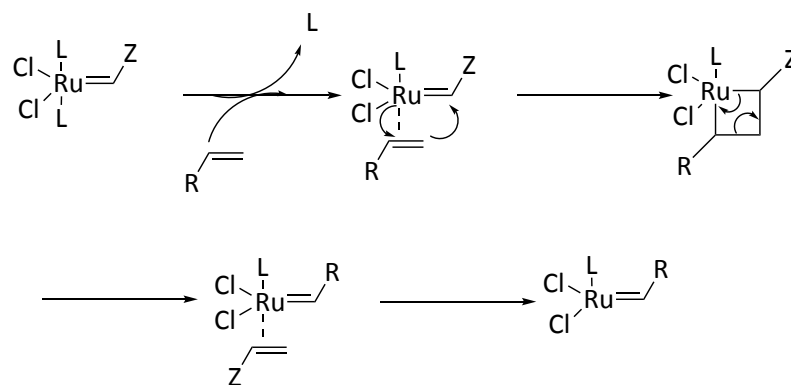


Scheme 47. Lipshutz's cross metathesis reaction in the presence of CuI

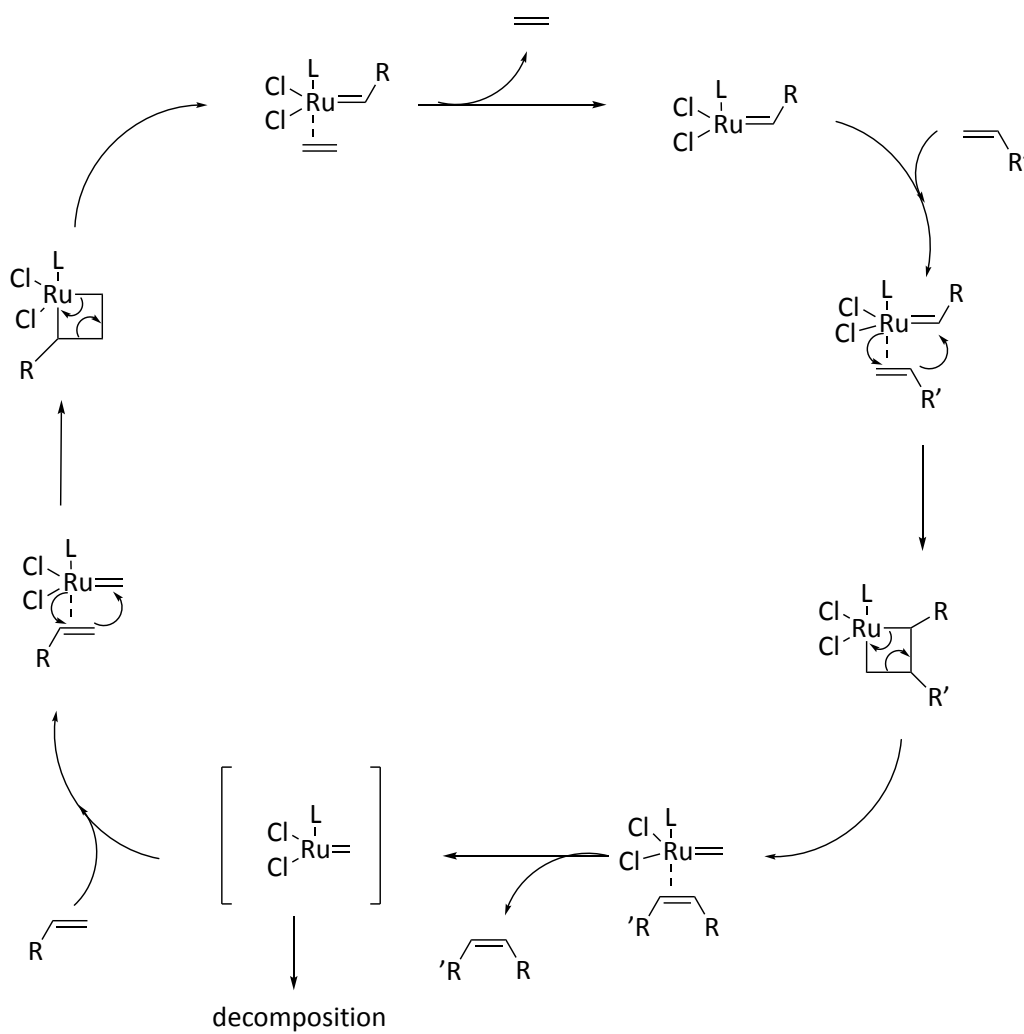
It was also proposed that copper (I) has the ability to scavenge the phosphine ligand, however this mode of action would not apply to our reaction conditions as Hoveyda-Grubbs 2nd generation catalyst does not have a phosphine ligand. To this end, the thioester **192** and 2,2'-dimethyl alcohol **188** were "clipped" together *via* an olefin cross metathesis reaction, and the best turnover of the metathesis product **196** occurred when the reaction was carried out in DCE at 40 °C resulting in 86% yield (Scheme 48).



Scheme 48. Cross-metathesis reaction for the cyclization precursor **196**



Scheme 49. Mechanism of olefin metathesis initiation



Scheme 50. The catalytic cycle of olefin metathesis

The proposed reaction mechanism proceeds *via* the Chauvin catalytic cycle.⁷⁴ Whereby the pre-catalyst undergoes ligand dissociation from the metal centre, followed by coordination of the alkene to form a metallacyclobutane in a cycloaddition reaction (Scheme 49). The metallacyclobutane then cycloreverts to release the initial carbene ligand and form the active 14 e⁻ complex. In a productive cross-metathesis, a different alkene then adds to the activated complex to form the metallacyclobutane ring (Scheme 50). The metalocycle then cycloeliminates to form the desired metathesis product and ethene as a by-product.

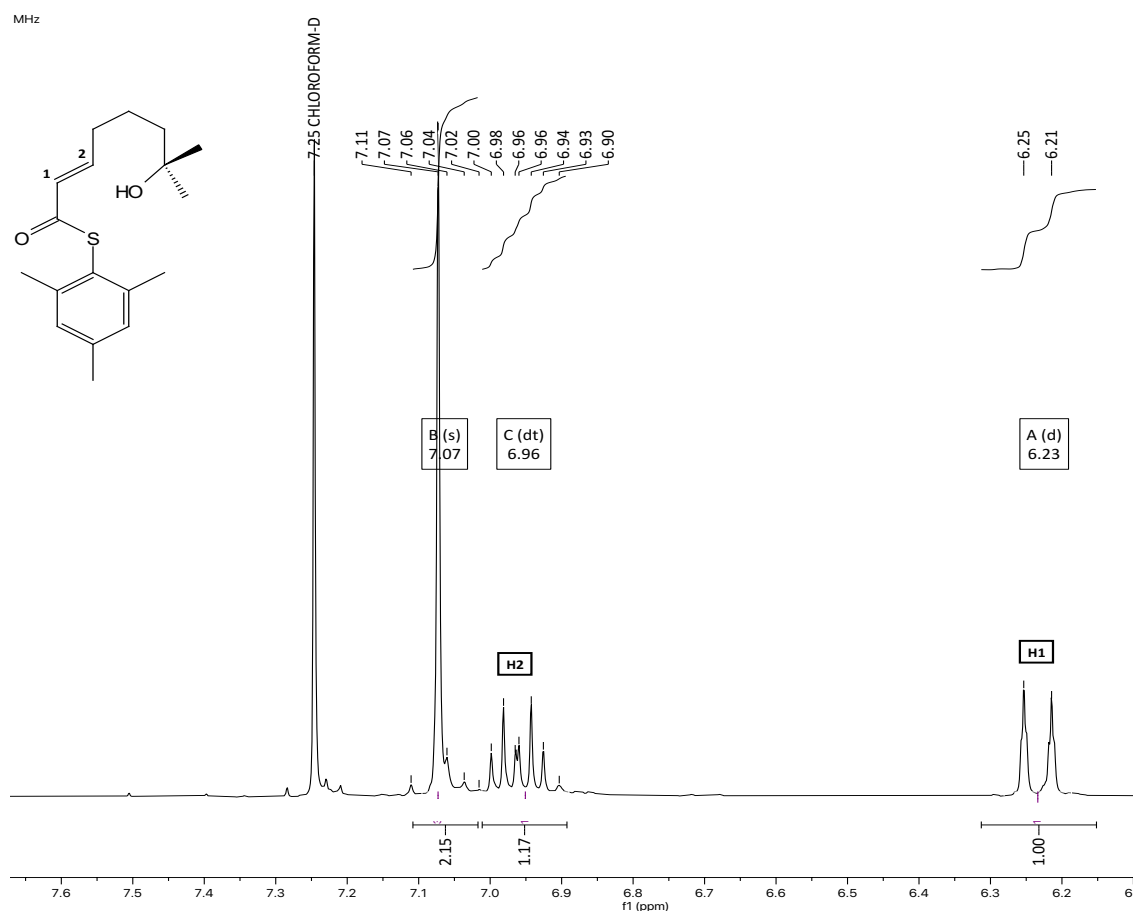


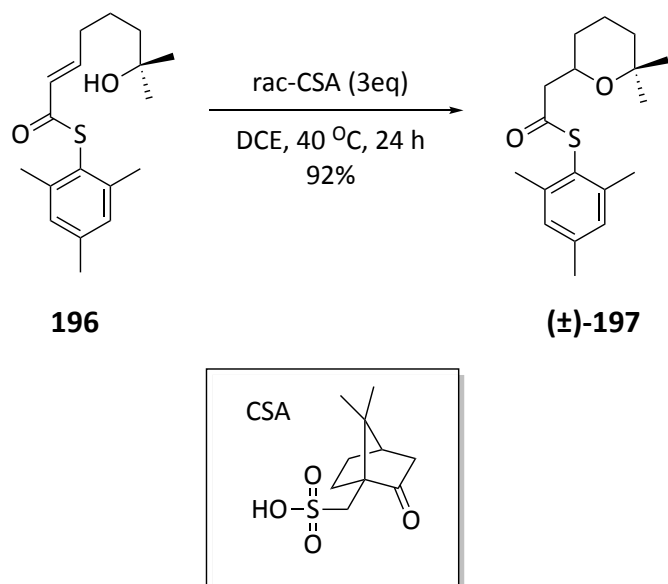
Figure 9. ¹H NMR of **196** shows the signals of the α and β -protons in the alkene region.

The formation of the *trans* double bond is usually favoured under thermodynamic control as it has lower energy than the *cis* counterpart.⁷⁵ The formation of *trans* product

was observed in our 'clip' reaction and that confirmed by the *J*-coupling value of the alkene proton in the ¹H NMR (Figure 9). The α- proton H-1 produced a doublet (d) signal at 6.23 ppm and coupled with the adjacent β-proton H-2 with a high ³*J*-coupling constant of 15.7 Hz, which corresponding to *trans*-alkene coupling. The β-proton H-2 gave rise to a dt signal at 6.96 ppm and this was due to the coupling with α- proton H-1 and the CH₂ protons with ³*J*-coupling constants of 15.7 and 6.8 Hz respectively.

2.1.3 Brønsted Acid Catalysed Cyclization

With the synthesis of the cyclization precursor **196** complete, we were in a position to close the tetrahydropyran ring using the Brønsted acid catalysed cyclization. In order to determine an enantiomeric ratio, a racemic standard was required to properly assign the peaks that represent both enantiomers. To do this, a cyclization reaction was carried out using an excess of racemic (±)-camphorsulfonic acid (rac-CSA) in DCE at 40 °C. As a result, racemic 2,2'-dimethyl THP **197** was isolated with a yield of 92% (Scheme 51).



Scheme 51. Cyclization of 2,2'-dimethyl substrate **196** to give racemic **197**

The assignment of the ^1H NMR of **197** is shown in Figure 10 which was arrived at using 1-D and 2-D NMR. The proton of the stereocenter H-9 that formed after cyclization appeared as dddd peak at 4.06 ppm ($J = 11.4$ Hz, 7.8 Hz, 5.0 Hz, 2.7 Hz) with corresponding carbon peak at 68.3 ppm confirmed by the HMQC spectrum shown in Figure 11. On the other hand, the two protons on C-8 (50.7 ppm) appeared as two dd peaks at 2.79 ppm ($J = 14.2$ Hz, 7.8 Hz) and 2.61 ppm ($J = 14.2$ Hz, 5.0 Hz) respectively as shown in the HMQC spectrum. This was confirmed by the COSY spectrum in Figure 12 which showed the H-H coupling of the H-8 and H-8' with each other and also with H-9.

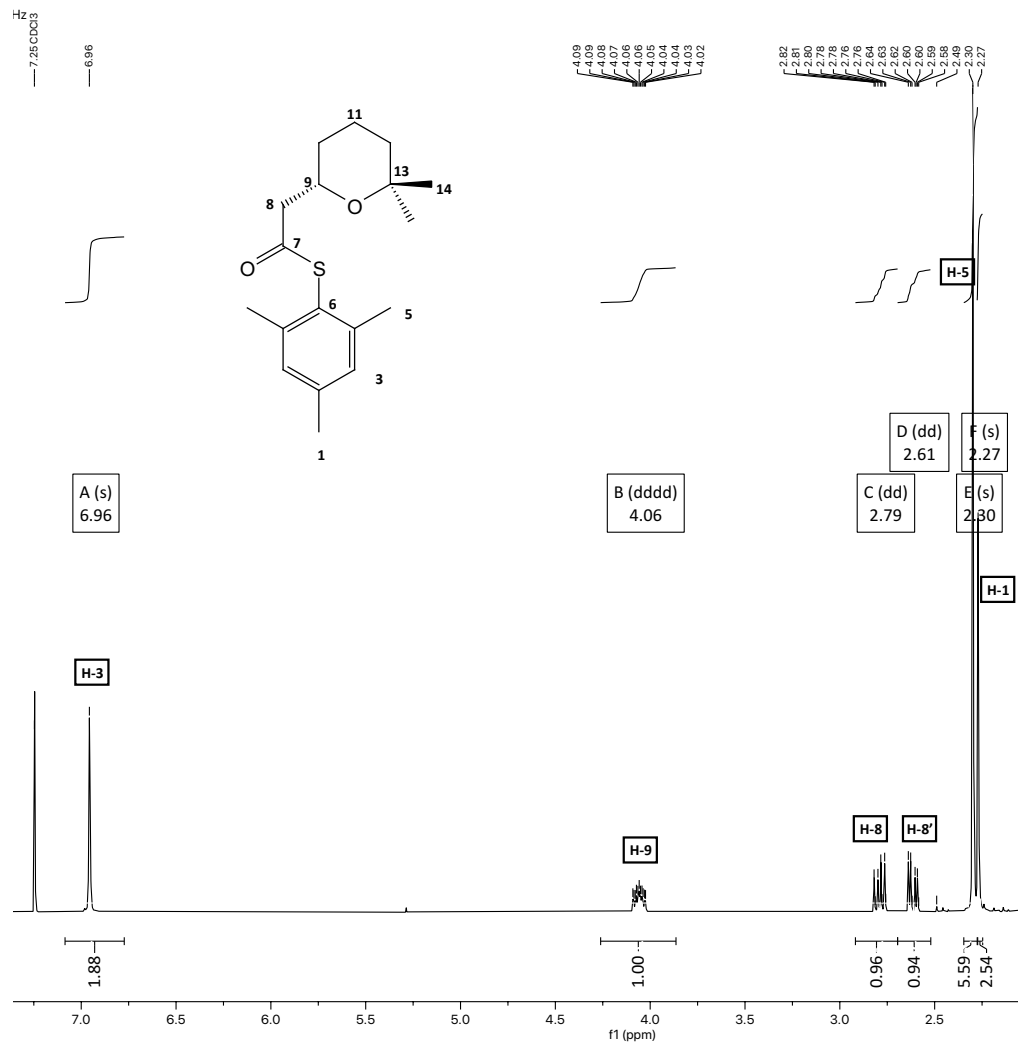


Figure 10. ^1H NMR of **197**

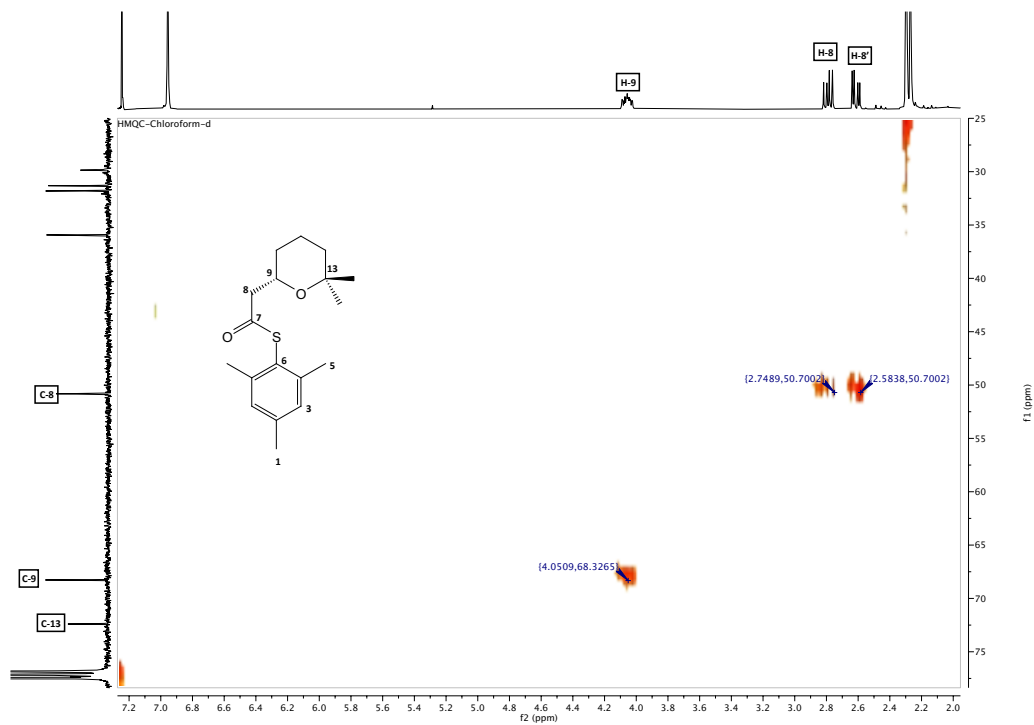


Figure 11. HMQC spectrum showing C-8 and C-9 with respective protons in **197**

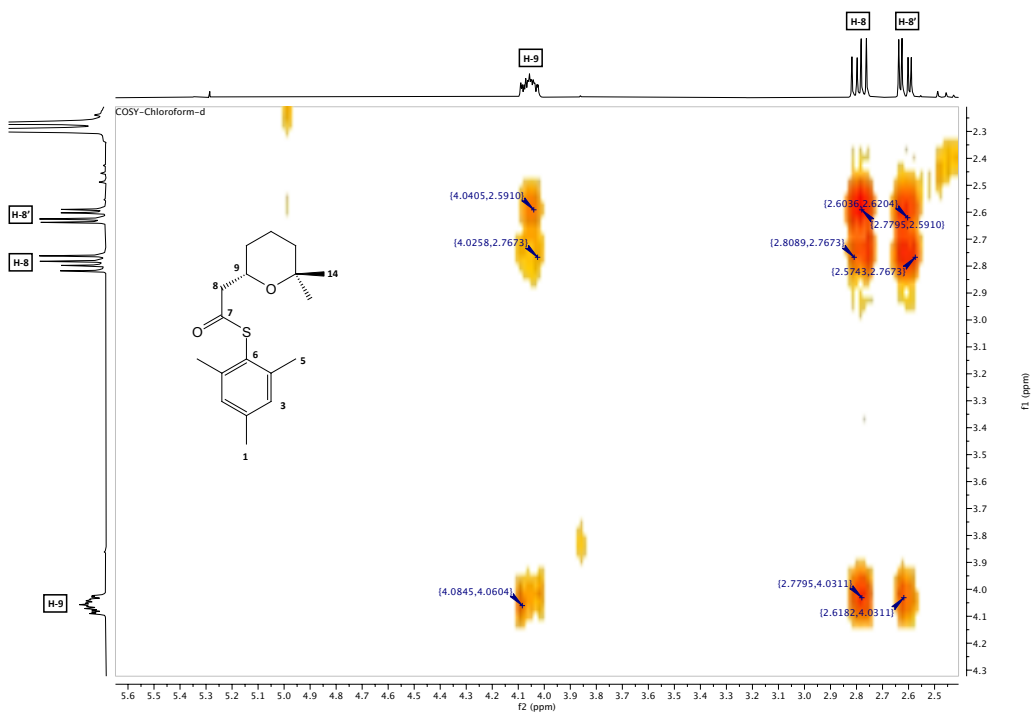


Figure 12. COSY spectrum showing correlation between H-8, H-8', and H-9 in **197**

The reaction led to the formation of a new stereogenic centre forming two enantiomers (*R*) and (*S*). Enantiomers have the same physical properties and differ by their ability to rotate plane polarised light. Therefore, the two commonly used methods to distinguish between a pair of enantiomers is polarimetry or chiral-HPLC methods. Using chiral-HPLC columns allowed us to precisely determine the enantiomeric ratio of the two enantiomers and hence the % ee, therefore different conditions could be screened. The IA, IB, IC, IG, and AD-H immobilised polysaccharide columns were used in the initial screening process. Various organic selector molecules are attached to the sugar in the polysaccharide stationary phase (either amylose or cellulose). This allows for resolution of the sample immobilized chiral mixture, as different interactions between the two enantiomers and the selectors enable the separation of the mixture. During the process of developing the separation method, it was found that altering the chiral column had the greatest impact on enhancing the resolution of the mixture. Adjusting solvent ratios (hexane\IPA), flow rate or temperature, on the other hand, allowed some control over resolution. Following the screening of conditions, the CHIRALPAK AD-H column eluting with hexane/2-propanol (98:2) at flow rate of 1.0 ml/min at a temperature of 25 °C was found to separate the two enantiomers within 30 min (Figure 13). As expected, we observed two peaks in the HPLC with a retention time of 24.77 min and 29.6 min. The fact that the integrated area of both peaks showed a 50:50 ratio confirming that rac-CSA did indeed produced a racemic mixture.

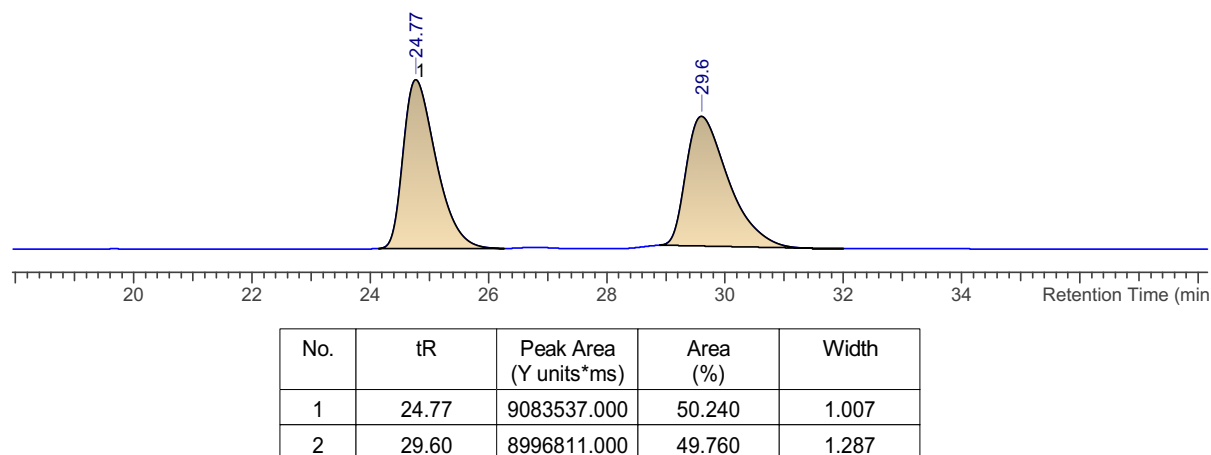
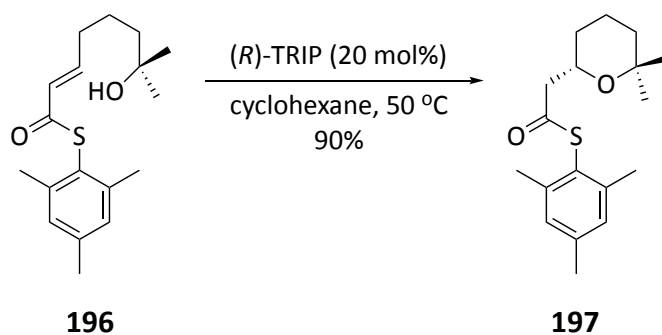


Figure 13. HPLC chromatogram of the synthesised THP 197 with rac-CSA

Having been able to successfully complete the synthesis of the racemic THP, we proceeded with the asymmetric reactions. The initial cyclization was carried out under the same conditions that had previously been used successfully used within the group for the synthesis of substituted piperidines⁷⁰, namely (*R*)-TRIP in cyclohexane at 50 °C (Scheme 52). The crude residue was then analysed by ¹H NMR spectroscopy (Figure 14).



Scheme 52. Cyclization of 2,2'-dimethyl substrate with (*R*)-TRIP

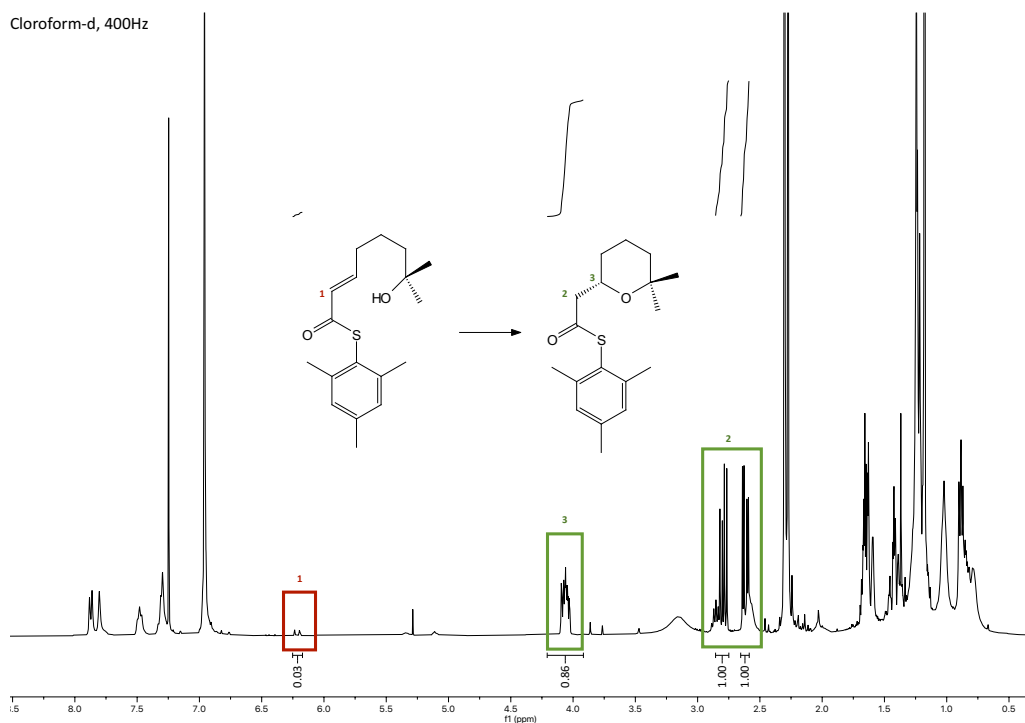


Figure 14. ¹H NMR of the crude produced from asymmetric reaction of **197** using (*R*)-TRIP

Product formation was confirmed using two distinct traits of the NMR spectrum which are highlighted in green. Firstly, the signals that represent the proton of the stereocentre H-3 observed as a dddd at 4.05 ppm ($J = 11.4$ Hz, 7.8 Hz, 5.0 Hz, 2.7 Hz). Secondly, the dd signals of H-2 and H2' observed at 2.86 ($J = 14.2$ Hz, 7.8 Hz) and 2.60 ppm ($J = 14.2$ Hz, 5.0 Hz) respectively that represent the α -protons. Conversion was calculated to be 97% using the integral of peaks from unreacted cyclization precursor H-1 observed at 6.23 ppm, which highlighted in red, and the peaks of the product that are highlighted in green at either 4.05, 2.86, or 2.60 ppm (Figure 14).

With the developed HPLC method that were used with the racemic product, the enantioselectivity of the asymmetric product could be determined. Submission of the product of the (*R*)-TRIP cyclised reaction **197** to HPLC analysis gave the chromatogram depicted in Figure 15 with the major peak having a retention time of 24.88 mins while the minor peak observed at 30.46 mins. Enantiomeric excess (% ee) was calculated from the integrated area under the observed peaks that represent both enantiomers as follow: $[(\text{major} - \text{minor}) / (\text{major} + \text{minor})] \times 100$ and it was encouraging to see enantioselectivity of 69%.

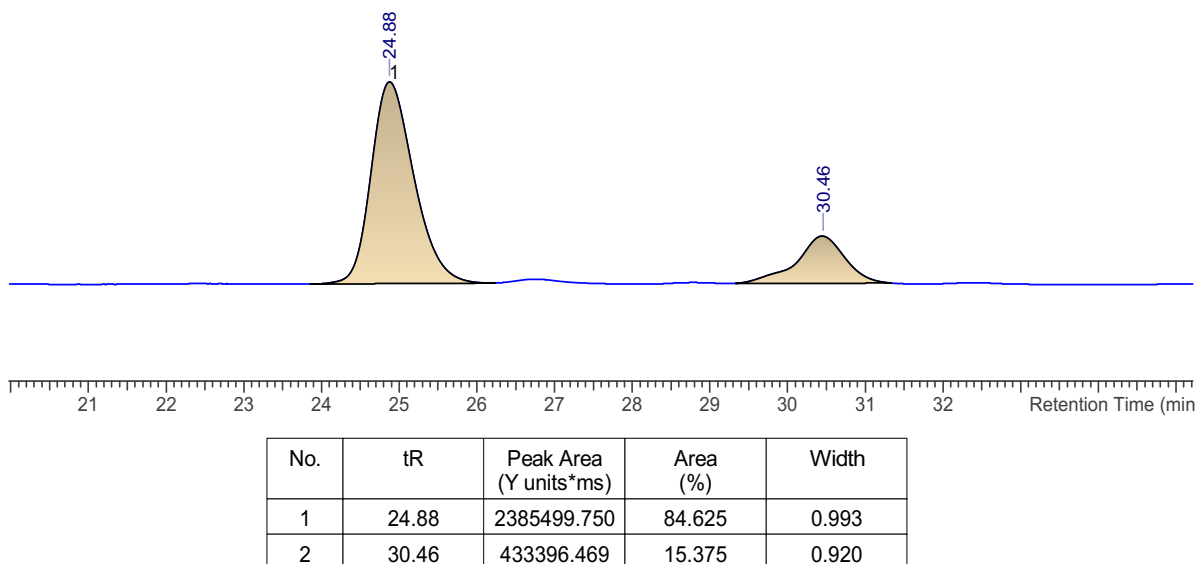


Figure 15. HPLC chromatogram of the synthesised THP **197** with (*R*)-TRIP

Preliminary DFT calculations based on the energy differences between the enantiomers indicated that the major enantiomer was predicted to be S at expected 77% ee with mesityl thioester, (*R*)-TRIP catalyst at 50 °C. At the same conditions, the experimental enantioselectivity found to be 69% which showed a good correlation with the computational studies.

Using mesityl thioester as the activating group did increase the enantioselectivity to 69% as compared with 18% ee obtained from tolyl thioester, however, there was potentially room for improvement if conditions were modified. Therefore, our next step were focused on improving the enantioselectivities while maintaining high conversions.

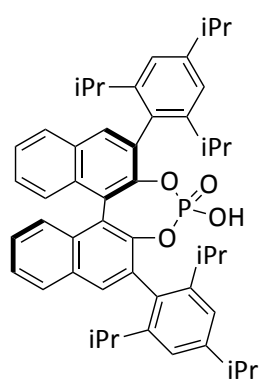
2.1.4 Optimization of the Reaction Conditions

In order to facilitate the screening process and optimisation of conditions, there were four parameters, namely temperature, time, solvent, and catalyst, that could be easily altered without requiring the substrate to be modified. In order to improve both the reaction conversion and enantioselectivity, we decided to change each of these parameters in turn and observe the reaction outcomes.

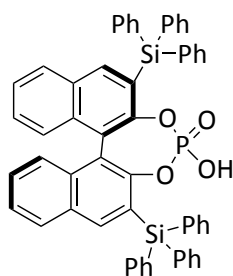
Previous work within the group showed that the use of low polarity solvent such as cyclohexane were best, presumably as they do not interact with the catalyst. However, there may be difficulties associated with the solubility of more polar substrates in cyclohexane, particularly at lower temperatures. As a result, toluene and DCE were chosen as alternative solvents for the screening process as they have higher boiling points (110 °C and 84 °C, respectively) and may be more able to solubilise substrate and catalyst.

Due to these two primary considerations, the selection of chiral catalysts was dependent on how readily available they were in the commercial market. First, it allows for rapid testing of conditions, which is important because CPA catalysts need to be made through a multistep synthesis. Second, it would be more viable in both research and industrial contexts if the catalyst can be acquired from a chemical supplier. In order to

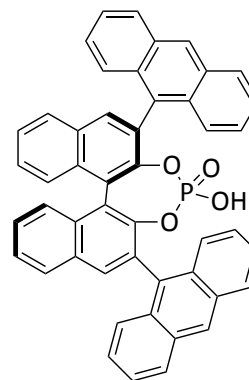
accomplish this goal, the catalyst that were chosen were (*R*)-TRIP **199**, (*R*)-TIPSY **200**, (*R*)-Anth **201**, (*R*)-phenanth **202**, (*R*)-VAPOL **203**, and (*R*)-SPINOL **204**, as illustrated in Figure 16.



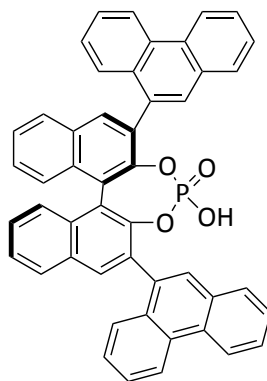
(*R*)-TRIP
199



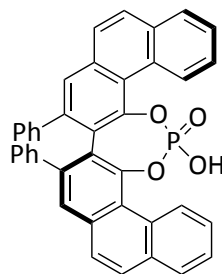
(*R*)-TIPSY
200



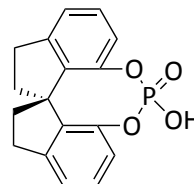
(*R*)-Anth
201



(*R*)-Phenanth
202

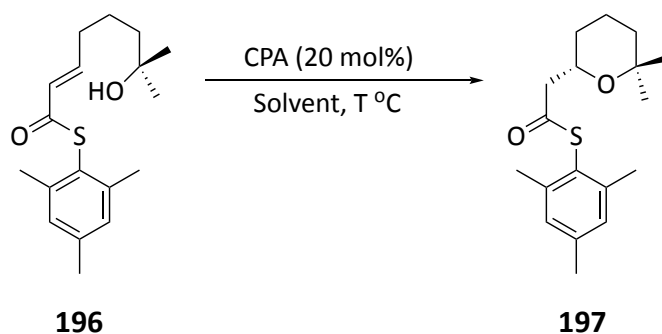


(*R*)-VAPOL
203



(*R*)-SPINOL
204

Figure 16. Structure of chiral phosphoric acid catalysts used in reaction screening



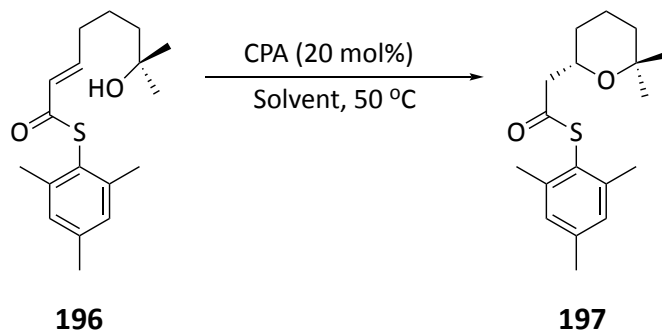
Scheme 53. Asymmetric Michael reaction for the synthesis of THPs

Entry	Solvent	Temperature °C	CPA	Conversion %	ee %
1	Cyclohexane	50	(<i>R</i>)-TRIP	97	69
2	Cyclohexane	rt	(<i>R</i>)-TRIP	20	44
3	Cyclohexane	75	(<i>R</i>)-TRIP	100	66
4	Toluene	rt	(<i>R</i>)-TRIP	10	10
5	Toluene	50	(<i>R</i>)-TRIP	69	60
6	Toluene	75	(<i>R</i>)-TRIP	97	61
7	DCE	rt	(<i>R</i>)-TRIP	6	9

Table 3. Conditions screening for the synthesis of THPs

Initial screening was done by variation of the solvent and the temperature of the reaction. The data in Table 3, entry 1 shows the already tested conditions of cyclohexane, (*R*)-TRIP at 50 °C for 24 hours, which gave conversion of 97% and 69% ee. When the temperature was lowered to room temperature (entry 2), a drastic fall in the conversion to 20% was observed while the enantioselectivity dropped to 44%. The decrease of the conversion at lower temperature was not surprising as the rate of the reaction would also be expected to drop. On the other hand, when the reaction exposed to higher temperature (75 °C), a quantitative conversion was observed but with slightly drop of the enantioselectivity to 66% (entry 3). To screen the different solvents in the reaction, the catalyst remained unchanged but different temperatures were used. Lowering the

temperature would allow for easier comparison of the effect of solvent on both conversion and enantioselectivity. If any significant increase in yield was observed by varying the solvent, it would be more noticeable when increasing the conversion from 20 % at room temperature than when increasing from either 96% at 50 °C or 100% at 75 °C. As can be seen by comparison Table 2, entries 2, 4, and 7, the effect of solvent had a significant impact on both the reaction conversion and enantioselectivity. Cyclohexane at room temperature gave a conversion of 20% and enantioselectivity of 69%, while both toluene and DCE showed a drop of the conversion to 10% and 6% and the enantioselectivity to 10% and 9% respectively. Running the reaction with toluene at either 50 °C or 75 °C did not improve both the reaction conversion and the enantioselectivity.



Scheme 54. Asymmetric Michael reaction for the synthesis of THPs

Entry	Solvent	CPA	Conversion %	ee %
1	Cyclohexane	(<i>R</i>)-TRIP	96	69
2	Cyclohexane	(<i>R</i>)-TIPSY	23	40
3	Cyclohexane	(<i>R</i>)-Phenanth	3	2
4	Toluene	(<i>R</i>)-Phenanth	6	12
5	Cyclohexane	(<i>R</i>)-Anth	96	21
6	Cyclohexane	(<i>R</i>)-VAPOL	79	0
7	Cyclohexane	(<i>R</i>)-SPINOL	85	0

Table 4. Conditions screening for the synthesis of THPs

Cyclohexane at 50 °C appeared to be the ideal conditions for the reaction to achieve high conversions, however, variations in these conditions did not seem to have a significant effect on the enantioselectivity. Therefore, it appeared that the only way to influence enantioselectivity would be through catalyst selection. Catalyst screen (Table 4, entry 2) showed moderate enantioselectivity for (*R*)-TIPSY (40%) but low conversion of 23%. (*R*)-Phenanth seemed to have solubility issues in cyclohexane, giving very poor conversion of 3% and rendering the product essentially racemic (entry 3). Upon replacing cyclohexane with toluene, a marginal improvement was observed in both conversion and enantioselectivity (entry 4). Catalysts (*R*)-Anth, (*R*)-VAPOL, and (*R*)-SPINOL gave the product with 79 to 96% conversions (entries 5, 6, and 7). In the case of enantioselectivity, (*R*)-anth gave the product in 21% ee while both (*R*)-VAPOL and (*R*)-SPINOL rendering the product racemic.

In another attempt to improve the enantioselectivity of the reaction, the nature of the thioester group on the substrate was examined. Based on the previous DFT calculations of both tolyl **207** and mesityl **208** thioester, it was found that increasing the steric bulk of the thioester group would enable us to obtain the substituted THPs with higher enantioselectivities (Figure 17). To this end, it was assumed that increasing the steric bulk of the substitution on the thioester, such as iso-propyl (*i*-Pr) **209**, would increase the enantioselectivity of the reaction further.

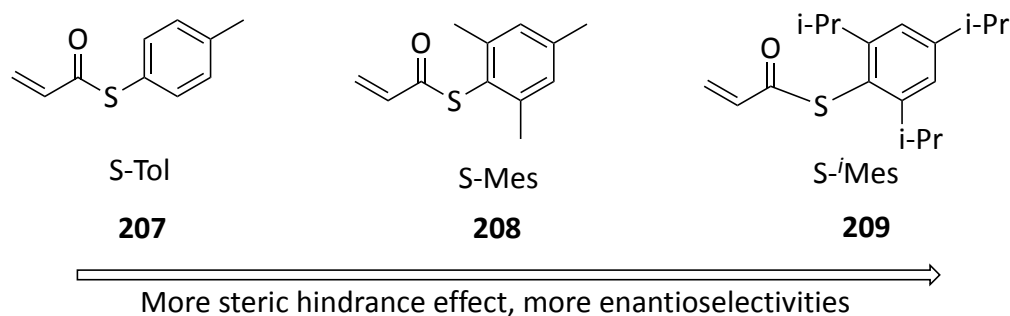
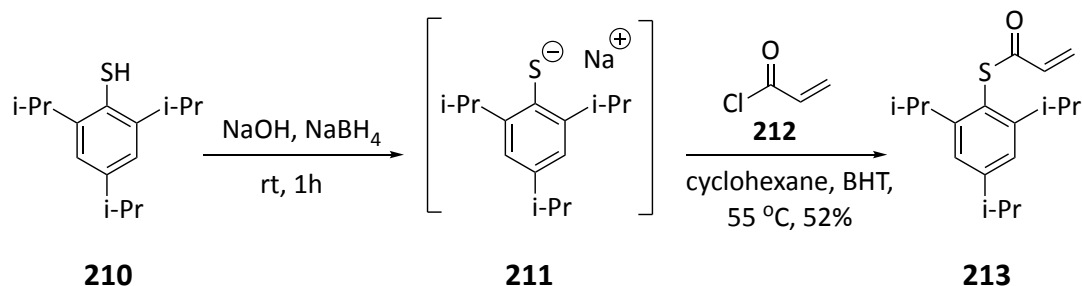


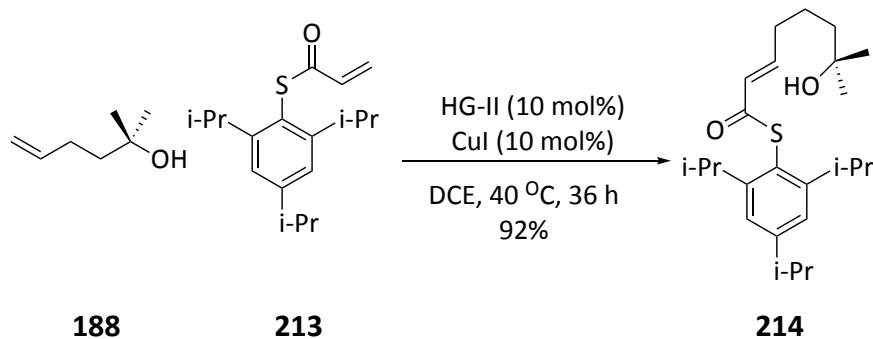
Figure 17. The effect of the nature of the thioester on the enantioselectivity of the reaction

In order to confirm our hypothesis, synthesis of triisopropyl thioacrylate **213** and then the cyclization precursors **214** was first attempted. Mirroring the synthesis of mesityl thioacrylate **192**, the triisopropyl thioacrylate **213** was synthesized from 2,4,6-triisopropylthiophenol **210** to give the product in 52% yield (Scheme 55).



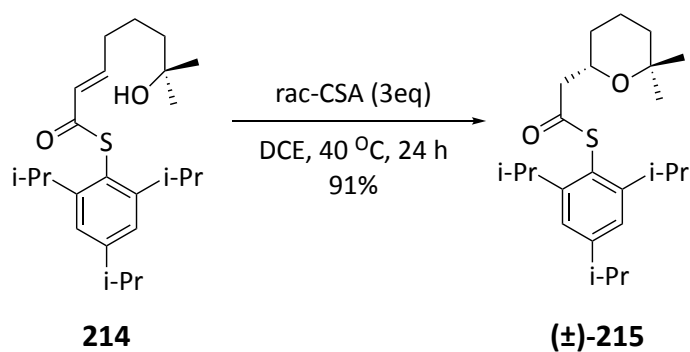
Scheme 55. Synthesis of triisopropyl thioacrylate **213**

The newly formed triisopropyl thioacrylate **213** could be then coupled to the 2,2-dimethyl alcohol **188** under the metathesis conditions (Scheme 56). It was found that cross metathesis reaction for **214** required 30 h for the starting material to be consumed completely by TLC with a quantitative conversion compared to the mesityl product **205** and afforded the product **214** in excellent yield (92%).



Scheme 56. Cross-metathesis reaction for the cyclization precursor **214**

Upon isolation of the pure **214**, the cyclization with CSA was carried out to optimize the HPLC condition and separate the two enantiomers (Scheme 57). Different HPLC conditions were investigated to achieve the best separation of the two enantiomers. The CHIRALPAK IA column eluting with hexane/2-propanol (99:1) at flow rate of 0.6 ml/min at a temperature of 40 °C was found to separate the two enantiomers in a short time (Figure 18). As expected, we observed two peaks in the HPLC with a retention time of 6.95 min and 9.88 min. The fact that the integrated area of both peaks showed a 50:50 ratio confirming that rac-CSA did indeed produced a racemic mixture.



Scheme 57. Cyclization to give racemic 2,2'-dimethyl THP **215**

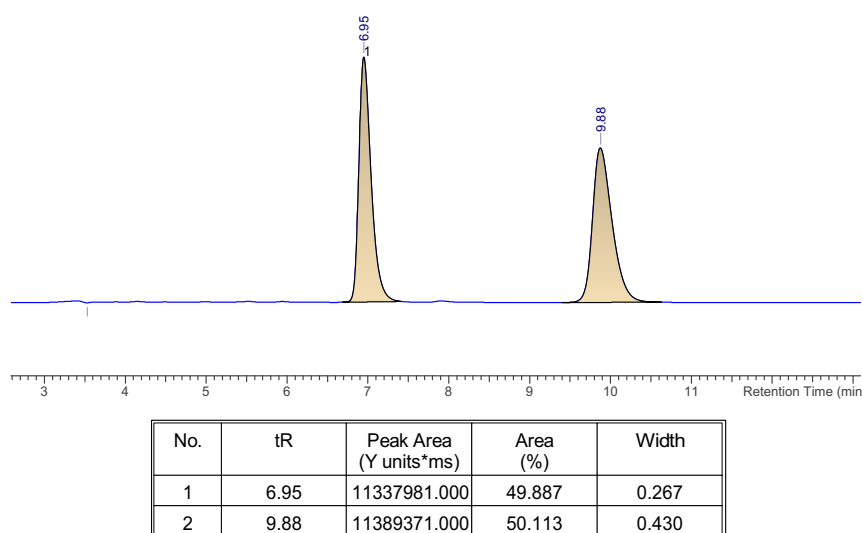
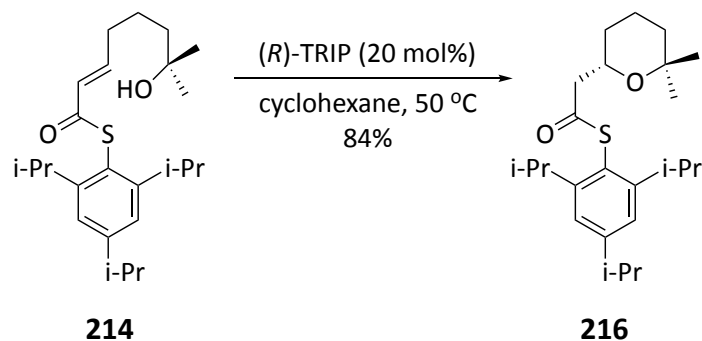


Figure 18. HPLC chromatogram of the synthesised THP **215** with rac-CSA

Using this HPLC method, it was possible to ascertain the enantiomer ratio and hence the enantioselectivity of the asymmetric reaction. Therefore, the asymmetric cyclization with chiral phosphoric acid, (*R*)-TRIP, in cyclohexane at 50 °C was attempted and the cyclized product **216** was obtained in 84% yield (Scheme 58).



Scheme 58. Cyclization of 2,2'-dimethyl THP **216** with (*R*)-TRIP

Submitting the asymmetric product **216** of the (*R*)-TRIP reaction to HPLC analysis gave the chromatogram depicted in Figure 19. This chromatogram showed that the major peak had a retention time of 6.82 min, while the minor peak had a retention time of 9.63 min. The enantioselectivity was determined to be 98% after the peaks were integrated.

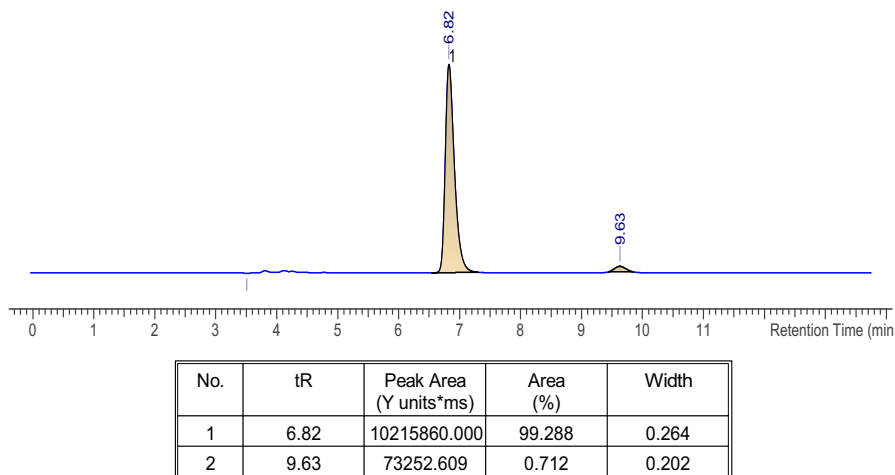


Figure 19. HPLC chromatogram of the synthesised THP **216** with (*R*)-TRIP

After obtaining such encouraging results, the following step was to extend the substrate scope of the reaction and to determine whether or not the cyclization conditions were universal for other substituents at the 2,2'-position.

2.2 Substrate Scope of 'Clip-Cycle' Reaction

2.2.1 Scope of the reaction for 2,2'-disubstitution

The geminal di-methyl substitution provided a simple and straightforward substrate for the purpose of optimising the reaction conditions. However, modifying the substitution at the 2-position could have the potential to provide a higher level of synthetic complexity and reveal the boundaries of the reaction.

In 2009, Lovering introduced the concept of "escape from flatland" and brought to light the fact that a prevalent number of molecules within compound libraries that were utilised in High Throughput Screening (HTS) were contained sp^2 carbons and were consequently composed of 2-dimensional 'flat' structures.⁷⁶ If the diversity of libraries were increased to include more 3-dimensional structures, such as molecules rich in sp^3 -carbons, drug development programmes would have access to a wider range of the chemical universe. Therefore, because of the 3-dimensional nature of drug targets, it was suggested that the incorporation of molecules with sp^3 -rich carbons would lead to a greater number potential hits with higher selectivity for drug targets. To this end, the formation of spirocycles allows for an increase the amount of three dimensionality, or sp^3 character, of a molecule and consequently, identifying potential compounds that move away from the more common sp and sp^2 rich systems seen in the majority of "lead-like" molecules.⁷⁷ Therefore, the introduction of spirocyclic functionality to the tetrahydropyran was investigated.

To synthesise the spirocyclic compounds, the process that was employed in the production of the 2,2'-geminal dimethyl substrate was used with only slight alterations

being necessary. To modify the 2,2'-substitution, a variety of cycloketones as well as non-cyclic ketones like diphenyl ketone and ketomalonate were chosen to test how well they were tolerated in the cyclization reaction (Figure 20).

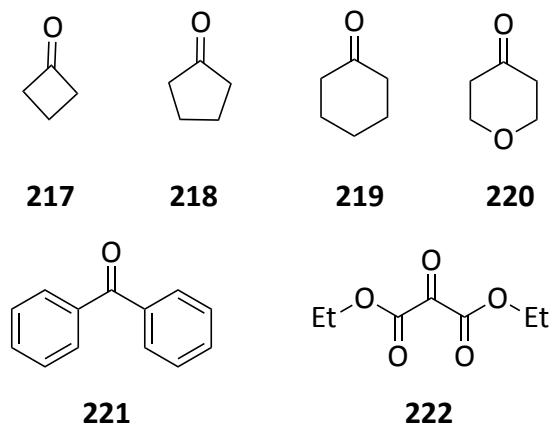
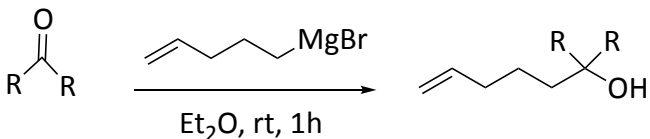


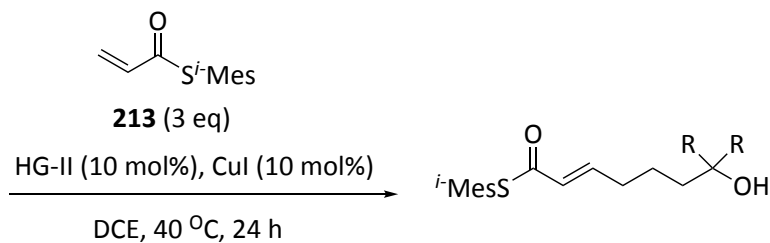
Figure 20. ketones selected to test 2,2'-substituted scope

In a manner similar to the dimethyl precursor, ketones were alkylated *via* Grignard reaction with metallated 4-bromobut-1-ene to afford the corresponding alcohols in good to excellent yields. The resultant tertiary alcohols were then “clipped” with isopropyl thioacrylate **213** *via* alkene metathesis using HG-II and CuI (Scheme 59). It was discovered that subjecting alcohol **232** to the metathesis conditions at 40 °C resulted in the formation of the cyclized product instead with 71% yield. However, by lowering the reaction temperature to room temperature, we were able to obtain the cyclization precursor **238** in 82% yield within 36 hours. Furthermore, carrying out the metathesis reaction of **233** led to the formation of the dimer product instead with 67% yield. To overcome this, the reaction was carried out at 60 °C and also another portion of HG-II catalyst was added which led to successfully obtaining the metathesis product **239** in excellent yield.



223: R = cyclobutyl
224: R = cyclopentyl
225: R = cyclohexyl
226: R = THP
227: R = phenyl
228: R = CO₂Et

229: R = cyclobutyl, 81%
230: R = cyclopentyl, 79%
231: R = cyclohexyl, 57%
232: R = THP, 67%
233: R = phenyl, 72%
234: R = CO₂Et, 61%



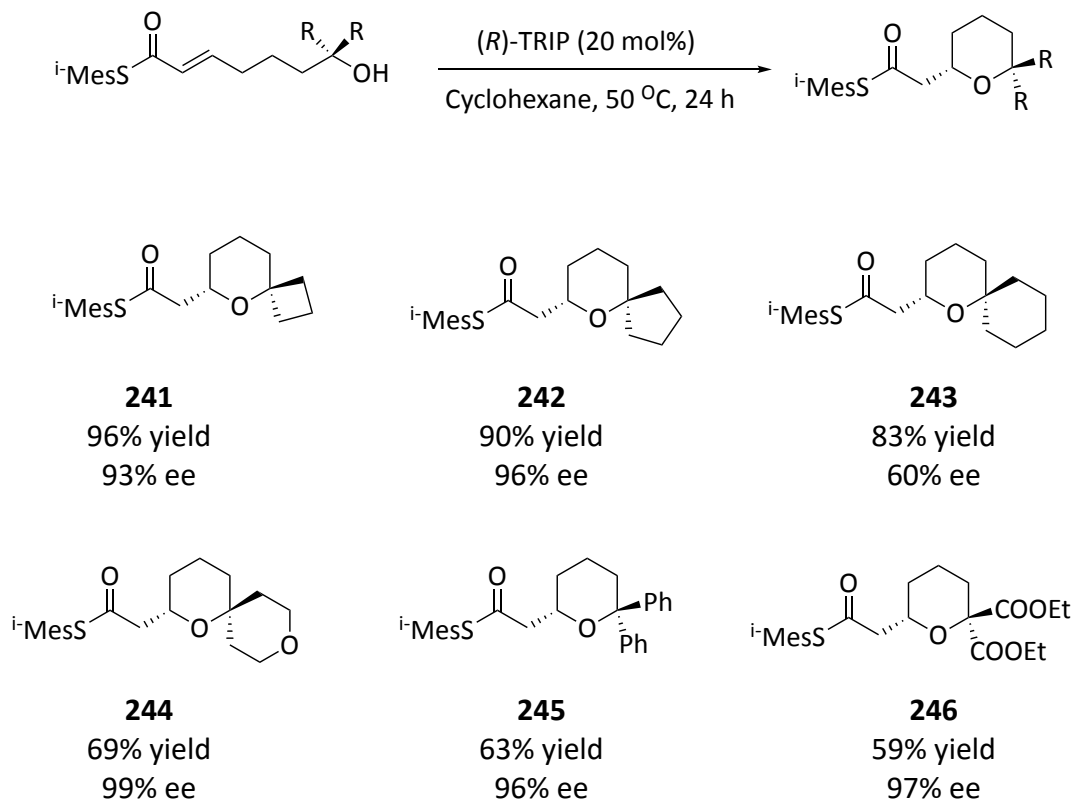
213 (3 eq)

235: R = cyclobutyl, 85%
236: R = cyclopentyl, 81%
237: R = cyclohexyl, 86%
238: R = THP, 82%
239: R = phenyl, 88%
240: R = CO₂Et, 87%

Scheme 59. Synthesis of 2,2'-substituted precursors

Having the precursors in hand, the conditions that had proven to be effective in cyclizing the 2,2'-dimethyl tetrahydropyran (cyclohexane, (*R*)-TRIP at 50 °C) were applied to the substrates (Scheme 60). Fortuitously, all substrates underwent the cyclization reaction smoothly and generated tetrahydropyran products in good to excellent yields. The enantioselectivities of the reaction turned out to be excellent with all substrates producing tetrahydropyran products in more than 90% ee. The exception to this was the spiro-cyclohexyl substrate which produced the product **243** in a moderate 60% ee, and we do not know the reason why the spiro-cyclohexyl substrate has a lower ee than either spiro-cyclopentyl **242** or spiro-THP **244**. The lower yields observed for spiro-THP **244**, diphenyl

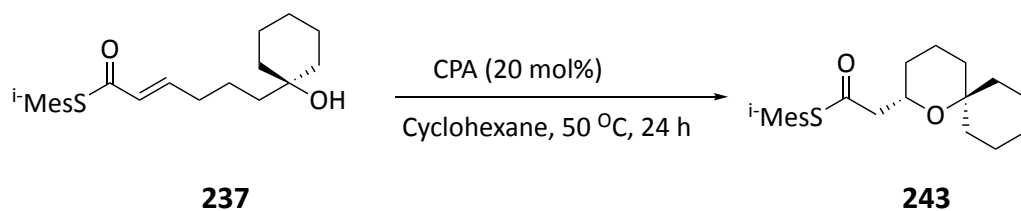
245, and diester **246** THPs could be attributed to a combination of steric and electronic factors, though it is unclear to what extent these different factors affect the reaction. Our hope had been that increasing the steric bulk of the thioester would increase the energy gap between the reaction transition states which led to either the (*R*) or (*S*) enantiomer. However, it appears that large substituents disfavour the cyclization and the uncyclized starting material was retrieved.



Scheme 60. Asymmetric cyclisation to form 2,2'-substituted tetrahydropyrans

In an attempt to improve the enantioselectivity of the spiro-cyclohexyl substrate **243**, a catalyst screen was conducted (Scheme 61, Table 5). Unfortunately, no improvement was seen on either the reaction conversion or enantioselectivity (entries

2,3,5, and 6). Catalyst (*R*)-Anth produced the THP product **243** in a quantitative yield but with very poor enantioselectivity of 19% ee (entry 4).



Scheme 61. Asymmetric synthesis of 2,2'-spirocyclohexyl THP **243**

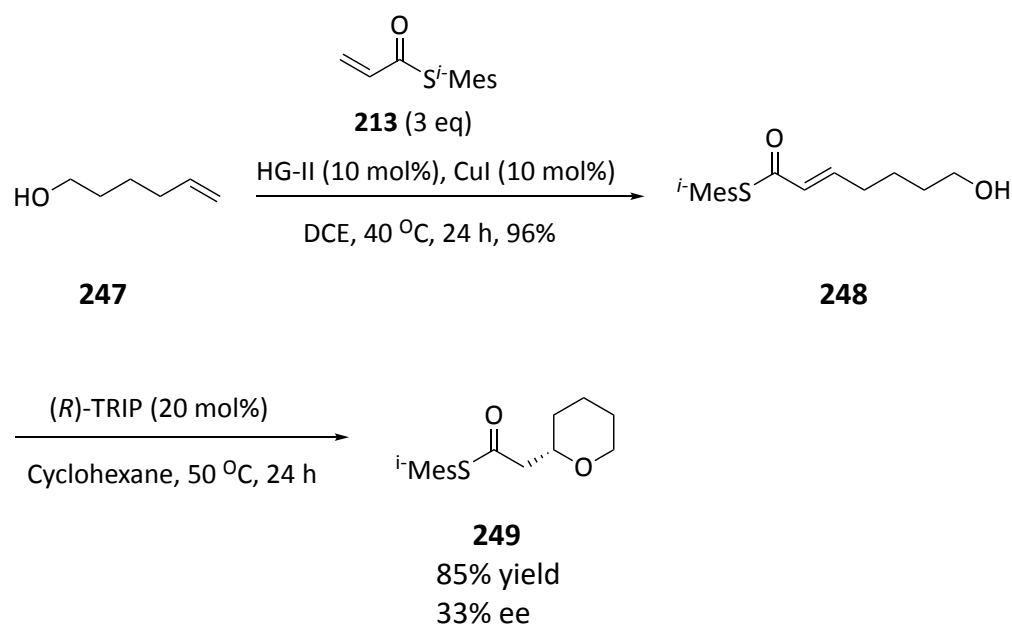
Entry	CPA	Conversion %	ee %
1	(<i>R</i>)-TRIP	83	60
2	(<i>R</i>)-TIPSY	46	32
3	(<i>R</i>)-phenanth	11	12
4	(<i>R</i>)-anth	100	19
5	(<i>R</i>)-VAPOL	80	5
6	(<i>R</i>)-SPINOL	73	0

Table 5. Catalyst screening for the synthesis of 2,2'-spirocyclohexyl THP **243**

The good yields and high enantioselectivities observed for the synthesis of 2,2'-substituted tetrahydropyrans using (*R*)-TRIP at 50 °C in cyclohexane for 24 hours were quite encouraging. At this point, it was determined that additional screening of reaction conditions would not be beneficial, as any advances in either enantioselectivities or yields would be minimal, and the current set of conditions avoided the employment of hazardous solvents or specialised catalysts. Therefore, the unsubstituted tetrahydropyran, which had not been explored previously, seemed like the natural choice as a new substrate to try next.

2.2.2 Synthesis of an unsubstituted tetrahydropyran

The formation of the unsubstituted precursor was accomplished by subjecting 6-hexen-1-ol **247** with thioacrylate **213** to the metathesis condition that had been previously reported, and the unsubstituted precursor **248** was obtained in a high yield of 96% (Scheme 62). The precursor **248** was then exposed to the cyclization conditions of (*R*)-TRIP for a period of 24 hours at a temperature of 50 °C in cyclohexane. Under these conditions, the substrate was able to undergo cyclization successfully, resulting in a high yield of 85%; however, the selectivity suffered a considerable decrease, falling to 33% ee (Scheme 62). Despite the fact that the initial conditions for the 2,2'-dimethyl substrate proved to be the best, the lower selectivity observed for the unsubstituted tetrahydropyran **249** warranted another screen of the conditions.



Scheme 62. Synthesis of the unsubstituted tetrahydropyran **249**

As previously discussed, it was hypothesised that increasing the steric bulk through substitution would favour particular catalytic transition states and also provide a Thorpe-Ingold effect that would improve the reaction rate.

The Thorpe-Ingold effect describes how ring substitutions increase the rate of the ring-forming reaction. The internal angle reduction was the first explanation for the gem-dialkyl effect.⁸² In 1915, Beesley, Ingold and Thorpe discovered a link between changes in the bond angles of carbons in an open-chain structure and the formation and stability of the corresponding cyclized product.^{83,84} They discovered that substituting methylene hydrogens with more sterically demanding alkyl groups causes an internal angle (θ) compression. As a result, the reactive units, X and Y, at the system's end move closer together, facilitating the cyclization (Figure 21).

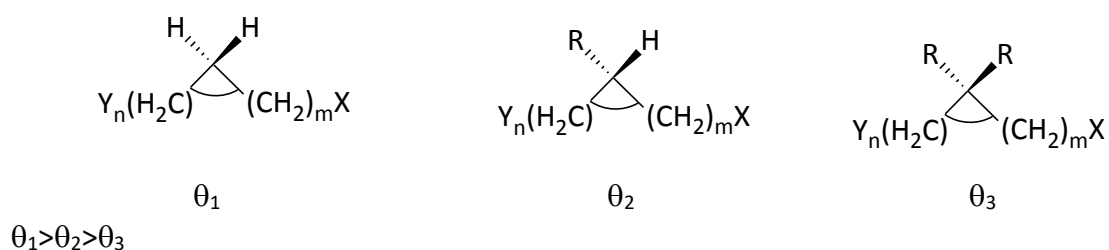
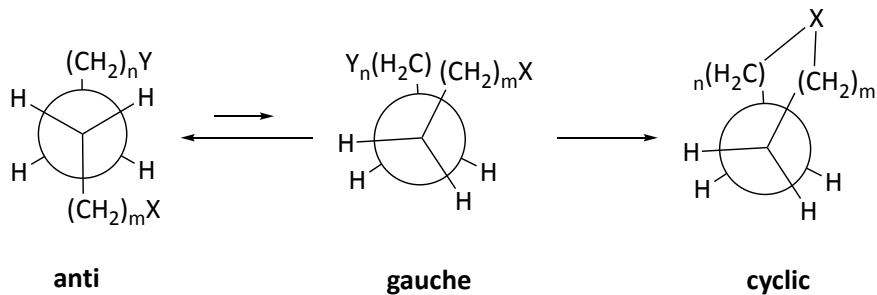


Figure 21. Thorpe-Ingold effect

It was found that the previous explanation is more applicable to the formation of small ring because in the case for five and six membered rings, there is very little or no change in bond angle. The Newman projections for the cyclization of generic (a) unsubstituted and (b) substituted open chains are shown in Figure 22.⁸² In both cases, the reactive units X and Y must approach each other for cyclization to occur, which requires rotation about the central C-C bonds. The rotation of an unsubstituted carbon chain (a) converts the most stable (and thus more highly populated) *anti* conformation into the *gauche* conformation (reactive rotamer). When one or two substituents are substituted for the methylene hydrogens, the energy of the "*gauche*" rotamer required for cyclization is lowered to be similar to the energy of the corresponding "*anti*" rotamer. As a result, a higher population of the reactive rotamer facilitates the cyclization of the substituted compound.

a) Unsubstituted



b) Substituted

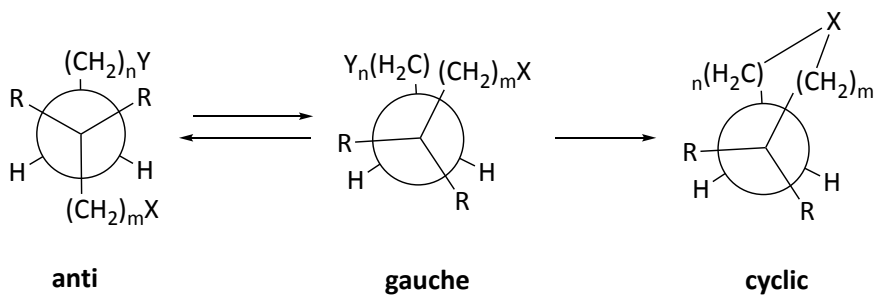


Figure 22. Reactive-rotamer effect on cyclization, Thorpe-Ingold effect

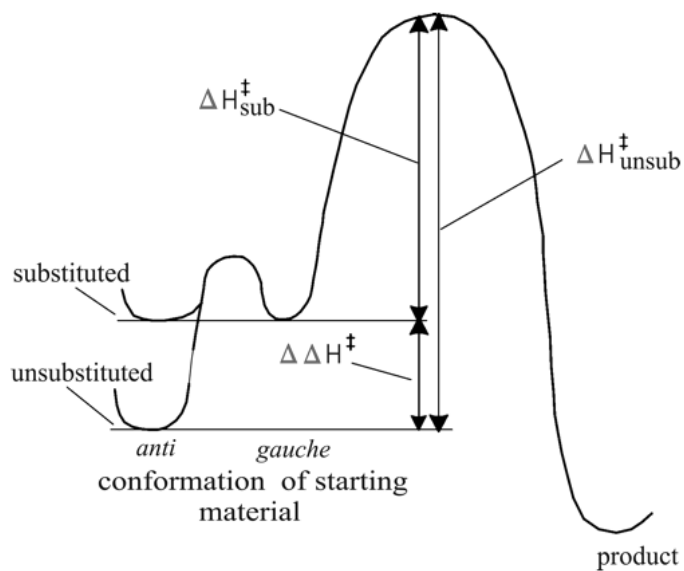
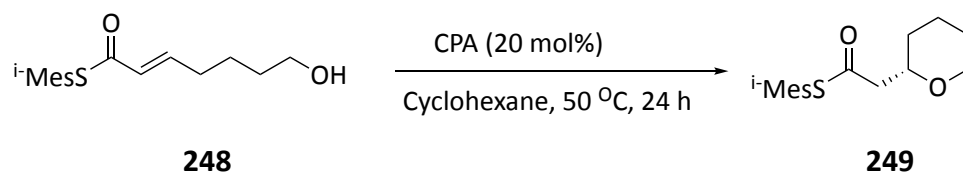


Figure 23. Reactive rotamer effect and the energy diagram for the cyclization⁸²

In terms of energy, substitution increases the energy of the ground state (Figure 23), so that the activation energy for cyclization of the substituted compound (ΔH^\ddagger sub) is lower than that of the unsubstituted (ΔH^\ddagger unsub).

Without this substitution, there is a possibility that the rates as well as the enantioselectivity could be affected. Clearly, the enantioselectivity decreased when the previously optimised conditions were used.

Previous work in the group on the asymmetric synthesis of pyrrolidines revealed that cyclization of unsubstituted pyrrolidine with (*R*)-TIPSY yielded the highest enantioselectivity among the chiral phosphoric acid catalysts (CPAs) tested,⁷⁸ so a catalyst screen was conducted to improve the enantioselectivity of the unsubstituted tetrahydropyran **249** (Scheme 63, Table 6). Neither the conversion nor the enantioselectivity of the product were improved by screening alternative catalysts, and (*R*)-TRIP remained the catalyst of choice for THP substrates (entry 1).



Scheme 63. Synthesis of the unsubstituted tetrahydropyran **249**

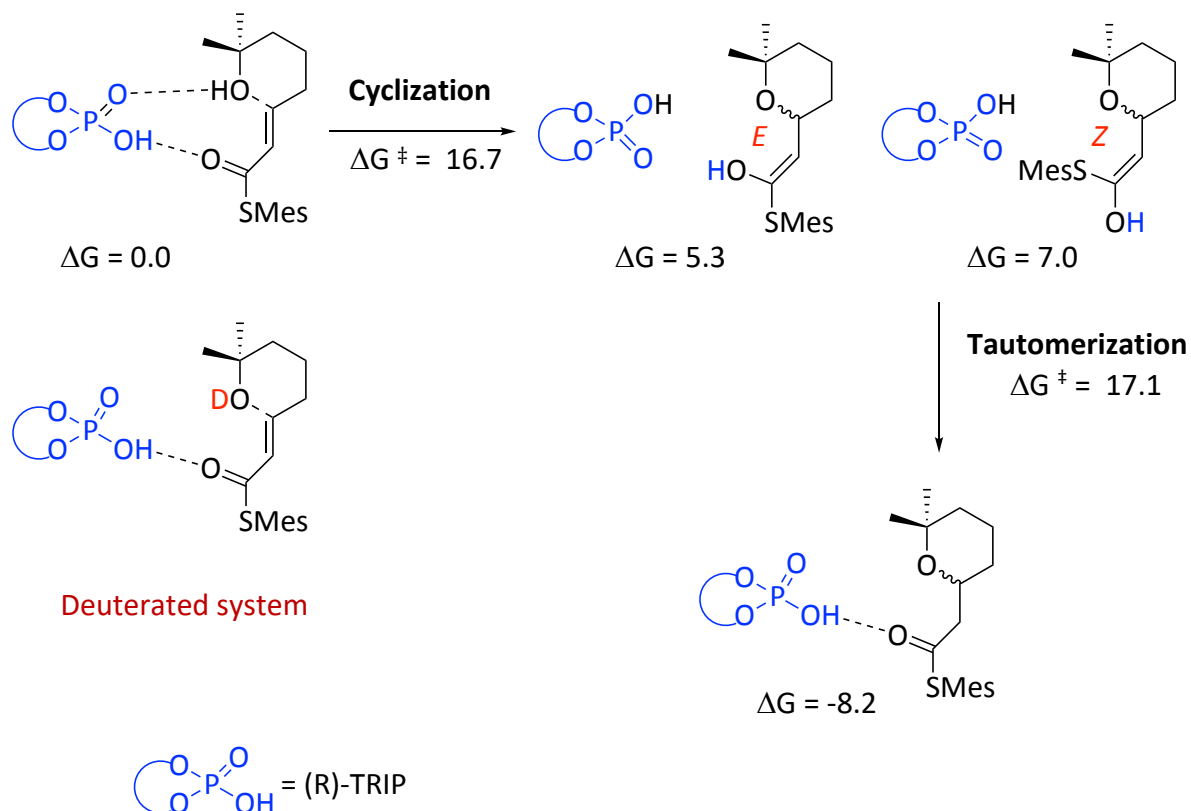
Entry	CPA	Conversion %	ee %
1	(<i>R</i>)-TRIP	85	33
2	(<i>R</i>)-TIPSY	43	14
3	(<i>R</i>)-Phenanth	32	4
4	(<i>R</i>)-Anth	21	0

Table 6. Conditions screen for the unsubstituted tetrahydropyran **249**

2.3 Computational Studies and Determination of Absolute Configuration and the Enantioselective Determining Step

2.3.1 Computational studies and kinetic isotope effect (KIE)

The full oxa-Michael mechanistic pathway was modelled in collaboration with Dr. Kristaps Ermanis, University of Nottingham in order to identify the enantioselectivity determining step.⁸⁶ All starting materials, intermediates, and products were subjected to extensive conformational searches. For each, carefully selected conformations were optimised with B3LYP17/6-31G**/SMD(cyclohexane), and single-point energies were calculated with M06-2X/def2-TZVP/SMD (cyclohexane). It was discovered that the reaction's possible stereochemical determining steps, either cyclization or tautomerization, were both predicted to produce opposite enantiomers (Scheme 64).

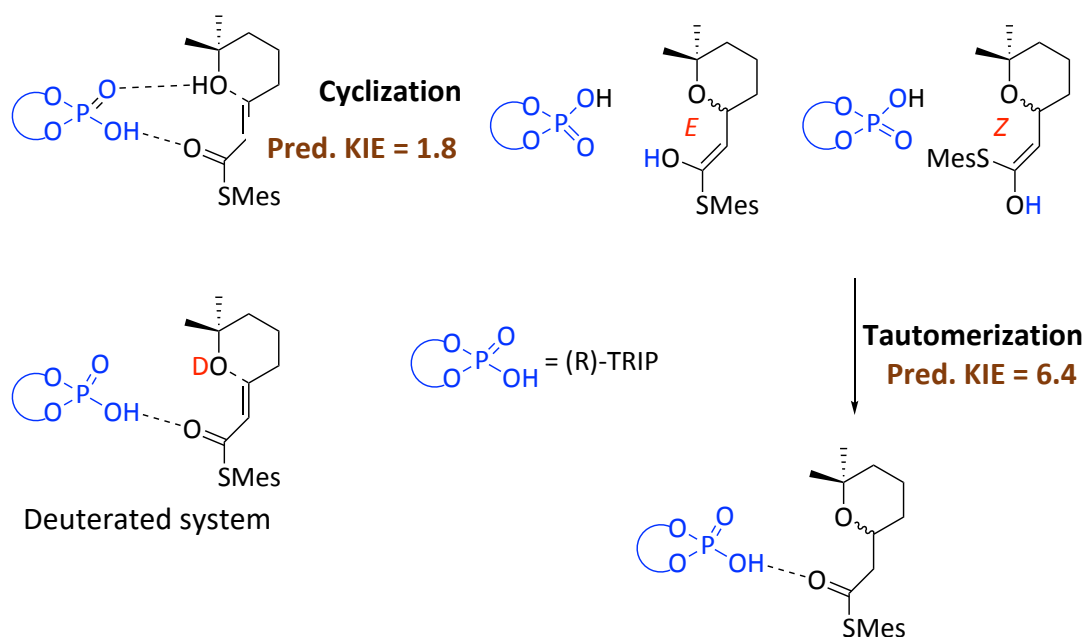


Scheme 64. Computational exploration of the CPA-catalysed oxa-Michael reaction mechanism.

The lowest barriers for cyclization and tautomerization in the resulting pathway were very close, with activation free energies of 16.7 and 17.1 kcal mol⁻¹, respectively. Since the difference is smaller than the margin of error associated with DFT approaches, either of the two steps might, in theory, determine the enantioselectivity. Cyclization has the potential to establish the stereochemistry, which would then be followed by a more rapid tautomerization. Alternately, the reaction could demonstrate Curtin–Hammett control. This would involve a reversible cyclization followed by an enantioselective tautomerization that would determine the selectivity of the reaction. Consequently, there was a requirement for an alternative method of finding the rate- and selectivity-determining step.

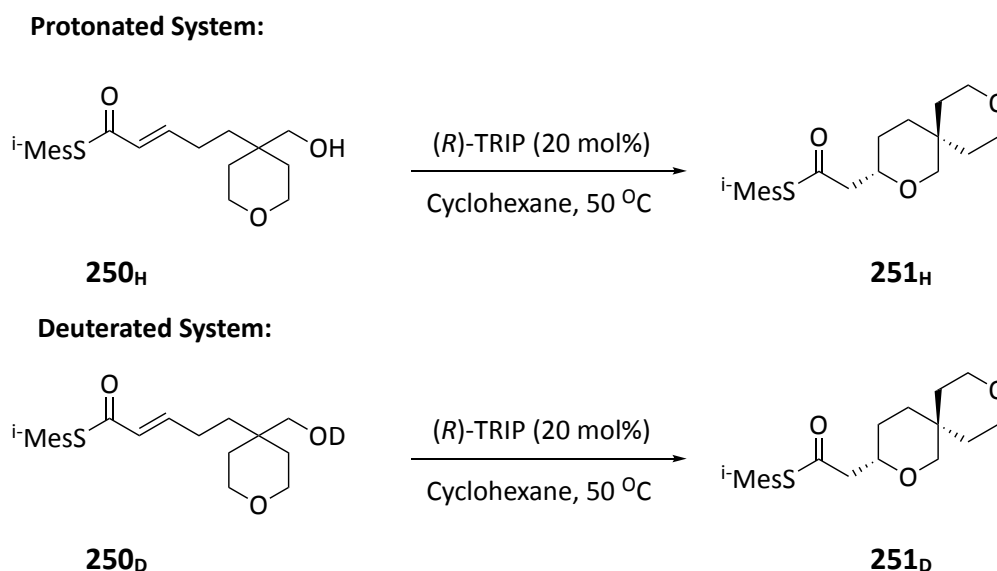
2.3.2 Predicted and experimental Kinetic isotope effect (KIE)

Another method for assessing the rate and selectivity-determining step was required since the activation energy differences between cyclization and tautomerization are so small. In order to accomplish this, the H/D KIEs for both steps were calculated (Scheme 65).



Scheme 65. Predicted KIE of the CPA-catalysed oxa-Michael reaction mechanism

The computational results showed that the cyclization H/D KIE was 1.8, while the tautomerization H/D KIE was 6.4 (Scheme 65). Both protonated and deuterated systems were tested to determine which is the enantioselective determining step. The deuterated cyclization precursor **250_D** was synthesized using the same procedure as the protonated **250_H** and then dissolved in deuterated methanol (CH₃OD) allowing for the H/D exchange, which was confirmed by mass spectrometry. Then, both systems were subjected to the optimized cyclization conditions using (*R*)-TRIP in cyclohexane at 50 °C (Scheme 66).



Scheme 66. Cyclization of H/D KIE reaction

The mixture of both systems was subjected to ¹H NMR analysis at regular intervals of twenty minutes (20 min) to track the formation of the products and the consumption of the starting materials over the course of the experiment. This allowed for the accurate calculation of the reaction's rate of conversion (Table 7).

Time/ min	Conversion %	
	251 _H	251 _D
20	69	53
40	79	71
60	90	82
80	100	90

Table 7. Conversion of 251_{H/D} over the time at 50 °C

KIE is defined as the ratio of rate constants for two isotopologue reactants, K_L/K_H , where K_L is the lighter isotopologue rate constant and K_H is the heavier isotopologue rate constant. For hydrogen and deuterium transfer, KIE is typically the ratio K_H/K_D between the rate constants K_H and K_D , respectively. The reaction rates of both systems, K_H (blue) and K_D (orange), were calculated by plotting $\ln[SM]$ vs time of both systems (Figure 24). The KIE was determined experimentally as the ratio K_H/K_D to be 1.2 which is closest to the 1.8 calculated for the cyclization. This provides to the evidence that the cyclization step is the rate and selective determining step in the reaction (Figure 24).

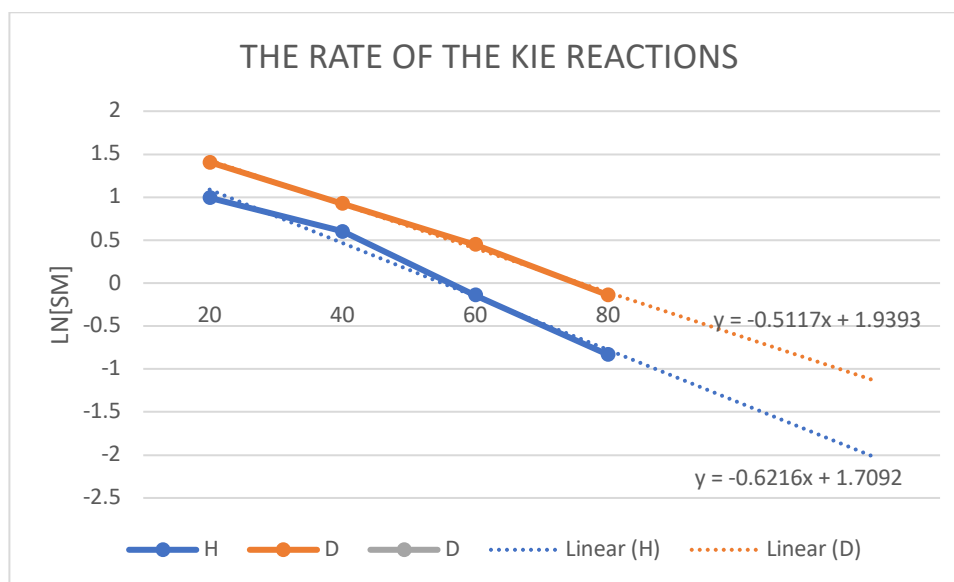
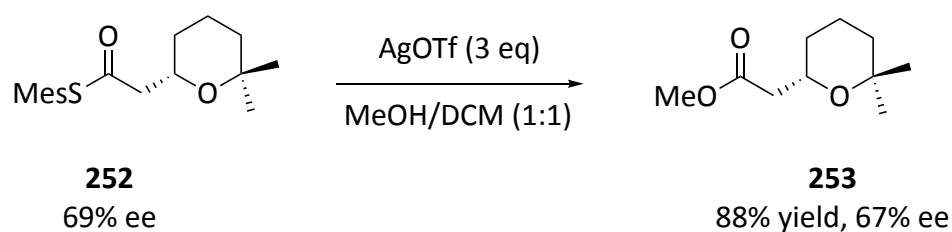


Figure 24. Experimental KIE of 251_{H/D}

2.3.3 Determination of the absolute stereochemistry

One of the benefits of using a thioester is its versatility in that it can be used for the final stage modification or as a linker unit to attach the tetrahydropyran subunit to a larger molecule. In processes that are analogous to those used to modify an oxoester, such as by reduction, hydrolysis, or transesterification, the thioester can also be altered usually under much milder conditions. The transesterification method was of interest because it could be used to determine the stereochemistry of the stereogenic centre formed during cyclisation.

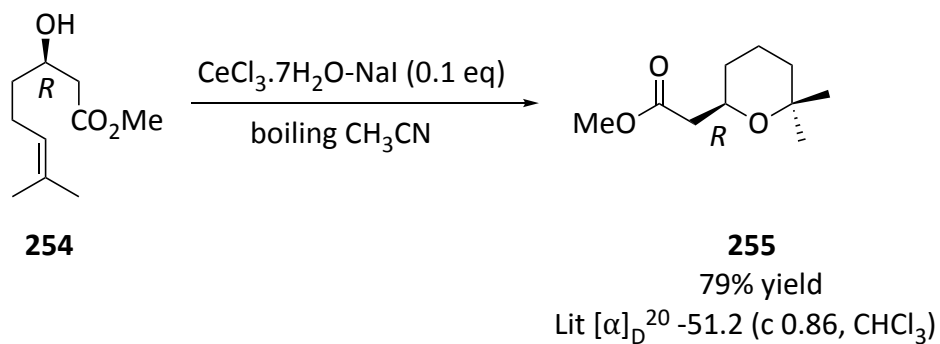
To our good fortune, methods for producing oxoesters from corresponding thioesters have been reported in the literature. Hanessian *et al.* described a method for converting a thiophenyl ester to a methyl ester using AgOTf in MeOH/CH₂Cl₂.⁷⁹ Using these conditions, the 2,2'-dimethyl tetrahydropyran **252** was smoothly converted into the corresponding methyl ester **253** in 62 % yield and with minimal enantioselectivity change (Scheme 67).



Scheme 67. Transesterification using silver triflate and methanol

The synthesis of the tetrahydropyran methyl ester **253** was performed for two primary reasons; first, to demonstrate the transesterification procedure, and second, to allow for determination of the absolute stereochemistry of the product. According to a publication by Rosini *et al*, who synthesised (*R*)-2,2'-dimethyl tetrahydropyran acetic acid ester **255** *via* cyclization of pure chiral starting material **254** with cerium (III) chloride

heptahydrate and sodium iodide in boiling acetonitrile with complete retention of the absolute configuration of the starting material (Scheme 68).⁸⁰



Scheme 68. Synthesis of (*R*)-2,2'-dimethyl tetrahydropyran acetic acid ester **255**

Because this product was derived from an enantiomerically pure starting material in the synthesis, the value for the optical rotation of the molecule would allow the determination of configuration in the (*R*)-TRIP catalysed cyclisation. The optical rotation of the methyl ester derived **253** from the cyclised thioester **252** was $[\alpha]_D^{20} + 26.4^\circ$ (c 0.71, CHCl₃) while the value for the literature compound was Lit $[\alpha]_D^{20} -51.2$ (c 0.86, CHCl₃).⁸⁰ When the sign of optical rotation was compared to the literature value, it was determined that the configuration of the tetrahydropyran methyl ester **253** was (*S*) and thus the thioester **252** must also be (*S*)- because there appeared to be no racemisation of the stereocentre.

This confirmed the DFT calculations' prediction, which predicted the (*S*)-enantiomer, and even the initial low-level MMFF calculations. As the tautomerization was calculated to give the opposite enantioselectivity, it indirectly added support to cyclisation as the rate and stereochemical determining step.

2.4 Scope of the reaction for 3,3'-disubstitution and One Pot Reaction

2.4.1 Scope of the reaction for 3,3'-disubstitution

To extend the substrate scope from the 2,2'-substituted tetrahydropyrans, 3,3'-substituted precursors were synthesised from commercially available esters using the procedures which had been reported in the literature.⁸¹ The same carbocycles including heterocycle, dimethyl and diphenyl functionality was included in the selection of substitution (Figure 25).

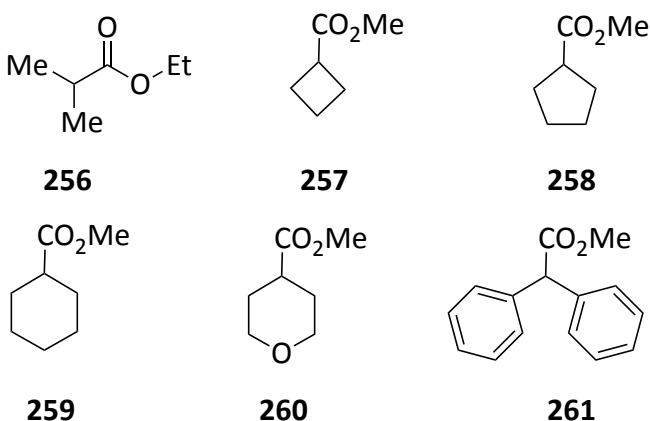
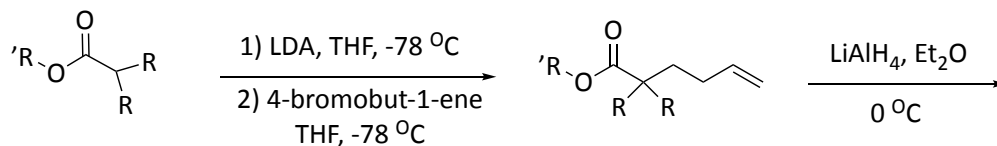


Figure 25. Esters selected to test 3,3'-disubstituted scope

The first synthetic step to synthesise the precursors was to alkylate the substituted esters with 4-bromobut-1-ene after deprotonation with LDA (Scheme 69). This formed the corresponding alkyl esters in good to excellent yields. The reduction of the resultant esters with LiAlH_4 to produce the corresponding primary alcohols proceeded well for most substrates, with particularly high yields being observed for the carbocyclic precursors. The THP **272** and diphenyl **273** substrates seemed to have solubility issues in diethyl ether, however, upon replacing the solvent with tetrahydrofuran, the THP **278** and diphenyl **279** alcohols were obtained in 75% and 74% yields respectively. The resultant alcohols were then clipped with thioacrylate **213** *via* alkene metathesis to generate the cyclization precursors. The lower yields compared to the 2,2'-substituted substrates were due to the

self-cyclization of the precursors to the THP either during the metathesis reaction or during the purification of the products possibly as a result of Thorpe-Ingold effect.



262: R = Me, R' = Et

263: R = cyclobutyl, R' = Me

264: R = cyclopentyl, R' = Me

265: R = cyclohexyl, R' = Me

266: R = THP, R' = Me

267: R = phenyl, R' = Me

268: R = Me, R' = Et, 70%

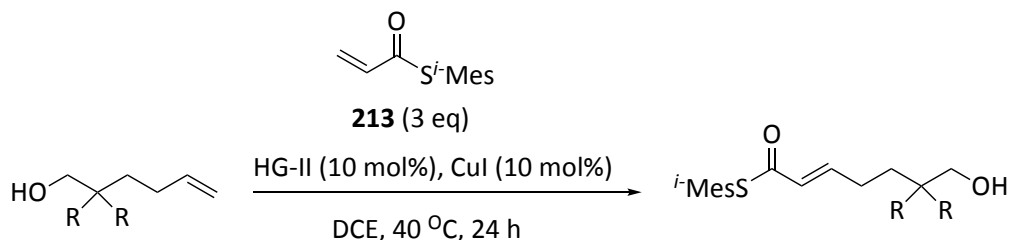
269: R = cyclobutyl, R' = Me, 66%

270: R = cyclopentyl, R' = Me, 91%

271: R = cyclohexyl, R' = Me, 80%

272: R = THP, R' = Me, 73%

273: R = phenyl, R' = Me, 70%



274: R = Me, 96%

275: R = cyclobutyl, 92%

276: R = cyclopentyl, 94%

277: R = cyclohexyl, 87%

278: R = THP, 75%

279: R = phenyl, 74%

280: R = Me, 71%

281: R = cyclobutyl, 51%

282: R = cyclopentyl, 64%

283: R = cyclohexyl, 61%

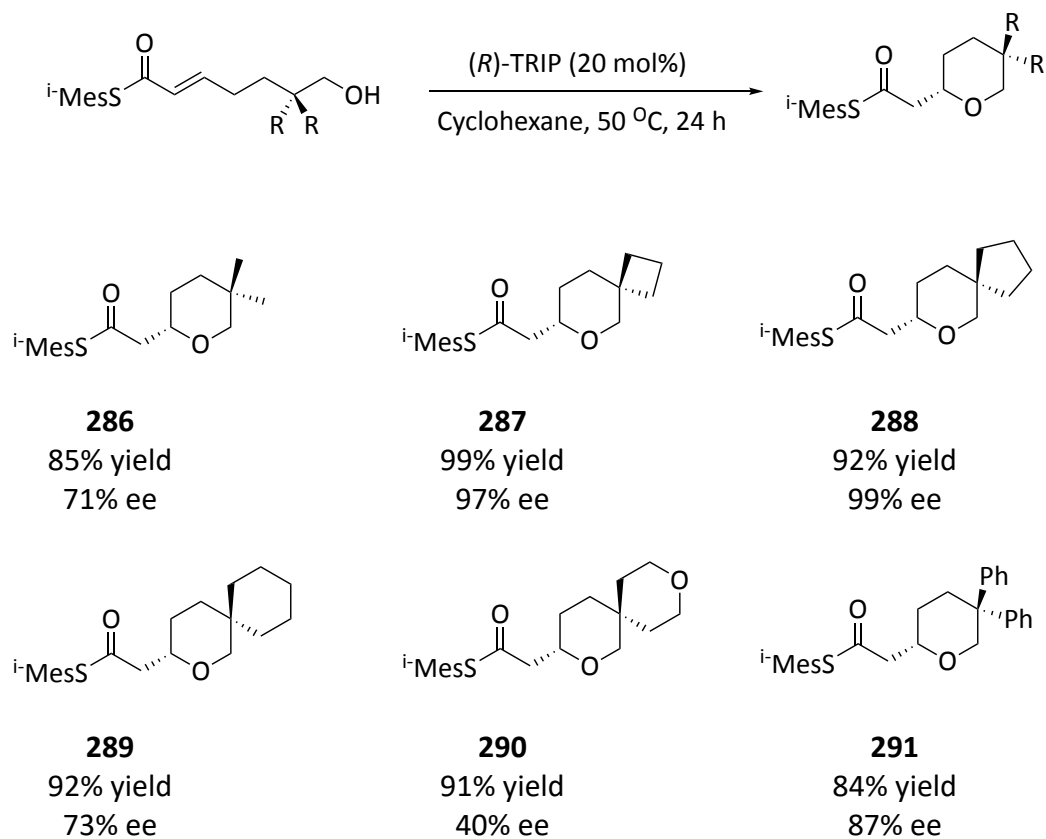
284: R = THP, 52%

285: R = phenyl, 48%

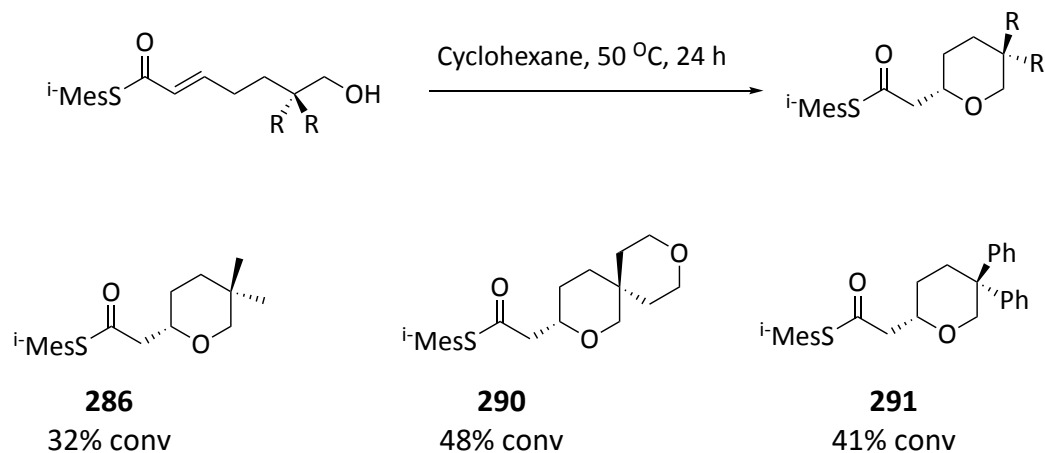
Scheme 69. Synthesis of 3,3'-substituted precursors

These newly synthesised precursors were then subjected to the cyclisation conditions previously developed (cyclohexane, (*R*)-TRIP, 50 °C). As can be seen from Scheme 70, the reaction was able to tolerate 3,3'-substitution well, and resulted in excellent yields and good to excellent enantioselectivities for the generation of enantiomerically enriched products. The lower enantioselectivities observed for dimethyl **286**, spiro-THP **290**, and diphenyl **291** substrates could be due to the uncatalyzed background reaction. To confirm this, the "Clip" products were left to stir in cyclohexane at 50 °C for 24 hours. The

conversions were then determined using the crude material ^1H NMR, demonstrating that there is background cyclization occurring within the reaction (Scheme 71).

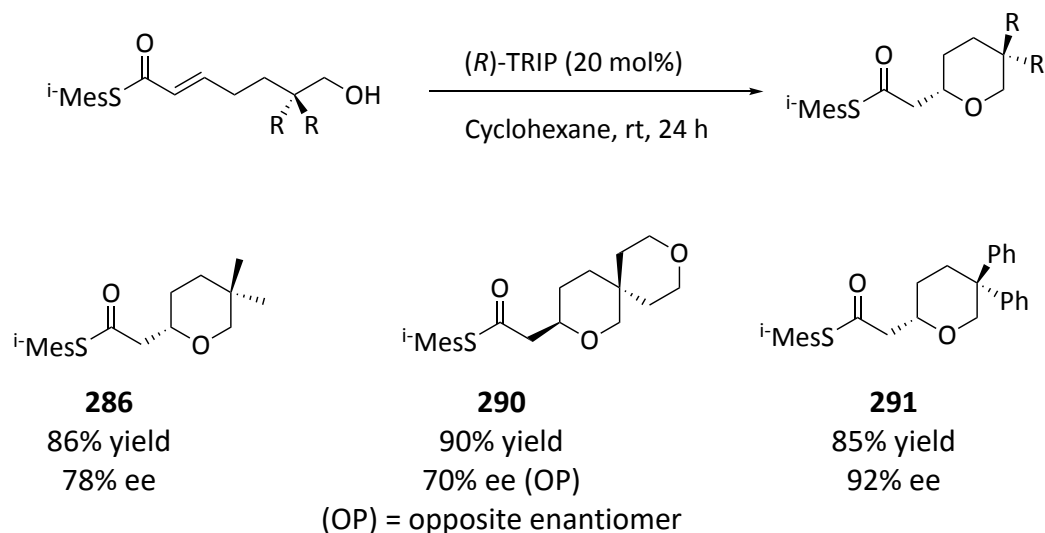


Scheme 70. Asymmetric cyclisation to form 3,3'-substituted tetrahydropyrans



Scheme 71. Background cyclization of 3,3'-substituted tetrahydropyrans

To overcome this, we devised that lowering the temperature could minimize the uncatalyzed background cyclisation of the reaction and hence enhance the enantioselectivity of the product. The cyclization reaction was carried out room temperature (rt) (Scheme 72). It was interesting to note that when the cyclization reaction was performed at rt, all THP products were isolated with excellent yields and also with higher enantioselectivities than when the reaction were carried out at 50 °C (Scheme 72).



Scheme 72. Asymmetric cyclisation to form 3,3'-substituted tetrahydropyrans at rt

More intriguingly, lowering the temperature caused an inversion of the product's configuration for the spiro-THP substrate **290** (Figures 26, 27 and 28). The experiments were repeated three times to confirm the outcomes and the same results were obtained. This observation will be discussed in greater detail later.

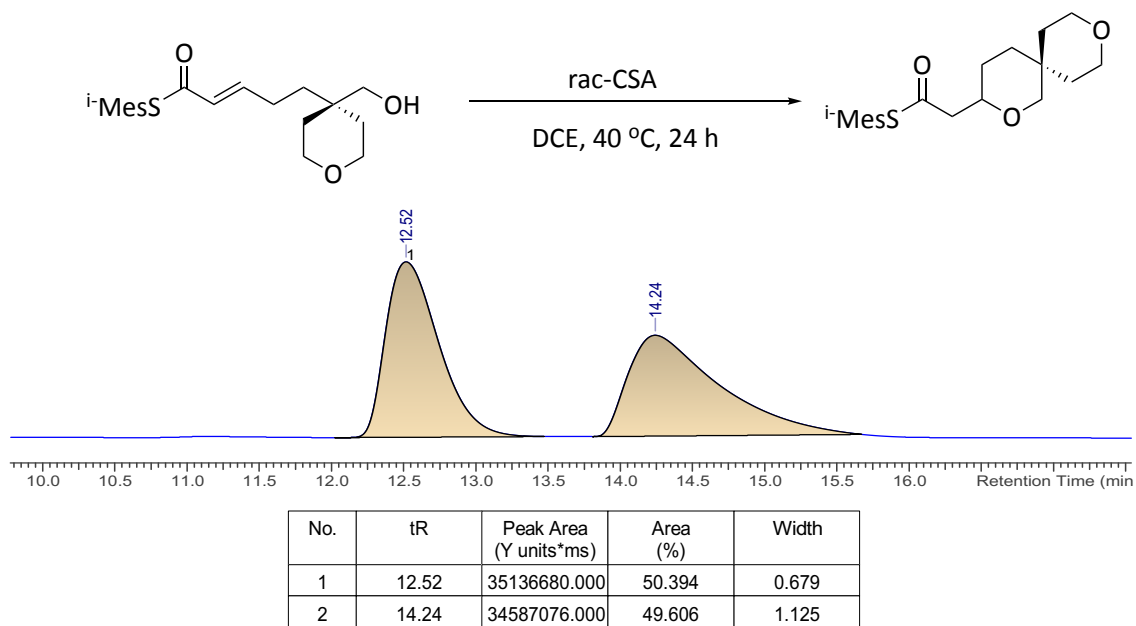


Figure 26. HPLC chromatogram of the synthesised racemic 3,3'-spiroTHP product **290** with *rac*-(CSA)

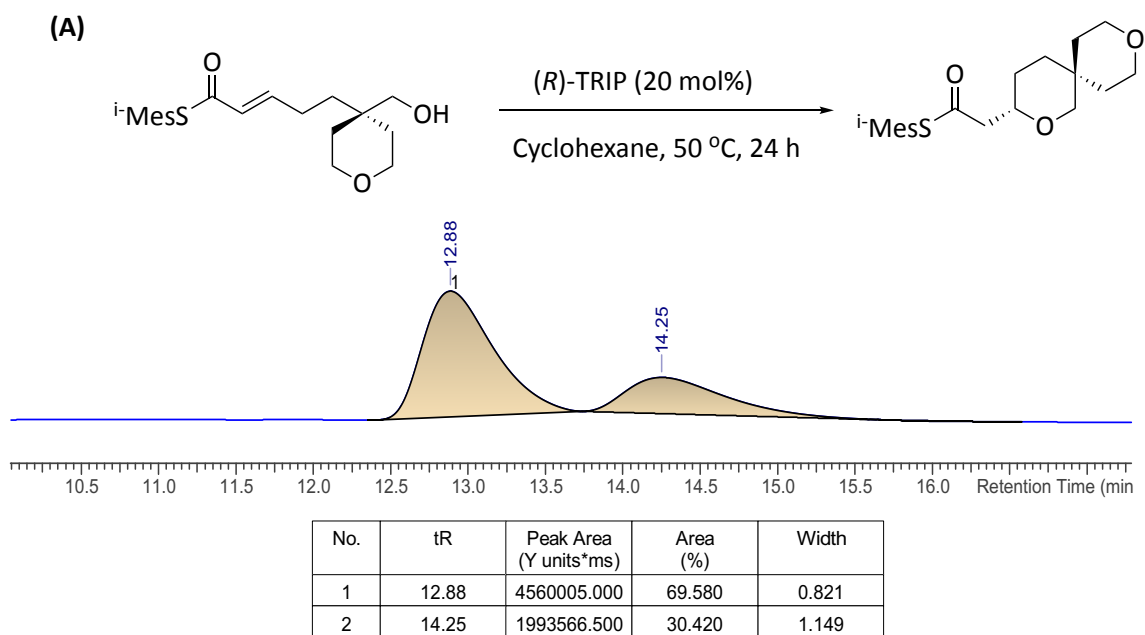


Figure 27. HPLC chromatogram of the synthesised 3,3'-spiroTHP product **290** with (*R*)-TRIP at 50 °C

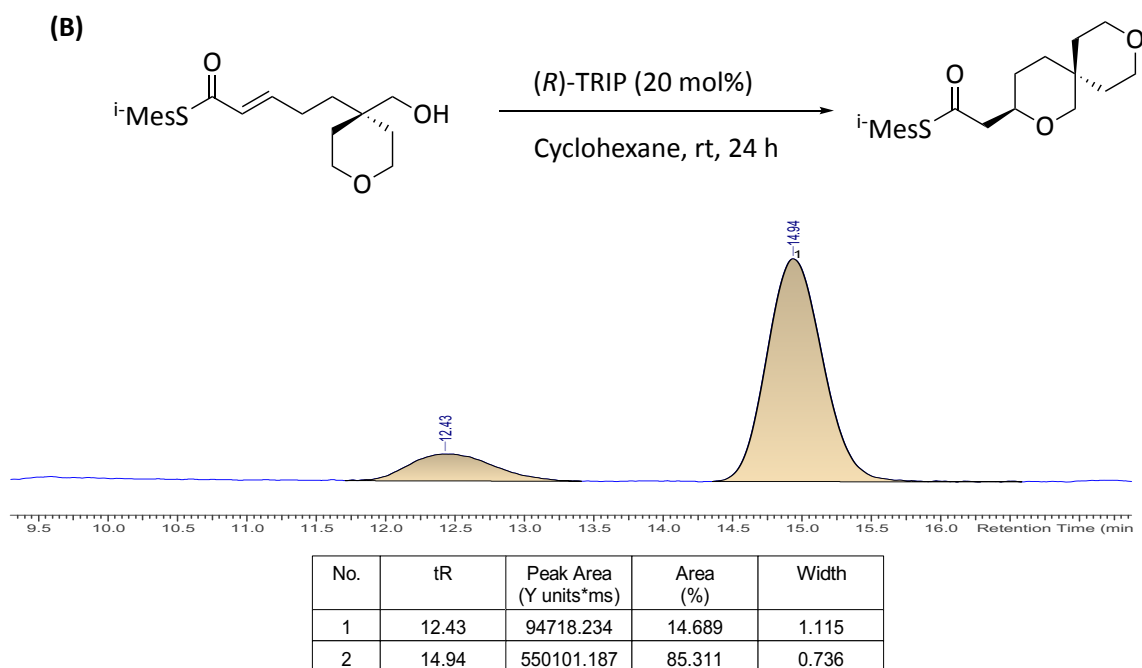


Figure 28. HPLC chromatogram of the synthesised 3,3'-spiroTHP product **290** with (*R*)-TRIP at room temperature

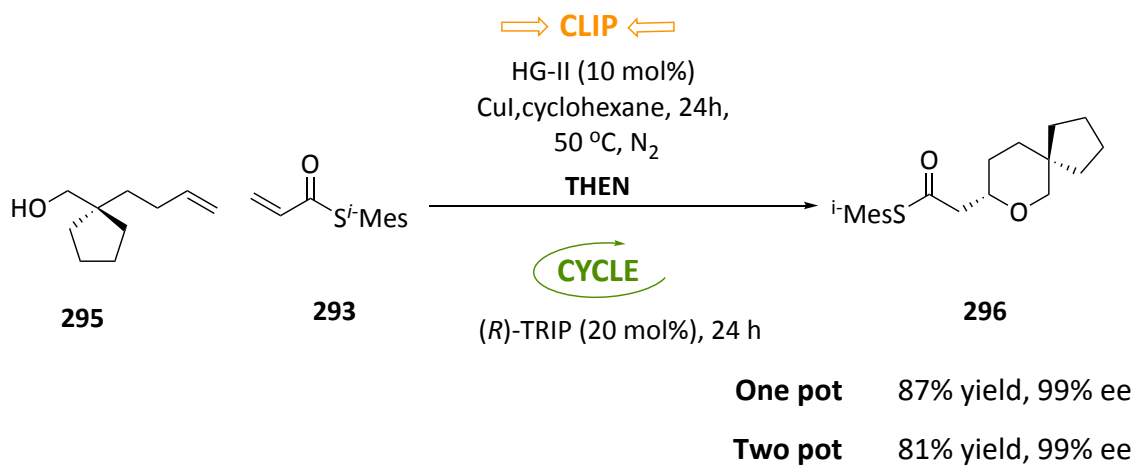
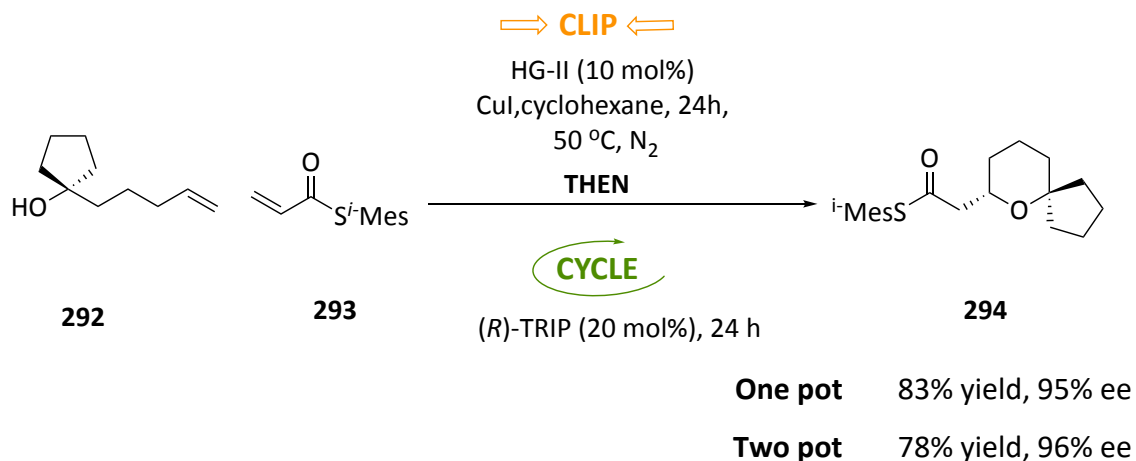
With the realisation of a two-pot procedure for the synthesis of substituted tetrahydropyrans, the focus shifted to the re-development of a one-pot procedure. High efficiency and operational simplicity are intrinsic benefits of one-pot processes, which eliminate the intermediate purification step to conserve resources and reduce waste.

2.4.2 One pot reaction

In terms of enantioselective domino, one-pot, and multicomponent reactions, organocatalysis, for example, has demonstrated its potential for the formation of multiple bonds and stereocenters. These latter strategies enable a quick, environmentally friendly, and simple approach to the formation of complex molecules with a minimum of manual operations and purification steps, making methodologies that employ these strategies highly desirable.⁸⁵

Tetrahydropyrans are essential organic chemistry building blocks, and a one-pot method would be an efficient and appealing approach to obtain them. Such a technique eliminates the need for intermediate product purification, the use of multiple vessels, less solvent requirements, and simplifies the overall procedure. However, for our purposes, the main advantage of a one-pot reaction is the reduced time frame of the stages leading to the final product.

The investigation of the 'Clip-Cycle' protocol's one-pot reaction started with clipping the homoallylic alcohol **292/295** with thioacrylate **293** *via* alkene metathesis in cyclohexane at 50 °C. When there was no alkene detected by TLC, (*R*)-TRIP catalyst was added and the reaction stirred at the same temperature for a further 24 hours while being monitored by TLC, afterwards the reaction was quenched with 0.2 M triethylamine (Scheme 73). The 2,2'- and 3,3'- spiro cyclopentyl substrates were chosen to test the efficiency of the one-pot reaction. It has been demonstrated that the 'Clip-Cycle' process can be carried out in a single pot without loss of yield or enantioselectivity. It was observed that the overall yield for both substrates improved while maintaining the high enantioselectivity; this is most likely due to the inherent increased efficiency of one-pot reactions, which eliminates factors such as product loss during transfer to other vessels or during the purification process. It also demonstrated that neither copper iodide nor the Hoveyda-Grubbs catalyst interfered with the intramolecular Michael cyclisation with (*R*)-TRIP.



Scheme 73. Asymmetric “Clip-Cycle” synthesis of substituted tetrahydropyrans in a one-pot reaction

2.4.3 Summary of results

It has been demonstrated that, α,β -unsaturated thioesters can act as Michael acceptors in an intramolecular asymmetric oxa-Michael reaction. Initial comparisons of tolyl-, mesityl-, and isopropyl-mesityl thioesters revealed that the latter produced higher yields and enantioselectivity than the other substrates. Following a series of optimizations, high yields and enantioselectivity were achieved when (R)-TRIP catalyst was used in the

synthesis of 2,2'-substituted tetrahydropyrans. In addition, the same conditions resulted in the formation of 3,3'-substituted tetrahydropyrans as well, with higher selectivity, particularly with spirocarbocyclic substitution, when compared to 2,2'-substituted tetrahydropyrans. The exact cause for the difference in selectivity is unknown, but the proximity of the substitution, and thus steric bulk, to the nucleophile as well as the Thorpe-Ingold effect, could play a role.

The extent to which each variable affected the yield and selectivity of the reaction was revealed by screening the reaction conditions. The yield and enantioselectivity of the reactions were affected by the solvent used, with cyclohexane performing best in all cases. In general, higher temperatures (75 °C instead of 50 °C) increased yield while slightly decreasing enantioselectivity. The catalyst choice was the most important factor in determining the enantioselectivity of the reaction, with (*R*)-TRIP providing the best selectivity for both substituted and unsubstituted tetrahydropyrans. We were able to determine a general set of conditions for the asymmetric synthesis of tetrahydropyrans through this optimization process: isopropyl-mesityl thioester as a Michael acceptor, (*R*)-TRIP, cyclohexane, 50 °C for 24 h. These conditions proved useful for the synthesis of a variety of spirocyclic and di-substituted tetrahydropyrans.

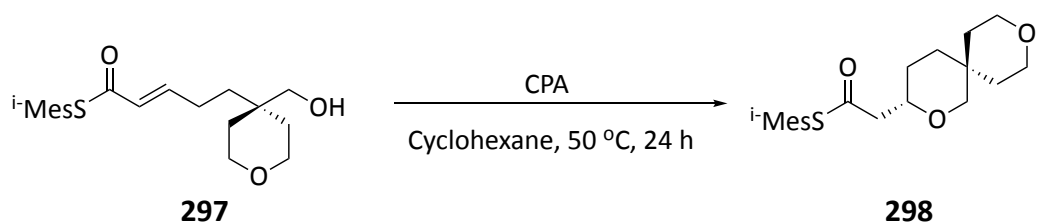
The 'Clip-Cycle' process has been demonstrated to be capable of producing enantiomerically enriched substituted tetrahydropyrans in a single pot reaction. The one-reaction improved the overall yield of the product while maintaining the high enantioselectivity; this is most likely due to the one-pot reaction's inherent increased efficiency.

After a reasonable substrate scope had been investigated, the focus shifted to do further investigation on the enantio-inversion observation that was seen in the 3,3'-spiro THP by lowering the reaction temperature.

2.5 The enantio-inversion Observation of Spiro-THP Substrate

2.5.1 The enantio-inversion observation

As previously discussed, when the cyclization precursor **297** was subjected to the optimal cyclization conditions, (*R*)-TRIP (20 mol%), cyclohexane at 50 °C (Scheme 74, Table 8, entry 1), the THP product **298** was obtained in 91% yield with only 40% ee. We believed that the lower enantioselectivity observed, when compared with other substrates, was due to the uncatalyzed background reaction. To confirm that, the reaction of **297** was carried out in cyclohexane at 50 °C without the catalyst (Scheme 74, Table 8, entry 2). The racemic THP product **298** was obtained in 42% yield.



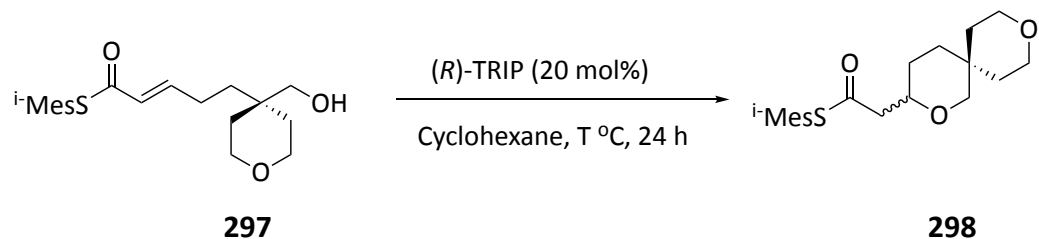
Scheme 74. Asymmetric synthesis of spiro-THP **298**

Entry	CPA	Conv. %	Yield %	ee %
1	(<i>R</i>)-TRIP	100	91	40
2	-	48	42	0

Table 8. Synthesis of spiro-THP **298**

It is possible to modify the reaction conditions in order to decrease the background reaction and, as a consequence, increase the enantioselectivity of the product. This can be accomplished by either lowering the temperature or increasing the catalyst loading in order to increase the amount of substrate that is passed through the catalyst system. To this end,

the reaction was carried out with different catalyst loadings of (*R*)-TRIP at different temperatures.



Scheme 75. Asymmetric synthesis of spiro-THP **298** at different temperatures

Entry	T °C	ee%	Abs. Conf.
1	50	40	<i>S</i> ^a
2	40	31	<i>S</i>
3	35	27	<i>S</i>
4	30	8	<i>S</i>
5	25	23	<i>R</i>
6	20	71	<i>R</i>

^a Absolute configuration for 3,3'- spiro-THP was assumed to be *S* as it has already determined for the 2,2'-dimethyl substrate.

Table 9. Asymmetric synthesis of spiro-THP **298** at different temperatures

Initial modification was done by lowering the temperature of the reaction while keeping the catalyst loading constant at 20 mol% (Table 9). The data in table 9, entry 1 shows the previously tested conditions which yielded the (*S*)-enantiomer product, assuming that the product's configuration would be the same as the 2,2'-dimethyl THP, with 40% ee (Figure 29-A). When the temperature was reduced to either 40 °C or 35 °C, the product was isolated in a lower enantioselectivity of 31% and 27%, respectively (entries 2 and 3). Running the reaction at 30 °C gave a nearly racemic product (entry 4). More interestingly, a decrease in the temperature to 25 °C or room temperature, which was 20 °C, resulted in an

inversion of the product configuration, (*R*)-enantiomer, (entries 5 and 6) with an increase in the enantioselectivity to reach 71% at 20 °C (entry 6-Figure 29-B).

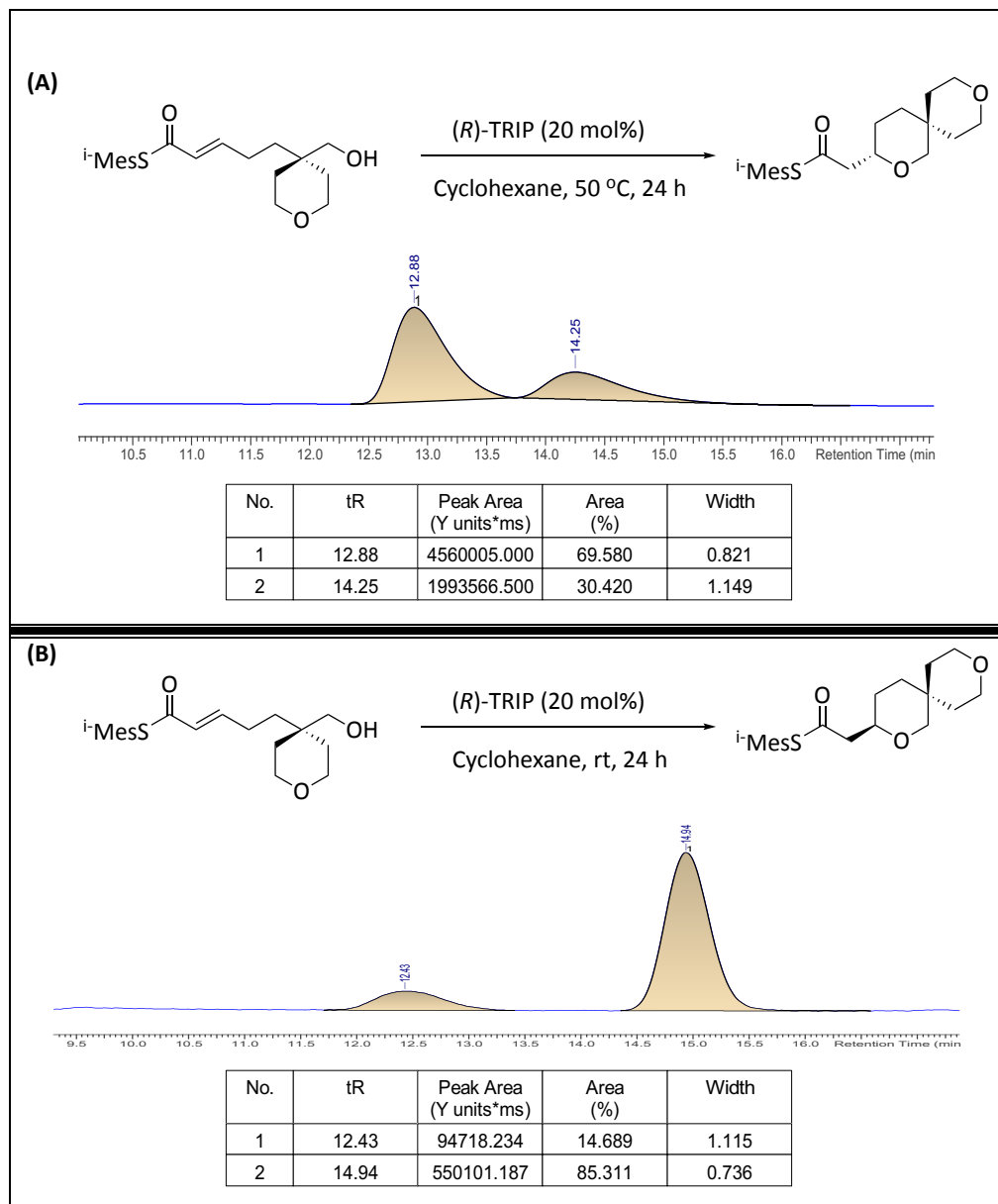
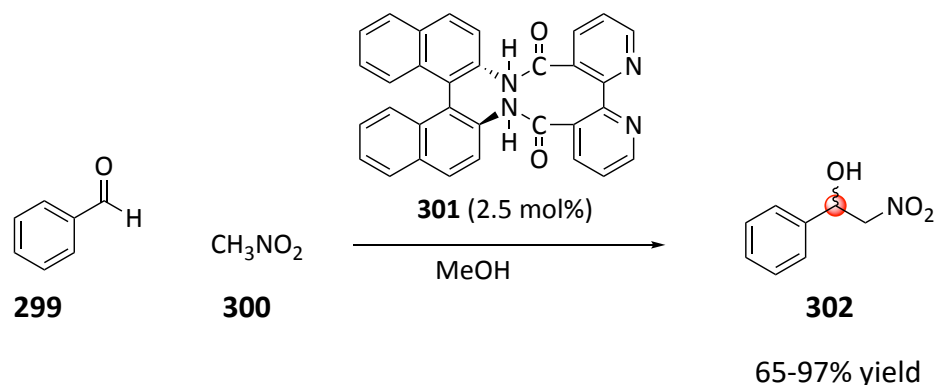


Figure 29. HPLC chromatogram of the synthesised 3,3'-spiroTHP product **298** with (*R*)-TRIP at 50 °C (A), and 20 °C (B)

The unexpected inversion of the configuration as a result of lowering the temperature was reported previously by Siva and co-workers.⁸⁷ In their research on enantioselective Henry reactions, the reaction of benzaldehyde **299** with nitromethane **300** in the presence of chiral catalyst **301** was carried out at different reaction temperatures (Scheme 76, Table 10). It was found that the best combination results of yield and enantioselectivity was obtained at 30 °C (entry 1). An increase in the temperatures from 30 °C up to 60 °C resulted in a decrease in both yields and ee (entries 2 and 3). More interestingly, lowering the reaction temperature from 30 °C to 5 °C, -10 °C, and -20 °C caused an inversion of the product's configuration (entries 5-7). The unexpected inversion was reasoned to the restricted interaction between the catalyst and substrate upon lowering the temperature from 30 °C to -20 °C.

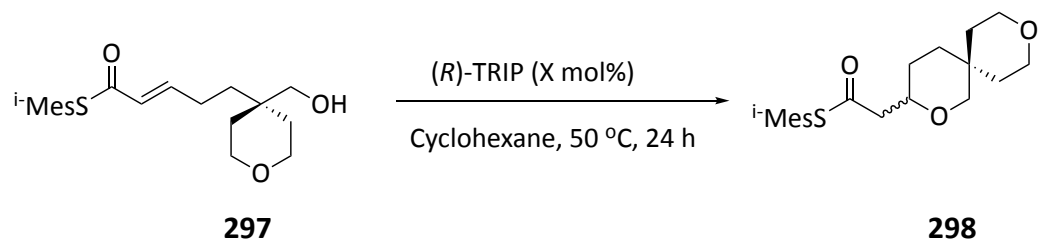


Scheme 76. The enantioselective Henry reaction under various temperature conditions

Entry	T °C	Time (h)	yield %	ee %	Abs. Conf.
1	30	6	97	98	S
2	50	6	81	78	S
3	60	6	65	67	S
4	15	7	82	70	S
5	5	7	75	74	R
6	0	8	90	91	R
7	-10	9	92	93	R
8	-20	10	95	97	R

Table 10. The enantioselective Henry reaction under various temperature conditions

The next step, that was attempted to reduce the uncatalyzed background reaction, was by increasing the catalyst loading to increase the amount of substrate that passed through the catalyst system (Scheme 77, Table 11).



Scheme 77. Asymmetric synthesis of spiro-THP **298** with different catalyst loading of (*R*)-TRIP at 50 °C

Entry	(<i>R</i>)-TRIP (X mol%)	ee%	Abs. Conf.
1	20	40	<i>S</i> ^a
2	30	57	<i>S</i>
3	40	66	<i>S</i>
4	15	38	<i>S</i>
5	10	34	<i>S</i>
6	5	30	<i>S</i>
7	0	0	(±)-Racemic

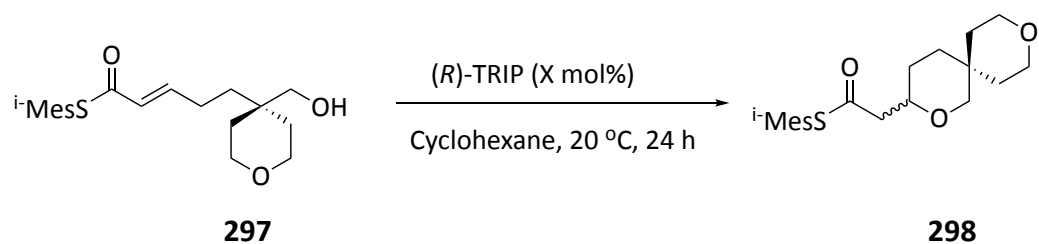
^a Absolute configuration for 3,3'- spiro-THP was assumed to be *S* as it has already determined for the 2,2'-dimethyl substrate.

Table 11. Asymmetric synthesis of spiro-THP **298** with different catalyst loading of (*R*)-TRIP at 50 °C

Initial screening was done by increasing the catalyst loading while keeping the temperature of the reaction constant at 50 °C. The data in table 11, entry 1 shows the previously tested conditions which yielded the (*S*)-enantiomer product. Increasing the catalyst loading of (*R*)-TRIP from 20 mol% up to 40 mol% increased the enantioselectivity of the isolated product up to 66% ee (entries 2 and 3). Running the reaction at 50 °C yielded

the product with an (*S*)-configuration with respect to any catalyst loading even with lower catalyst loading including 15, 10, and 5 mol% (entries 4-6). The absence of the catalyst yield the racemic product (entry 7).

As the enantio-inversion of the reaction outcome was seen by lowering the temperature from 50 to 20 °C, The inversion of the configuration was investigated further by conducting reactions at several catalyst loadings of (*R*)-TRIP at 20 °C (Scheme 78, Table 12).



Scheme 78. Asymmetric synthesis of spiro-THP **298** with different catalyst loading of (*R*)-TRIP at 20 °C

Entry	(<i>R</i>)-TRIP (X mol%)	ee%	Abs. Conf.
1	50	38	<i>S</i> ^a
2	40	32	<i>S</i>
3	30	21	<i>S</i>
4	20	71	<i>R</i>
5	15	68	<i>R</i>
6	10	65	<i>R</i>
7	5	48	<i>R</i>
8	0	0	(±)-Racemic

^a Absolute configuration for 3,3'- spiro-THP was assumed to be *S* as it has already determined for the 2,2'-dimethyl substrate.

Table 12. Asymmetric synthesis of spiro-THP **298** with different catalyst loading of (*R*)-TRIP at 20 °C

The THP product was obtained with an (*S*)-configuration when the reaction was subjected to high catalyst loadings of 30, 40, and 50 mol% at 20 °C (Table 12, entries 1-3). In contrast, subjecting the reaction to 20 mol% of (*R*)-TRIP led to an inversion of the configuration with high enantioselectivity of 71% (entry 4). Lowering the catalyst concentration further down to 5 mol% yielded the THP product with an (*R*)-configuration and an decrease of the enantioselectivity of the isolated product was also seen from 68 to 48 % ee (entries 5-7).

In light of these three studies, the enantio-inversion of the product was observed by either lowering the temperature of the reaction or changing the catalyst concentration. Therefore, we decided to find out if there was something different about the catalyst under these conditions that could explain the inversion that was seen in the absolute configuration of the product.

2.5.2 NMR- spectroscopic investigation of the catalyst species

Inversion being present both at temperature changes and catalyst concentration changes would suggest some monomeric/dimeric catalysis was going on. Thus, NMR-spectroscopic studies were performed with different catalyst loadings and at both 20 and 50 °C. The initial investigation began with running the ³¹P NMR spectrum with a low catalyst loading of 20 mol% at a low temperature of 20 °C. A phosphorus signal was observed at 2.61 ppm (Figure 30), which was confirmed to be the monomer speciation of the catalyst by comparing the phosphorus signal with what has been reported in the literature.⁸⁸

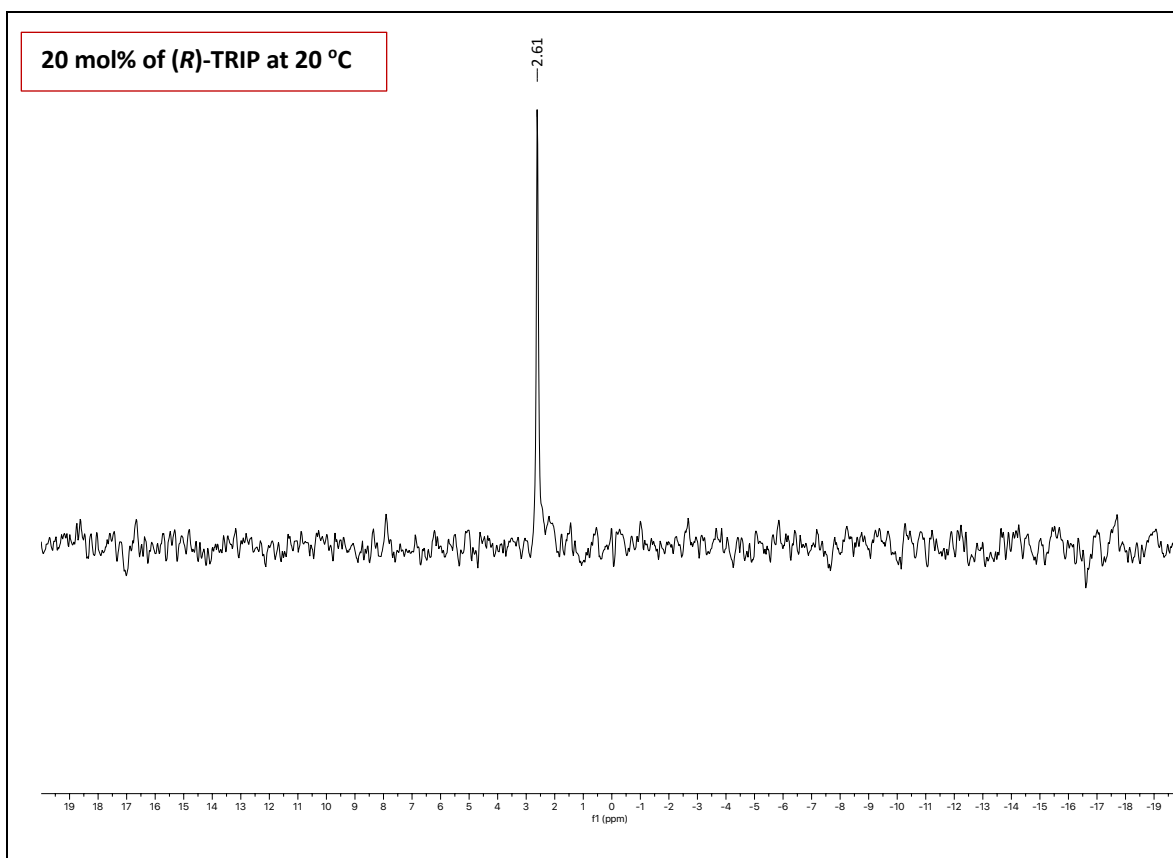


Figure 30. ^{31}P NMR of 20 mol% (R)-TRIP at 20 °C

A shift downfield of the phosphorus signal in the ^{31}P NMR spectrum from 2.82 ppm to 4.97 ppm was seen upon increasing the loading of the catalyst to 50 mol% at 20 °C, which indicated the presence of the dimeric speciation of the catalyst. On the other hand, a signal at 5.13 ppm was observed when the temperature was increased to 50 °C. The presence of the dimeric speciation of the catalyst at high catalyst loading and/or high temperature was indicated by the change in the chemical shift of the phosphorus signals, although the chemical shift of these dimers is not the same (4.97 ppm and 5.13 ppm).

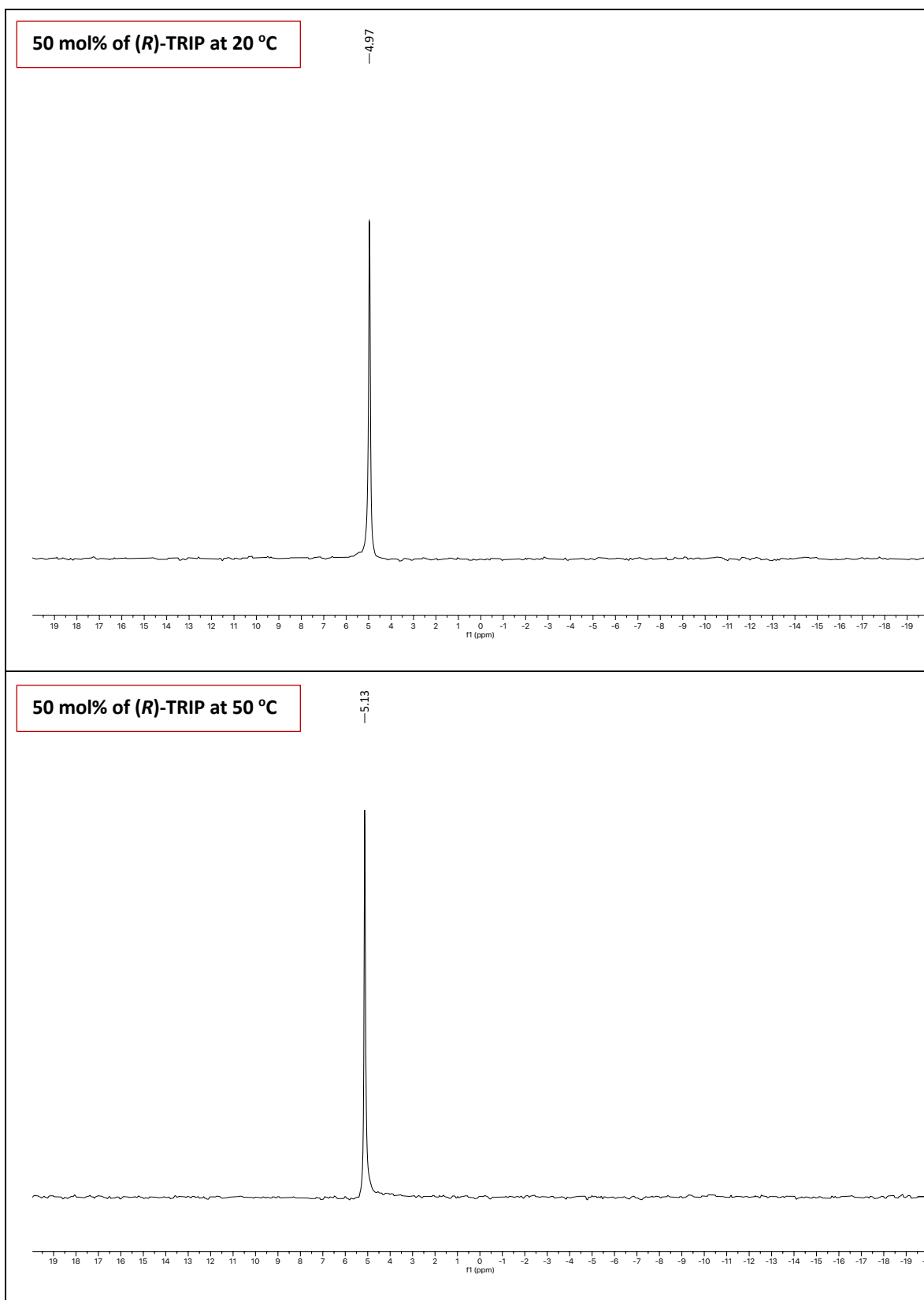
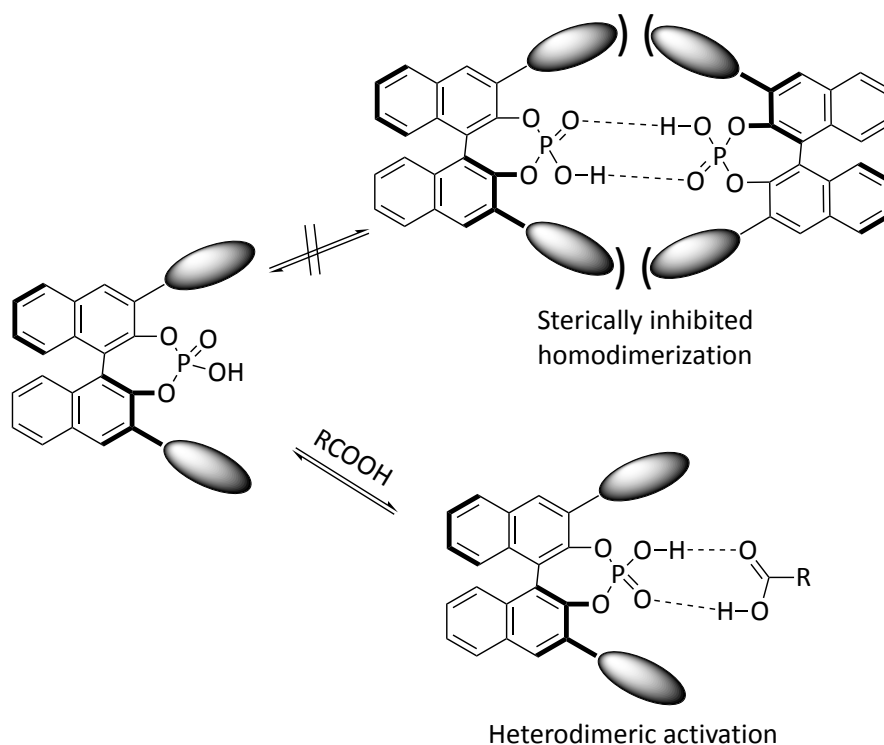


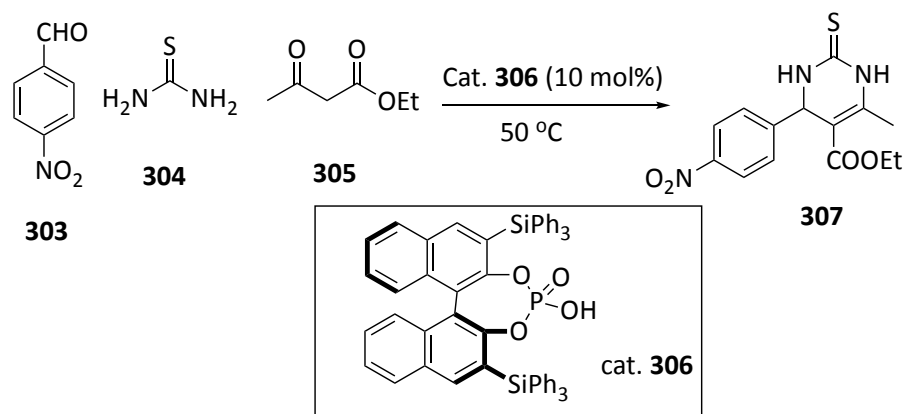
Figure 31. ^{31}P NMR of 20 mol% (R)-TRIP with different catalyst loadings at different temperatures

The presence of monomeric/dimeric speciation in the catalyst was confirmed by NMR spectroscopy. This, however, contradicted what List has reported. He originally reported that homodimerization in sterically demanding catalysts (e.g. 3,3'-disubstituted BINOL-derived catalyst) is sterically disfavored, whereas heterodimerization with small molecules like carboxylic acid is possible (Scheme 79).^{88,89} Due to their intrinsic structural features, sterically demanding catalysts prevent classical donor-acceptor stabilisation, resulting in 'frustrated' Brønsted pairs. In fact, an intramolecular hydrogen bond within the phosphate moiety (between the P=O and P-OH functionalities) is geometrically impossible. At the same time, intermolecular homodimerization is sterically undesirable (Scheme 79). However, these characteristics create a distinct chiral pocket in which heterodimeric associations with small amphoteric molecules are thermodynamically highly favoured, making them particularly effective.



Scheme 79. Chiral sterically demanding phosphoric acids: inhibited homodimerization and novel heterodimeric activation

A literature search was then conducted to find an explanation for our observations and the cause of the enantio-inversion when the reaction was carried out at different catalyst loadings of (*R*)-TRIP. Unlike List, Gong and co-workers demonstrated that the dimerization of phosphoric acid can occur and that asymmetric amplification in reactions catalyzed by phosphoric acids arose from the formation of less soluble supramolecular structures of the racemic phosphoric acid that participate in hydrogen bonds with the crystalline water molecules.⁹⁰ Throughout their research on the phosphoric acid catalyzed Biginelli reaction (Scheme 80), they discovered a strong positive nonlinear effect (NLE) for the reaction of *para*-nitrobenzaldehyde **303**, thiourea **304**, and ethyl acetoacetate **305** in the presence of 10 mol% of the non-enantiopure 3,3'-ditriphenylsilyl binol-derived phosphoric acid **306** in toluene (Figure 32-A). On the other hand, running the same reaction with same conditions except using chloroform for the reaction medium instead of toluene resulted in absolutely linear effect (Figure 32-B). Also, they discovered that highly enantioselective reactions can be observed even with using non-optimally pure phosphoric acids, which led to a strong non-linear effect (Scheme 80).⁹⁰



Scheme 80. Asymmetric amplification in the Biginelli reaction catalyzed by phosphoric acid

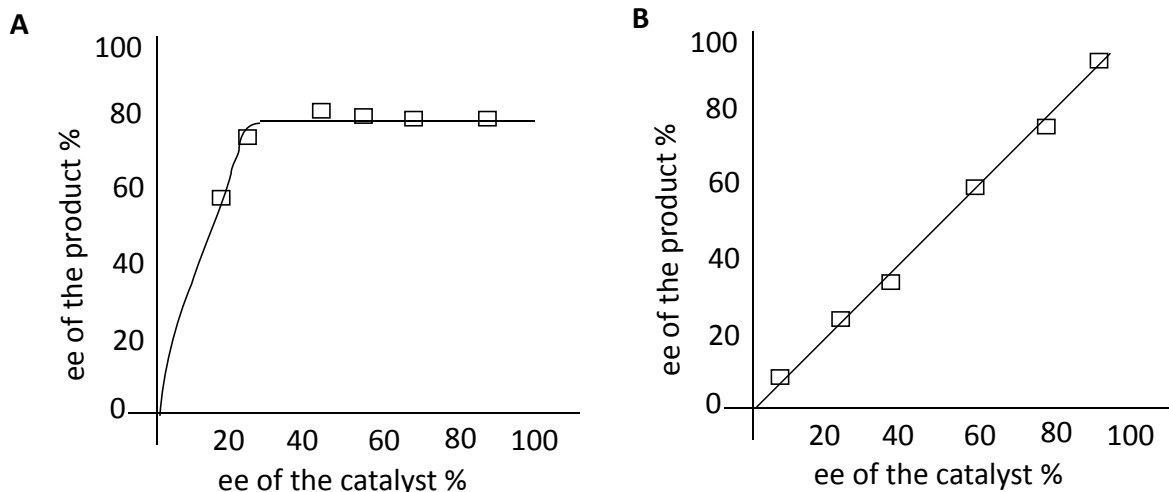


Figure 32. Asymmetric amplification in the Biginelli reaction catalyzed by phosphoric acid
 A: non-linear effect in toluene, B: linear effect in chloroform

In light of this knowledge, as well as the fact that our catalyst, (*R*)-TRIP, was not mentioned in Gong's paper. We decided to investigate the non-linear effect of (*R*)-TRIP.

2.5.3 Non-linear effect of the catalyst (NLE)

In asymmetric catalysis, non-linear effects (NLEs) occur when the enantiomeric excess of the product does not scale linearly with the enantiomeric excess of the catalyst.⁹² In the non-linear effect, the relation between the enantioselectivity of the product and the enantiopurity of the catalyst can be modified as positive or negative non-linear effect (Figure 33).⁹³ In an asymmetric reaction, a positive nonlinear effect, (+)-NLE (Figure 33-red line), is present, resulting in a higher enantioselectivity of the product than predicted by an ideal linear situation (Figure 33-black line). It is also known as asymmetric amplification. In contrast, a negative non-linear effect, known as asymmetric depletion, occurs when a product's enantioselectivity is lower than predicted by an ideal linear situation (Figure 33-blue line).

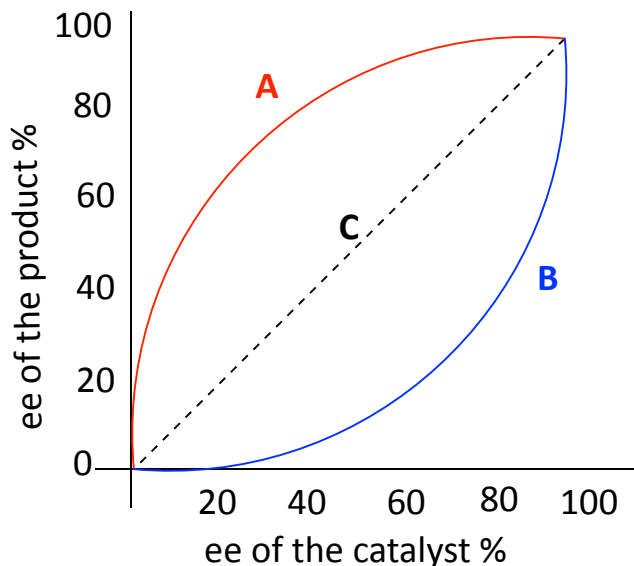
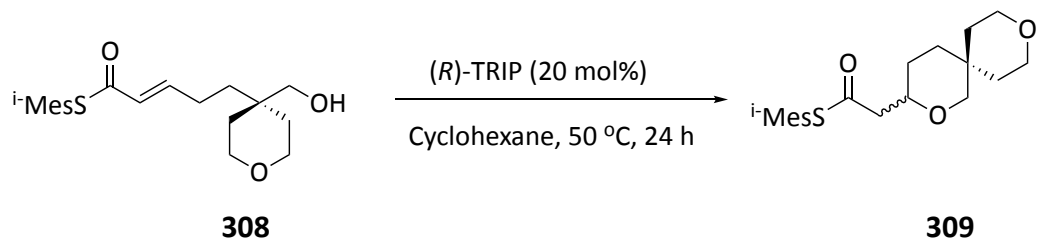


Figure 33. The relation between the enantioselectivity of the product and the enantiopurity of the catalyst

NLEs have been regarded as ubiquitous phenomena that provide additional information about the catalyst's aggregation state or the formation of multiligand species.^{92–94} To that end, the nonlinear effect of (*R*)-TRIP was investigated by running the cyclization reaction at 50 °C with various enantiomeric excesses of (*R*)-TRIP of 100, 75, 50, and 25% ee (Scheme 82). Decreasing the enantiopurity of the catalyst caused a decrease in the enantioselectivity of the products (Table 13). To determine the nonlinear effect of the catalyst, the enantioselectivity of the products were plotted against the enantiopurity of the catalyst. From the plot, it clearly that the catalyst had a positive non-linear effect at 50 °C as shown in Table 13 and by the curve in Figure 34.



Scheme 81. Asymmetric synthesis of spiro-THP **309** with different enantiopurity of (*R*)-TRIP

Entry	Enantiopurity of cat. %	ee%	Abs. conf.
1	100	39	S
2	75	33	S
3	50	24	S
4	25	14	S

Table 13. Asymmetric synthesis of spiro-THP **309** with different enantiopurity of (*R*)-TRIP

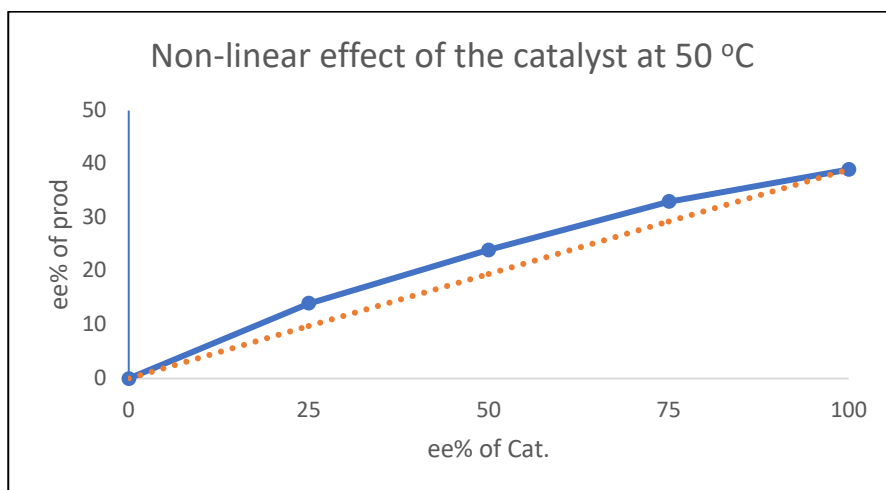
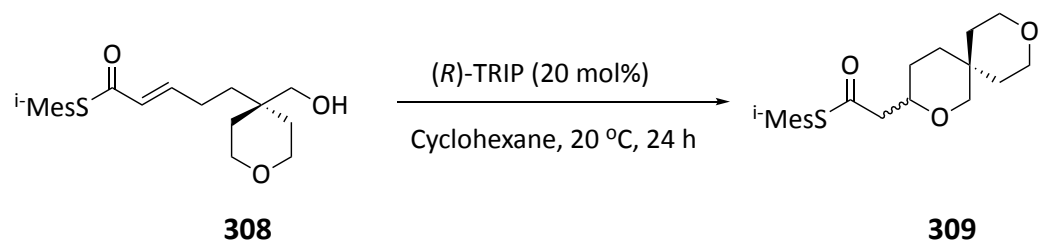


Figure 34. Non-linear effect of (*R*)-TRIP at 50 °C

In parallel, another investigation of the same type in the enantiopurity of the catalyst was carried out at 20 °C (Scheme 83, Table 14). A plot of the enantioselectivities of the products versus the enantiopurity of (*R*)-TRIP was constructed to determine the nonlinear effect of the catalyst. In contrast to the result that was obtained at 50 °C, a greater positive non-linear effect was observed when the temperature of the reaction was lowered to 20 °C (Figure 35).



Scheme 82. Asymmetric synthesis of spiro-THP **309** with different enantiopurity of (*R*)-TRIP

Entry	Enantiopurity of cat. %	ee%	Abs. conf.
1	100	71	<i>R</i>
2	75	65	<i>R</i>
3	50	46	<i>R</i>
4	25	28	<i>R</i>

Table 14. Asymmetric synthesis of spiro-THP **309** with different enantiopurity of (*R*)-TRIP

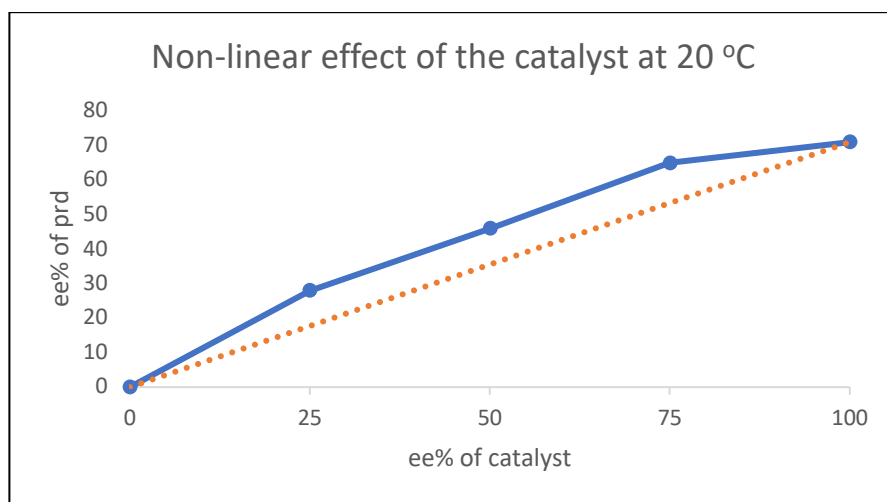


Figure 35. Non-linear effect of (*R*)-TRIP at 50 °C

Even though the nonlinear effect that we observed was not particularly significant, the fact that the heterodimer participated in the solutions demonstrates that

heterodimerization was at least theoretically possible. As a direct consequence of this, we should expect to observe catalyst aggregation. Therefore, a ^{31}P NMR sample of (*R*)-TRIP with 50% ee was submitted. Additional evidence of the catalyst aggregation was provided by the detection of monomeric and dimeric speciation at 2.62 and 5.5 ppm, respectively (Figure 36).

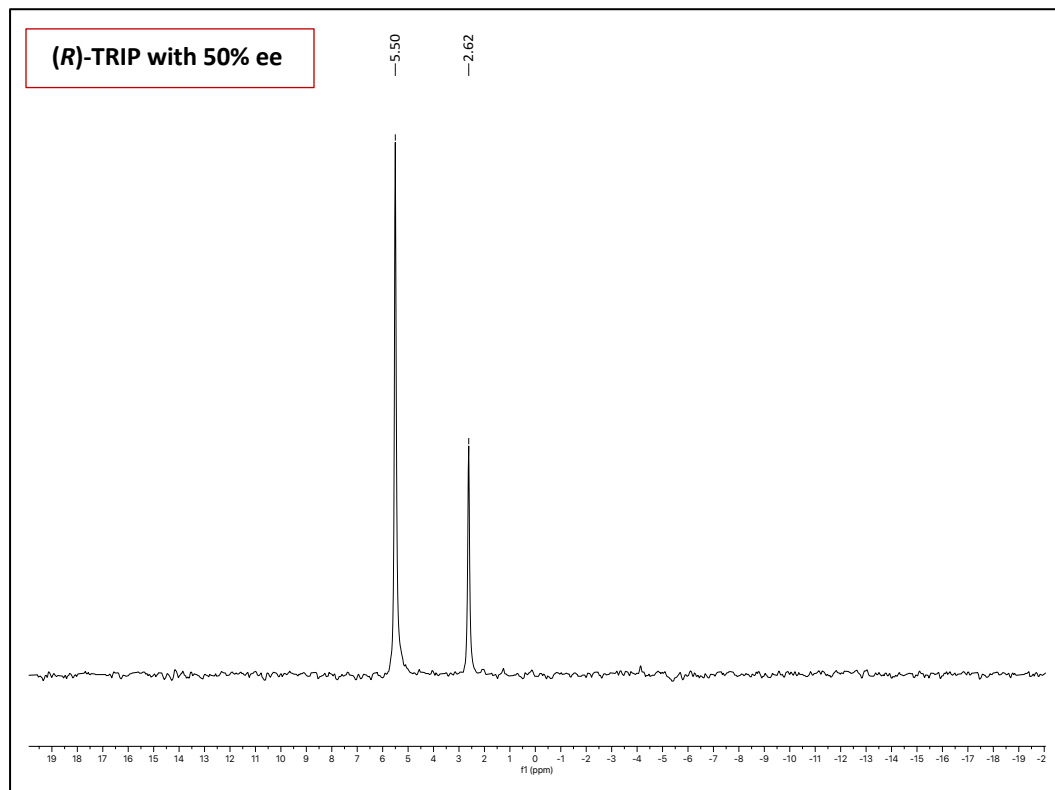


Figure 36. ^{31}P NMR of (*R*)-TRIP with 50% ee

2.5.4 Catalyst orders and aggregation

In such mechanistic scenarios, the order in catalysts is a good indicator of the distribution of the catalyst between monomeric and dimeric species. Orders close to one indicate that a significant percentage of the catalyst is present as the monomeric species, whereas orders close to 0.5 indicate that the majority of the catalyst is present as the inactive dimer. The Variable Time Normalisation Analysis (VTNA) makes use of widely

available concentration-versus-time reaction profiles. Almost any reaction-monitoring technique currently available, such as NMR and HPLC, can directly obtain these profiles. By comparing concentrations to time profiles, the order in the catalyst can be identified. In 2016, Bures reported a simple graphical method to determine the order in catalyst which used a normalized time scale, $t[\text{cat}]^{-n}$, to adjust the entire reaction profile constructed with concentration data (Figure 37).⁹⁵

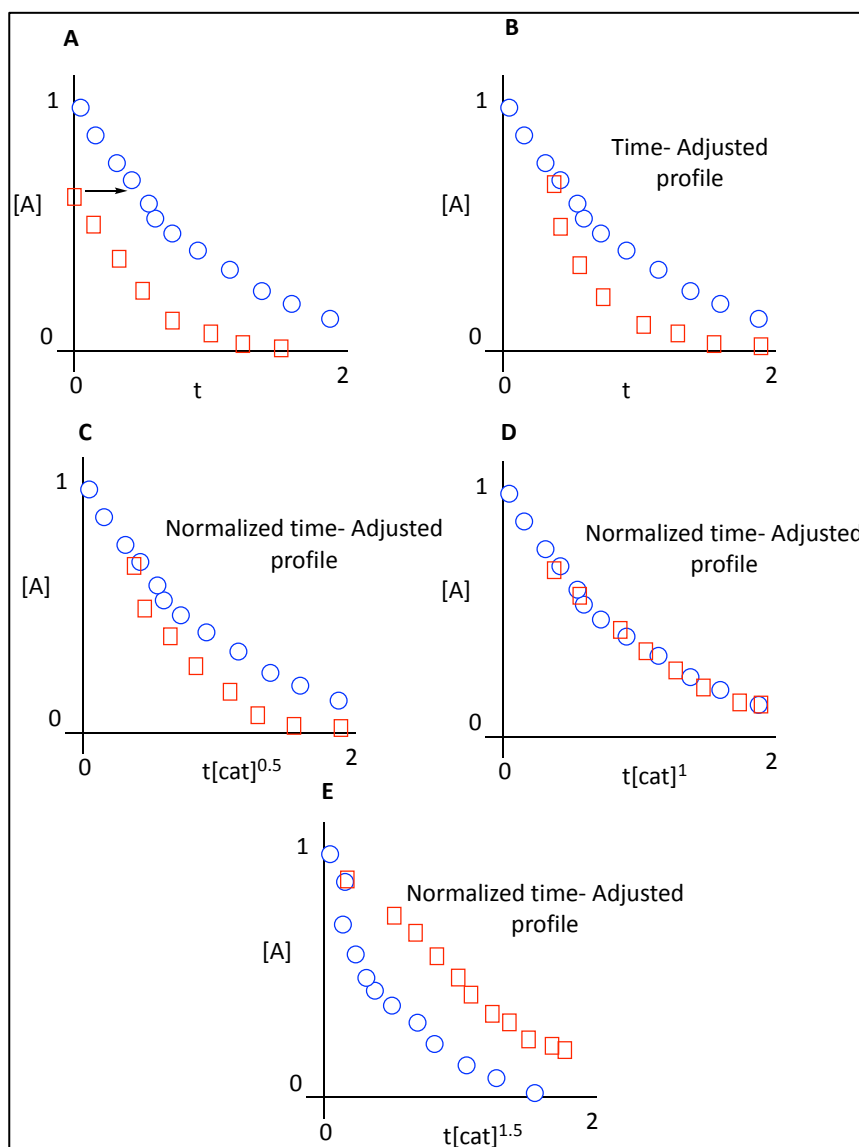


Figure 37. Bures' analysis to determine the order in catalyst

To facilitate a visual comparison between the profiles, the profile of the reaction initiated with a lower concentration of starting materials must be shifted to the right on the time scale until the first point of the profile overlapped with the point of the second profile (Figure 37-B). Each time point was normalised by multiplying it by the total concentrations of catalyst used in each experiment, raised to an arbitrary power (Figure 37, C-E). This power value was tweaked until all of the corrected conversion curves overlapped and that would be the order in catalyst.

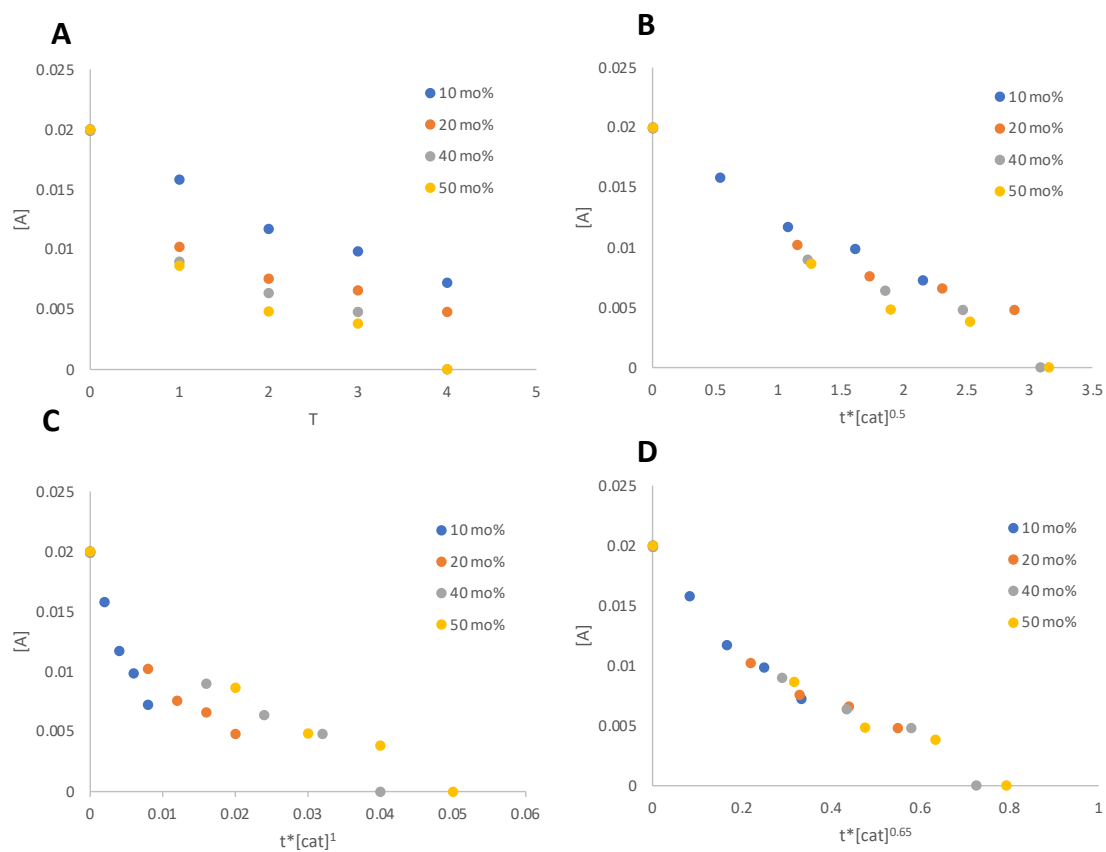


Figure 38. Catalyst order determination at 20 °C: initial rates (A), normalized initial rates with different power values (B, C, D)

A series of experiments with different concentrations of catalyst were used to determine the reaction orders of the catalyst in both regimes. Bures' method was used to give a graphical analysis to determine the order in the catalyst in our reaction. As the enantio-inversion was observed when different catalyst loadings of (*R*)-TRIP was used at 20 °C, the initial analysis used a range loadings of (*R*)-TRIP including 10, 20, 40, and 50 mol% at 20 °C (Figure 38).

Figure 38 depicts the procedures used to determine the order of the catalyst, beginning with a plot of the primary data of starting material concentrations [A] versus time (Figure 38-graph A). After that, the time scale was adjusted by multiplying it by the total concentrations of the catalyst to a power of the catalyst's order (Figure 38, graphs B, C, and D). In this case, the corrected order in catalyst was 0.65, which caused all of the curves to overlap.

Since the enantio-inversion was seen when the catalyst loading was changed, we decided to determine the order in catalyst for each regime separately. The order in the catalyst was calculated to be 0.9 when the reaction was carried out using low catalyst loadings (5, 10, 15, and 20 mol%) at 20 °C (Figure 39-A). In contrast, a catalyst order of 0.5 was seen when higher loadings were used (30, 35, 40, and 50 mol%) at the same temperature 20 °C (Figure 39-B). By increasing the temperature to 50 °C, the calculated order of the catalyst was found to be 0.5 in all catalyst loadings (Figure 39-C and D).

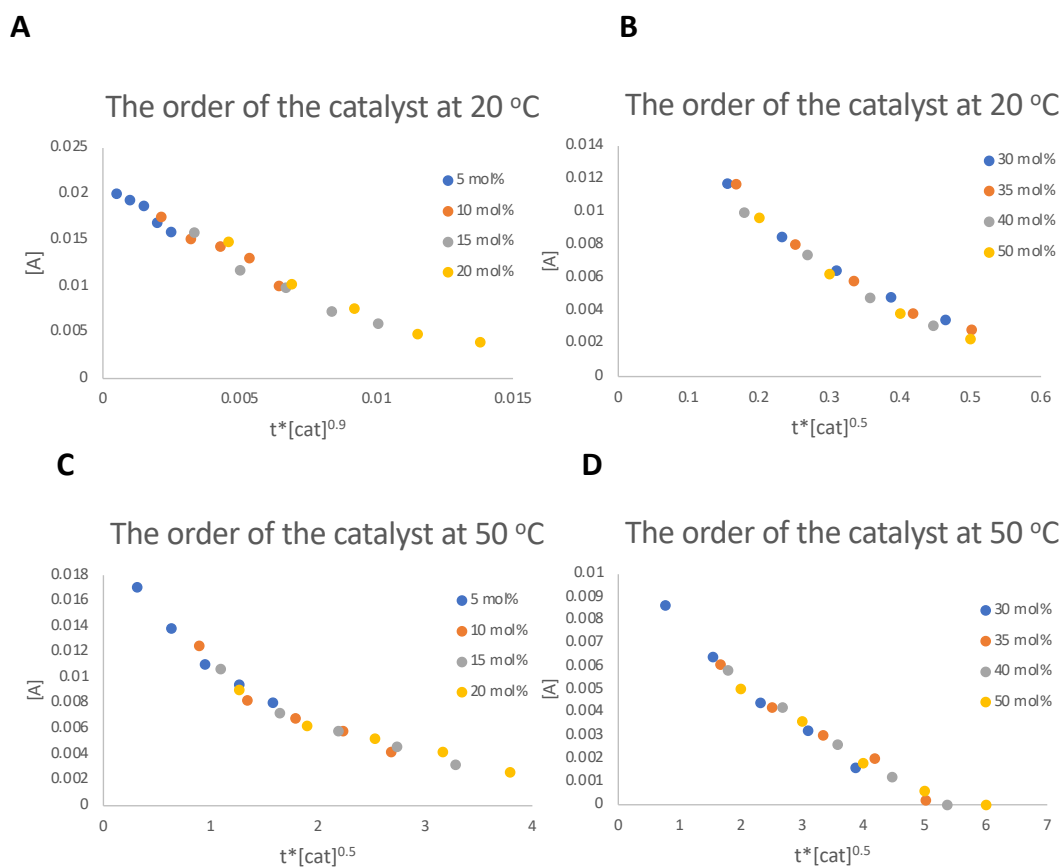


Figure 39. Catalyst order determination: low cat. loadings at 20 °C (A), high cat. loadings at 20 °C (B), Low cat. loadings at 50 °C (C), high cat. loadings at 50 °C (D)

The determination of the order in a catalyst indicated the distribution of the catalyst between monomeric and dimeric species. When the order determined to be close to one, it indicated that a major percentage of the catalyst presented as the monomeric species. On the other hand, orders in the catalyst close to 0.5 indicated that the majority of the catalyst was presented as the inactive dimer.

To draw additional conclusions regarding the catalyst speciation and relative activity of each catalytic species, we expressed the fraction of the starting material consumed by the monomeric species (Y_{mono}) as a function of the order in the catalyst ($\varepsilon_{[\text{cat}]T}^{\text{renant}}$) and the fraction of the catalyst in the monomeric form (f_{mono}) (Figure 40). The plot of this function

is extraordinarily useful for visualising the relative stability and activity of each catalytic species, not only in the extreme limit cases of monomeric catalytic species being the minor catalytic species and the most productive one ($f_{\text{mono}} \approx 0$, $Y \approx 1$, $\varepsilon_{[\text{cat}]T}^{\text{renant}} \approx 0.5$), or being the major catalytic species and the least productive one ($f_{\text{mono}} \approx 1$, $Y \approx 0$, $\varepsilon_{[\text{cat}]T}^{\text{renant}} \approx 2$), but also with more complex scenarios with orders in the catalyst between 0.5 and 2.

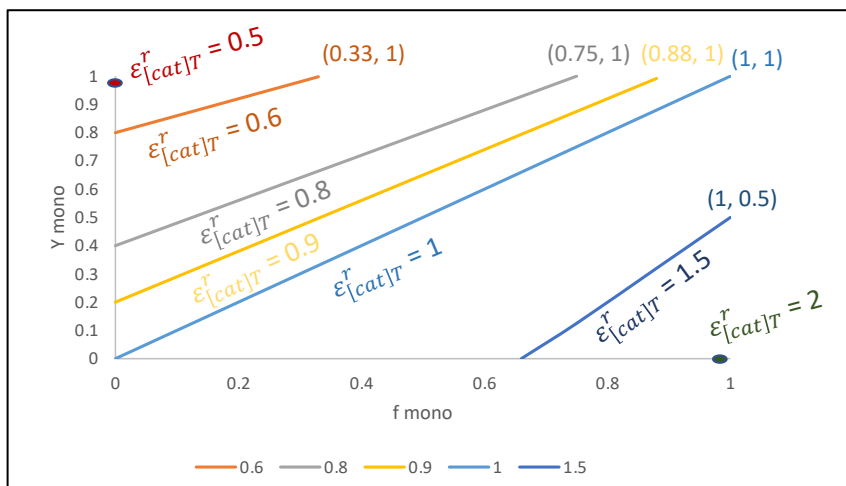


Figure 40. Possible fraction of the catalyst as a monomeric species (f_{mono}) and fraction of the starting material consumed by the monomeric species (Y_{mono}) for different orders of catalyst

In the case when the catalyst order was measured to be 0.9 (Figure 40-Yellow line), we can conclude that at least 12% of the catalyst was present as a dimeric species and the monomeric species consumed at least 20% of the starting material and the dimeric species consumed less than 80% of the starting material (Figure 40).

After that, our attention shifted to investigate if there was a change in the mechanism and the enantioselective determining step of both regimes.

2.5.5 Computational studies and kinetic isotope effect (KIE)

As previously discussed, DFT calculations revealed two possible enantioselective determining steps: cyclization and tautomerization, both of which were predicted to yield the opposite enantiomers. Kinetic isotope effect was calculated for cyclization and tautomerization and predicted to be 1.8 and 6.4 respectively (Figure 41).

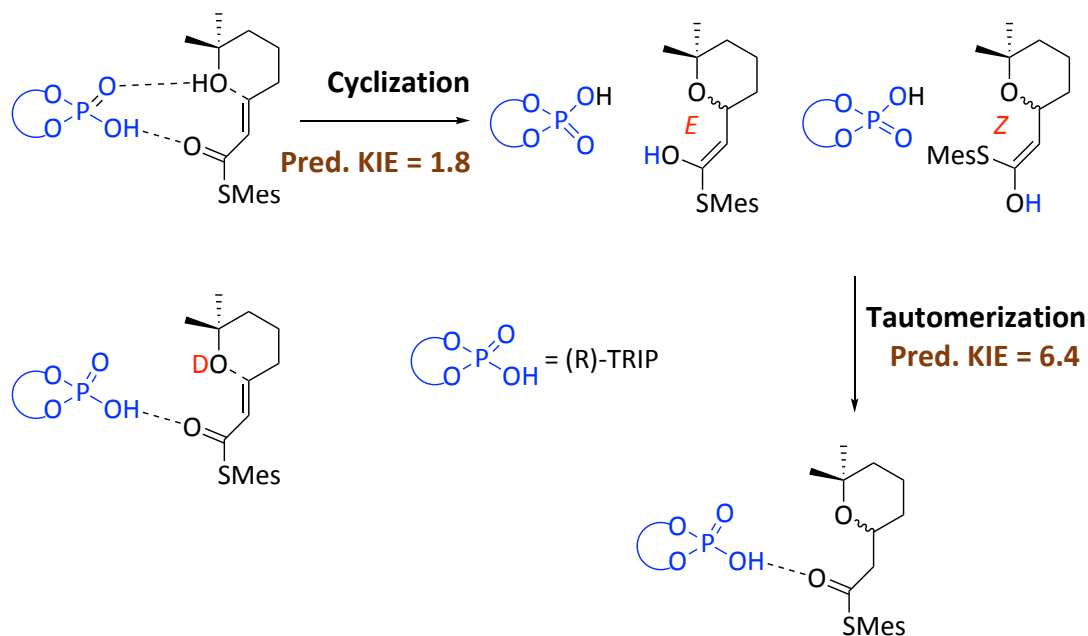


Figure 41. Predicted KIE of the CPA-catalyzed oxa-Michael reaction mechanism

The kinetic isotope effect was calculated experimentally using a deuterated substrate for all regimes (Table 15). The KIE was found to be 1.1 for 50 mol% of catalyst at 20 °C and 1.17 for a low catalyst concentration of 20 mol% at 50 °C, indicating that the cyclization is the enantioselective determining step. On the other hand, with 20 mol% of catalyst at 20 °C, the KIE was found to be 0, and that could be due to D/H exchange occurring on the proton of the cyclizing hydroxyl and that did not participate in the mechanism. To overcome this, we decided to recalculate KIE for all regimes using a deuterated catalyst (Table 15). The KIE of 50 mol% of catalyst at 20 °C and 20 mol% of catalyst at 20 °C using D-(R)-TRIP matched the previous calculations using deuterated substrates and were found to

be 1.11 and 1.23, respectively. In contrast, a KIE of 3.17 was obtained for a low catalyst loading of 20 mol% of catalyst at 20 °C, indicating that tautomerization is the enantioselective determining step in this case. Thus, the observed switch in enantioselectivity can be explained by the change in the mechanism and the enantioselective determining step between regimes.

Entry	Regime	KIE	
		D-substrate	D-(R)-TRIP
1	50 mol% of catalyst at 20 °C	1.1	1.11
2	20 mol% of catalyst at 20 °C	0	3.17
3	20 mol% of catalyst at 50 °C	1.17	1.23

Table 15. Calculated KIE of the CPA-catalysed oxa-Michael reaction mechanism at different regimes

After explaining the reason that caused the enantio-inversion, the only thing that we were not sure about was the reason behind observing dimer species of catalyst at higher temperatures. We suspected that it might be an enthalpic contribution. As a result, the next step was to compute ΔS^\ddagger and ΔH^\ddagger for both regimes.

2.5.6 Determination of ΔH and ΔS

The Eyring equation used in chemical kinetics to describe changes in the rate of a chemical reaction against temperature. An Eyring plot allows the activation parameters ΔS^\ddagger and ΔH^\ddagger to be determined from the temperature dependence of the rate constant. A series of experiments with different temperatures were used to determine the activation parameters in both regimes using Eyring plot. The linear form of the Eyring Equation is given below:

$$\ln \frac{k}{t} = \frac{-\Delta H^\ddagger}{RT} + \ln \frac{k_b}{h} + \frac{\Delta S^\ddagger}{R}$$

Where k is the rate constant, t is temperature, ΔH^\ddagger is activation enthalpy, R is ideal gas constant, K_b is Boltzmann constant, h is Plank constant, and ΔS^\ddagger is the activation entropy.

The values for ΔS^\ddagger and ΔH^\ddagger can be determined from kinetic data obtained from a $\ln \frac{k}{t}$ vs $\frac{1}{T}$ plot. The equation is represented by straight line with a negative slope, $\frac{-\Delta H^\ddagger}{R}$, and a y-intercept, $\ln \frac{k_b}{h} + \frac{\Delta S^\ddagger}{R}$. In order to determine the activation parameters, both regimes were plotted (Figure 42) and consequently the activation parameters ΔH^\ddagger and ΔS^\ddagger can be calculated using the values of the slope and intercept, respectively (Table 16).

The initial investigation was carried out by running the reaction at different temperatures, which were 15 °C, 20 °C, and 25 °C, as the products of these reaction temperatures were obtained with the same absolute configuration. At regular intervals (1 hour), the reaction mixture was analyzed by ^1H NMR to monitor the formation of the products and the consumption of the starting materials over time and consequently determine the rate of the reaction by plotting the concentration of the starting material versus the time (Figure 42).

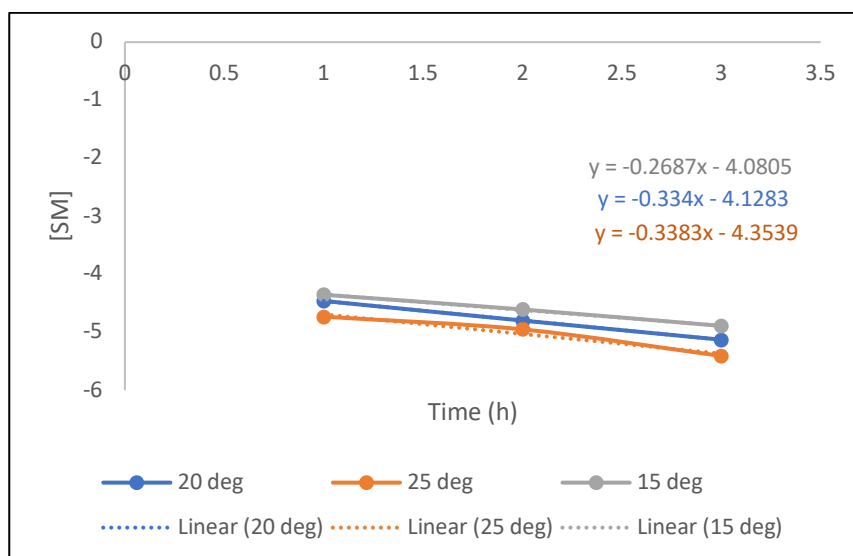


Figure 42. Rate of reaction under various temperature conditions

Using the kinetic data of the reactions conducted at 15 °C, 20 °C, and 25 °C, an Eyring plot ($\ln \frac{k}{T}$ vs $\frac{1}{T}$) was plotted (Figure 43). The values of the slope and intercept were used further to calculate the activation parameters ΔH^\ddagger and ΔS^\ddagger , respectively (Table 16).

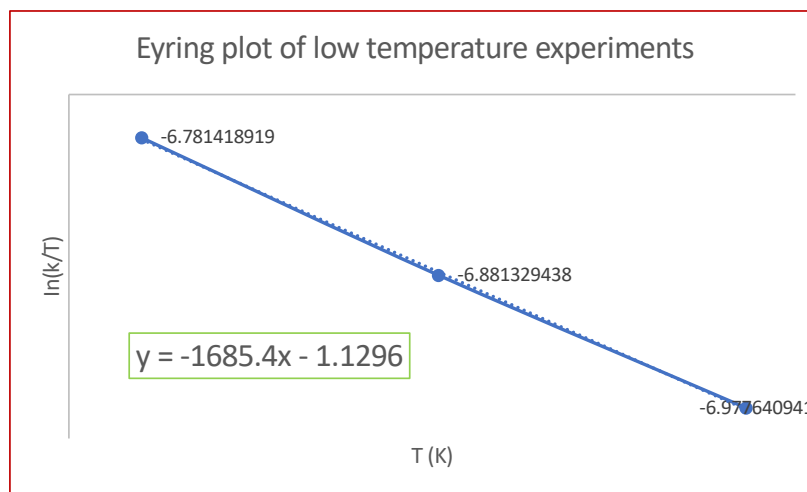


Figure 43. Eyring plot at low temperature reactions

On the other hand, a set of reactions were carried out at higher temperatures, 35 °C, 40 °C, and 50 °C, to determine how temperature changes affect the activation parameters by increasing the temperatures (Figure 44). The reaction mixture was analyzed by ^1H NMR at regular intervals (20 min) to calculate the conversion and, as a result, determine the rate of the reaction by plotting the concentration of the starting material versus time (Figure 44-A). Following that, an Eyring plot was created to allow the activation parameters to be determined (Figure 44-B).

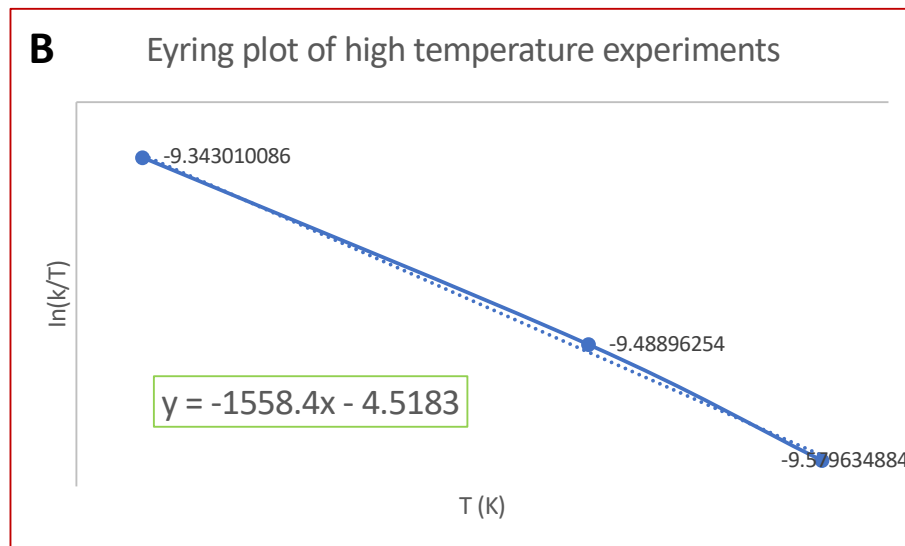
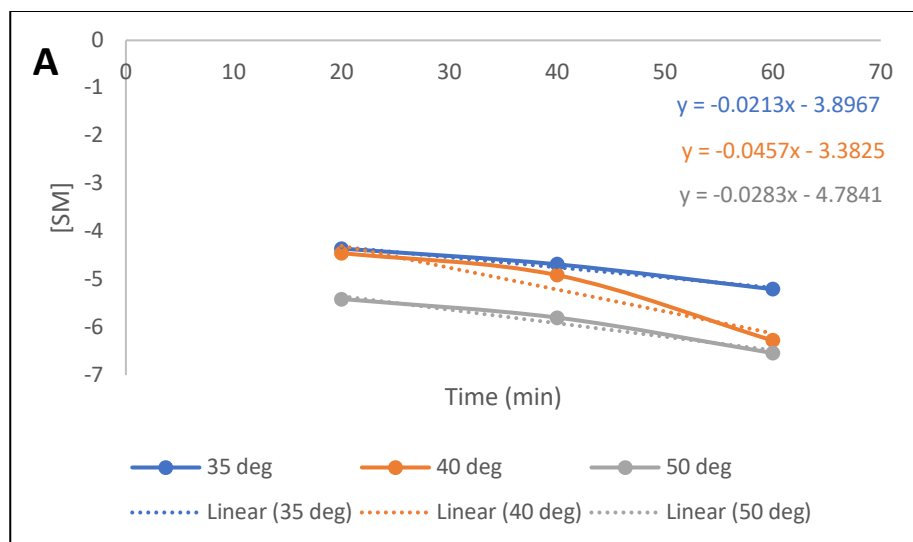


Figure 44. A: Rate of reaction under various temperature conditions

B: Eyring plot at high temperature reactions

After plotting an Eyring plot of both regimes, the activation parameters ΔH^\ddagger and ΔS^\ddagger were determined using the values of the slopes and intercepts, respectively (Table 16).

Entry	Regime	ΔH^\ddagger (KJ/mol)	ΔS^\ddagger (J/mol.K)
1	Low temperature	14.01	-206.94
2	High temperature	12.96	-235.12

Table 16. The calculated activation parameters for both regimes

The results in Table 16 showed that the activation enthalpy was constant in both regimes and was found to be 14.01 for low temperature and 12.96 for high temperature. Furthermore, the activation entropy becomes more negative with increasing the reaction temperature, indicating that the transition state is more ordered with higher temperatures.

2.5.7 Summary of results

When the spiro-THP substrate was subjected to the optimal cyclization conditions, the THP product was obtained with only 40% ee. The low enantioselectivity of the product was caused by the uncatalyzed background reaction. To address this issue, the reaction was altered by either lowering the temperature of the reaction or increasing the amount of catalyst used.

When the reaction was carried out at lower temperatures, the enantioselectivity of the product decreased. Surprisingly, running the reaction at 20 °C resulted in a product with a higher enantioselectivity of 71 % ee and an inversion of the absolute configuration. On the other hand, changing the catalyst loading at 50 °C did change the enantioselectivity of the product; however, the absolute configuration remained constant across all catalyst loadings. In contrast to the result obtained at 50 °C, an inversion of the configuration was observed by the change in the catalyst concentrations when the reaction was conducted at 20 °C. Higher catalyst loadings yielded the (*S*)-enantiomer, whereas the low catalyst loadings produced the (*R*)-enantiomer.

A further investigation was conducted to explain the enantio-inversion observation of all regimes. It was found that the catalyst existed as a dimer at both regimes (50 mol% , 20 °C and 20 mol%, 50 °C). Moreover, at both regimes, the order in the catalyst was calculated to be 0.5, indicating that the reaction was catalysed by a small amount of monomer. The cyclization was the rate and stereochemistry determining step, as confirmed by KIE studies.

At 20 mol% and 20 °C, the catalyst existed as a monomer as shown by ³¹P NMR and confirmed by having an order in the catalyst of 0.9. Furthermore, KIE studies revealed that tautomerization was the rate and enantioselective determining step in this case.

3 Conclusion

A novel asymmetric synthesis of substituted tetrahydropyrans catalysed by chiral phosphoric acid *via* the oxa-Michael reaction has been developed. The development of a methodology involved extensive optimisation of reaction conditions. The use of chiral phosphoric acid enabled excellent yields from the start, but other parameters needed to be adjusted in order to improve the enantioselectivity. It was discovered that increasing the steric bulk of the thioester led to the formation of a product with excellent yield and enantioselectivity.

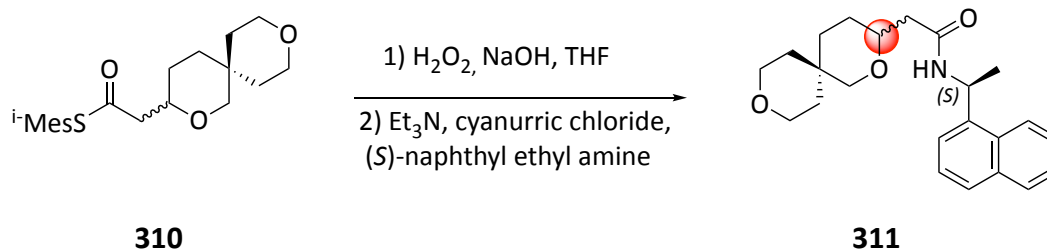
The scope of the cyclisation was demonstrated by the synthesis of a variety of 2,2'- and 3,3'-spirocyclic and disubstituted tetrahydropyrans using the optimised conditions of (*R*)-TRIP in cyclohexane at 50 °C. In general, high enantioselectivity was obtained for 2,2'-substituted THPs, whereas lower enantioselectivity was observed in some of 3,3'-substituted THPs and that was due to the uncatalyzed background reaction. The conditions for transesterification for the 2,2'-dimethyl THP thioester were found, and the formation of the methyl ester allowed the absolute stereochemistry to be assigned as (*S*).

Modifying the reaction conditions of the 3,3'-sipro-THP substrate, either by lowering the temperature or increasing the catalyst concentration, was conducted to minimize the uncatalyzed background reaction. Lowering the temperature of the reaction to 20 °C resulted in an inversion of the absolute configuration of the product. On the other hand, increasing the catalyst concentrations at 50 °C increased the enantioselectivity of the product with constant absolute configuration across all the catalyst loadings. Changing the catalyst loadings at 20 °C caused the enantio-inversion of the reaction outcomes. An additional investigation was carried out to explain the observed enantio-inversion in all regimes. The catalyst was discovered to exist as a dimer in both regimes (50 mol%, 20 °C and 20 mol%, 50 °C) with order in the catalyst of 0.5 in both regimes. The KIE studies confirmed that cyclization was the rate and stereochemistry determining step. In contrast, the catalyst existed as a monomer at 20 mol% and 20 °C and order in the catalyst of 0.9.

Furthermore, KIE studies revealed that in this case, tautomerization was the rate and enantioselective determining step.

4 Future Work

With promising results have been obtained with the enantio-inversion experiment, the next step is to investigate the hydrolysis of the thioester and derivatise the acid to form THP **311** (Scheme 84).

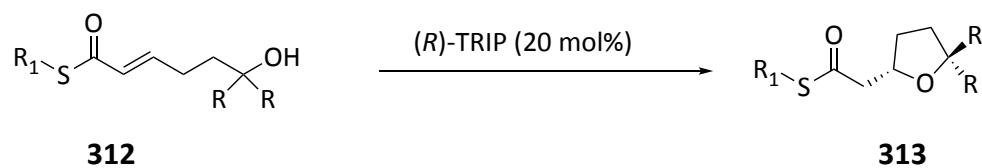


Scheme 83. Possible conditions to derivatise THP 308

The key to this synthesis is to determine the absolute configuration of the THP **310**. The original assignment of the absolute stereochemistry was based on the original DFT calculations of the 2,2'-dimethyl THP thioester substrate and comparison with known 2,2'-dimethyl THP methyl ester. The DFT calculations predicted the *S* enantiomer and the major enantiomer was confirmed as *S*. In fact, we actually have no evidence that the 3,3'-system actually cyclise to give the same absolute stereochemistry as the 2,2'-system. Thus, determination of the absolute configuration of 3,3'-system is required. In addition, one of the question that left unanswered was that is spiro-THP the only substrate showed enantio-inversion of the reaction outcomes by either temperature or catalyst concentration changes. Substrate scope could be extended including carbocyclic and heterocyclic substitutions.

Another area of interest is the use of the α,β -unsaturated thioester as a Michael acceptor in the cyclisation of tetrahydrofuran (Scheme 85). Although modifications to the procedure may be required, the selectivity observed in the THP cyclisation has the potential

to form enantioenriched THF. Changing the thioester's substitution may be required to improve yields or selectivity, but this tuning ability is what makes the thioester an appealing motif.



Scheme 84. Potential application of use of α,β -unsaturated thioester as a Michael acceptor for the synthesis of THF

5 Experimental

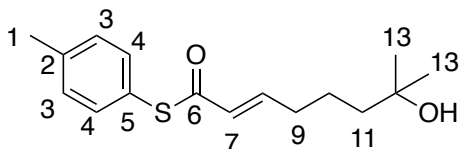
5.1 General Experimental

Unless otherwise noted all compounds were bought from commercial suppliers and used without further purification. Where a solvent is described as “dry” it was purified by PureSolv alumina columns from Innovative Technologies. Melting points were determined using a Stuart SMP3 apparatus. Infra-red spectra were acquired on a ThermoNicolet Avatar 370 FT-IR spectrometer. Nuclear magnetic resonance spectra were recorded on a Jeol ECS-400, a Jeol 500 Avance III HD 500 or a Jeol AV500 at ambient temperature. Coupling constants (J) are quoted in Hertz. Mass spectrometry was performed by the University of York mass spectrometry service using electron spray ionisation (ESI) technique. Thin layer chromatography was performed on glass-backed plates coated with Merck Silica gel 60 F₂₅₄. The plates were developed using ultraviolet light, acidic aqueous ceric ammonium molybdate or basic aqueous potassium permanganate. Liquid chromatography was performed using forced flow (flash column) with the solvent systems indicated. The stationary phase was silica gel 60 (220–240 mesh) supplied by Fluorochem or silica gel Merck TLC grade 11695 supplied by Sigma-Aldrich. NMR assignments were made using 2D NMR including COSY, HMBC, HSQC techniques which can be accessed at DOI: 10.15124/8ff9123f-ee1a-4ae2-a60e-7626c989e5a0. All numbering on the structures below is for the benefit of characterization and does not necessarily conform to IUPAC rules.

5.2 Experimental Details for the 'Clip-Cycle' Reactions

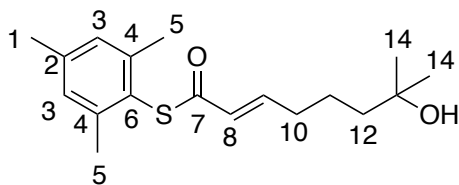
5.2.1 Synthesis of 'Clip-Cycle' Precursors

(*E*)-*S*-*p*-Tolyl 7-hydroxy-7-methyloct-2-enethioate (**184**)



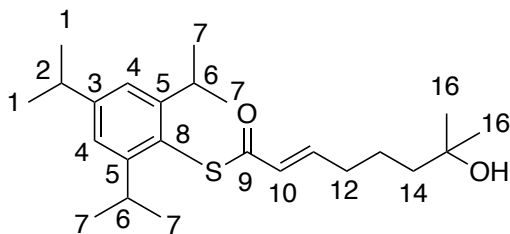
A solution of unsaturated alcohol **188** (102 mg, 0.80 mmol, 1.0 eq) and thioester **183** (427 mg, 2.40 mmol, 3.0 eq) were dissolved in dry Et₂O (5 mL) under a nitrogen atmosphere. To this, copper (I) iodide (15.3 mg, 0.08 mmol, 10 mol%) and Hovyeda-Grubbs 2nd generation catalyst (50.2 mg, 0.08 mmol, 10 mol%) were added as solids in a single portion and the mixture was stirred at 40 °C for 24 hours. The mixture was then concentrated and purified by column chromatography on silica using 10-15 % ethyl acetate in n-hexane to yield **184** as a brown oil (193 mg, 87% yield). ¹H NMR (400 MHz, CDCl₃): δ 7.31 (2H, d, *J* = 8.0 Hz, H-3), 7.21 (2H, d, *J* = 8.0 Hz, H-4), 6.97 (1H, dt, *J* = 15.6 Hz, 7.0 Hz, H-8), 6.17 (1H, dt, *J* = 15.6 Hz, 1.4 Hz, H-7), 2.36 (3H, s, H-1), 2.27-2.21 (2H, m, H-9), 1.61-1.55 (2H, m, H-11), 1.53-1.46 (2H, m, H-10), 1.22 (6H, s, H-13) ppm; ¹³C NMR (101 MHz, CDCl₃): δ 188.7 (C-6), 146.3 (C-7), 139.7 (C-2), 134.7 (C-4), 130.1 (C-3), 128.2 (C-8), 124.1 (C-5), 70.9 (C-12), 43.3 (C-11), 32.7 (C-9), 29.4 (C-13), 22.9 (C-10), 21.4 (C-1) ppm; IR (film NaCl): ν_{max} 3383, 2964, 2924, 2853, 1687, 1631, 1494, 1464, 1398, 1376, 1284, 1160, 1017, 972, 807 cm⁻¹; HRMS (ESI): *m/z* calcd for C₁₆H₂₂NaO₂S⁺ (M+Na)⁺ 301.1233; found 301.1230.

(*E*)-*S*-Mesityl 7-hydroxy-7-methyloct-2-enethioate (**196**)



196 was synthesised using the same procedure as **184** with unsaturated alcohol **188** (76.8 mg, 0.61 mmol, 1.0 eq), thioester **192** (373 mg, 1.81 mmol, 3.02 eq), copper (I) iodide (11.5 mg, 0.06 mmol, 10 mol%) and Hovyeda-Grubbs 2nd generation catalyst (37.6 mg, 0.06 mmol, 10 mol%) The mixture was purified by column chromatography on silica using 10% ethyl acetate in petroleum ether to yield **196** as a brown oil (158 mg, 86% yield). ¹H NMR (400 MHz, CDCl₃): δ 7.00-6.92 (3H, m, H-3, H-9), 6.22 (1H, d, *J* = 15.6 Hz, H-8), 2.32 (6H, s, H-5), 2.31 (3H, s, H-1), 2.28-2.21 (2H, m, H-10), 1.60-1.47 (4H, m, H-11, H-12), 1.22 (6H, s, H-14) ppm; ¹³C NMR (101 MHz, CDCl₃): δ 187.9 (C-7), 145.9 (C-9), 142.8 (C-4), 140.0 (C-2), 129.3 (C-3), 128.3 (C-8), 123.6 (C-6), 71.0 (C-13), 43.4 (C-12), 32.7 (C-10), 29.4 (C-14), 22.9 (C-11), 21.7 (C-5), 21.3 (C-1) ppm; IR (film NaCl): ν_{max} 3412, 2969, 2940, 1684, 1631, 1464, 1375, 1284, 1156, 1040, 972, 907, 851, 799, 765, 715 cm⁻¹; HRMS (ESI): *m/z* calcd for C₁₈H₂₆NaO₂S⁺ (M+Na)⁺ 329.1546; found 329.1551.

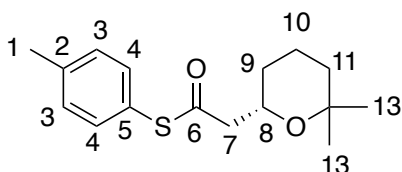
(*E*)-S-(2,4,6-Triisopropylphenyl) 7-hydroxy-7-methyloct-2-enethioate (214**)**



214 was synthesised using the same procedure as **184** with unsaturated alcohol **188** (76.8 mg, 0.60 mmol, 1.0 eq), thioester **213** (373 mg, 1.81 mmol, 3.0 eq), copper (I) iodide (4.2 mg, 0.02 mmol, 10 mol%) and Hovyeda-Grubbs 2nd generation catalyst (13.7 mg, 0.02 mmol, 10 mol%) The mixture was purified by column chromatography on silica using 10% ethyl acetate in n-hexane to yield **214** as a brown oil (216 mg, 92% yield). ¹H NMR (400 MHz, CDCl₃): δ 7.07 (2H, s, H-4), 6.96 (1H, dt, *J* = 17.5 Hz, 6.7 Hz, H-11), 6.23 (1H, d, *J* = 17.5 Hz, H-10), 3.39 (2H, sept, *J* = 6.9 Hz, H-6), 2.90 (1H, sept, *J* = 6.9 Hz, H-2), 2.28-2.21 (2H, m, H-12), 1.95-1.55 (2H, m, H-14), 1.53-1.48 (2H, m, H-13), 1.25 (6H, d, *J* = 6.9 Hz, H-1), 1.23 (6H, s, H-16), 1.17 (12H, d, *J* = 6.9 Hz, H-7) ppm; ¹³C NMR (101 MHz, CDCl₃): δ 189.0 (C-9), 152.7 (C-5), 151.1 (C-3), 145.7 (C-11), 128.2 (C-10), 122.1 (C-4), 121.6 (C-8), 71.0 (C-15), 43.5 (C-14),

34.5 (C-2), 32.8 (C-12), 32.0 (C-6), 29.4 (C-16), 24.5 (C-13), 24.0 (C-7), 22.9 (C-1) ppm; IR (ATR): ν_{\max} 3412, 2969, 2940, 1684, 1631, 1464, 1375, 1284, 1156, 1040, 972, 907, 851, 799, 765, 715 cm^{-1} ; HRMS (ESI): m/z calcd for $\text{C}_{24}\text{H}_{38}\text{NaO}_2\text{S}^+$ ($\text{M}+\text{Na}$) $^+$ 413.2485; found 413.2488.

***S*-*p*-Tolyl-2-(6,6-dimethyltetrahydro-2*H*-pyran-2-yl)ethanethioate (**185**)**



Racemic-CSA

To a solution of **184** (28.9 mg, 0.10 mmol) in DCE (5 mL), a portion of CSA (73.0 mg, 0.31 mmol, 3 eq) was added and heated under reflux at 80 °C for 24 hours. The reaction was quenched with Et_3N (1.0 mL), washed with NaHCO_3 solution (2 x 5 mL) and brine solution (2 x 5 mL), dried over anhydrous Na_2SO_4 and filtered. The filtrate was concentrated *in vacuo* to give a crude yellow oil. The oil was purified by column chromatography on silica using 5% Et_2O in hexane to yield **185** as a yellow oil (13.0 mg, 45 % yield).

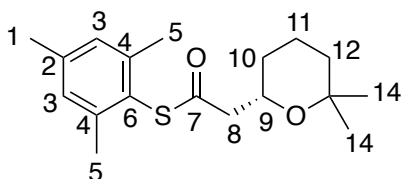
Asymmetric-(*R*)-TRIP, 50 °C, cyclohexane

The cyclization precursor **184** (18.5 mg, 0.07 mmol) was dissolved in cyclohexane (3.3 mL). To this, (*R*)-TRIP **199** (10.1 mg, 0.01 mmol, 20 mol %) was added and stirred at 50 °C under a nitrogen atmosphere for 24 hours. The reaction mixture was quenched by (0.2 ml) of Et_3N then concentrated *in vacuo* and purified by column chromatography on silica using 5% Et_2O in hexane to yield the product as a yellow oil (10.4 mg, 56% yield, 18% ee).

^1H NMR (400 MHz, CDCl_3): δ 7.27 (d, 2H, $J = 8.1$ Hz, H-3), 7.20 (2H, d, $J = 8.1$ Hz, H-4), 4.04 (1H, dddd, $J = 11.5$ Hz, 6.6 Hz, 4.1 Hz, 2.7 Hz, H-8), 2.82 (1H, dd, $J = 14.8$ Hz, 6.6 Hz, H-7), 2.64 (1H, dd, $J = 14.8$ Hz, 4.1 Hz, H-7), 2.36 (3H, s, H-1), 1.67-1.61 (3H, m, H-9, H-10), 1.45-1.32 (2H, m, H-11), 1.19 (3H, s, H-13), 1.18 (3H, s, H-13), 1.13 (1H, m, H-10) ppm; ^{13}C NMR (101 MHz, CDCl_3): δ 196.1 (C-6), 139.7 (C-2), 134.5 (C-4), 130.1 (C-3), 124.5 (C-5), 72.4 (C-12), 67.6 (C-8), 50.8 (C-7), 35.9 (C-11), 31.8 (C-13), 31.3 (C-9), 21.9 (C-1), 21.4 (C-13'), 19.9 (C-10) ppm;

IR (film NaCl): ν_{\max} 2973, 2928, 1707, 1494, 1460, 1379, 1360, 1281, 1213, 1137, 1065, 1043, 974, 900, 867, 806, 746 cm^{-1} ; HRMS (ESI): m/z calcd for $\text{C}_{16}\text{H}_{22}\text{NaO}_2\text{S}^+$ ($\text{M}+\text{Na}$)⁺ 301.1233; found 301.1227; $[\alpha]_{\text{D}}^{20} + 6.1^\circ$ (c 0.52, CHCl_3), for 18% ee.

S-Mesityl 2-(6,6-dimethyltetrahydro-2H-pyran-2-yl)ethanethioate (197)



Racemic-CSA

197 was synthesised using the same procedure as **185** with alcohol-thioester **196** (18.5 mg, 0.06 mmol) and rac- CSA (41.7 mg, 0.18 mmol, 3 eq.) The crude was purified by column chromatography on silica using 5% Et_2O in hexane to yield **197** as a yellow oil (17.0 mg, 92 % yield).

Asymmetric-(R)-TRIP, 50 °C, PhMe

197 was synthesised using the same procedure as **185** with alcohol-thioester **196** (20.0 mg, 0.07 mmol) and (R)-TRIP **199** (9.91 mg, 0.01 mmol, 20 mol %). The crude was purified by column chromatography on silica using 5% Et_2O in hexane to yield **197** as a yellow oil (13.4 mg, 66% yield, 60% ee).

Asymmetric-(R)-TRIP, 50 °C, cyclohexane

197 was synthesised using the same procedure as **185** with alcohol-thioester **196** (18.7 mg, 0.07 mmol) and (R)-TRIP **199** (9.32 mg, 0.01 mmol, 20 mol %). **197** yielded as a yellow oil (16.8 mg, 90% yield, 69% ee).

Asymmetric-(R)-TRIP, 75 °C, cyclohexane

197 was synthesised using the same procedure as **185** with alcohol-thioester **196** (19.8 mg, 0.07 mmol) and (*R*)-TRIP **199** (9.81 mg, 0.01 mmol, 20 mol %). **197** yielded as a yellow oil (17.9 mg, 90% yield, 66% ee).

Asymmetric-(R)-TIPSY, 50 °C, cyclohexane

197 was synthesised using the same procedure as **185** with alcohol-thioester **196** (14.6 mg, 0.05 mmol) and (*R*)-TIPSY **200** (8.6 mg, 0.01 mmol, 20 mol %). **197** yielded as a yellow oil (3.1 mg, 22% yield, 40% ee).

Asymmetric-(R)-anthr, 50 °C, cyclohexane

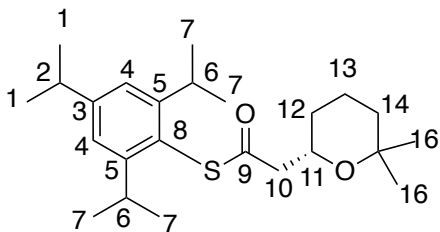
197 was synthesised using the same procedure as **185** with alcohol-thioester **196** (12.5 mg, 0.04 mmol) and (*R*)-Anth **201** (5.8 mg, 0.01 mmol, 20 mol %). **197** yielded as a yellow oil (11.9 mg, 95% yield, 21% ee).

Asymmetric-(R)-phenanth, 50 °C, cyclohexane

197 was synthesised using the same procedure as **185** with alcohol-thioester **196** (12.5 mg, 0.05 mmol) and (*R*)-Phenanth **202** (5.8 mg, 0.01 mmol, 20 mol %). **197** yielded as a yellow oil (0.4 mg, 3% yield, 2% ee).

¹H NMR (400 MHz, CDCl₃): δ 6.96 (2H, s, H-3), 4.05 (1H, dddd, *J* = 11.4 Hz, 7.8 Hz, 5.0 Hz, 2.7 Hz, H-9), 2.78 (1H, dd, *J* = 14.2 Hz, 7.8 Hz, H-8), 2.60 (1H, dd, *J* = 14.2 Hz, 5.0 Hz, H-8), 2.30 (6H, s, H-5), 2.27 (3H, s, H-1), 1.66-1.63 (3H, m, H-10, H-11), 1.55-1.42 (3H, m, H-11, H-12), 1.18 (6H, s, H-14) ppm; ¹³C NMR (101 MHz, CDCl₃): δ 195.4 (C-7), 142.6 (C-2), 139.9 (C-4), 129.2 (C-3), 124.1 (C-6), 72.4 (C-13), 68.2 (C-9), 50.8 (C-8), 35.9 (C-12), 31.8 (C-14), 31.3 (C-14'), 29.8 (C-10), 21.7 (C-5), 21.3 (C-1), 20.0 (C-11) ppm; IR (film NaCl): ν_{max} 2972, 2926, 1702, 1461, 1377, 1364, 1278, 1138, 1063, 1043, 978, 901, 849, 797, 737, 717 cm⁻¹. HRMS (ESI): *m/z* calcd for C₁₈H₂₆NaO₂S⁺ (M+Na)⁺ 329.1546; found 329.1548; [α]_D²⁰ + 32.4° (c 0.84, CHCl₃), for 66% ee.

**(S)-S-(2,4,6-Triisopropylphenyl) 2-(6,6-dimethyltetrahydro-2H-pyran-2-yl)ethanethioate
(216)**



Racemic-CSA

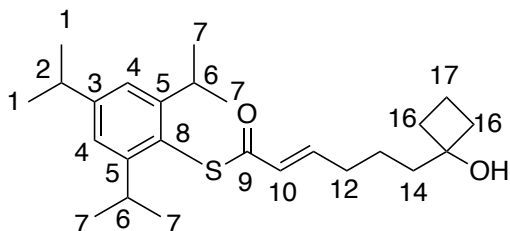
216 was synthesised using the same procedure as **185** with alcohol-thioester **214** (20.3 mg, 0.05 mmol) and rac- CSA (36.3 mg, 0.16 mmol, 3 eq). The crude was purified by column chromatography on silica using 5% Et₂O in hexane to yield **216** as a yellow oil (18.5 mg, 91% yield).

Asymmetric-(R)-TRIP

216 was synthesised using the same procedure as **185** with alcohol-thioester **214** (25.3 mg, 0.07 mmol) and (*R*)-TRIP (9.700 mg, 0.013 mmol, 20 mol %). **216** yielded as a yellow oil (21.3 mg, 84% yield, 98% ee).

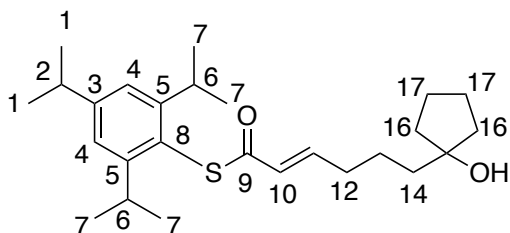
¹H NMR (400 MHz, CDCl₃): δ 7.06 (2H, s, H-4), 4.08 (1H, dddd, *J* = 11.4 Hz, 8.4 Hz, 4.4 Hz, 2.7 Hz, H-11), 3.42 (2H, sept, *J* = 6.9 Hz, H-6), 2.89 (1H, sept, *J* = 6.9 Hz, H-2), 2.81 (1H, dd, *J* = 14.5 Hz, 8.4 Hz, H-10), 2.63 (1H, dd, *J* = 14.5 Hz, 4.4 Hz, H-10), 1.82-1.63 (2H, m, H-12), 1.61-1.55 (2H, m, H-14), 1.47-1.37 (2H, m, H-13), 1.25 (12H, d, *J* = 6.9 Hz, H-7), 1.19 (3H, s, H-16), 1.16 (6H, d, *J* = 6.9 Hz, H-1), 0.87 (3H, s, H-16') ppm; ¹³C NMR (101 MHz, CDCl₃): δ 196.5 (C-9), 152.4 (C-3), 151.0 (C-5), 122.0 (C-8), 122.0 (C-4), 72.2 (C-15), 68.2 (C-11), 50.7 (C-10), 35.8 (C-14), 34.4 (C-2), 31.8 (C-16), 31.2 (C-16'), 29.7 (C-7), 24.0 (C-1), 21.7 (C-12), 20.0 (C-13) ppm; IR (ATR): ν_{max} 2924, 2857, 1702, 1459, 1376, 1069, 993, 901, 849, 797, 737, 717 cm⁻¹; HRMS (ESI): *m/z* calcd for C₂₄H₃₉O₂S⁺ (M+H)⁺ 391.2665; found 391.2662; [α]_D²⁰ + 65.8° (c 0.96, CHCl₃).

(E)-S-(2,4,6-Triisopropylphenyl) 6-(1-hydroxycyclobutyl)hex-2-enethioate (235)



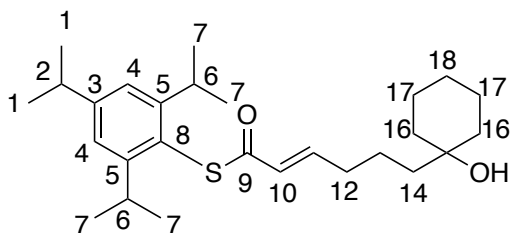
235 was synthesised using the same procedure as **184** with unsaturated alcohol **229** (69.2 mg, 0.49 mmol, 1.0 eq), thioester **213** (305 mg, 1.48 mmol, 3.0 eq), copper (I) iodide (9.00 mg, 0.04 mmol, 10 mol%) and Hovyeda-Grubbs 2nd generation catalyst (29.0 mg, 0.04 mmol, 10 mol%). The mixture was purified by column chromatography on silica using 10% ethyl acetate in n-hexane to yield the product **235** as a brown oil (168 mg, 85% yield). ^1H NMR (400 MHz, CDCl_3): δ 7.07 (2H, s, H-4), 6.98 (1H, dt, $J=17.4$ Hz, 6.8 Hz, H-11), 6.24 (1H, d, $J=17.4$ Hz, H-10), 3.38 (2H, sept, $J=6.8$ Hz, H-6), 2.88 (1H, sept, $J=6.8$ Hz, H-2), 2.28-2.23 (2H, m, H-12), 1.81-1.78 (2H, m, H-14), 2.00-1.97 (2H, m, H-16), 1.63-1.59 (3H, m, H-13, H-16), 1.56-1.53 (3H, m, H-13, H-17), 1.26 (6H, d, $J=6.8$ Hz, H-1), 1.17 (12H, d, $J=6.8$ Hz, H-7) ppm; ^{13}C NMR (101 MHz, CDCl_3): δ 189.0 (C-9), 152.7 (C-5), 151.1 (C-3), 145.8 (C-11), 128.2 (C-10), 122.1 (C-4), 121.6 (C-8), 75.3 (C-15), 39.0 (C-14), 36.3 (C-16), 34.5 (C-2), 32.6 (C-12), 32.0 (C-6), 24.0 (C-7), 23.6 (C-1), 22.1 (C-13), 12.2 (C-17) ppm; IR (ATR): ν_{max} 3412, 2969, 2940, 1684, 1631, 1464, 1375, 1284, 1156, 1040, 972, 907, 851, 799, 765, 715 cm^{-1} ; HRMS (ESI): m/z calcd for $\text{C}_{25}\text{H}_{38}\text{NaO}_2\text{S}^+$ ($\text{M}+\text{Na}$) $^+$ 425.2485; found 425.2491.

(E)-S-(2,4,6-Triisopropylphenyl) 6-(1-hydroxycyclopentyl)hex-2-enethioate (236)



236 was synthesised using the same procedure as **184** with unsaturated alcohol **230** (71.2 mg, 0.46 mmol, 1.0 eq), thioester **213** (401 mg, 1.46 mmol, 3.0 eq), copper (I) iodide (6.20 mg, 0.04 mmol, 10 mol%) and Hovyeda-Grubbs 2nd generation catalyst (25.0 mg, 0.04 mmol, 10 mol%). The mixture was purified by column chromatography on silica using 10% ethyl acetate in n-hexane to yield the product **236** as a brown oil (155 mg, 81% yield). ¹H NMR (400 MHz, CDCl₃): δ 7.07 (2H, s, H-4), 6.96 (1H, dt, *J* = 17.5 Hz, 6.8 Hz, H-11), 6.24 (1H, d, *J* = 17.5 Hz, H-10), 3.38 (2H, sept, *J* = 6.9 Hz, H-6), 2.87 (1H, sept, *J* = 6.9 Hz, H-2), 2.28-2.23 (2H, m, H-12), 1.81-1.78 (2H, m, H-14), 1.69-1.64 (2H, m, H-16), 1.63-1.60 (4H, m, H-16, H-17), 1.59-1.49 (4H, m, H-13, H-17), 1.25 (6H, d, *J* = 6.9 Hz, H-7) 1.15 (12H, d, *J* = 6.9 Hz, H-1) ppm; ¹³C NMR (101 MHz, CDCl₃): δ 189.0 (C-9), 152.7 (C-5), 151.1 (C-3), 145.8 (C-11), 128.1 (C-10), 122.1 (C-4), 121.6 (C-8), 82.5 (C-15), 41.1 (C-14), 39.8 (C-16), 34.5 (C-2), 32.8 (C-12), 32.1 (C-6), 24.5 (C-1), 24.0 (C-7), 23.8 (C-17), 23.3 (C-13) ppm; IR (ATR): ν_{max} 3412, 2969, 2940, 1684, 1631, 1464, 1375, 1284, 1156, 1040, 972, 907, 851, 799, 765, 715 cm⁻¹; HRMS (ESI): *m/z* calcd for C₂₆H₄₀NaO₂S⁺ (M+Na)⁺ 439.2641; found 439.2643.

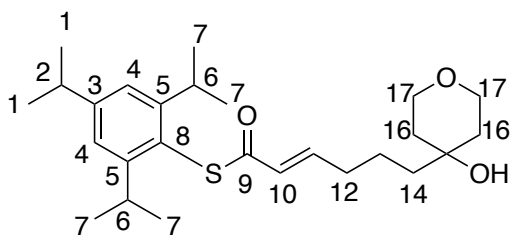
(E)-S-(2,4,6-Triisopropylphenyl) 6-(1-hydroxycyclohexyl)hex-2-enethioate (237)



237 was synthesised using the same procedure as **184** with unsaturated alcohol **231** (49.8 mg, 0.29 mmol, 1.0 eq), thioester **213** (256 mg, 0.88 mmol, 3.0 eq), copper (I) iodide (6.00 mg, 0.03 mmol, 10 mol%) and Hovyeda-Grubbs 2nd generation catalyst (14.4 mg, 0.03 mmol, 10 mol%). The mixture was purified by column chromatography on silica using 10% ethyl acetate in n-hexane to yield the product **237** as a brown oil (107 mg, 86% yield). ¹H NMR (400 MHz, CDCl₃): δ 7.07 (2H, s, H-4), 6.97 (1H, dt, *J* = 17.5 Hz, 6.8 Hz, H-11), 6.23 (1H,

d, $J=17.5$ Hz, H-10), 3.38 (2H, sept, $J = 6.9$ Hz, H-6), 2.89 (1H, sept, $J = 6.9$ Hz, H-2), 2.27-2.16 (2H, m, H-12), 1.62-1.59 (2H, m, H-14), 1.57-1.52 (5H, m, H-13, H-16), 1.50-1.48 (5H, m, H-13, H-17), 1.43-1.41 (2H, m, H-17), 1.25 (6H, d, $J = 6.9$ Hz, H-7) 1.17 (12H, d, $J = 6.9$ Hz, H-1) ppm; ^{13}C NMR (101 MHz, CDCl_3): δ 189.0 (C-9), 152.7 (C-5), 151.1 (C-3), 145.9 (C-11), 128.1 (C-10), 122.1 (C-4), 121.6 (C-8), 71.4 (C-15), 37.5 (C-16), 34.5 (C-14), 32.9 (C-2), 32.0 (C-6), 25.9 (C-12), 24.5 (C-18), 24.0 (C-7), 23.6 (C-13), 22.3 (C-1), 21.5 (C-17) ppm; IR (ATR): ν_{max} 3412, 2969, 2940, 1684, 1631, 1464, 1375, 1284, 1156, 1040, 972, 907, 851, 799, 765, 715 cm^{-1} ; HRMS (ESI): calcd for $\text{C}_{27}\text{H}_{42}\text{NaO}_2\text{S}^+$ ($\text{M}+\text{Na}$) $^+$ 453.2798; found 453.2807.

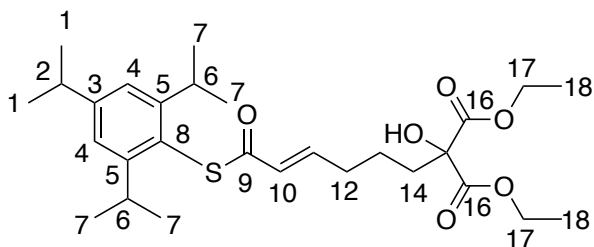
(*E*)-*S*-(2,4,6-Triisopropylphenyl) 6-(4-hydroxytetrahydro-2*H*-pyran-4-yl)hex-2-enethioate (238)



238 was synthesised using the same procedure as **184** with unsaturated alcohol **232** (76.0 mg, 0.40 mmol, 1.0 eq), thioester **213** (373 mg, 1.19 mmol, 3.0 eq), copper (I) iodide (25 mg, 0.04 mmol, 10 mol%) and Hovyeda-Grubbs 2nd generation catalyst (7.52 mg, 0.04 mmol, 10 mol%). The mixture was purified by column chromatography on silica using 60% ethyl acetate in *n*-hexane to yield the product **238** as a brown oil (142 mg, 82% yield). ^1H NMR (400 MHz, CDCl_3): δ 7.07 (2H, s, H-4), 6.95 (1H, dt, $J = 17.5$ Hz, 6.7 Hz, H-11), 6.24 (1H, d, $J = 17.5$ Hz, H-10), 3.76-3.73 (4H, m, H-17), 3.38 (2H, sept, $J = 6.9$ Hz, H-6), 2.88 (1H, sept, $J = 6.9$ Hz, H-2), 2.28-2.22 (2H, m, H-12), 1.73-1.60 (2H, m, H-14), 1.59-1.50 (2H, m, H-16), 1.50-1.44 (4H, m, H-13, H-16), 1.25 (6H, d, $J = 6.9$ Hz, H-1), 1.17 (12H, d, $J = 6.9$ Hz, H-7) ppm; ^{13}C NMR (101 MHz, CDCl_3): δ 188.9 (C-9), 152.6 (C-5), 151.2 (C-3), 145.4 (C-11), 128.3 (C-10), 122.1 (C-4), 121.5 (C-8), 69.0 (C-15), 63.9 (C-16), 43.0 (C-14), 37.7 (C-17), 34.5 (C-2), 32.6 (C-

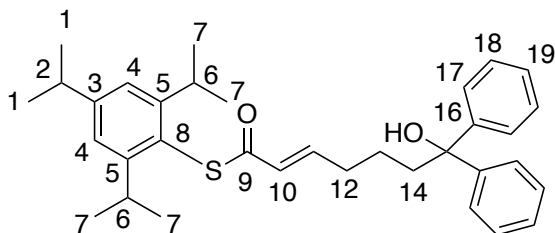
12), 32.1 (C-6), 29.8 (C-13), 24.0 (C-7), 21.1 (C-1) ppm; IR (ATR): ν_{\max} 3421, 2959, 2928, 2866, 1698, 1640, 1598, 1459, 1362, 1300, 1238, 1104, 1022, 908, 877, 839, 757, 537 cm^{-1} ; HRMS (ESI): m/z calcd for $\text{C}_{26}\text{H}_{40}\text{NaO}_3\text{S}^+$ ($\text{M}+\text{Na}$) $^+$ 455.2590; found 455.2595.

(E)-Diethyl 2-hydroxy-2-(6-oxo-6-((2,4,6-triisopropylphenyl)thio)hex-4-en-1-yl)malonate (240)



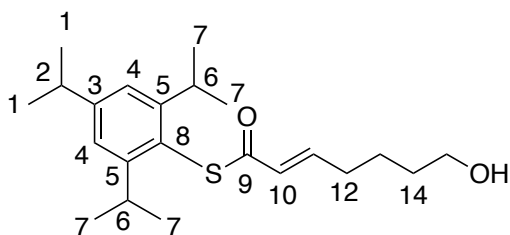
240 was synthesised using the same procedure as **184** with unsaturated alcohol **234** (146 mg, 0.57 mmol, 1.0 eq), thioester **213** (500 mg, 1.72 mmol, 3.0 eq), copper (I) iodide (39.1 mg, 0.06 mmol, 10 mol%) and Hovyeda-Grubbs 2nd generation catalyst (10.4 mg, 0.06 mmol, 10 mol%). The mixture was purified by column chromatography on silica using 30% ethyl acetate in n-hexane to yield the product **240** as a brown oil (251 mg, 87% yield). ^1H NMR (400 MHz, CDCl_3): δ 7.07 (2H, s, H-4), 6.94 (1H, dt, $J=17.5$ Hz, 6.7 Hz, H-11), 6.23 (1H, d, $J=17.5$ Hz, H-10), 4.29-4.24 (4H, q, $J=7.1$ Hz, H-17), 3.37 (2H, sept, $J=6.9$ Hz, H-6), 2.89 (1H, sept, $J=6.8$ Hz, H-2), 2.29-2.23 (2H, m, H-12), 2.09-2.05 (2H, m, H-14), 1.50-1.42 (2H, m, H-13), 1.28-1.27 (6H, t, $J=7.1$ Hz H-18), 1.25 (6H, d, $J=6.9$ Hz, H-1), 1.17 (12H, d, $J=6.9$ Hz, H-7) ppm; ^{13}C NMR (101 MHz, CDCl_3): δ 188.8 (C-9), 170.5 (C-16), 152.7 (C-5), 151.1 (C-3), 144.9 (C-11), 128.4 (C-10), 122.1 (C-4), 121.5 (C-8), 78.8 (C-15), 62.7 (C-17), 62.1 (C-14), 34.4 (C-2), 34.1 (C-12), 32.0 (C-6), 24.5 (C-13), 24.0 (C-7), 21.8 (C-1), 14.1 (C-18) ppm; IR (ATR): ν_{\max} 3484, 3077, 2932, 1739, 1641, 1445, 1369, 1225, 1132, 1024, 1006, 910, 861, 733, 634 cm^{-1} ; HRMS (ESI): m/z calcd for $\text{C}_{28}\text{H}_{42}\text{NaO}_6\text{S}^+$ ($\text{M}+\text{Na}$) $^+$ 529.2594; found 529.2593.

(E)-S-(2,4,6-Triisopropylphenyl) 7-hydroxy-7,7-diphenylhept-2-enethioate (239)



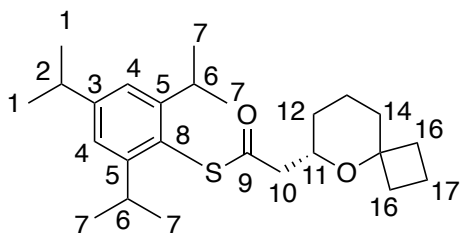
239 was synthesised using the same procedure as **184** with unsaturated alcohol **233** (174 mg, 0.69 mmol, 1.0 eq), thioester **213** (600 mg, 2.67 mmol, 3.0 eq), copper (I) iodide (43.0 mg, 0.07 mmol, 10 mol%) and Hovyeda-Grubbs 2nd generation catalyst (131 mg, 0.07 mmol, 10 mol%). The mixture was purified by column chromatography on silica using 20% ethyl acetate in n-hexane to yield the product **239** as a brown oil (312 mg, 88% yield). ¹H NMR (400 MHz, CDCl₃): δ 7.41-7.38 (4H, m, H-17), 7.33-7.30 (4H, m, H-18), 7.23-7.21 (2H, m, H-19), 7.07 (2H, s, H-4), 6.90 (1H, dt, *J* = 17.5 Hz, 6.7 Hz, H-11), 6.17 (1H, d, *J* = 17.5 Hz, H-10), 3.38 (2H, sept, *J* = 6.9 Hz, H-6), 2.88 (1H, sept, *J* = 6.9 Hz, H-2), 2.34-2.31 (2H, m, H-12), 2.30-2.21 (2H, m, H-14), 1.55-1.48 (2H, m, H-13), 1.25 (6H, d, *J* = 6.9 Hz, H-1), 1.16 (12H, d, *J* = 6.9 Hz, H-7) ppm; ¹³C NMR (101 MHz, CDCl₃): δ 188.9 (C-9), 152.7 (C-5), 151.1 (C-3), 146.9 (C-16), 145.5 (C-11), 128.4 (C-18), 128.3 (C-10), 127.1 (C-19), 126.1 (C-17), 122.1 (C-4), 121.5 (C-8), 78.2 (C-15), 41.5 (C-14), 34.4 (C-2), 32.5 (C-12), 32.0 (C-6), 24.5 (C-1), 24.0 (C-7), 22.4 (C-13) ppm; IR (ATR): ν_{max} 3485, 2960, 2928, 2869, 1674, 1630, 1598, 1461, 1447, 1362, 1169, 1032, 975, 911, 877, 851, 755, 700, 645 cm⁻¹; HRMS (ESI): *m/z* calcd for C₃₄H₄₂NaO₂S⁺ (M+Na)⁺ 537.2798; found 537.2796.

(E)-S-(2,4,6-Triisopropylphenyl) 7-hydroxyhept-2-enethioate (248)



248 was synthesised using the same procedure as **184** with unsaturated alcohol hex-5-en-1-ol (53.3 mg, 0.53 mmol, 1.0 eq), thioester **213** (463 mg, 1.59 mmol, 3.0 eq), copper (I) iodide (33.1 mg, 0.05 mmol, 10 mol%) and Hovyeda-Grubbs 2nd generation catalyst (10.1 mg, 0.05 mmol, 10 mol%). The mixture was purified by column chromatography on silica using 20% ethyl acetate in n-hexane to yield the product as a brown oil (184 mg, 96% yield). ^1H NMR (400 MHz, CDCl_3): δ 7.07 (2H, s, H-4), 6.95 (1H, dt, $J = 17.5$ Hz, 6.7 Hz, H-11), 6.23 (1H, d, $J = 17.5$ Hz, H-10), 3.68-3.65 (2H, m, H-15), 3.38 (2H, sept, $J = 6.9$ Hz, H-6), 2.89 (1H, sept, $J = 6.9$ Hz, H-2), 2.33-2.20 (2H, m, H-12), 1.62-1.56 (4H, m, H-14-H-13), 1.25 (6H, d, $J = 6.9$ Hz, H-1), 1.17 (12H, d, $J = 6.9$ Hz, H-7) ppm; ^{13}C NMR (101 MHz, CDCl_3): δ 188.9 (C-9), 152.7 (C-5), 151.1 (C-3), 145.5 (C-11), 128.2 (C-10), 122.1 (C-4), 121.6 (C-8), 62.7 (C-15), 34.5 (C-14), 32.3 (C-2), 32.1 (C-6), 24.5 (C-12), 24.3 (C-1), 24.0 (C-7), 23.6 (C-13) ppm; IR (ATR): ν_{max} 3412, 2969, 2940, 1684, 1631, 1464, 1375, 1284, 1156, 1040, 972, 907, 851, 799, 765, 715 cm^{-1} ; HRMS (ESI): m/z calcd for $\text{C}_{22}\text{H}_{34}\text{NaO}_2\text{S}^+$ ($\text{M}+\text{Na}$) $^+$ 385.2172; found 385.2172.

(S)-S-(2,4,6-Triisopropylphenyl) 2-(5-oxaspiro[3.5]nonan-6-yl)ethanethioate (241)



Racemic-CSA

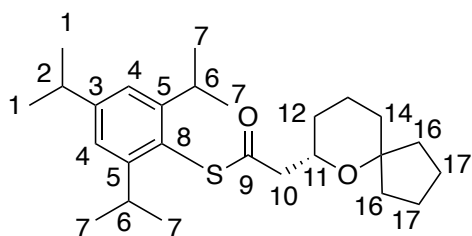
241 was synthesised using the same procedure as **216** with alcohol-thioester **235** (7.94 mg, 0.02 mmol) and rac-CSA (13.9 mg, 0.06 mmol, 3 eq). **241** yielded as yellow oil (7.62 mg, 97% yield) after column chromatography on silica using 5% Et_2O in hexane.

Asymmetric-(R)-TRIP

241 was synthesised using the same procedure as **216** with alcohol-thioester **235** (16.7 mg, 0.06 mmol) and (*R*)-TRIP **199** (8.80 mg, 0.01 mmol, 20 mol %). **241** yielded as yellow oil (16.0 mg, 96% yield, 93% ee) after column chromatography on silica using 5% Et₂O in hexane.

¹H NMR (400 MHz, CDCl₃): δ 7.08 (2H, s, H-4), 3.85 (1H, dddd, *J* = 11.3 Hz, 8.1 Hz, 4.3 Hz, 2.6 Hz, H-11), 3.44 (2H, sept, *J* = 6.9 Hz, H-6), 2.91-2.83 (2H, m, H-2, H-10), 2.62 (1H, dd, *J* = 14.5 Hz, 4.3 Hz, H-10), 2.10-2.00 (1H, m, H-14), 1.99-1.90 (3H, m, H-14, H-16), 1.79-1.70 (3H, m, H-12, H-13), 1.61-1.52 (4H, m, H-16, H-17), 1.42-1.39 (1H, m, H-12), 1.25 (12H, d, *J* = 6.9 Hz, H-7), 1.18 (6H, d, *J* = 6.9 Hz, H-1) ppm; ¹³C NMR (101 MHz, CDCl₃): δ 196.4 (C-9), 152.7 (C-3), 151.1 (C-5), 122.7 (C-8), 122.0 (C-4), 77.3 (C-15), 69.4 (C-11), 50.1 (C-10), 34.8 (C-14), 34.4 (C-2), 32.8 (C-12), 31.9 (C-6), 30.8 (C-16), 30.6 (C-16'), 29.7 (C-1), 24.0 (C-7), 20.1 (C-13), 12.6 (C-17) ppm; IR (ATR): ν_{max} 2924, 2859, 1702, 1468, 1376, 1261, 1079, 804 cm⁻¹; HRMS (ESI): *m/z* calcd for C₂₅H₃₈NaO₂S⁺ (M+Na)⁺ 425.2485; found 425.2483; [α]_D²⁰ + 39.2° (c 0.38, CHCl₃).

(S)-*S*-(2,4,6-Triisopropylphenyl)2-(6-oxaspiro[4.5]decan-7-yl)ethanethioate (**242**)



Racemic-CSA

242 was synthesised using the same procedure as **216** with alcohol-thioester **236** (26.0 mg, 0.07 mmol) and rac-CSA (44.1 mg, 0.19 mmol, 3 eq). **242** yielded as yellow oil (24.2 mg, 93% yield) after column chromatography on silica using 5% Et₂O in hexane.

Asymmetric-(R)-TRIP

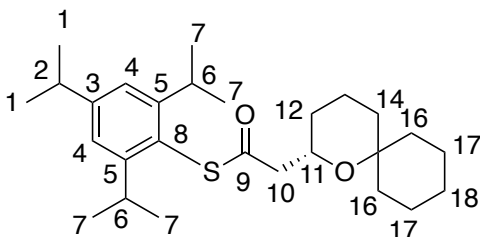
242 was synthesised using the same procedure as **216** with alcohol-thioester **236** (16.7 mg, 0.06 mmol) and (*R*)-TRIP **199** (8.80 mg, 0.01 mmol, 20 mol %). **242** yielded as yellow oil (15.0 mg, 90% yield, 96% ee) after column chromatography on silica using 5% Et₂O in hexane.

One-pot reaction

A solution of unsaturated alcohol **230** (30.0 mg, 0.19 mmol, 1.0 eq) and thioester **213** (170 mg, 0.57 mmol, 3.0 eq) were dissolved in cyclohexane (10 mL) under a nitrogen atmosphere. To this, copper (I) iodide (3.62 mg, 0.02 mmol, 10 mol%) and Hovyeda-Grubbs 2nd generation catalyst (11.9 mg, 0.02 mmol, 10 mol%) were added as solids in a single portion and the mixture was stirred at 50 °C for 24 hours. The reaction was monitored by TLC and after completion, (*R*)-TRIP **199** (29 mg, 0.04 mmol, 20 mol %) was added to the reaction and left to stir for 24 hours. The reaction mixture was quenched by (0.2 ml) of Et₃N then concentrated in *vacuo* and purified by column chromatography on silica using 5% Et₂O in hexane to yield the product as a yellow oil (57.4 mg, 71% yield, 95% ee).

¹H NMR (400 MHz, CDCl₃): δ 7.06 (2H, s, H-4), 4.00 (1H, dddd, *J* = 11.3 Hz, 8.3 Hz, 4.1 Hz, 2.8 Hz, H-11), 3.38 (2H, sept, *J* = 6.7 Hz, H-6), 3.00-2.72 (2H, m, H-2, H-10), 2.63 (1H, dd, *J* = 14.6 Hz, 4.1 Hz, H-10) 1.89-1.83 (1H, m, H-14), 1.77-1.64 (5H, m, H-14, H-16), 1.62-1.52 (4H, m, H-12, H-17), 1.51-1.41 (4H, m, H-13, H-17), 1.25 (6H, d, *J* = 6.7 Hz, H-1), 1.16 (12H, d, *J* = 6.7 Hz, H-7) ppm; ¹³C NMR (101 MHz, CDCl₃): δ 196.4 (C-9), 152.5 (C-3), 151.0 (C-5), 122.1 (C-8), 122.0 (C-4), 84.4 (C-15), 69.2 (C-11), 50.6 (C-10), 41.6 (C-14), 34.7 (C-16), 34.4 (C-16'), 32.7 (C-2), 31.9 (C-6), 31.3 (C-10), 24.5 (C-1), 24.0 (C-7), 24.0 (C-17), 23.3 (C-17'), 21.2 (C-13) ppm; IR (ATR): ν_{max} 2958, 2867, 1699, 1461, 1362, 1091, 973, 906, 876, 731, 650, 471 cm⁻¹; HRMS (ESI): *m/z* calcd for C₂₆H₄₀NaO₂S⁺ (M+Na)⁺ 439.2641; found 439.2643; [α]_D²⁰ + 41.7° (c 0.62, CHCl₃).

(S)-S-(2,4,6-Triisopropyl) 2-(1-oxaspiro[5.5]undecane-2-yl)ethanethioate (243)



Racemic-CSA

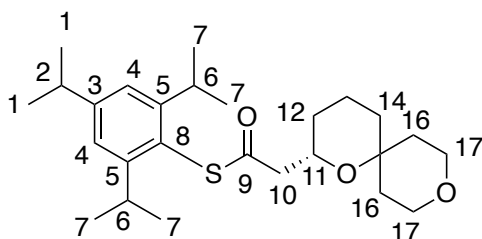
243 was synthesised using the same procedure as **216** with alcohol-thioester **237** (23.1 mg, 0.07 mmol) and rac-CSA (48.7 mg, 0.21 mmol, 3 eq). **243** yielded as yellow oil (21.9 mg, 95% yield) after column chromatography on silica using 5% Et₂O in hexane.

Asymmetric-(R)-TRIP

243 was synthesised using the same procedure as **216** with alcohol-thioester **237** (19.9 mg, 0.06 mmol) and (*R*)-TRIP **199** (8.79 mg, 0.01 mmol, 20 mol %). **243** yielded as yellow oil (16.5 mg, 83% yield, 60% ee) after column chromatography on silica using 5% Et₂O in hexane.

¹H NMR (400 MHz, CDCl₃): δ 7.06 (2H, s, H-4), 4.07 (1H, dddd, *J* = 11.5 Hz, 7.9 Hz, 4.6 Hz, 2.7 Hz, H-11), 3.42 (2H, sept, *J* = 7.0 Hz, H-6), 2.94-2.83 (2H, m, H-2, H-10), 2.63 (1H, dd, *J* = 14.6 Hz, 4.6 Hz, H-10) 2.07-2.03 (1H, m, H-14), 1.75-1.64 (2H, m, H-16), 1.63-1.56 (2H, m, H-16), 1.55-1.44 (6H, m, H-14, H-17- H-18), 1.43-1.34 (2H, m, H-12), 1.41-1.35 (3H, m, H-13, H-18), 1.23 (12H, d, *J* = 7.0 Hz, H-7), 1.16 (6H, d, *J* = 7.0 Hz, H-1) ppm; ¹³C NMR (101 MHz, CDCl₃): δ 196.3 (C-9), 152.5 (C-3), 150.9 (C-5), 122.1 (C-8), 122.0 (C-4), 72.7 (C-15), 66.4 (C-11), 50.8 (C-10), 40.4 (C-14), 35.1 (C-2), 34.4 (C-6), 31.9 (C-16), 31.5 (C-16'), 29.7 (C-12), 26.5 (C-18), 23.9 (C-1), 23.9 (C-7), 21.6 (C-17), 21, 3 (C-17'), 19.2 (C-13).ppm; IR (ATR): ν_{max} 2959, 2931, 2866, 1703, 1687, 1461, 1386, 1070, 987, 876, 746, 653, 473 cm⁻¹; HRMS (ESI): *m/z* calcd for C₂₇H₄₂NaO₂S⁺ (M+Na)⁺ 453.2798; found 453.2807; [α]_D²⁰ + 11.4° (c 0.75, CHCl₃).

(S)-S-(2,4,6-Triisopropylphenyl) 2-(1,9-dioxaspiro[5.5]undecan-2-yl)ethanethioate (244)



Racemic-CSA

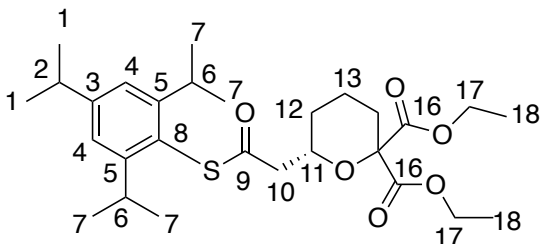
244 was synthesised using the same procedure as **216** with alcohol-thioester **238** (15.9 mg, 0.04 mmol) and rac- CSA (35.6 mg, 0.11 mmol, 3 eq). The reaction mixture was purified by column chromatography on silica using 40% EtOAc in hexane to yield **244** as a yellow oil (13.7 mg, 86% yield).

Asymmetric-(R)-TRIP

244 was synthesised using the same procedure as **216** with alcohol-thioester **238** (18.7 mg, 0.04 mmol) and (*R*)-TRIP (6.52 mg, 0.01 mmol, 20 mol %). **244** yielded as yellow oil (12.9 mg, 69% yield, 99% ee).

^1H NMR (400 MHz, CDCl_3): δ 7.07 (2H, s, H-4), 4.08 (1H, dddd, $J = 11.4$ Hz, 8.6 Hz, 4.3 Hz, 2.7 Hz, H-11), 3.81 (1H, ddd, $J = 11.7$ Hz, 4.4 Hz, 4.1 Hz, H-17), 3.65 (1H, ddd, $J = 11.7$ Hz, 4.4 Hz, 2.3 Hz, H-17), 3.63-3.56 (2H, m, H-17), 3.43 (2H, sept, $J = 6.8$ Hz, H-6), 2.93-2.86 (2H, m, H-2, H-10), 2.65 (1H, dd, $J = 14.5$ Hz, 4.3 Hz, H-10), 2.14-2.03 (1H, m, H-14), 1.73-1.60 (5H, m, H-14, H-16), 1.53-1.35 (3H, m, H-12, H-13), 1.34-1.29 (1H, m, H-13), 1.25 (12H, d, $J = 6.8$ Hz, H-7), 1.15 (6H, d, $J = 6.8$ Hz, H-1) ppm; ^{13}C NMR (101 MHz, CDCl_3): δ 196.4 (C-9), 152.2 (C-3), 151.1 (C-5), 122.1 (C-4), 121.8 (C-8), 70.4 (C-15), 66.8 (C-11), 63.3 (C-17), 63.3 (C-17'), 50.5 (C-10), 40.3 (C-16), 35.7 (C-14), 34.4 (C-16'), 32.0 (C-2), 31.3 (C-6), 30.4 (C-12), 24.4 (C-1), 24.0 (C-7), 18.9 (C-13) ppm; IR (ATR): ν_{max} 3421, 2959, 2928, 2866, 1698, 1640, 1598, 1459, 1362, 1300, 1238, 1104, 1022, 908, 877, 839, 757, 537 cm^{-1} ; HRMS (ESI): m/z calcd for $\text{C}_{26}\text{H}_{41}\text{O}_3\text{S}^+$ ($\text{M}+\text{H}^+$) 433.2771; found 433.2783; $[\alpha]_{\text{D}}^{20} - 51.2^\circ$ (c 0.55, CHCl_3).

(S)-Diethyl-6-(2-oxo-2-((2,4,6-triisopropylphenyl)thio)ethyl)tetrahydro-2H-pyran-2,2-dicarboxylate (246)



Racemic-CSA

246 was synthesised using the same procedure as **216** with alcohol-thioester **240** (16.8 mg, 0.03 mmol) and rac- CSA (32.1 mg, 0.10 mmol, 3 eq). The reaction mixture was purified by column chromatography on silica using 20% Et₂O in hexane to yield the product as a yellow oil (14.6 mg, 87% yield).

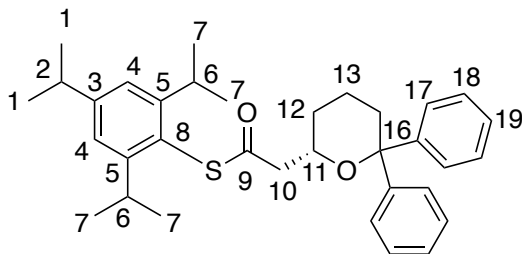
Asymmetric-(R)-TRIP

246 was synthesised using the same procedure as **216** with alcohol-thioester **240** (21.6 mg, 0.04 mmol) and (*R*)-TRIP (6.41 mg, 0.01 mmol, 20 mol %). **246** yielded as yellow oil (12.7 mg, 59% yield, 97% ee).

¹H NMR (400 MHz, CDCl₃): δ 7.05 (2H, s, H-4), 4.23 (4H, q, *J* = 7.0 Hz, H-17), 4.06 (1H, dddd, *J* = 11.5 Hz, 6.0 Hz, 4.2 Hz, 2.8 Hz, H-11), 3.39 (2H, sept, *J* = 6.9 Hz, H-6), 3.09 (1H, dd, *J* = 14.7 Hz, 6.0 Hz, H-10), 2.89 (1H, sept, *J* = 6.9 Hz, H-2), 2.80 (1H, dd, *J* = 14.7 Hz, 4.2 Hz, H-10), 2.36 (1H, dd, *J* = 11.2 Hz, 2.7 Hz, H-14), 1.77-1.70 (1H, m, H-12), 1.69-1.64 (3H, m, H-12, H-13, H-14), 1.40-1.35 (1H, m, H-14), 1.28 (6H, d, *J* = 6.9 Hz, H-1), 1.22 (6H, t, *J* = 7.0 Hz, H-18), 1.15 (12H, d, *J* = 6.9 Hz, H-7) ppm; ¹³C NMR (101 MHz, CDCl₃): δ 195.1 (C-9), 168.6 (C16), 168.3 (C-16'), 152.4 (C-3), 151.0 (C-5), 122.0 (C-4), 121.8 (C-8), 82.2 (C-15), 71.8 (C-11), 62.0 (C-17), 61.8 (C-17'), 49.7 (C-10), 34.4 (C-14), 31.9 (C-6), 29.7 (C-12), 29.3 (C-2), 23.9 (C-7), 23.9 (C-1), 19.9 (C-13), 14.1 (C-18), 14.0 (C-18) ppm; IR (ATR): ν_{max} 3077, 2932, 1739, 1641, 1445,

1369, 1225, 1132, 1024, 1006, 910, 861, 733, 634 cm^{-1} ; HRMS (ESI): m/z calcd for $\text{C}_{28}\text{H}_{43}\text{O}_6\text{S}^+$ ($\text{M}+\text{H}^+$) 507.2775; found 507.2777; $[\alpha]_{\text{D}}^{20}$ -40.6° (c 0.41, CHCl_3).

(S)-S-(2,4,6-Triisopropylphenyl) 2-(6,6-diphenyltetrahydro-2H-pyran-2-yl)ethanethioate (245)



Racemic-CSA

245 was synthesised using the same procedure as **216** with alcohol-thioester **239** (28.9 mg, 0.06 mmol) was and rac-CSA (54.4 mg, 0.17 mmol, 3 eq). The reaction mixture was purified by column chromatography on silica using 30% Et_2O in hexane to yield **245** as a yellow oil (25.4 mg, 99% yield).

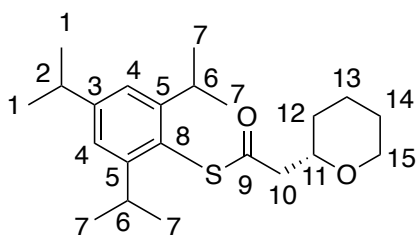
Asymmetric-(R)-TRIP

245 was synthesised using the same procedure as **216** with alcohol-thioester **239** (22.3 mg, 0.043 mmol) and (*R*)-TRIP (6.5 mg, 0.086 mmol, 20 mol %). **245** yielded as yellow oil (14.0 mg, 63% yield, 96% ee).

^1H NMR (400 MHz, CDCl_3): δ 7.43-7.40 (4H, m, H-17), 7.32-7.29 (2H, m, H-19), 7.23-7.10 (4H, m, H-18), 7.07 (2H, s, H-4), 4.06 (1H, dddd, $J=11.6$ Hz, 9.1 Hz, 3.5 Hz, 2.7 Hz, H-11), 3.42 (2H, sept, $J=6.9$ Hz, H-6), 3.12 (1H, dd, $J=14.6$ Hz, 9.1 Hz, H-10), 2.90 (1H, sept, $J=6.9$ Hz, H-2), 2.72 (1H, dd, $J=14.6$ Hz, 3.5 Hz, H-10), 1.81-1.70 (3H, m, H-12, H-14), 1.50-1.41 (3H, m, H-13, H-14), 1.25 (12H, d, $J=6.9$ Hz, H-7), 1.09 (6H, d, $J=6.9$ Hz, H-1) ppm; ^{13}C NMR (101 MHz, CDCl_3): δ 196.0 (C-9), 151.0 (C-3), 151.0 (C-5), 149.1 (C-16), 142.4 (C-16'), 128.6 (C-17), 127.9 (C-17'), 127.4 (C-18), 126.8 (C-19), 126.1 (C-19'), 124.8 (C-18'), 122.1 (C-8), 122.0 (C-

4), 80.3 (C-15), 68.6 (C-11), 50.5 (C-10), 34.8 (C-14), 34.4 (C-2), 32.0 (C-6), 31.1 (C-12), 29.7 (C-1), 23.9 (C7), 20.4 (C-13) ppm; IR (ATR): ν_{\max} 2960, 2936, 2861, 1804, 1670, 1603, 1462, 1380, 1095, 976, 700, 686 cm^{-1} ; HRMS (ESI): m/z calcd for $\text{C}_{34}\text{H}_{42}\text{NaO}_2\text{S}^+$ ($\text{M}+\text{Na}$) $^+$ 537.2798; found 537.2796; $[\alpha]_{\text{D}}^{20}$ - 42.3° (c 0.60, CHCl_3).

(S)-S-(2,4,6-Triisopropylphenyl) 2-(tetrahydro-2H-pyran-2-yl)ethanethioate (249)



Racemic-CSA

249 was synthesised using the same procedure as **216** with alcohol-thioester **248** (8.51 mg, 0.02 mmol) and rac- CSA (22.7 mg, 0.07 mmol, 3 eq). The reaction mixture was purified by column chromatography on silica using 5% Et_2O in hexane to yield **249** as a yellow oil (7.57 mg, 89% yield).

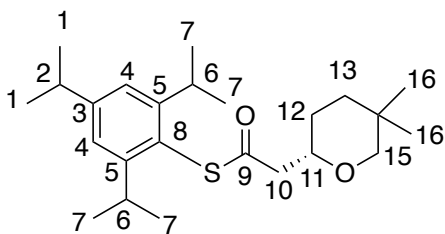
Asymmetric-(R)-TRIP

249 was synthesised using the same procedure as **216** with alcohol-thioester **248** (10.9 mg, 0.03 mmol) and (*R*)-TRIP (4.53 mg, 0.01 mmol, 20 mol %). **249** yielded as yellow oil (9.27 mg, 85% yield, 33% ee).

^1H NMR (400 MHz, CDCl_3): δ 7.06 (2H, s, H-4), 3.97 (1H, ddd, J = 10.3 Hz, 4.6 Hz, 2.7 Hz, H-15), 3.80 (1H, dddd, J = 11.6 Hz, 7.8 Hz, 4.4 Hz, 2.5 Hz, H-11), 3.46-3.40 (3H, m, H-6, H-15), 2.92-2.84 (2H, m, H-2, H-10), 2.67 (1H, dd, J = 14.5 Hz, 4.4 Hz, H-10), 1.86-1.81 (1H, m, H-14), 1.67-1.54 (3H, m, H-12, H-14), 1.51-1.34 (2H, m, H-13), 1.25 (6H, d, J = 6.9 Hz, H-1), 1.15 (12H, d, J = 6.9 Hz, H-7) ppm; ^{13}C NMR (101 MHz, CDCl_3): δ 196.3 (C-9), 152.5 (C-3), 151.1

(C-5), 122.1 (C-4), 122.0 (C-8), 75.4 (C-15), 68.7 (C-11), 50.2 (C-10), 34.4 (C-14), 31.9 (C-6), 31.6 (C-2), 29.8 (C-12), 25.7 (C-1), 24.0 (C-7), 23.4 (C-13) ppm; IR (ATR): ν_{\max} 2924, 2857, 1702, 1459, 1376, 1069, 993, 901, 849, 797, 737, 717 cm^{-1} ; HRMS (ESI): m/z calcd for $\text{C}_{22}\text{H}_{34}\text{NaO}_2\text{S}^+$ ($\text{M}+\text{Na}$) $^+$ 385.2172; found 385.2172; $[\alpha]_{\text{D}}^{20} + 7.23^\circ$ (c 0.44, CHCl_3).

(S)-S-(2,4,6-Triisopropylphenyl) 2-(5,5-dimethyltetrahydro-2H-pyran-2-yl)ethanethioate (286)



The cyclization precursor **280** was synthesised using the same procedure as **184** with unsaturated alcohol **274** (82.0 mg, 0.64 mmol, 1.0 eq), thioester **213** (560 mg, 1.93 mmol, 3.0 eq), copper (I) iodide (12.2 mg, 0.06 mmol, 10 mol%) and Hovyeda-Grubbs 2nd generation catalyst (40.1 mg, 0.06 mmol, 10 mol%). The mixture was then concentrated and used for the cyclization without further purification.

Racemic-CSA

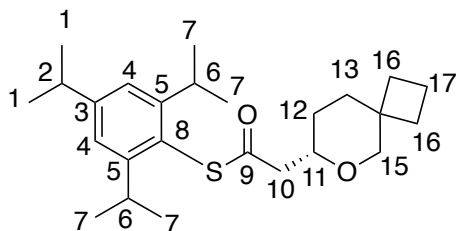
286 was synthesised using the same procedure as **216** with alcohol-thioester **280** (29.2 mg, 0.07 mmol) was and rac-CSA (52.1 mg, 0.23 mmol, 3 eq). The reaction mixture was purified by column chromatography on silica using 5% Et_2O in hexane to yield **286** as a yellow oil (20.0 mg, 94% yield).

Asymmetric-(R)-TRIP

286 was synthesised using the same procedure as **216** with alcohol-thioester **280** (33.3 mg, 0.07 mmol) and (*R*)-TRIP (12.9 mg, 0.017 mmol, 20 mol %). **286** yielded as yellow oil (28.3 mg, 85% yield, 71% ee).

^1H NMR (400 MHz, CDCl_3): δ 7.06 (2H, s, H-4), 3.70 (1H, dddd, $J = 11.6$ Hz, 7.8 Hz, 4.1 Hz, 2.6 Hz, H-11), 3.45 (1H, d, $J = 11.1$ Hz, H-15), 3.38 (2H, sept, $J = 6.9$ Hz, H-6), 3.17 (1H, d, $J = 11.1$ Hz, H-15), 2.93-2.85 (2H, m, H-2, H-10), 2.73 (1H, dd, $J = 14.5$ Hz, 4.1 Hz, H-10) 1.58-1.52 (2H, m, H-12), 1.49-1.39 (2H, m, H-13), 1.25 (6H, d, $J = 6.9$ Hz, H-1), 1.16 (12H, d, $J = 6.9$ Hz, H-7), 1.02 (3H, s, H-16), 0.80 (3H, s, H-16) ppm; ^{13}C NMR (101 MHz, CDCl_3): δ 196.2 (C-9), 152.5 (C-3), 151.1 (C-5), 122.1 (C-4), 122.0 (C-8), 78.5 (C-15), 75.4 (C-11), 49.9 (C-10), 36.7 (C-14), 34.4 (C-2), 32.0 (C-6), 29.9 (C-12), 27.9 (C-13), 27.2 (C-16), 24.4 (C-1), 24.0 (C-7), 23.7 (C-16') ppm; IR (ATR): ν_{max} 2924, 2857, 1702, 1459, 1376, 1069, 993, 901, 849, 797, 737, 717 cm^{-1} ; HRMS (ESI): m/z calcd for $\text{C}_{24}\text{H}_{39}\text{O}_2\text{S}^+$ ($\text{M}+\text{H}$) $^+$ 391.2665; found 391.2662; $[\alpha]_{\text{D}}^{20} - 32.14^\circ$ (c 0.87, CHCl_3).

(S)-S-(2,4,6-Triisopropylphenyl) 2-(6-oxaspiro[3.5]nonan-7-yl)ethanethioate (287)



The cyclization precursor **281** was synthesised using the same procedure as **184** with unsaturated alcohol **275** (110 mg, 0.78 mmol, 1.0 eq), thioester **213** (684 mg, 2.35 mmol, 3.0 eq), copper (I) iodide (14.9 mg, 0.08 mmol, 10 mol%) and Hovyeda-Grubbs 2nd generation catalyst (50.1 mg, 0.08 mmol, 10 mol%). The mixture was then concentrated and used for the cyclization without further purification.

Racemic-CSA

287 was synthesised using the same procedure as **216** with alcohol-thioester **281** (10.3 mg, 0.03 mmol) and rac- CSA (25.2 mg, 0.08 mmol, 3 eq). The reaction mixture was then

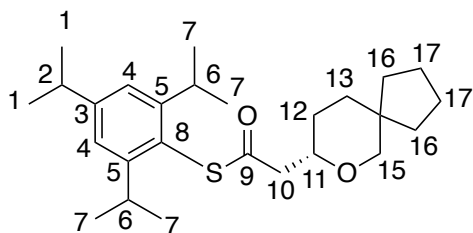
concentrated in *vacuo* and purified by column chromatography on silica using 5% Et₂O in hexane to yield **287** as a yellow oil (9.7 mg, 94% yield).

Asymmetric-(R)-TRIP

287 was synthesised using the same procedure as **216** with alcohol-thioester **281** (10.5 mg, 0.03 mmol) and (*R*)-TRIP (3.92 mg, 0.02mmol, 20 mol %). **287** yielded as yellow oil (9.7 mg, 99% yield, 97% ee).

¹H NMR (400 MHz, CDCl₃): δ 7.06 (2H, s, H-4), 3.83 (1H, d, *J* = 11.1 Hz, H-15), 3.70 (1H, dddd, *J* = 11.7 Hz, 8.5 Hz, 4.7 Hz, 2.6 Hz, H-11), 3.40 (2H, sept, *J* = 6.8 Hz, H-6), 3.23 (1H, d, *J* = 11.1 Hz, H-15), 2.90-2.83 (2H, m, H-2, H-10), 2.67 (1H, dd, *J* = 14.6 Hz, 4.7 Hz, H-10) 2.05-1.99 (1H, m, H-12), 1.90-1.82 (3H, m, H-12, H-16), 1.78-1.72 (1H, m, H-13), 1.62-1.51 (5H, m, H-13, H-16, H-17), 1.25 (6H, d, *J* = 6.8 Hz, H-1), 1.16 (12H, d, *J* = 6.8 Hz, H-7) ppm; ¹³C NMR (101 MHz, CDCl₃): δ 196.1 (C-9), 152.4 (C-3), 151.0 (C-5), 122.0 (C-4), 121.9 (C-8), 76.4 (C-15), 74.8 (C-11), 49.7 (C-10), 37.7 (C-14), 35.6 (C-16), 34.4 (C-12), 31.9 (C-12), 30.4 (C-2), 29.0 (C-6), 28.1 (C-13), 23.9 (C-1), 23.9 (C-7), 15.3 (C-17) ppm; IR (ATR): ν_{max} 2924, 2859, 1702, 1468, 1376, 1261, 1079, 804 cm⁻¹; HRMS (ESI): *m/z* calcd for C₂₅H₃₈NaO₂S⁺ (M+Na)⁺ 425.2485; found 425.2483; [α]_D²⁰ – 55.23° (c 0.48, CHCl₃).

(*S*)-*S*-(2,4,6-Triisopropylphenyl) 2-(6-oxaspiro[4.5]decan-7-yl)ethanethioate (**288**)



The cyclization precursor **282** was synthesised using the same procedure as **184** with unsaturated alcohol **276** (60.0 mg, 0.40 mmol, 1.0 eq), thioester **213** (399 mg, 1.67 mmol, 3.0 eq), copper (I) iodide (7.40 mg, 0.04 mmol, 10 mol%) and Hovyeda-Grubbs 2nd

generation catalyst (24.0 mg, 0.04 mmol, 10 mol%). The mixture was then concentrated and used for the cyclization without further purification.

Racemic-CSA

288 was synthesised using the same procedure as **216** with alcohol-thioester **282** (22.0 mg, 0.05 mmol) and rac- CSA (51.0 mg, 0.16 mmol, 3 eq). The reaction mixture was then concentrated in *vacuo* and purified by column chromatography on silica using 5% Et₂O in hexane to yield **288** as a yellow oil (21.3 mg, 97% yield).

Asymmetric-(R)-TRIP

288 was synthesised using the same procedure as **216** with alcohol-thioester **282** (30.9 mg, 0.07 mmol) and (*R*)-TRIP (11.2 mg, 0.02 mmol, 20 mol). **288** yielded as yellow oil (28.4 mg, 92% yield, 99% ee).

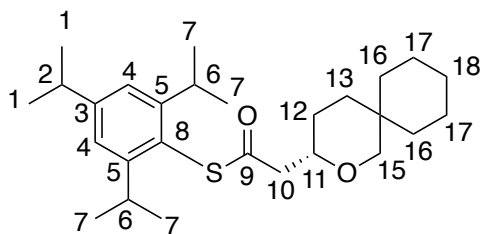
One-pot reaction

288 was synthesised using the same procedure as **242** with unsaturated alcohol **276** (30.0 mg, 0.19 mmol, 1.0 eq), thioester **213** (170 mg, 0.57 mmol, 3.0 eq), copper (I) iodide (3.62 mg, 0.02 mmol, 10 mol%), Hovyeda-Grubbs 2nd generation catalyst (11.9 mg, 0.02 mmol, 10 mol%) and (*R*)-TRIP (29.0 mg, 0.04 mmol, 20 mol). **288** yielded as yellow oil (57.0 mg, 70% yield, 99% ee).

¹H NMR (400 MHz, CDCl₃): δ 7.06 (2H, s, H-4), 3.75 (1H, dddd, *J* = 11.2 Hz, 6.9 Hz, 3.7 Hz, 2.5 Hz, H-11), 3.52 (1H, d, *J* = 11.1 Hz, H-15), 3.40 (2H, sept, *J* = 6.9 Hz, H-6), 3.20 (1H, d, *J* = 11.1 Hz, H-15), 2.92-2.85 (2H, m, H-2, H-10), 2.71 (1H, dd, *J* = 14.5 Hz, 3.7 Hz, H-10) 1.87-1.82 (1H, m, H-12), 1.63-1.53 (6H, m, H-12, H-13, H-16,), 1.53-1.43 (2H, m, H-13, H-17), 1.43-1.27 (2H, m, H-13, H-17), 1.25 (6H, d, *J* = 6.9 Hz, H-1), 1.22-1.199 (1H, m, H-16), 1.16 (12H, d, *J* = 6.9 Hz, H-7) ppm; ¹³C NMR (101 MHz, CDCl₃): δ 196.2 (C-9), 152.5 (C-3), 151.1 (C-5), 122.1 (C-4), 122.0 (C-8), 76.6 (C-15), 75.3 (C-11), 49.9 (C-10), 41.9 (C-14), 36.8 (C-16), 36.1 (C-16'), 34.6 (C-12), 34.4 (C-2), 32.0 (C-6), 29.2 (C-13), 25.2 (C-17), 24.8 (C-17'), 24.0 (C-7), 23.7 (C-1) ppm; IR (ATR): ν_{max} 2958, 2867, 1699, 1461, 1362, 1091, 973, 906, 876, 731, 650, 471 cm⁻¹

¹; HRMS (ESI): *m/z* calcd for C₂₆H₄₀NaO₂S⁺ (M+Na)⁺ 439.2641; found 439.2652; [α]_D²⁰ – 64.44° (c 0.75, CHCl₃).

(S)-S-(2,4,6-Triisopropylphenyl) 2-(2-oxaspiro[5.5]undecan-3-yl)ethanethioate (289)



The cyclization precursor **283** was synthesised using the same procedure as **184** with unsaturated alcohol **277** (83.8 mg, 0.50 mmol, 1.0 eq), thioester **213** (434 mg, 1.49 mmol, 3.0 eq), copper (I) iodide (9.48 mg, 0.05 mmol, 10 mol%) and Hovyeda-Grubbs 2nd generation catalyst (31.2 mg, 0.05 mmol, 10 mol%). The mixture was then concentrated and used for the cyclization without further purification.

Racemic-CSA

289 was synthesised using the same procedure as **216** with alcohol-thioester **283** (29.8 mg, 0.07 mmol) and rac- CSA (48.0 mg, 0.21 mmol, 3 eq). The reaction mixture was then concentrated in *vacuo* and purified by column chromatography on silica using 5% Et₂O in hexane to yield **289** as a yellow oil (27.6 mg, 95% yield).

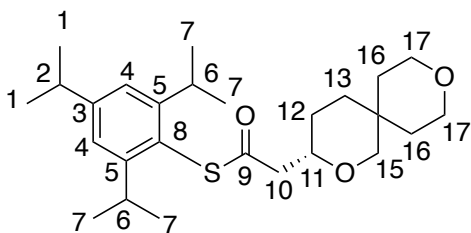
Asymmetric-(R)-TRIP

289 was synthesised using the same procedure as **216** with alcohol-thioester **283** (33.0 mg, 0.08 mmol) and (*R*)-TRIP (11.5 mg, 0.02 mmol, 20 mol). **289** yielded as yellow oil (30.4 mg, 92% yield, 73% ee).

¹H NMR (400 MHz, CDCl₃): δ 7.06 (2H, s, H-4), 3.76-3.69 (2H, m, H-11, H-15), 3.40 (2H, sept, *J* = 7.1 Hz, H-6), 3.09 (1H, d, *J* = 11.2 Hz, H-15), 2.93-2.84 (2H, m, H-2, H-10), 2.73 (1H, dd, *J*

= 14.7 Hz, 4.6 Hz, H-10) 1.80-1.75 (1H, m, H-12), 1.61-1.53 (2H, m, H-16), 1.52-1.44 (3H, m, H-12, H-16), 1.44-1.38 (4H, m, H-17), 1.34-1.28 (1H, m, H-13), 1.25 (6H, d, $J = 7.1$ Hz, H-1), 1.22-1.19 (1H, m, H-13), 1.16 (12H, d, $J = 7.1$ Hz, H-7), 1.12-1.08 (2H, m, H-18) ppm; ^{13}C NMR (101 MHz, CDCl_3): δ 196.2 (C-9), 152.5 (C-3), 151.1 (C-5), 122.1 (C-4), 122.0 (C-8), 77.0 (C-15), 75.9 (C-11), 49.9 (C-10), 36.6 (C-14), 34.5 (C-2), 34.0 (C-12), 32.1 (C-6), 32.0 (C-16), 31.4 (C-16'), 27.2 (C-17), 26.9 (C-17'), 24.4 (C-1), 24.0 (C-7), 21.6 (C-13), 21.6 (C-18) ppm; IR (ATR): ν_{max} 2959, 2931, 2866, 1703, 1687, 1461, 1386, 1070, 987, 876, 746, 653, 473 cm^{-1} ; HRMS (ESI): m/z calcd for $\text{C}_{27}\text{H}_{42}\text{NaO}_2\text{S}^+$ ($\text{M}+\text{Na}$) $^+$ 453.2798; found 453.2807; $[\alpha]_{\text{D}}^{20} - 34.65^\circ$ (c 1.40, CHCl_3).

(S)-S-(2,4,6-Triisopropylphenyl) 2-(2,9-dioxaspiro[5.5]undecan-3-yl)ethanethioate (290)



The cyclization precursor **284** was synthesised using the same procedure as **184** with unsaturated alcohol **278** (42.0 mg, 0.25 mmol, 1.0 eq), thioester **213** (215 mg, 0.74 mmol, 3.0 eq), copper (I) iodide (4.70 mg, 0.03 mmol, 10 mol%) and Hovyeda-Grubbs 2nd generation catalyst (15.5 mg, 0.03 mmol, 10 mol%). The mixture was then concentrated and used for the cyclization without further purification.

Racemic-CSA

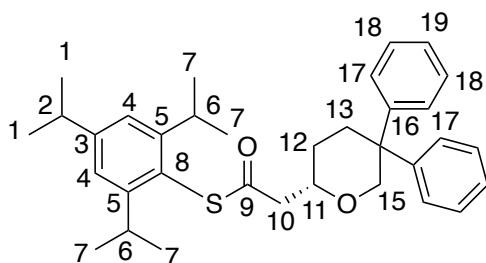
290 was synthesised using the same procedure as **216** with alcohol-thioester **284** (14.3 mg, 0.03 mmol) and rac- CSA (20.9 mg, 0.09 mmol, 3 eq). The reaction mixture was then concentrated in *vacuo* and purified by column chromatography on silica using 40% EtOAc in hexane to yield **290** as a yellow oil (13.4 mg, 94% yield).

Asymmetric-(*R*)-TRIP

290 was synthesised using the same procedure as **216** with alcohol-thioester **284** (14.3 mg, 0.03 mmol) and (*R*)-TRIP (4.99 mg, 0.07 mmol, 20 mol %). **290** yielded as yellow oil (13.0 mg, 91% yield, 40% ee).

^1H NMR (400 MHz, CDCl_3): δ 7.06 (2H, s, H-4), 3.88 (1H, d, $J = 11.4$ Hz, H-15), 3.79-3.72 (1H, m, H-11), 3.69-3.65 (2H, m, H-17), 3.64-3.61 (1H, m, H-17), 3.59-3.53 (1H, m, H-17), 3.40 (2H, sept, $J = 6.8$ Hz, H-6), 3.15 (1H, d, $J = 11.4$ Hz, H-15), 2.92-2.86 (2H, m, H-2, H-10), 2.73 (1H, dd, $J = 14.3$ Hz, 4.1 Hz, H-10) 1.89-1.84 (1H, m, H-16), 1.82-1.76 (1H, m, H-16), 1.65-1.58 (2H, m, H-16), 1.57-1.49 (2H, m, H-12), 1.36-1.30 (2H, m, H-13), 1.25 (6H, d, $J = 6.8$ Hz, H-1), 1.16 (12H, d, $J = 6.8$ Hz, H-7) ppm; ^{13}C NMR (101 MHz, CDCl_3): δ 196.1 (C-9), 152.4 (C-3), 151.2 (C-5), 122.1 (C-4), 121.9 (C-8), 75.9 (C-15), 75.8 (C-11), 64.0 (C-17), 63.4 (C-17'), 49.7 (C-10), 36.0 (C-13), 34.4 (C-2), 34.1 (C-16), 32.0 (C-6), 31.8 (C-16'), 30.2 (C-14), 26.9 (C-12), 24.4 (C-1), 24.0 (C-7) ppm; IR (ATR): ν_{max} 3421, 2959, 2928, 2866, 1698, 1640, 1598, 1459, 1362, 1300, 1238, 1104, 1022, 908, 877, 839, 757, 537 cm^{-1} ; HRMS (ESI): m/z calcd for $\text{C}_{26}\text{H}_{41}\text{O}_3\text{S}^+$ ($\text{M}+\text{H}$) $^+$ 433.2771; found 433.2776; $[\alpha]_{\text{D}}^{20} - 9.14^\circ$ (c 0.57, CHCl_3).

(*S*)-*S*-(2,4,6-Triisopropylphenyl) 2-(5,5-diphenyltetrahydro-2*H*-pyran-2-yl)ethanethioate (**291**)



The cyclization precursor **285** was synthesised using the same procedure as **184** with unsaturated alcohol **279** (190 mg, 0.75 mmol, 1.0 eq), thioester **213** (657 mg, 2.26 mmol, 3.0 eq), copper (I) iodide (144 mg, 0.75 mmol, 1.0 eq) and Hovyeda-Grubbs 2nd generation

catalyst (47.2 mg, 0.08 mmol, 10 mol%). The mixture was then concentrated and used for the cyclization without further purification.

Racemic-CSA

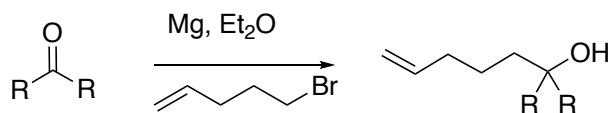
291 was synthesised using the same procedure as **216** with alcohol-thioester **285** (28.9 mg, 0.06 mmol) and rac-CSA (54.4 mg, 0.17 mmol, 3 eq). The reaction mixture was then concentrated in *vacuo* and purified by column chromatography on silica using 20% EtOAc in hexane to yield **291** as a yellow oil (24.9 mg, 86% yield).

Asymmetric-(R)-TRIP

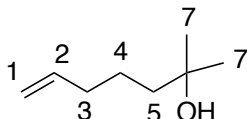
291 was synthesised using the same procedure as **216** with alcohol-thioester **285** (9.51 mg, 0.018 mmol) and (*R*)-TRIP (2.78 mg, 0.003 mmol, 20 mol %). **291** yielded as yellow oil (6.94 mg, 73% yield, 87% ee).

¹H NMR (400 MHz, CDCl₃): δ 7.43-7.31 (2H, m, H-19), 7.309-7.23 (4H, m, H-17), 7.20-7.14 (2H, m, H-18), 7.06 (2H, s, H-4), 4.61 (1H, d, *J* = 11.1 Hz, H-15), 3.95 (1H, dddd, *J* = 11.4 Hz, 8.4 Hz, 4.4 Hz, 2.7 Hz, H-11), 3.55 (1H, d, *J* = 11.1 Hz, H-15), 3.46 (2H, sept, *J* = 6.9 Hz, H-6), 2.94-2.85 (2H, m, H-2, H-10), 2.68 (1H, dd, *J* = 14.5 Hz, 4.4 Hz, H-10), 2.51 -2.41 (1H, m, H-12), 1.68-1.51 (2H, m, H-13), 1.25 (6H, d, *J* = 6.9 Hz, H-1), 1.11 (12H, d, *J* = 6.9 Hz, H-7) ppm; ¹³C NMR (101 MHz, CDCl₃): δ 196.0 (C-9), 153.0 (C-3), 151.1 (C-5), 146.5 (C-16), 145.7 (C-16'), 129.0 (C-17), 128.3 (C-17'), 128.1 (C-18), 127.0 (C-18'), 126.4 (C-19), 125.8 (C-19'), 122.0 (C-4), 121.8 (C-8), 75.0 (C-15), 75.0 (C-11), 49.7 (C-10), 45.8 (C-14), 34.5 (C-2), 34.4 (C-6), 31.9 (C-12), 29.7 (C-13), 27.7 (C-1), 23.9 (C-7) ppm, IR (ATR): ν_{max} 2960, 2936, 2861, 1804, 1670, 1603, 1462, 1380, 1095, 976, 700, 686 cm⁻¹; HRMS (ESI): *m/z* calcd for C₃₄H₄₂NaO₂S⁺ (M+Na)⁺ 537.2798; found 537.2796; [α]_D²⁰ + 21.45° (c 0.32, CHCl₃).

5.2.2 2,2-Disubstituted alcohols

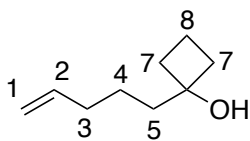


2-Methylhept-6-en-2-ol (188)



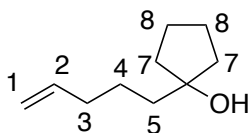
A degassed solution of 5-bromo-1-pentene (5.10 mL, 43.1 mmol) in Et₂O (20 mL) was added 0.3 ml/min, to a mixture of magnesium turnings (1.20 g, 49.4 mmol) in dry Et₂O (40 mL) under a nitrogen atmosphere. The reaction mixture was left to stir at room temperature for two hours. The solution of Grignard reagent was added (5 ml/min) to a solution of dry acetone (3.15 mL, 43.1 mmol) in Et₂O (20 mL). A white precipitate formed within 2 min. The reaction mixture was then quenched with excess saturated aq NH₄Cl solution and the white precipitate was filtered. The organic layer was separated and washed with H₂O, dried over anhydrous Na₂SO₄ and filtered. It was then concentrated *in vacuo* to give a colourless oil. The oil was purified by flash column chromatography on silica with 10% of ethyl acetate in n-hexane to yield **188** as a colourless oil (1.61 g, 53% yield). ¹H NMR (400 MHz, CDCl₃): δ 5.78 (1H, ddt, *J* = 17.0 Hz, 10.4 Hz, 7.6 Hz, H-2), 5.00 (1H, ddt, *J* = 17.0 Hz, 2.0 Hz, 1.4 Hz, H-1_{trans}), 4.95 (1H, ddt, *J* = 10.4 Hz, 2.0 Hz, 1.4 Hz, H-1_{cis}), 2.03 (2H, dt, *J* = 7.6 Hz, 7.4 Hz, H-3), 1.45-1.43 (4H, m, H-5, H-4), 1.19 (6H, s, H-7) ppm; ¹³C NMR (101 MHz, CDCl₃): δ 138.9 (C-2), 114.7 (C-1), 71.1 (C-6), 43.4 (C-5), 34.3 (C-3), 29.3 (C-7), 23.8 (C-4) ppm; IR (ATR): ν_{max} 3369, 3078, 2971, 1641, 1377, 1151, 992, 908, 764 cm⁻¹; HRMS (APCI): *m/z* calcd for C₈H₁₇O (M-H)⁺ 129.1274; found 129.1271.

1-(Pent-4-en-1-yl)cyclobutanol (**229**)



229 was synthesised using the same procedure as **188** with a solution of cyclobutanone (1.97 mL, 29.7 mmol) in Et₂O (20 mL). The oil was purified by flash column chromatography on silica with 10% of ethyl acetate in n-hexane to yield **229** as a colourless oil (3.43 g, 81% yield). ¹H NMR (400 MHz, CDCl₃): δ 5.80 (1H, ddt, *J* = 17.1 Hz, 10.4 Hz, 6.6 Hz, H-2), 5.01 (1H, ddt, *J* = 17.1 Hz, 2.0 Hz, 1.4 Hz, H-1_{trans}), 4.94 (1H, ddt, *J* = 10.4 Hz, 2.0 Hz, 1.4 Hz, H-1_{cis}), 2.10-1.94 (6H, m, H-3, H-5, H-7), 1.75-1.67 (1H, m, H-4), 1.59-1.55 (2H, m, H-7), 1.49-1.44 (3H, m, H-4, H-8) ppm; ¹³C NMR (101 MHz, CDCl₃): δ 138.9 (C-2), 114.7 (C-1), 75.3 (C-6), 39.0 (C-5), 36.0 (C-7), 34.1 (C-3), 22.8 (C-4), 12.2 (C-8) ppm; IR (ATR): ν_{max} 3385, 3076, 2931, 2860, 1641, 1447, 1414, 1354, 1255, 1165, 990, 969, 908 cm⁻¹; HRMS (APCI): *m/z* calcd for C₉H₁₇O (M-H)⁺ 141.1274; found 141.1264.

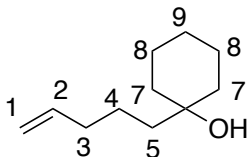
1-(Pent-4-en-1-yl)cyclopentanol (**230**)



230 was synthesised using the same procedure as **188** with a solution of cyclopentanone (3.11 mL, 29.3 mmol) in Et₂O (20 mL). The oil was purified by flash column chromatography on silica with 10% of ethyl acetate in n-hexane to yield **230** as a colourless oil (3.61 g, 79% yield). ¹H NMR (400 MHz, CDCl₃): δ 5.77 (1H, ddt, *J* = 17.1 Hz, 10.4 Hz, 6.6 Hz, H-2), 4.97 (1H, ddt, *J* = 17.1 Hz, 2.0 Hz, 1.4 Hz, H-1_{trans}), 4.90 (1H, ddt, *J* = 10.4 Hz, 2.0 Hz, 1.4 Hz, H-1_{cis}), 2.03 (2H, dt, *J* = 6.6 Hz, 6.4 Hz, H-3), 1.77-1.74 (2H, m, H-5), 1.61-1.55 (5H, m, H-4, H-7, H-8), 1.51-1.42 (5H, m, H-4, H-7, H-8) ppm; ¹³C NMR (101 MHz, CDCl₃): δ 138.9 (C-2), 114.6 (C-1), 82.5 (C-6), 41.0 (C-5), 39.7 (C-3), 34.3 (C-7), 24.1 (C-4), 23.9 (C-8) ppm; IR (ATR): ν_{max} 3381, 2943,

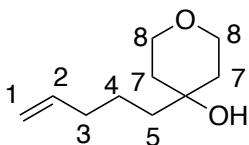
2871, 1711, 1641, 1283, 1095, 992, 908, 733, 630, 554 cm^{-1} ; HRMS (APCI): m/z calcd for $\text{C}_{10}\text{H}_{19}\text{O}$ (M-H)⁺ 155.14304; found 155.14272.

1-(Pent-4-en-1-yl)cyclohexanol (**231**)



231 was synthesised using the same procedure as **188** with a solution of cyclohexanone (3.11 mL, 29.9 mmol) in Et_2O (20 mL). The oil was purified by flash column chromatography on silica with 10% of ethyl acetate in n-hexane to yield **231** as a colourless oil (4.12 g, 57% yield). ^1H NMR (400 MHz, CDCl_3): δ 5.77 (1H, ddt, $J = 17.1$ Hz, 10.4 Hz, 6.6 Hz, H-2), 4.98 (1H, ddt, $J = 17.1$ Hz, 2.0 Hz, 1.4 Hz, H-1_{trans}), 4.92 (1H, ddt, $J = 10.4$ Hz, 2.0 Hz, 1.4 Hz, H-1_{cis}), 2.02 (2H, dt, $J = 6.6$ Hz, 6.5 Hz, H-3), 1.59-1.53 (2H, m, H-5), 1.51-1.44 (4H, m, H-7, H-8), 1.43-1.34 (7H, m, H-4, H-7, H-8, H-9), 1.31-1.17 (1H, m, H-9) ppm; ^{13}C NMR (101 MHz, CDCl_3): δ 139.0 (C-2), 114.6 (C-1), 71.5 (C-6), 41.9 (C-5), 37.5 (C-7), 34.3 (C-3), 25.9 (C-4), 22.3 (C-8), 22.3 (C-9) ppm; IR (ATR): ν_{max} 3385, 3076, 2931, 2860, 1641, 1447, 1414, 1354, 1255, 1165, 990, 969, 908 cm^{-1} ; HRMS (APCI): m/z calcd for $\text{C}_{11}\text{H}_{21}\text{O}$ (M-H)⁺ 169.1590; found 169.1594.

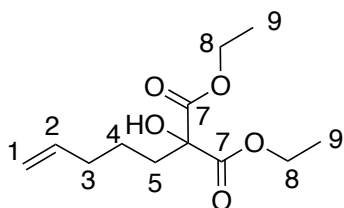
4-(Pent-4-en-1-yl)tetrahydro-2H-pyran-4-ol (**232**)



232 was synthesised using the same procedure as **188** with a solution of tetrahydro-4H-pyran-4-one (3.22 mL, 29.7 mmol) in Et_2O (20 mL). The oil was purified by flash column chromatography on silica with 40% of ethyl acetate in n-hexane to yield **232** as a colourless

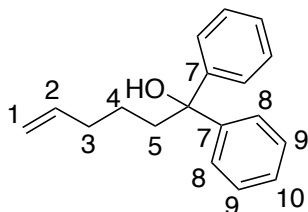
oil (3.34 g, 67% yield). ^1H NMR (400 MHz, CDCl_3): δ 5.77 (1H, ddt, $J = 17.1$ Hz, 10.4 Hz, 6.6 Hz, H-2), 4.98 (1H, ddt, $J = 17.1$ Hz, 2.0 Hz, 1.4 Hz, H-1_{trans}), 4.93 (1H, ddt, $J = 10.4$ Hz, 2.0 Hz, 1.4 Hz, H-1_{cis}), 3.75-3.65 (4H, m, H-8), 2.03 (2H, dt, $J = 6.6$ Hz, 6.5 Hz, H-3), 1.89-1.76 (1H, m, H-5), 1.67-1.59 (2H, m, H-7), 1.45-1.41 (5H, m, H-4, H-5, H-7) ppm; ^{13}C NMR (101 MHz, CDCl_3): δ 138.6 (C-2), 114.9 (C-1), 68.9 (C-6), 63.9 (C-8), 42.8 (C-5), 37.6 (C-7), 34.1 (C-3), 21.8 (C-4) ppm; IR (ATR): ν_{max} 3414, 3077, 2941, 2866, 2241, 1640, 1417, 1357, 1097, 909, 873, 647, 537 cm^{-1} ; HRMS (ESI): m/z calcd for $\text{C}_{10}\text{H}_{19}\text{O}_2$ (M-H) $^+$ 171.1380; found 171.1373.

Diethyl 2-hydroxy-2-(pent-4-en-1-yl)malonate (**234**)



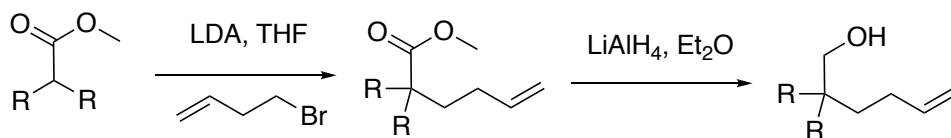
234 was synthesised using the same procedure as **188** with a solution of diethyl keto malonate (4.21 mL, 29.9 mmol) in Et_2O (20 mL). The oil was purified by flash column chromatography on silica with 20% of ethyl acetate in n-hexane to yield **234** as a colourless oil (4.51 g, 61% yield). ^1H NMR (400 MHz, CDCl_3): δ 5.75 (1H, ddt, $J = 17.1$ Hz, 10.2 Hz, 7.3 Hz, H-2), 5.00 (1H, ddt, $J = 17.1$ Hz, 2.5 Hz, 1.4 Hz, H-1_{trans}), 4.93 (1H, ddt, $J = 10.2$ Hz, 2.5 Hz, 1.4 Hz, H-1_{cis}), 4.26-4.21 (4H, m, H-8), 2.09-1.98 (4H, m, H-3, H-5), 1.44-1.39 (2H, m, H-4), 1.28-1.24 (6H, t, $J = 7.1$ Hz, H-9) ppm; ^{13}C NMR (101 MHz, CDCl_3): δ 170.7 (C-7), 138.2 (C-2), 115.1 (C-1), 79.0 (C-6), 62.5 (C-8), 34.1 (C-5), 33.5 (C-3), 22.4 (C-4), 14.1 (C-9) ppm; IR (ATR): ν_{max} 3493, 2981, 2939, 1736, 1391, 1219, 1196, 1024, 9123, 732, 597 cm^{-1} ; HRMS (ESI): m/z calcd for $\text{C}_{12}\text{H}_{20}\text{NaO}_5$ (M-Na) $^+$ 267.1203; found 267.1198.

1,1-Diphenylhex-5-en-1-ol (**233**)

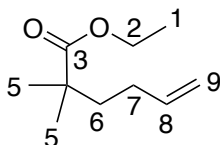


233 was synthesised using the same procedure as **188** with a solution of benzophenone (5.34 mL, 29.3 mmol) in Et₂O (20 mL). The oil was purified by flash column chromatography on silica with 20% of ethyl acetate in n-hexane to yield **233** as a colourless oil (5.31 g, 72% yield). ¹H NMR (400 MHz, CDCl₃): δ 7.44-7.41 (4H, m, H-8), 7.34-7.30 (4H, m, H-9), 7.26-7.23 (2H, m, H-10), 5.79 (1H, ddt, *J* = 17.1 Hz, 10.2 Hz, 7.3 Hz, H-2), 5.02 (1H, ddt, *J* = 17.1 Hz, 2.5 Hz, 1.4 Hz, H-1_{trans}), 4.99 (1H, ddt, *J* = 10.2 Hz, 2.5 Hz, 1.4 Hz, H-1_{cis}), 2.30 (2H, dt, *J* = 7.3 Hz, 7.1 Hz, H-3), 2.12-2.05 (2H, m, H-5), 1.46-1.37 (2H, m, H-4) ppm; ¹³C NMR (101 MHz, CDCl₃): δ 147.2 (C-7), 138.7 (C-2), 128.3 (C-8), 126.9 (C-10), 126.2 (C-9), 115.0 (C-1), 78.3 (C-6), 41.5 (C-5), 34.1 (C-3), 23.2 (C-4) ppm; IR (ATR): ν_{max} 3469.3, 3061.8, 2947.5, 2980.1, 1640.2, 1598.9, 1493.3, 1446.86, 1162.6, 1058.9, 994.1, 953.6, 907.5, 730.8, 697.5, 604.22 cm⁻¹; HRMS (ESI): *m/z* calcd for C₁₈H₂₀NaO⁺ (M-Na)⁺ 275.1406; found 275.1412.

5.2.3 3,3-Disubstituted alcohols



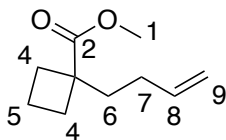
2,2-Dimethyl-hex-5-enoic acid ethyl ester (268)



To a solution of diisopropylamine (1.51 ml, 10.8 mmol) in dry THF (5 ml) at $-78\text{ }^{\circ}\text{C}$ under N_2 was added $n\text{-BuLi}$ (2.5 M in hexanes, 10.8 mmol) and the solution stirred for 45 mins. A solution of ethyl isobutyrate (1.30 ml, 9.91 mmol) in THF (5 ml) was added (1 ml/min) at $-78\text{ }^{\circ}\text{C}$ and reaction stirred for 45 mins. 4-Bromo-1-butene (1.00 ml, 9.91 mmol) was added over 1 min at $-78\text{ }^{\circ}\text{C}$ and the reaction warmed to room temperature. The reaction was stirred overnight and quenched with 1 M HCl (10 ml). The reaction was partitioned with diethyl ether (30 ml) and aqueous phase extracted with diethyl ether (2 x 30 ml), the organic fractions were combined, washed with saturated brine solution (30 ml), dried with MgSO_4 , filtered and concentrated *in vacuo*. The crude residue was purified by flash column chromatography (5% EtOAc/hexane) to afford product as a colorless oil (1.22 g, 70% yield). ^1H NMR (400 MHz, CDCl_3): δ 5.80 (1H, ddt, $J=16.8$ Hz, 9.9 Hz, 6.9 Hz, H-8), 4.99 (1H, ddt, $J=16.8$ Hz, 1.5 Hz, 1.5 Hz, H-9_{trans}), 4.93 (1H, ddt, $J=9.9$, 1.5 Hz, 1.5 Hz, H-9_{cis}), 4.11 (2H, q, $J=7.6$ Hz, H-2), 2.04-1.95 (2H, m, H-7), 1.61-1.59 (2H, m, H-6), 1.25 (3H, t, $J=7.6$ Hz, H-1), 1.16 (6H, s, H-5) ppm; ^{13}C NMR (101 MHz, CDCl_3): δ 177.9 (C-3), 138.7 (C-8), 114.5 (C-9), 60.3 (C-2), 42.1 (C-4), 39.9 (C-6), 29.5 (C-7), 25.2 (C-5), 14.3 (C-1) ppm; IR (ATR): ν_{max} 2978, 2938, 1726, 1641, 1473, 1450, 1473, 1386, 1365, 1319, 1280, 1199, 1143, 1094, 1027, 996, 909, 863, 774, 646, 580, 556, 503 cm^{-1} ; HRMS (APCI): m/z calcd for $\text{C}_{10}\text{H}_{19}\text{O}_2$ (M-H)⁺

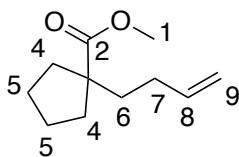
171.1380; found 171.1373. Spectroscopical data are in full agreement with those previously reported.¹

1-But-3-enyl-cyclobutanecarboxylic acid methyl ester (**269**)



269 was synthesized using the same procedure as **268** with diisopropylamine (0.68 ml, 4.82 mmol), n-BuLi (2.5 M in hexanes, 4.82 mmol), methyl cyclobutane carboxylate (0.5 ml, 4.38 mmol) and 4-bromo-1-butene (0.45 ml, 4.38 mmol). The crude residue was purified by flash column chromatography (2% EtOAc/hexane) to afford **269** as a colorless oil (285 mg, 66% yield). ¹H NMR (400 MHz, CDCl₃): δ 5.77 (1H, ddt, *J* = 16.8 Hz, 9.9 Hz, 6.1 Hz, H-8), 5.01 (1H, ddt, *J* = 16.8 Hz, 1.5 Hz, 1.5 Hz, H-9_{trans}), 4.94 (1H, ddt, *J* = 9.9 Hz, 1.5 Hz, 1.5 Hz, H-9_{cis}), 3.66 (3H, s, H-1), 2.43-2.32 (2H, m, H-4), 1.99-1.83 (8H, m, H-4, H-5, H-6, H-7) ppm; ¹³C NMR (101 MHz, CDCl₃): δ 177.6 (C-2), 138.3 (C-8), 114.7 (C-9), 51.8 (C-1), 47.5 (C-3), 37.3 (C-6), 30.1 (C-4), 29.4 (C-7), 15.7 (C-5) ppm; IR (ATR): ν_{max} 3077, 2948, 2869, 1731, 1693, 1641, 1434, 1329, 1283, 1244, 1201, 1142, 1112, 994, 911, 806, 692, 637, 458 cm⁻¹; HRMS (APCI): *m/z* calcd for C₁₀H₁₇O₂ (M-H)⁺ 169.12231; found 169.12218. Spectroscopical data are in full agreement with those previously reported.¹

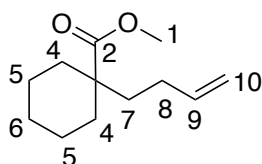
1-But-3-enyl-cyclopentanecarboxylic acid methyl ester (**270**)



270 was synthesized using the same procedure as **268** with diisopropylamine (1.50 ml, 11.0 mmol), n-BuLi (2.5 M in hexanes, 11.0 mmol), methyl cyclopentane carboxylate (1.32 g, 10.1 mmol) and 4-bromo-1-butene (1.00 ml, 10.1 mmol). **270** yielded as a colourless oil (1.4 g,

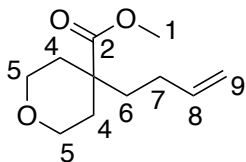
91% yield) after column chromatography (2% EtOAc/hexane). ^1H NMR (400 MHz, CDCl_3): δ 5.74 (1H, ddt, $J = 16.9$ Hz, 10.5 Hz, 6.9 Hz, H-8), 4.98 (1H, ddt, $J = 16.9$ Hz, 1.5 Hz, 1.5 Hz, H-9_{trans}), 4.92 (1H, ddt, $J = 10.5$ Hz, 1.5 Hz, 1.5 Hz, H-9_{cis}), 3.65 (3H, s, H-1), 2.19-2.07 (2H, m, H-4), 1.97-1.91 (2H, m, H-7), 1.70-1.65 (2H, m, H-6), 1.63-1.54 (4H, m, H-5), 1.50-1.45 (2H, m, H-4) ppm; ^{13}C NMR (101 MHz, CDCl_3): δ 178.3 (C-2), 138.5 (C-8), 114.5 (C-9), 53.9 (C-3), 51.8 (C-1), 38.5 (C-6), 36.1 (C-4), 30.5 (C-7), 25.0 (C-5); IR (ATR): ν_{max} 3078, 2951, 2871, 1730, 1641, 1452, 1339, 1255, 1196, 1162, 994, 910 cm^{-1} . Spectroscopical data are in full agreement with those previously reported.¹

1-But-3-enyl-cyclohexanecarboxylic acid methyl ester (**271**)



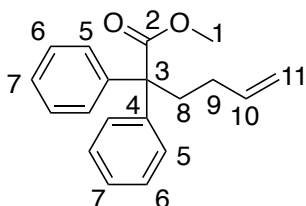
271 was synthesized using the same procedure as **268** with diisopropylamine (1.51 ml, 11.0 mmol), *n*-BuLi (2.5 M in hexanes, 11.0 mmol), methyl cyclohexane carboxylate (1.50 ml, 10.1 mmol) and 4-bromo-1-butene (1.00 ml, 10.1 mmol). The crude residue was purified by flash column chromatography (2% EtOAc/hexane) to afford **271** as a colorless oil (1.61 g, 80% yield). ^1H NMR (400 MHz, CDCl_3): δ 5.76 (1H, ddt, $J = 16.9$ Hz, 10.0 Hz, 6.3 Hz, H-9), 4.99 (1H, ddt, $J = 16.9$ Hz, 1.5 Hz, 1.5 Hz, H-10_{trans}), 4.93 (1H, ddt, $J = 10.0$ Hz, 1.5 Hz, 1.5 Hz, H-10_{cis}), 3.68 (3H, s, H-1), 2.14-2.04 (2H, m, H-4), 2.00-1.99 (2H, m, H-8), 1.65-1.50 (5H, m, H-5, H-6, H-7), 1.40-1.16 (5H, m, H-4, H-5, H-6) ppm; ^{13}C NMR (101 MHz, CDCl_3): δ 177.3 (C-2), 138.6 (C-9), 114.5 (C-10), 51.5 (C-1), 46.9 (C-3), 39.8 (C-7), 34.3 (C-4), 28.6 (C-8), 26.0 (C-6), 23.3 (C-5); IR (ATR): ν_{max} 3078, 2930, 2854, 1727, 1641, 1453, 1432, 1364, 1330, 1292, 1275, 1194, 1156, 1134, 1040, 995, 959, 909, 891, 850, 800, 765, 1649, 620, 567, 514 cm^{-1} ; HRMS (APCI) calcd for $\text{C}_{12}\text{H}_{21}\text{O}_2$ (M-H)⁺ 197.153606; found 197.154279. Spectroscopical data are in full agreement with those previously reported.¹

4-But-3-enyl-tetrahydro-pyran-4-carboxylic acid methyl ester (272)



272 was synthesized using the same procedure as **268** with diisopropylamine (1.54 ml, 11.0 mmol), n-BuLi (2.5 M in hexanes, 11.0 mmol), methyl tetrahydro-2H-pyran-4-carboxylate (1.54 ml, 10.1 mmol) and 4-bromo-1-butene (1.00 ml, 10.1 mmol). **272** yielded as a colourless oil (1.45 g, 73% yield) after column chromatography (10% EtOAc/hexane). ^1H NMR (400 MHz, CDCl_3): δ 5.75 (1H, ddt, $J = 16.9, 10.5, 6.4$ Hz, H-8), 5.00 (1H, ddt, $J = 16.9, 1.5$ Hz, H-9_{trans}), 4.95 (1H, ddt, $J = 10.5, 1.5$ Hz, H-9_{cis}), 3.83 (2H, ddd, $J = 11.7, 4.4, 4.1$ Hz, H-5), 3.72 (3H, s, H-1), 3.43 (2H, ddd, $J = 11.7, 2.3$ Hz, H-5), 2.10 (2H, ddd, $J = 13.7, 4.4, 2.3$ Hz, H-4), 2.02-1.91 (2H, m, H-7), 1.67-1.59 (2H, m, H-6), 1.52 (2H, ddd, $J = 13.7, 11.7, 4.1$ Hz, H-4) ppm; ^{13}C NMR (101 MHz, CDCl_3): δ 176.2 (C-2), 138.0 (C-8), 115.0 (C-9), 65.6 (C-5), 51.9 (C-1), 44.9 (C-3), 40.0 (C-6), 34.3 (C-4), 28.2 (C-7); IR (ATR): ν_{max} 3078, 2954, 2852, 1728, 1641, 1452, 1389, 1337, 1299, 1242, 1210, 1194, 1152, 1108, 1034, 1015, 997, 982, 912, 888, 840, 802, 775, 600, 561, 491, 462 cm^{-1} ; HRMS (ESI) calcd for $\text{C}_{11}\text{H}_{18}\text{NaO}_3$ ($\text{M} + \text{Na}$) $^+$ 211.1150; found 211.1150. Spectroscopical data are in full agreement with those previously reported.¹

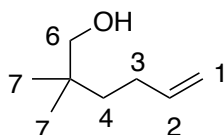
2,2-Diphenyl-hex-5-enoic acid methyl ester (273)



273 was synthesized using the same procedure as **268** with diisopropylamine (1.54 ml, 11.0 mmol), n-BuLi (2.5 M in hexanes, 11.0 mmol), diphenyl methyl acetate (2.24 g, 10.1 mmol)

and 4-bromo-1-butene (1.30 ml, 10.1 mmol). **273** yielded as a colourless oil (117 mg, 42% yield) after column chromatography (4% EtOAc/hexane). ^1H NMR (400 MHz, CDCl_3): δ 7.44-7.41 (4H, m, H-5), 7.34-7.30 (4H, m, H-6), 7.26-7.23 (2H, m, H-7), 5.75 (1H, ddt, $J = 16.8, 9.9, 6.5$ Hz, H-10), 5.01 (1H, ddt, $J = 16.8, 1.5$ Hz, H-11_{trans}), 4.96 (1H, ddt, $J = 9.9, 1.5$ Hz, H-11_{cis}), 3.68 (3H, s, H-1), 2.48-2.44 (2H, m, H-8), 1.83-1.77 (2H, m, H-9) ppm; ^{13}C NMR (101 MHz, CDCl_3): δ 174.8 (C-2), 142.8 (C-4), 138.4 (C-10), 129.0 (C-5), 128.0 (C-6), 126.9 (C-7), 114.6 (C-11), 60.3 (C-3), 52.5 (C-1), 37.4 (C-8), 29.8 (C-9) ppm; IR (ATR): ν_{max} 3024, 3060, 2950, 1729, 1640, 1598, 1495, 1445, 1221, 1121, 1063, 1033, 913, 784, 760, 699, 602, 576, 502, 481 cm^{-1} ; HRMS (ESI) calcd for $\text{C}_{19}\text{H}_{21}\text{O}_2$ ($\text{M} + \text{H}$) $^+$ 281.1528 ; found 281.1536. Spectroscopical data are in full agreement with those previously reported.¹

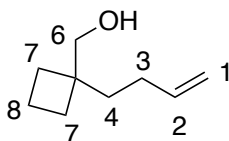
2,2-Dimethylhex-5-en-1-ol (**274**)



To a dry round bottom flask, LiAlH_4 (431mg, 11.5 mmol) was added, dry Et_2O (5ml) was then added to form a suspension and the flask was cooled to 0 °C. To this mixture, a solution of **268** (1.31 g, 7.72 mmol) in dry Et_2O (5ml) was added (1 ml /min). After completion of addition, the reaction was allowed to warm to rt as it was stirred overnight. Upon completion by TLC, the reaction was cooled to 0 °C and was quenched with 0.4 ml of water, 0.4 ml of 15% w/w NaOH solution, and then 1.2 ml of water. The reaction was stirred for 10 min at 0 °C before MgSO_4 was added. The resulting white slurry was stirred for 30 min at rt. The white solids were removed via filtration with Et_2O rinsing. The solution was then concentrated *in vacuo* and yielded the product as colorless oil (963 mg, 96% yield). ^1H NMR (400 MHz, CDCl_3): δ 5.80 (1H, ddt, $J = 17.1$ Hz, 10.4 Hz, 6.6 Hz, H-2), 5.03 (1H, ddt, $J = 17.1$ Hz, 2.0 Hz, 1.4 Hz, H-1_{trans}), 4.95 (1H, ddt, $J = 10.4$ Hz, 2.0 Hz, 1.4 Hz, H-1_{cis}), 3.31 (2H, s, H-6), 2.05-1.98 (2H, m, H-3), 1.35-1.30 (2H, m, H-4), 0.88 (6H, s, H-7) ppm; ^{13}C NMR(101 MHz, CDCl_3): δ 139.6 (C-2), 114.0 (C-1), 71.6 (C-6), 37.9 (C-5), 35.1 (C-3), 28.4 (C-4), 23.9 (C-

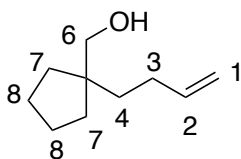
7) ppm; IR (ATR): ν_{\max} 3369, 3078, 2971, 1641, 1377, 1151, 992, 908, 764 cm^{-1} ; HRMS (ESI): m/z calcd for $\text{C}_8\text{H}_{16}\text{O}$ (M-H)⁺ 113.0966; found 113.0958.

(1-(But-3-en-1-yl)cyclobutyl)methanol (**275**)



275 was synthesized using the same procedure as **274** with LiAlH_4 (1.10 g, 6.45 mmol) and **269** (954 mg, 5.23 mmol). **275** yielded as a colourless oil (465 mg, 92% yield). ^1H NMR (400 MHz, CDCl_3): δ 5.83 (1H, ddt, J = 16.9 Hz, 10.0 Hz, 6.3 Hz, H-2), 5.01 (1H, ddt, J = 16.9 Hz, 1.5 Hz, 1.5 Hz, H-1_{trans}), 4.92 (1H, ddt, J = 10.0 Hz, 1.5 Hz, 1.5 Hz, H-1_{cis}), 3.53 (2H, s, H-6), 2.02-1.84 (2H, m, H-3), 1.82-1.80 (2H, m, H-7), 1.78-1.70 (3H, m, H-4, H-7), 1.68-1.60 (1H, m, H-4), 1.59-1.55 (2H, m, H-8) ppm; ^{13}C NMR (101 MHz, CDCl_3): δ 139.4 (C-2), 114.2 (C-1), 67.9 (C-6), 42.9 (C-5), 36.0 (C-3), 28.4 (C-4), 28.3 (C-7), 15.3 (C-8) ppm; IR (ATR): ν_{\max} 3343, 2980, 2933, 1641, 1442, 1253, 1168, 994, 955, 908, 633, 553 cm^{-1} ; HRMS (APCI): m/z calcd for $\text{C}_9\text{H}_{17}\text{O}$ (M-H)⁺ 141.1274; found 141.1264.

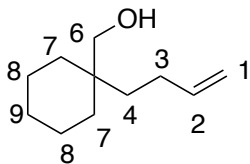
(1-(But-3-en-1-yl)cyclopentyl)methanol (**276**)



276 was synthesized using the same procedure as **274** with LiAlH_4 (294 mg, 7.85 mmol) and **270** (954 mg, 5.23 mmol). **276** yielded as a colourless oil (718 mg, 94% yield). ^1H NMR (400 MHz, CDCl_3): δ 5.81 (1H, ddt, J = 16.9 Hz, 10.0 Hz, 6.3 Hz, H-2), 5.00 (1H, ddt, J = 16.9 Hz, 1.5 Hz, 1.5 Hz, H-1_{trans}), 4.90 (1H, ddt, J = 10.0 Hz, 1.5 Hz, 1.5 Hz, H-1_{cis}), 3.37 (2H, s, H-6), 2.04-

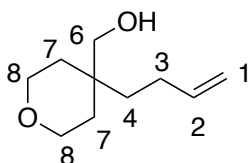
1.97 (2H, m, H-3), 1.84-1.72 (1H, m, H-4), 1.58-1.52 (3H, m, H-4, H-7), 1.46-1.39 (4H, m, H-7, H-8), 1.39-1.31 (2H, m, H-8) ppm; ^{13}C NMR (101 MHz, CDCl_3): δ 139.6 (C-2), 114.1 (C-1), 68.3 (C-6), 47.0 (C-5), 36.4 (C-3), 34.6 (C-7), 29.3 (C-4), 25.4 (C-8) ppm; IR (ATR): ν_{max} 3380.8, 2943.4, 2871.1, 1710.7, 1641.1, 1282.9, 1094.8, 991.7, 907.9, 733 cm^{-1} .

(1-(But-3-en-1-yl)cyclohexyl)methanol (**277**)



277 was synthesized using the same procedure as **274** with LiAlH_4 (571 mg, 15.2 mmol) and **271** (1.72 mg, 10.2 mmol). **277** yielded as a colourless oil (139 mg, 87% yield). ^1H NMR (400 MHz, CDCl_3): δ 5.81 (1H, ddt, J = 16.9 Hz, 10.0 Hz, 6.3 Hz, H-2), 5.00 (1H, ddt, J = 16.9 Hz, 1.5 Hz, 1.5 Hz, H-1_{trans}), 4.96 (1H, ddt, J = 10.0 Hz, 1.5 Hz, 1.5 Hz, H-1_{cis}), 3.40 (2H, s, H-6), 2.00-1.94 (2H, m, H-3), 1.44-1.38 (8H, m, H-7, H-8), 1.37-1.27 (4H, m, H-4, H-9) ppm; ^{13}C NMR (101 MHz, CDCl_3): δ 139.8 (C-2), 114.1 (C-1), 68.4 (C-6), 37.1 (C-5), 34.0 (C-3), 32.5 (C-7), 27.6 (C-4), 26.5 (C-9), 21.5 (C-8); IR (ATR): ν_{max} 3338, 3076, 2851, 1960, 1640, 1452, 1033, 906, 848, 632 cm^{-1} ; HRMS (APCI) m/z calcd for $\text{C}_{11}\text{H}_{21}\text{O}$ (M-H) $^+$ 169.1587; found 169.1592.

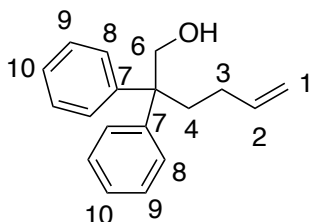
(4-(but-3-en-1-yl)tetrahydro-2H-pyran-4-yl)methanol (**278**)



278 was synthesized using the same procedure as **274** with LiAlH_4 (513 mg, 13.5 mmol) and **272** (1.79 g, 9.03 mmol). **278** yielded as a colourless oil (1.15 g, 75% yield). ^1H NMR (400 MHz, CDCl_3): δ 5.79 (1H, ddt, J = 16.9 Hz, 10.0 Hz, 6.3 Hz, H-2), 5.00 (1H, ddt, J = 16.9 Hz, 1.5

Hz, 1.5 Hz, H-1_{trans}), 4.94 (1H, ddt, $J = 10.0$ Hz, 1.5 Hz, 1.5 Hz, H-1_{cis}), 3.65-3.62 (4H, m, H-8), 3.47 (2H, s, H-6), 2.01-1.95 (2H, m, H-3), 1.53-1.45 (4H, m, H-7), 1.42 - 1.37 (2H, m, H-4) ppm; ^{13}C NMR (101 MHz, CDCl_3): δ 139.1 (C-2), 114.5 (C-1), 67.0 (C-6), 63.7 (C-8), 35.1 (C-5), 33.7 (C-3), 32.5 (C-7), 27.4 (C-4) ppm; IR (ATR): ν_{max} 3414.2, 3077.2, 2940.9, 2866.23, 2241.3, 1640.9, 1416.6, 1357.3, 1097.5, 909.8730.1, 646.5, 536.5 cm^{-1} ; HRMS (APCI): m/z calcd for $\text{C}_{10}\text{H}_{19}\text{O}_2$ (M-H)⁺ 171.1380; found 171.1371.

2,2-Diphenylhex-5-en-1-ol (279)

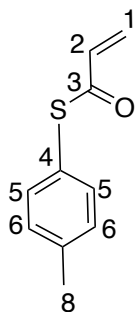


279 was synthesized using the same procedure as **274** with LiAlH_4 (513 mg, 13.5 mmol) and **273** (1.79 g, 9.03 mmol) in dry Et_2O (5 ml). **279** yielded as a colourless oil (1.10 g, 74% yield). ^1H NMR (400 MHz, CDCl_3): δ 7.32-7.30 (4H, m, H-8), 7.28-7.24 (2H, m, H-10), 7.22-7.18 (4H, m, H-9), 5.78 (1H, ddt, $J = 17.1$ Hz, 10.2 Hz, 7.3 Hz, H-2), 4.97 (1H, ddt, $J = 17.1$ Hz, 2.5 Hz, 1.4 Hz, H-1_{trans}), 4.92 (1H, ddt, $J = 10.2$ Hz, 2.5 Hz, 1.4 Hz, H-1_{cis}), 4.14 (2H, s, H-6), 2.27-2.23 (2H, m, H-3), 1.83-1.77 (2H, m, H-4) ppm; ^{13}C NMR (101 MHz, CDCl_3): δ 145.5 (C-7), 138.9 (C-2), 128.4 (C-8), 128.1 (C-9), 126.5 (C-10), 114.5 (C-1), 68.2 (C-6), 52.0 (C-5), 35.6 (C-3), 28.2 (C-4) ppm; IR (ATR): ν_{max} 3469, 3062, 2948, 2980, 1640, 1599, 1493, 1447, 1163, 1059, 994, 954, 908, 731, 698, 604 cm^{-1} ; HRMS (APCI): m/z calcd for $\text{C}_{18}\text{H}_{20}\text{NaO}$ (M-Na)⁺ 275.1406; found 275.1412.

5.3 Synthesis of Thioesters

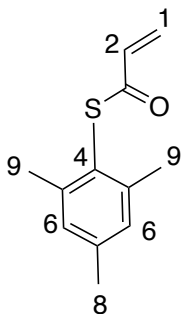
Note: In all cases competing 1,4-addition of the thiol was seen. This product could not be completely removed chromatographically so thioacrylates containing ~35% of the 1,4-addition product were used in the subsequent metathesis reaction.

Thioacrylic acid p-tolyl ester (**183**)



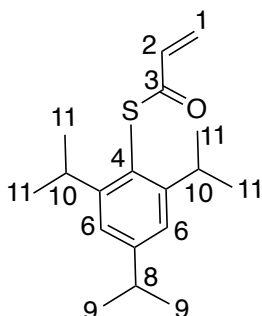
NaBH₄ (0.05 g, 1.32 mmol) and p-thiocresol (5.46 g, 44.0 mmol) were added in that order to a solution of NaOH (15% w/w aq. 20 ml) and stirred at room temperature for an hour and then cooled to 0 °C before use. In a separate flask, butylated hydroxytoluene (0.145 g, 0.66 mmol) and acryloyl chloride (5.36 ml, 66.0 mmol) were dissolved in cyclohexane (30 ml). To this solution under cooling at 0 °C, the borohydride solution was added (1ml/min) and stirred for 30 min. The solution was then heated to 55 °C and stirred for an hour. The reaction mixture was extracted with Et₂O (80 ml), washed with NaHCO₃ (100 ml) and brine solution (100 ml), and then dried over anhydrous MgSO₄. A portion of butylated hydroxytoluene (42.3 mg) was added prior to evaporation to prevent polymerization. **183** yielded as a pale-yellow oil (5.37 g, 68% yield) after column chromatography (2% Et₂O/hexane). ¹H NMR (400 MHz, CDCl₃): δ 7.33 (2H, d, *J* = 8.4 Hz, H-5) 7.24 (2H, d, *J* = 8.4 Hz, H-6), 6.45 (1H, dd, *J* = 17.5 Hz, 10.0 Hz, H-2), 6.38 (1H, dd, *J* = 17.5 Hz, 1.5 Hz, H-1), 5.75 (1H, dd, *J* = 10.0 Hz, 1.5 Hz, H-1), 2.39 (3H, s, H-8) ppm; ¹³C NMR (101 MHz, CDCl₃): δ 189.1 (C-3), 139.9 (C-7), 134.7 (C-5), 134.5 (C-2), 130.2 (C-6), 127.4 (C-1), 123.7 (C-4), 21.5 (C-8) ppm; IR (ATR): ν_{max} 3023, 2921, 1681, 1611, 1597, 1493, 1447, 1393, 1304, 1276, 1160, 986, 940, 803, 722, 704, 627, 528, 470 cm⁻¹; HRMS (ESI) *m/z* calcd for C₁₀H₁₁OS (M-H)⁺ 179.0536; found 179.0536

Thioacrylic acid 2,4,6-trimethyl-phenyl ester (**192**)



192 was synthesized using the same procedure as **183** with NaOH (15% w/w aq. 5 ml), NaBH₄ (0.015 g, 0.27 mmol), 2,4,6 trimethyl thiophenol (1.36 g, 8.93 mmol), butylated hydroxytoluene (0.030 g, 0.13 mmol) and acryloyl chloride (1.08 ml, 13.34 mmol). **192** yielded as a pale-yellow oil (1.26 g, 69% yield) after column chromatography (2% Et₂O/hexane). ¹H NMR (400 MHz, CDCl₃): δ 6.98 (2H, s, H-6), 6.49 (1H, dd, *J* =17.5 Hz, 10.0 Hz, H-2), 6.40 (1H, dd, *J* =17.5 Hz, 1.2 Hz, H-1), 5.74 (1H, dd, *J* =10.0 Hz, 1.2 Hz, H-1), 2.31 (6H, s, H-9), 2.29 (3H, s, H-8) ppm; ¹³C NMR (101 MHz, CDCl₃): δ 188.3 (C-3), 142.8 (C-4), 140.2 (C-2), 134.7 (C-6), 129.4 (C-7), 127.1 (C-1), 123.1 (C-5), 21.7 (C-9), 21.3 (C-8) ppm; IR (ATR): ν_{max} 2952, 2920, 1681, 1612, 1603, 1463, 1375, 1299, 1160, 1031, 994, 940, 850, 726, 631, 558 cm⁻¹; HRMS (ESI) *m/z* calcd for C₁₂H₁₅OS (M-H)⁺ 207.0838; found 207.0838.

Thioacrylic acid 2,4,6-triisopropyl-phenyl ester (**213**)

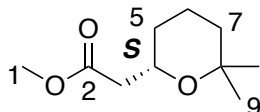


213 was synthesized using the same procedure as **183** with NaOH (15% w/w aq. 5 ml), NaBH₄ (4.80 mg, 0.131 mmol) and 2,4,6-triisopropylthiophenol (1.00 g, 4.23 mmol), butylated hydroxytoluene (9.33 mg, 0.04 mmol) and acryloyl chloride (1.00 ml, 6.74 mmol).

213 yielded as a pale-yellow oil (401 mg, 52% yield) after column chromatography (2% Et₂O/hexane). ¹H NMR (400 MHz, CDCl₃): δ 7.09 (2H, s, H-6), 6.50 (1H, dd, *J* =17.5 Hz, 10.0 Hz, H-2), 6.38 (1H, dd, *J* =17.5 Hz, 1.2 Hz, H-1), 5.74 (1H, dd, *J* =10.0 Hz, 1.2 Hz, H-1), 3.43-3.38 (2H, sept, *J* =6.9 Hz, H-10), 2.96-2.91 (1H, sept, *J* =6.9 Hz, H-8), 1.25 (6H, d, *J* =6.9 Hz, H-9), 1.18 (12H, d, *J* =6.9 Hz, H-11) ppm; ¹³C NMR (101 MHz, CDCl₃): δ 189.3 (C-3), 152.6 (C-5), 151.2 (C-7), 134.5 (C-1), 126.8 (C-2), 122.1 (C-6), 121.1 (C-4), 34.4 (C-8), 32.0 (C-10), 29.7 (C-10'), 23.9 (C-9), 22.7 (C-11) ppm. IR (ATR): ν_{max} 2952, 2920, 1681, 1612, 1603, 1463, 1375, 1299, 1160, 1031, 994, 940, 850, 726, 631, 558 cm⁻¹. HRMS (ESI) *m/z* calcd for C₁₈H₂₆OS (M-H)⁺ 291.1707; found 291.1704.

5.4 Determination of the Absolute Stereochemistry

(6,6-Dimethyl-tetrahydro-pyran-2-yl)-acetic acid methyl ester (253)



To solution of THP thioester **197** (25.0 mg, 0.09 mmol, 69% ee) in dry MeOH/DCM (1:1, 1 ml) was added AgOTf (67.1 mg, 0.26 mmol) and the reaction was stirred overnight. After completion of the reaction by TLC, the reaction was diluted with Et₂O (5 ml) and filtered through a silica plug followed by Et₂O (3 X 15 ml). The combined filtrate was concentrated *in vacuo* and the crude residue was purified by flash column chromatography 20% EtOAc/hexane to afford **197** as a pale yellow oil (14.1 mg, 88% yield, 67% ee). ¹H NMR (400 MHz, CDCl₃): δ 3.97 (1H, dddd, *J* = 11.4 Hz, 7.2 Hz, 4.7 Hz, 2.7 Hz, H-4), 3.65 (3H, s, H-1), 2.47 (1H, dd, *J* = 15.1 Hz, 7.2 Hz, H-3), 2.33 (1H, dd, *J* = 15.1 Hz, 4.7 Hz, H-3), 1.68-1.60 (3H, m, H-5, H-6), 1.45-1.30 (2H, m, H-7), 1.19 (3H, s, H-9), 1.16 (3H, s, H-9'), 1.13-1.08 (1H, m, H-6) ppm. ¹³C NMR (101 MHz, CDCl₃): δ 172.2 (C-2), 72.2 (C-8), 67.4 (C-4), 51.6 (C-1), 42.0 (C-3), 36.0 (C-5), 31.8 (C-9), 31.2 (C-7), 21.9 (C-9'), 19.9 (C-6) ppm. IR (ATR): ν_{max} 2974, 2935, 1740, 1435, 1380, 1192 cm⁻¹; ESI-MS: *m/z* calcd for C₁₀H₁₉NaO₃⁺ (M+Na)⁺ 209.1148; found 209.1151. [α]_D²⁰ + 26.4° (c 0.71, CHCl₃) [lit. [α]_D²⁰ - 51.2° (c 0.86, CHCl₃) for (*R*) enantiomer²].

5.5 Kinetic Isotope Studies

The deuterated cyclization precursor **250_D** was synthesized using the same procedure as the protonated **250_H** and then dissolved in deuterated methanol (CH₃OD) allowing for the H/D exchange, which was confirmed by mass spectrometry.

To a solution of alcohol-thioester **250_{H/D}** (20.0 mg, 0.05 mmol, 1 eq) in D₁₂-cyclohexane (2.3 ml), (*R*)-TRIP **199** (6.96 mg, 0.01 mmol, 20 mol %) was added and stirred at either 50 °C or room temperature. At regular intervals (20 min and 1 hour for the reaction carried out at 50 °C and room temperature respectively), the mixture was analyzed by ¹H NMR to monitor the formation of the products and the consumption of the starting materials over the time.

Time/ min	Conversion %	
	251_H	251_D
20	69	53
40	79	71
60	90	82
80	100	90

Table 17. Conversion of **250_{H/D}** over the time at 50 °C.

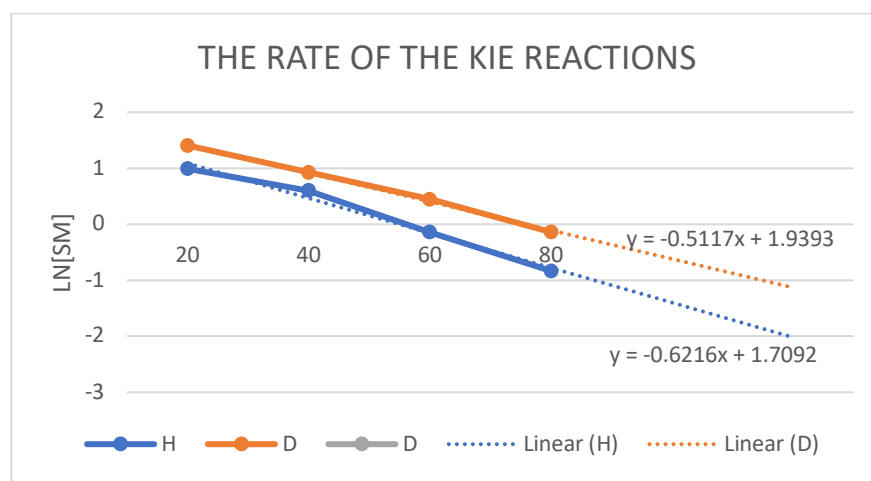


Figure 45. Experimental KIE of **251_{H/D}**

Time/ h	Conversion %	
	251 _H	251 _D
1	49	49
2	62	60
3	67	66

Table 18. Conversion of 251_{H/D} over the time at room temperature.

Time/ h	Conversion %	
	(R)-TRIP _H	(R)-TRIP _D
1	49	9
2	62	15
3	67	22
4	78	33
5	89	41

Table 19. Conversion of 251 over the time at room temperature with (R)-TRIP_{H/D}

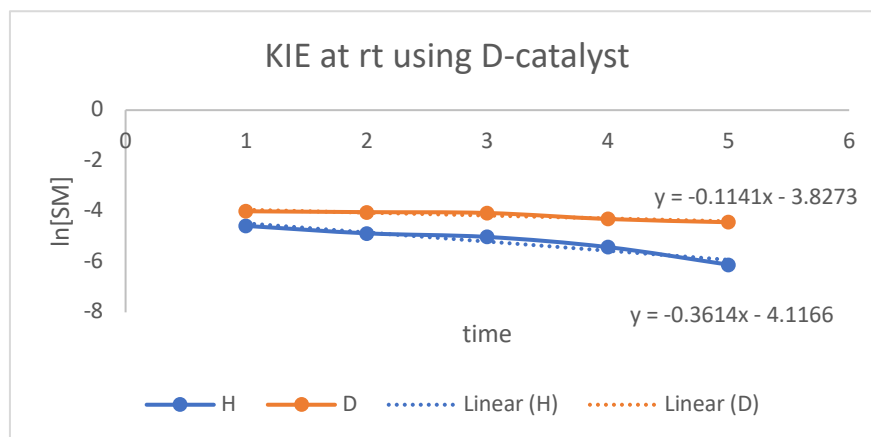
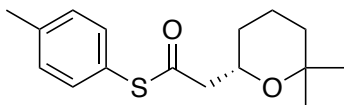


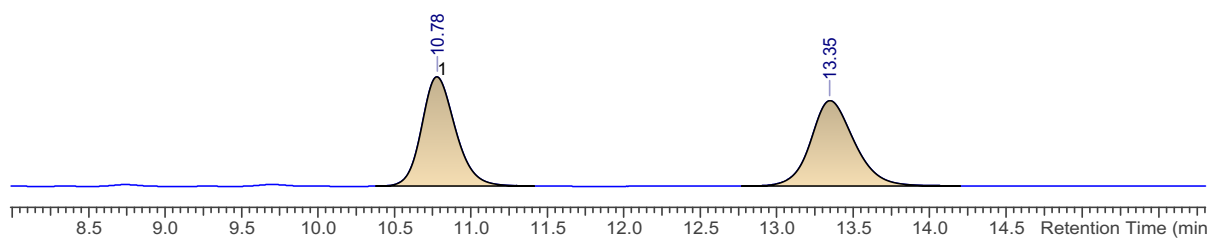
Figure 46. Experimental KIE of 251 at room temperature

5.6 HPLC Data



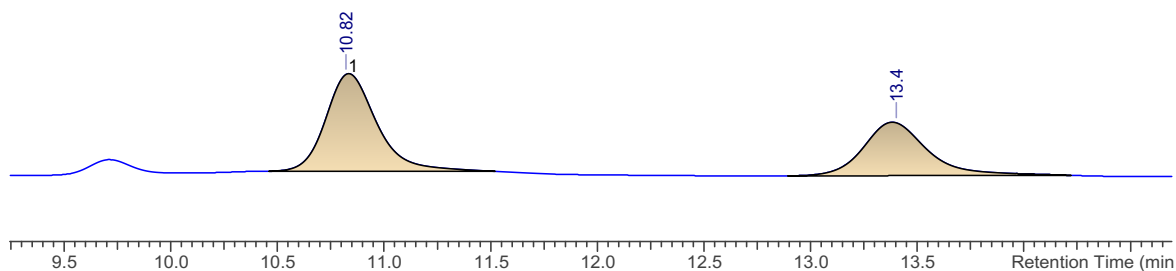
***S-p*-Tolyl-2-(6,6-dimethyltetrahydro-2*H*-pyran-2-yl)ethanethioate (185)**

HPLC separation conditions: CHIRALPAK AD-H column, hexane/2-propanol (95:5), flow rate: 0.9 ml/min, 25 °C; tR 10.78 min (major) and 13.35 min (minor).

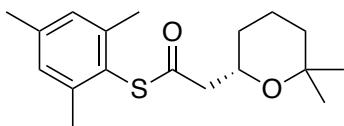


No.	tR	Peak Area (Y units*ms)	Area (%)	Width
1	10.78	1761496.375	49.782	0.394
2	13.35	1776920.750	50.218	0.503

(*R*)-TRIP, cyclohexane, 18% ee

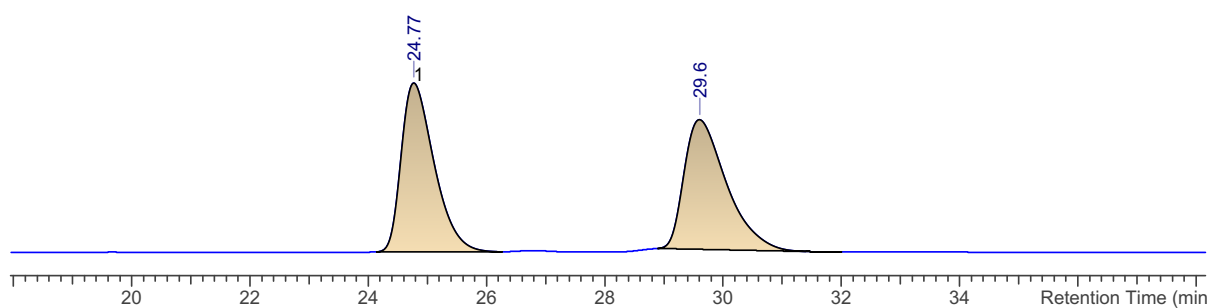


No.	tR	Peak Area (Y units*ms)	Area (%)	Width
1	10.82	685617.625	59.160	0.418
2	13.40	473311.531	40.840	0.515



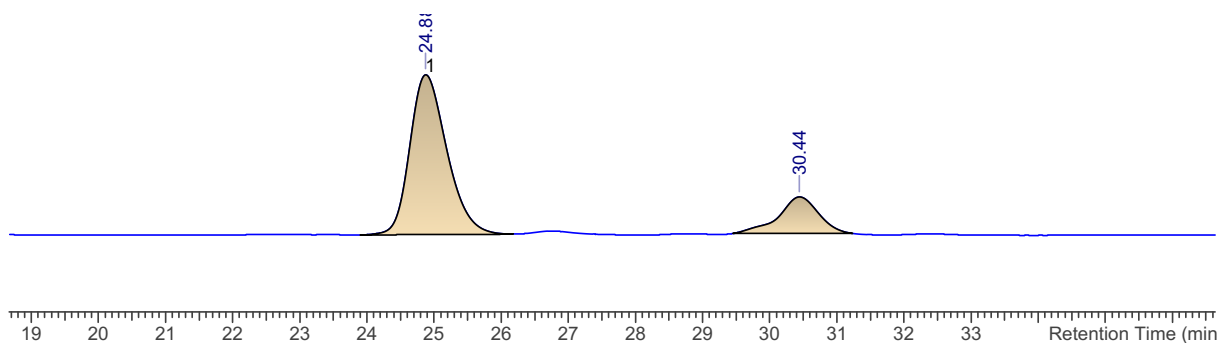
S-Mesityl 2-(6,6-dimethyltetrahydro-2H-pyran-2-yl)ethanethioate (197)

HPLC separation conditions: CHIRALPAK AD-H column, hexane/2-propanol (98:2), flow rate: 1.0 ml/min, 25 °C; tR 24.77 min (major) and 29.6 min (minor).



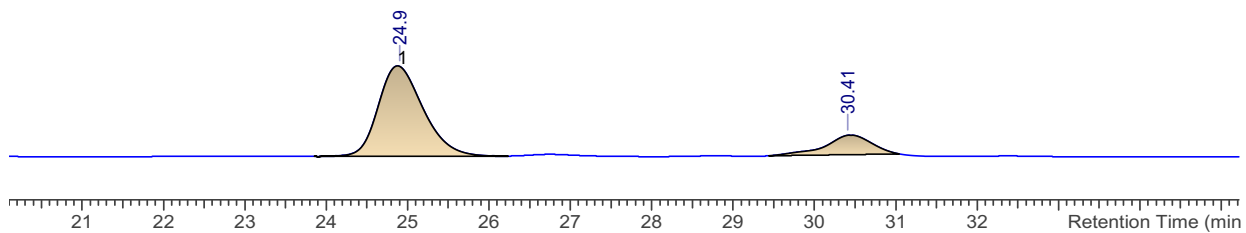
No.	tR	Peak Area (Y units*ms)	Area (%)	Width
1	24.77	9083537.000	50.240	1.007
2	29.60	8996811.000	49.760	1.287

(*R*)-TRIP, PhMe, 50 °C, 60% ee



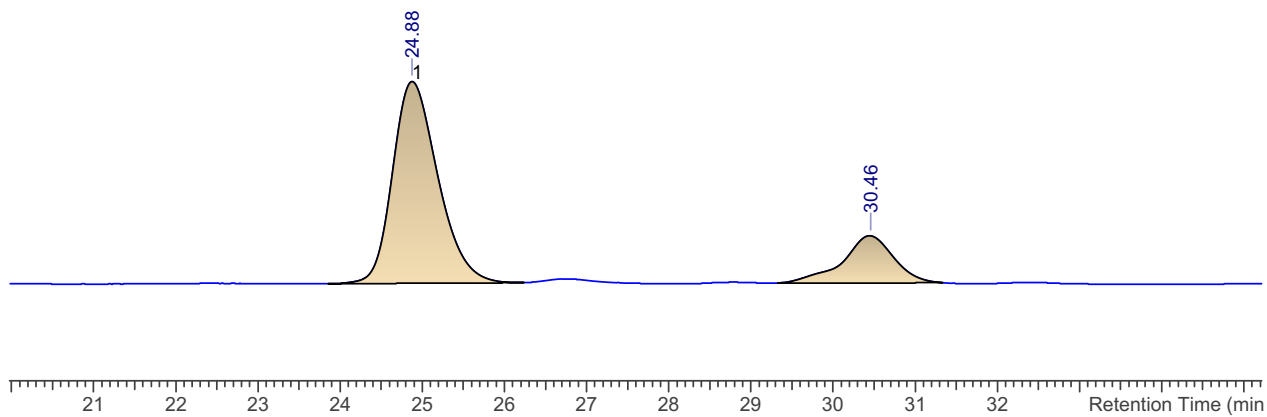
No.	tR	Peak Area (Y units*ms)	Area (%)	Width
1	24.88	2385430.250	80.086	0.994
2	30.44	593150.125	19.914	1.012

(*R*)-TRIP, cyclohexane, 75 °C, 66% ee

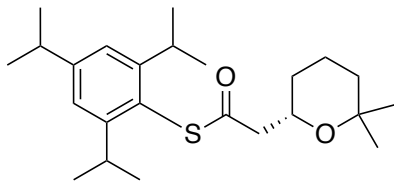


No.	tR	Peak Area (Y units*ms)	Area (%)	Width
1	24.90	2385430.250	83.245	0.998
2	30.41	480123.563	16.755	0.964

(*R*)-TRIP, cyclohexane, 50 °C, 69% ee

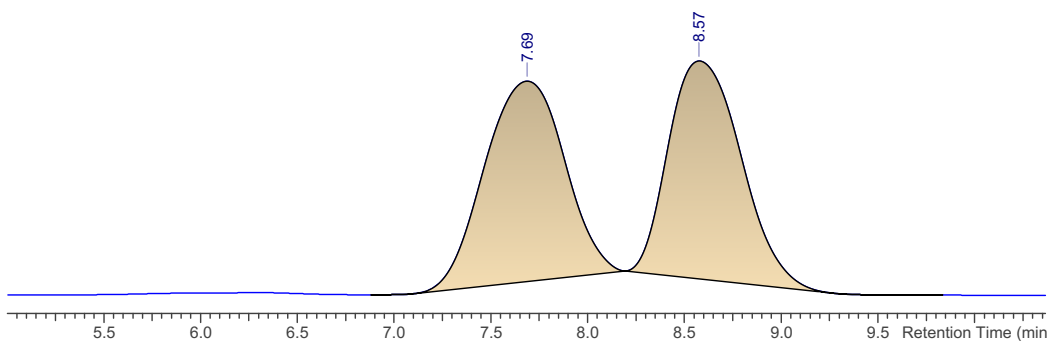


No.	tR	Peak Area (Y units*ms)	Area (%)	Width
1	24.88	2385499.750	84.625	0.993
2	30.46	433396.469	15.375	0.920

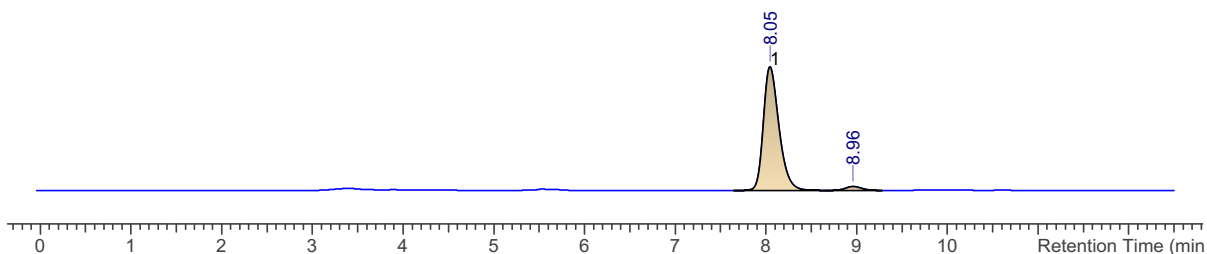


**(S)-S-(2,4,6-Triisopropylphenyl)2-(6,6-dimethyltetrahydro-2H-pyran-2-yl)ethanethioate
(216)**

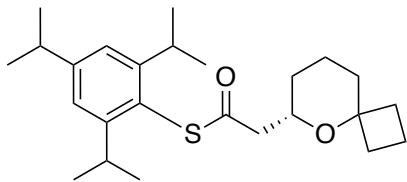
HPLC separation conditions: CHIRALPAK IA column, hexane/2-propanol (99:1), flow rate: 0.6 ml/min, 40 °C; tR 6.64 min (major) and 8.57 min (minor), 98% ee



No.	tR	Peak Area (Y units*ms)	Area (%)	Width
1	7.69	33347516.000	50.272	0.787
2	8.57	32986754.000	49.728	0.706

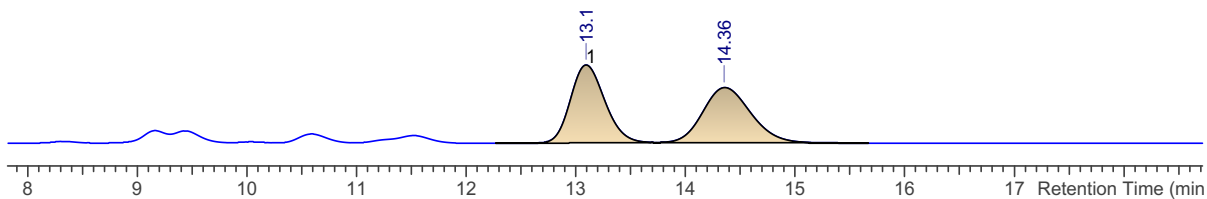


No.	tR	Peak Area (Y units*ms)	Area (%)	Width
1	8.05	7786344.000	99.037	0.305
2	8.96	75733.797	0.963	0.132

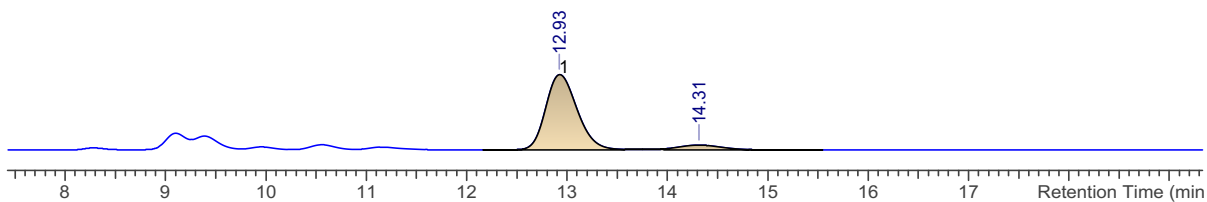


(S)-S-(2,4,6-Triisopropylphenyl) 2-(5-oxaspiro[3.5]nonan-6-yl)ethanethioate (241)

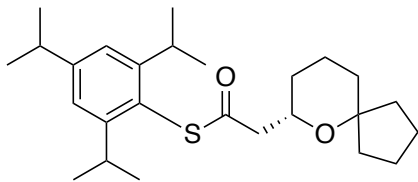
HPLC separation conditions: CHIRALPAK IA column, hexane/2-propanol (99:1), flow rate: 0.6 ml/min, 40 °C; tR 12.93 min (major) and 14.31 min (minor), 93% ee



No.	tR	Peak Area (Y units*ms)	Area (%)	Width
1	13.10	21178112.000	50.201	0.571
2	14.36	21008588.000	49.799	0.799

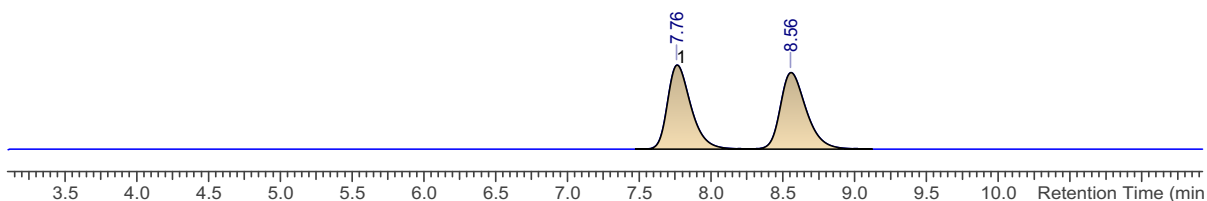


No.	tR	Peak Area (Y units*ms)	Area (%)	Width
1	12.93	34849340.000	96.445	0.569
2	14.31	1284388.500	3.555	0.588

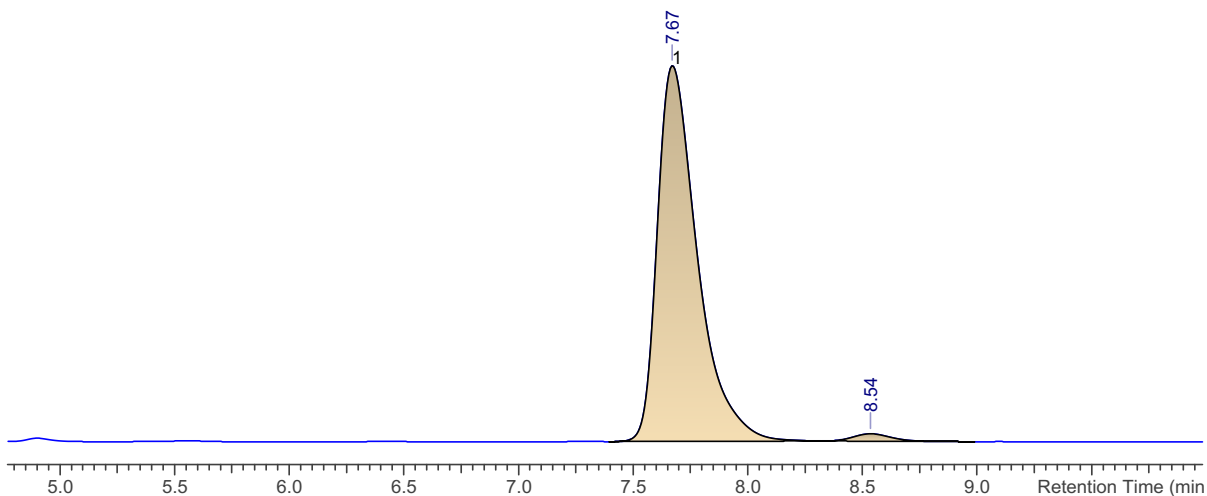


(S)-S-(2,4,6-Triisopropylphenyl)2-(6-oxaspiro[4.5]decan-7-yl)ethanethioate (242)

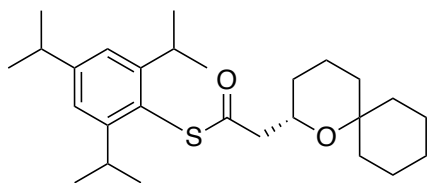
HPLC separation conditions: CHIRALPAK IA column, hexane/2-propanol (99:1), flow rate: 0.6 ml/min, 40 °C; tR 7.67 min (major) and 8.54 min (minor), 96% ee



No.	tR	Peak Area (Y units*ms)	Area (%)	Width
1	7.76	8561297.000	49.962	0.289
2	8.55	8574155.000	50.038	0.320

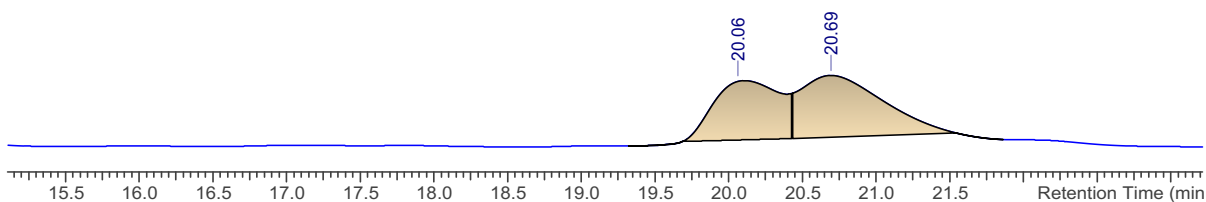


No.	tR	Peak Area (Y units*ms)	Area (%)	Width
1	7.67	21056412.000	98.199	0.304
2	8.54	386274.000	1.801	0.296

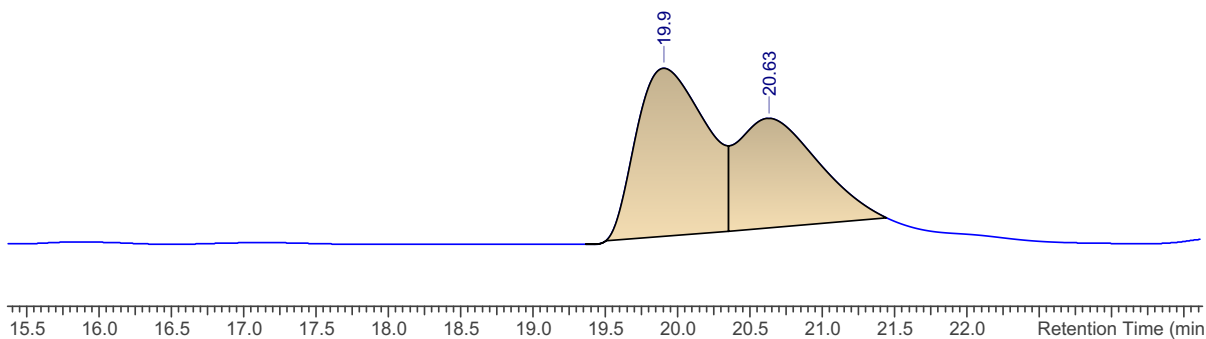


(S)-S-(2,4,6-Triisopropyl) 2-(1-oxaspiro[5.5]undecane-2-yl)ethanethioate (243)

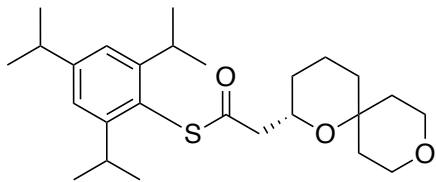
HPLC separation conditions: CHIRALPAK IC column, hexane/2-propanol (100:0), flow rate: 0.6 ml/min, 40 °C; tR 19.9 min (major) and 20.63 min (minor), 60% ee



No.	tR	Peak Area (Y units*ms)	Area (%)	Width
1	20.06	5220379.500	49.505	0.352
2	20.69	5324767.000	50.495	0.528

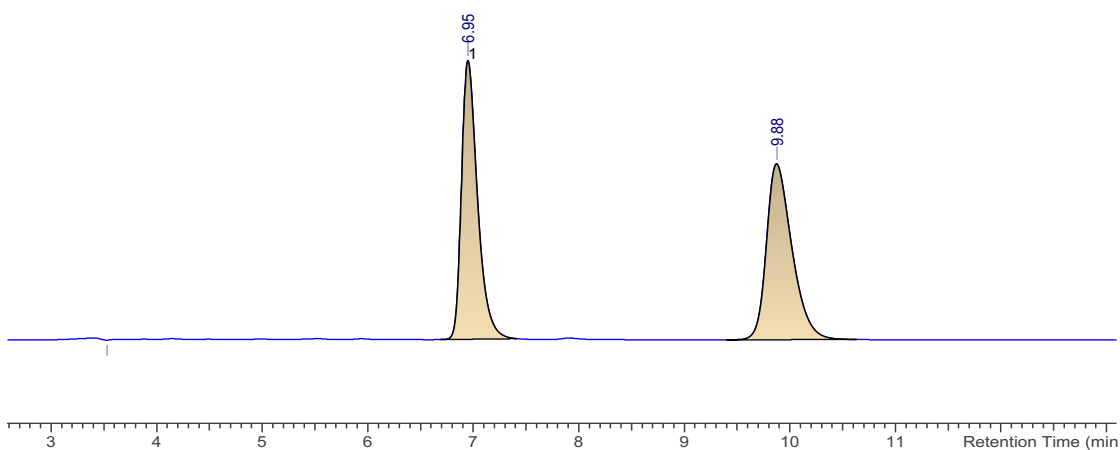


No.	tR	Peak Area (Y units*ms)	Area (%)	Width
1	19.90	2303106.250	19.967	0.068
2	20.63	9231700.000	80.033	1.229

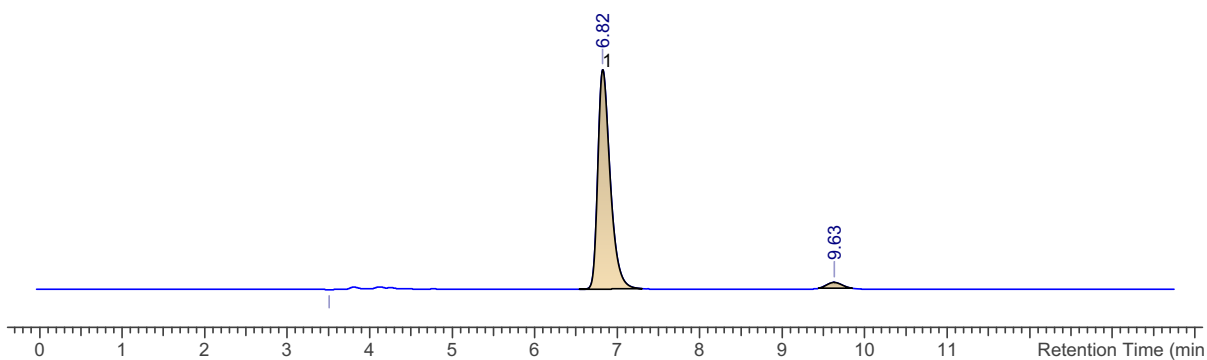


(S)-S-(2,4,6-Triisopropylphenyl)-2-(1,9-dioxaspiro[5.5]undecan-2-yl)ethanethioate (244)

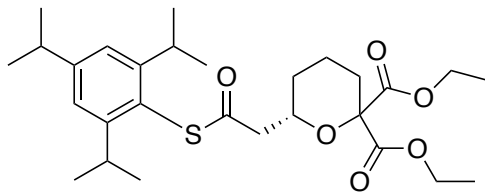
HPLC separation conditions: CHIRALPAK IA column, hexane/2-propanol (99:1), flow rate: 0.6 ml/min, 40 °C; tR 6.82 min (major) and 9.63 min (minor), 99% ee



No.	tR	Peak Area (Y units*ms)	Area (%)	Width
1	6.95	11337981.000	49.887	0.267
2	9.88	11389371.000	50.113	0.430

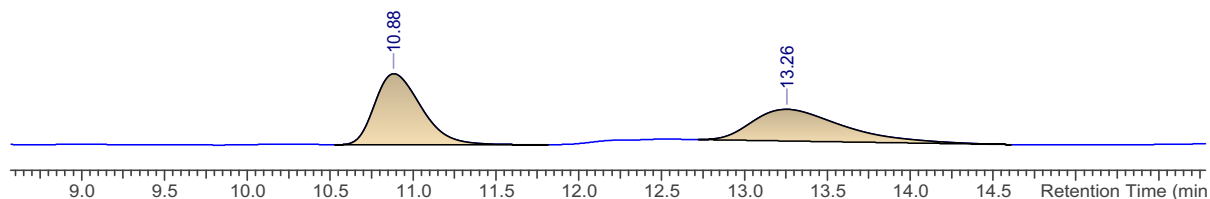


No.	tR	Peak Area (Y units*ms)	Area (%)	Width
1	6.82	10215860.000	99.288	0.264
2	9.63	73252.609	0.712	0.202

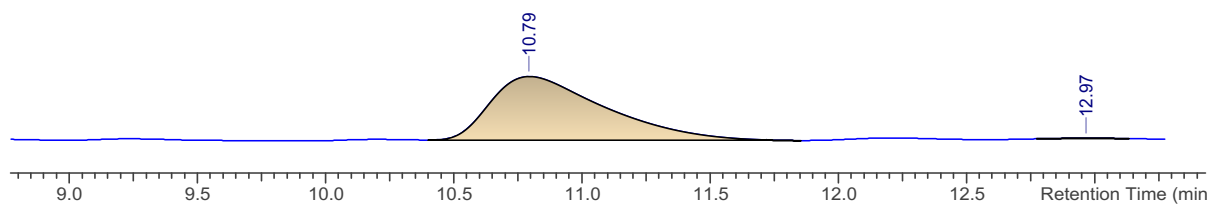


(S)-Diethyl-6-(2-oxo-2-((2,4,6-triisopropylphenyl)thio)ethyl)tetrahydro-2H-pyran-2,2-dicarboxylate (246)

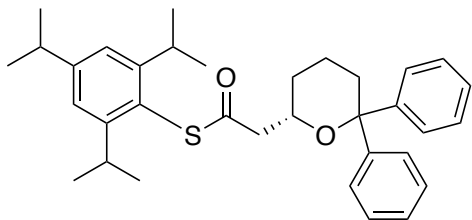
HPLC separation conditions: CHIRALPAK IA column, hexane/2-propanol (99:1), flow rate: 0.6 ml/min, 40 °C; tR 10.79 min (major) and 12.97 min (minor), 97% ee



No.	tR	Peak Area (Y units*ms)	Area (%)	Width
1	10.88	2911815.750	50.103	0.490
2	13.26	2899852.750	49.897	0.985

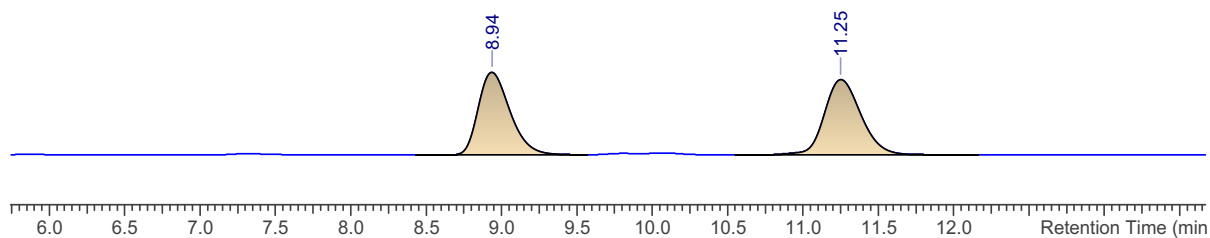


No.	tR	Peak Area (Y units*ms)	Area (%)	Width
1	10.79	2806635.500	98.734	0.810
2	12.97	36001.199	1.266	0.638

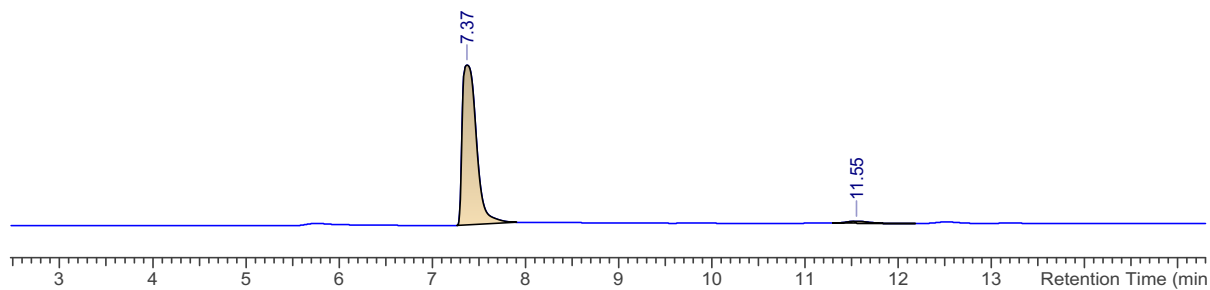


**(S)-S-(2,4,6-Triisopropylphenyl)2-(6,6-diphenyltetrahydro-2H-pyran-2-yl)ethanethioate
(245)**

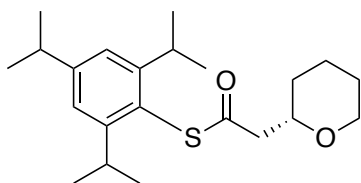
HPLC separation conditions: CHIRALPAK IA column, hexane/2-propanol (99:1), flow rate: 0.6 ml/min, 40 °C; tR 7.37 min (major) and 11.55 min (minor), 96% ee



No.	tR	Peak Area (Y units*ms)	Area (%)	Width
1	8.94	18180564.000	48.688	0.382
2	11.25	19160120.000	51.312	0.436

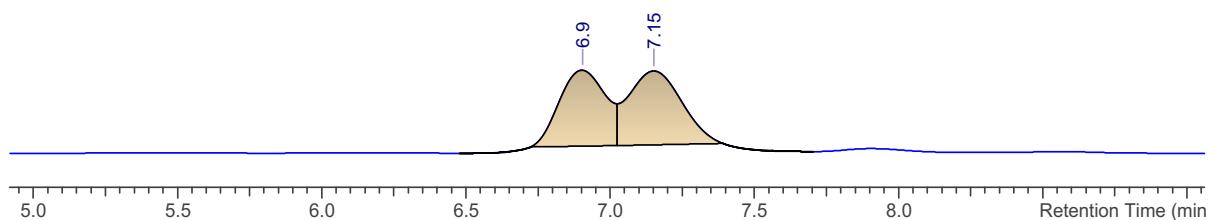


No.	tR	Peak Area (Y units*ms)	Area (%)	Width
1	7.37	22942132.000	98.099	0.276
2	11.55	444638.813	1.901	0.419

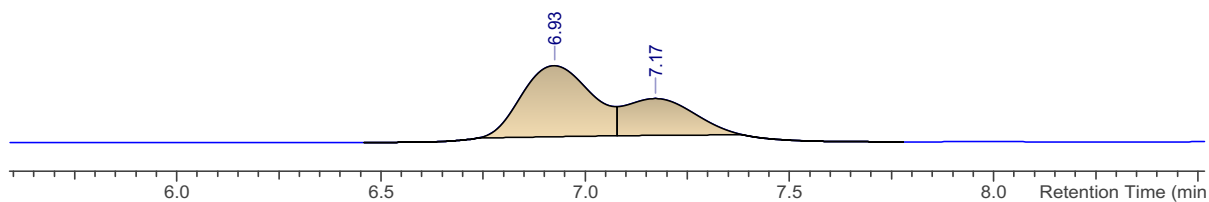


(S)-S-(2,4,6-Triisopropylphenyl) 2-(tetrahydro-2H-pyran-2-yl)ethanethioate (249)

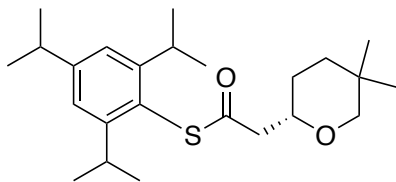
HPLC separation conditions: CHIRALPAK IA column, hexane/2-propanol (100:0), flow rate: 0.6 ml/min, 40 °C; tR 6.93 min (major) and 7.17 min (minor), 33% ee



No.	tR	Peak Area (Y units*ms)	Area (%)	Width
1	6.90	7088970.000	48.911	0.215
2	7.15	7404771.000	51.089	0.245

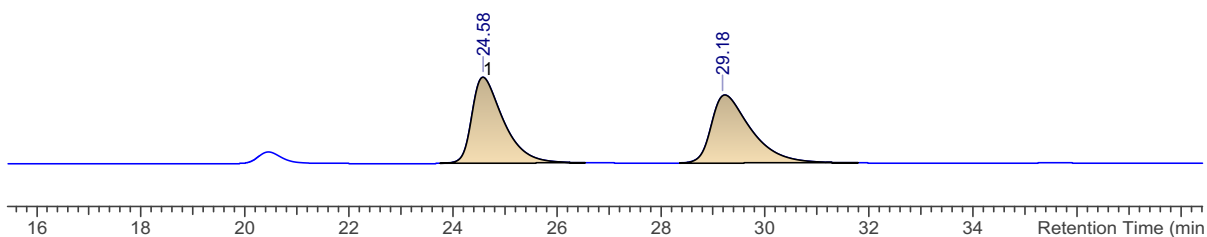


No.	tR	Peak Area (Y units*ms)	Area (%)	Width
1	6.93	18246696.000	66.289	0.344
2	7.17	9279316.000	33.711	0.201

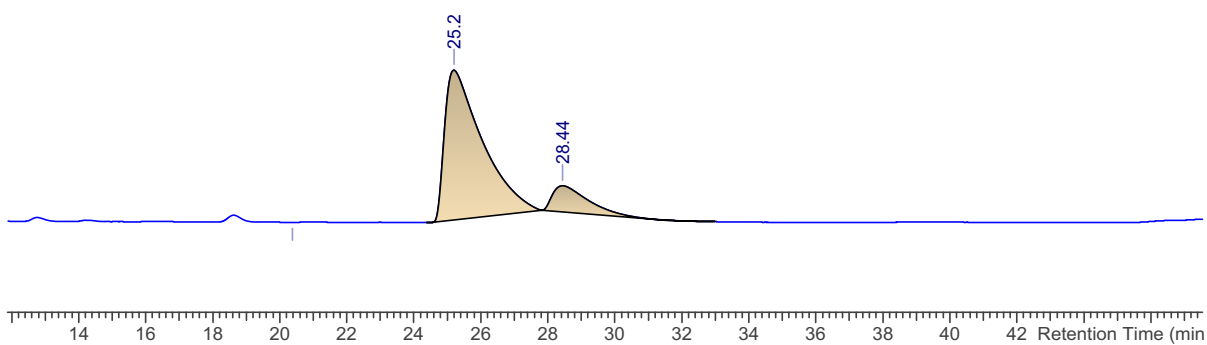


**(S)-S-(2,4,6-Triisopropylphenyl)2-(5,5-dimethyltetrahydro-2H-pyran-2-yl)ethanethioate
(286)**

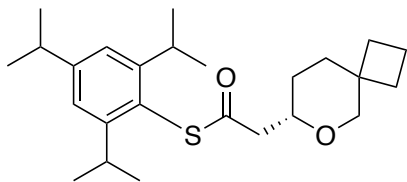
HPLC separation conditions: CHIRALPAK IA column, hexane/2-propanol (99:1), flow rate: 0.6 ml/min, 40 °C; tR 25.20 min (major) and 28.44 min (minor), 71% ee



No.	tR	Peak Area (Y units*ms)	Area (%)	Width
1	24.58	2426636.750	50.089	1.057
2	29.18	2417980.000	49.911	1.341

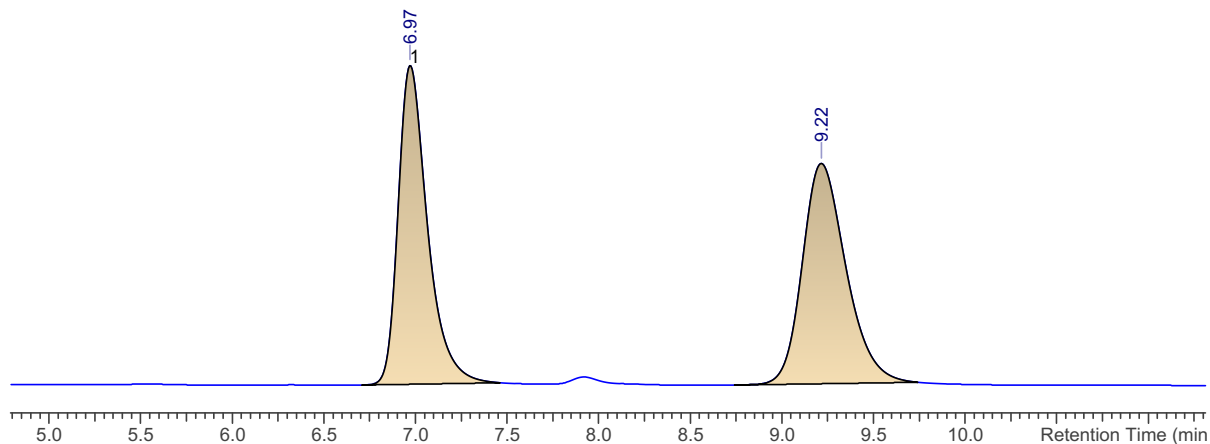


No.	tR	Peak Area (Y units*ms)	Area (%)	Width
1	25.20	7089395.000	85.629	1.999
2	28.44	1189756.625	14.371	1.882

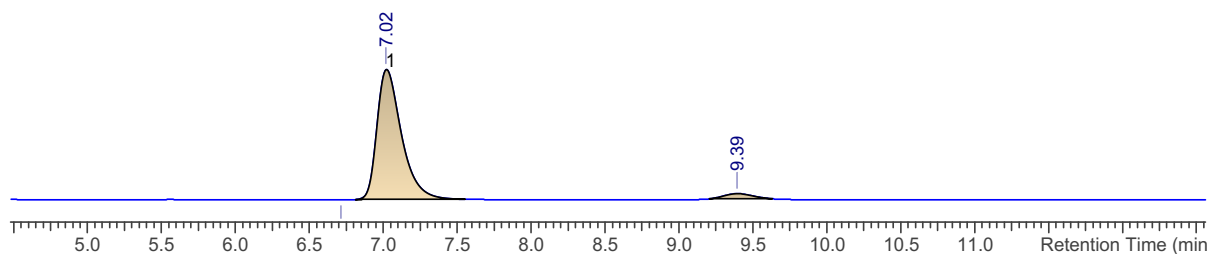


(S)-S-(2,4,6-Triisopropylphenyl) 2-(6-oxaspiro[3.5]nonan-7-yl)ethanethioate (287)

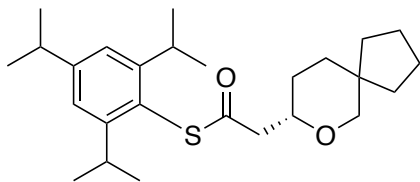
HPLC separation conditions: CHIRALPAK IA column, hexane/2-propanol (99:1), flow rate: 0.6 ml/min, 40 °C; tR 7.02 min (major) and 9.39 min (minor), 97% ee



No.	tR	Peak Area (Y units*ms)	Area (%)	Width
1	6.97	5266314.000	49.232	0.279
2	9.22	5430537.000	50.768	0.427

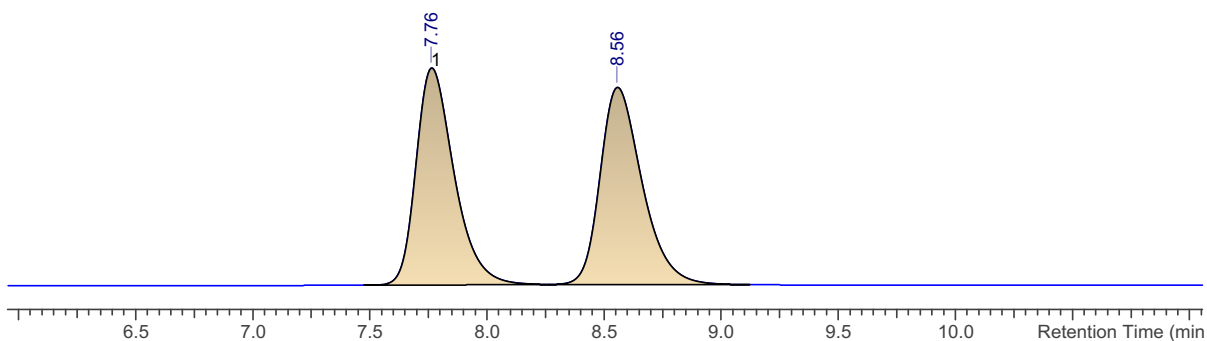


No.	tR	Peak Area (Y units*ms)	Area (%)	Width
1	7.02	14916656.000	98.607	0.291
2	9.39	210735.641	1.393	0.259

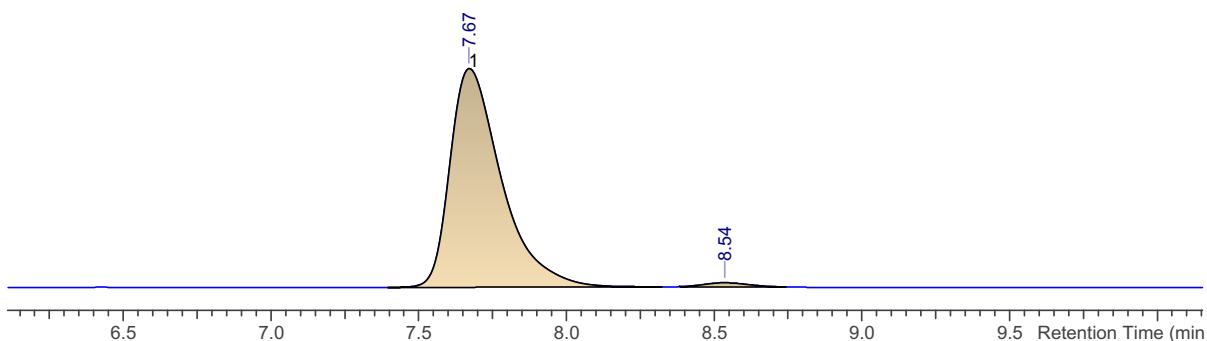


(S)-S-(2,4,6-Triisopropylphenyl) 2-(6-oxaspiro[4.5]decan-7-yl)ethanethioate (288)

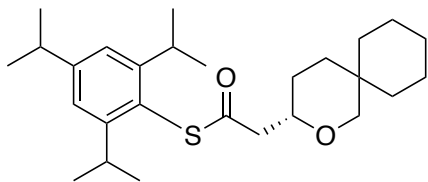
HPLC separation conditions: CHIRALPAK IA column, hexane/2-propanol (99:1), flow rate: 0.6 ml/min, 40 °C; tR 7.67 min (major) and 8.54 min (minor), 99% ee



No.	tR	Peak Area (Y units*ms)	Area (%)	Width
1	7.76	8561297.000	49.962	0.289
2	8.55	8574155.000	50.038	0.320

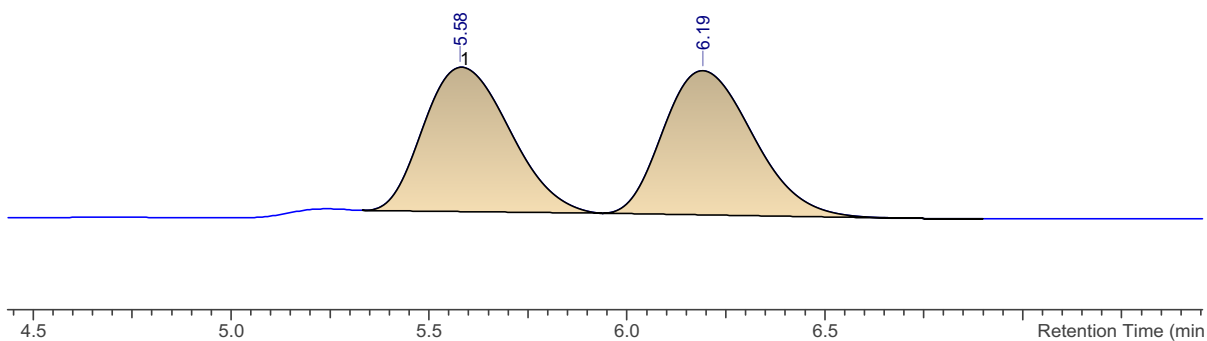


No.	tR	Peak Area (Y units*ms)	Area (%)	Width
1	7.67	21056412.000	99.399	0.304
2	8.54	127288.211	0.601	0.200

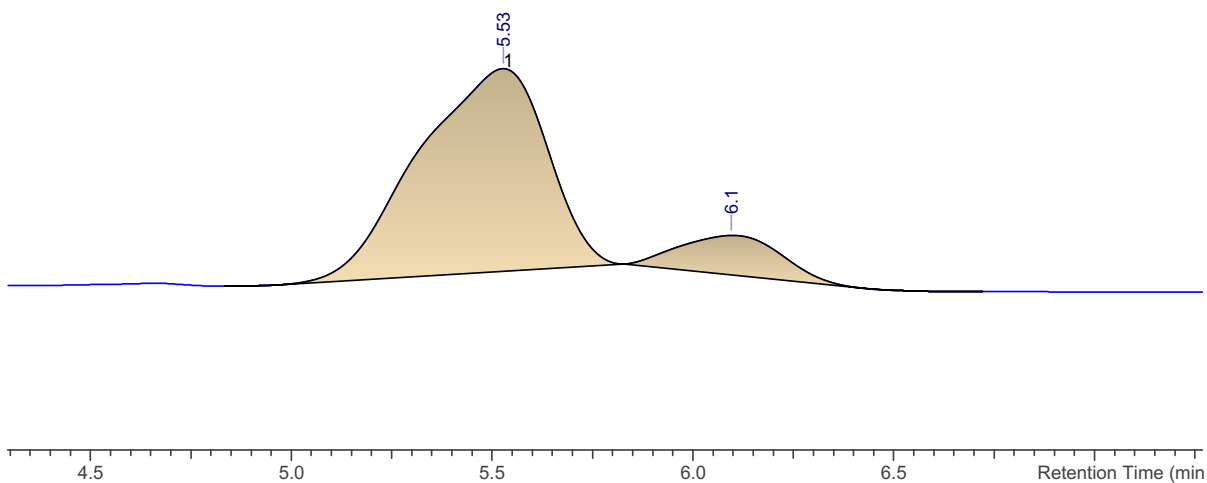


(S)-S-(2,4,6-Triisopropylphenyl) 2-(2-oxaspiro[5.5]undecan-3-yl)ethanethioate (289)

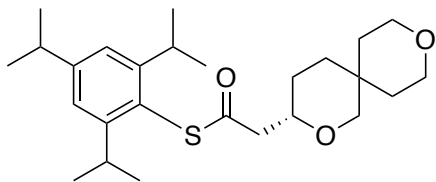
HPLC separation conditions: CHIRALPAK IB column, hexane/2-propanol (100:0), flow rate: 0.6 ml/min, 40 °C; tR 5.53 min (major) and 6.1 min (minor), 73% ee



No.	tR	Peak Area (Y units*ms)	Area (%)	Width
1	5.58	7373615.500	49.005	0.413
2	6.19	7672967.000	50.995	0.424

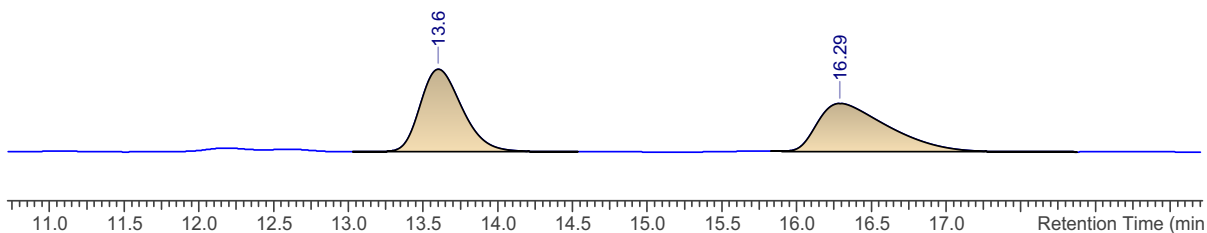


No.	tR	Peak Area (Y units*ms)	Area (%)	Width
1	5.53	1711052.125	86.592	0.636
2	6.10	264942.563	13.408	0.464

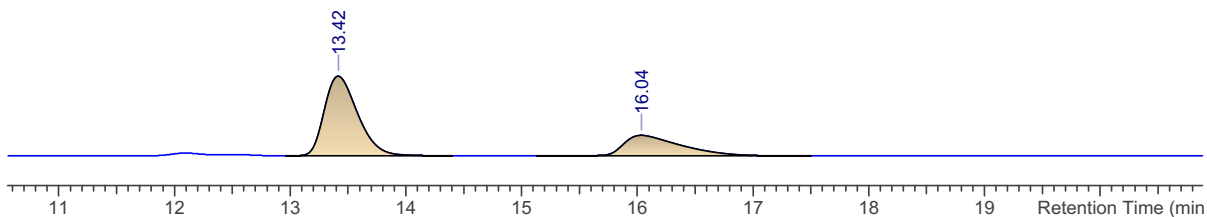


(S)-S-(2,4,6-Triisopropylphenyl) 2-(2,9-dioxaspiro[5.5]undecan-3-yl)ethanethioate (290)

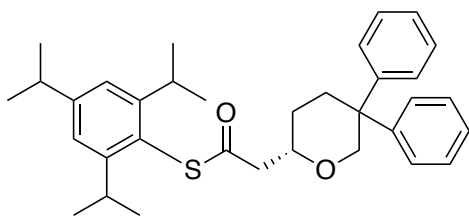
HPLC separation conditions: CHIRALPAK IA column, hexane/2-propanol (99:1), flow rate: 0.6 ml/min, 40 °C; tR 13.42 min (major) and 16.04 min (minor), 40% ee



No.	tR	Peak Area (Y units*ms)	Area (%)	Width
1	13.60	3270212.750	50.766	0.510
2	16.29	3171546.500	49.234	0.862

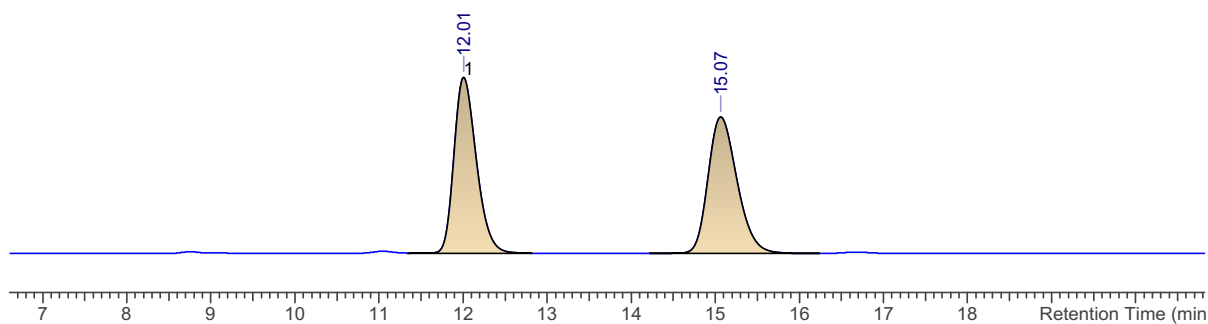


No.	tR	Peak Area (Y units*ms)	Area (%)	Width
1	13.42	9410043.000	69.551	0.524
2	16.04	4119725.250	30.449	0.885

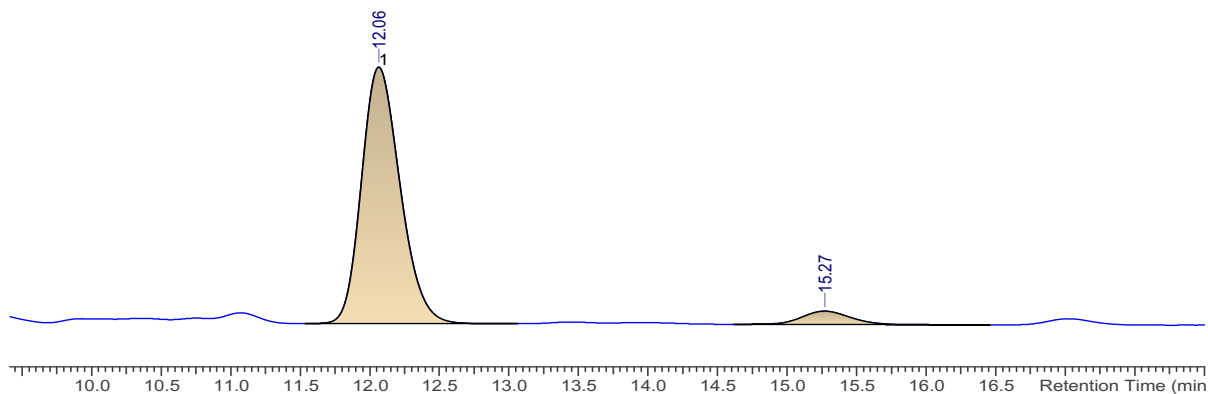


**(S)-S-(2,4,6-Triisopropylphenyl)2-(5,5-diphenyltetrahydro-2H-pyran-2-yl)ethanethioate
(291)**

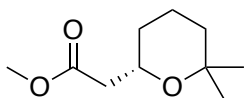
HPLC separation conditions: CHIRALPAK IA column, hexane/2-propanol (99:1), flow rate: 0.6 ml/min, 40 °C; t_R 12.06 min (major) and 15.27 min (minor), 87% ee



No.	tR	Peak Area (Y units*ms)	Area (%)	Width
1	12.01	7751497.500	49.846	0.482
2	15.07	7799358.000	50.154	0.626

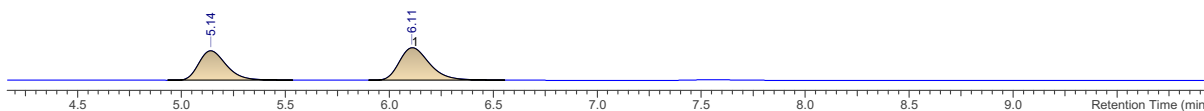


No.	tR	Peak Area (Y units*ms)	Area (%)	Width
1	12.06	5185279.500	93.809	0.506
2	15.27	342188.531	6.191	0.632

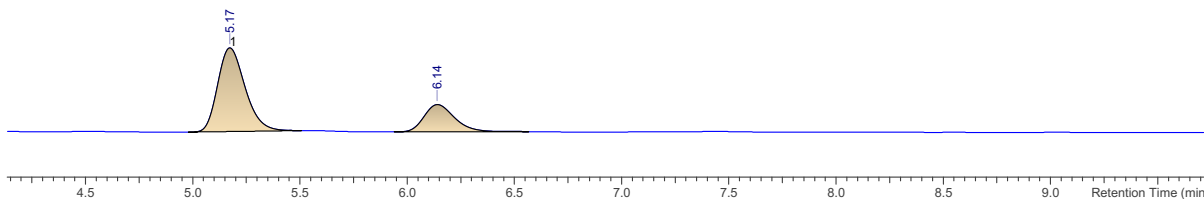


(6,6-Dimethyl-tetrahydro-pyran-2-yl)-acetic acid methyl ester (255)

HPLC separation conditions: CHIRALPAK IA column, hexane/2-propanol (95:5), flow rate: 1.0 ml/min, 25 °C; tR 5.17 min for (S)-enantiomer (major) and 6.14 min for (R)- enantiomer (minor), 66% ee

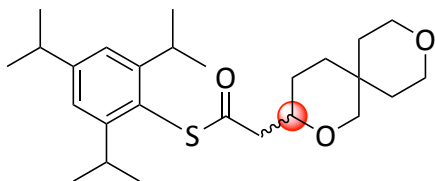


No.	tR	Peak Area (Y units*ms)	Area (%)	Width
1	5.14	6392892.000	49.743	0.233
2	6.11	6458914.500	50.257	0.235



No.	tR	Peak Area (Y units*ms)	Area (%)	Width
1	5.17	1077943.375	83.723	0.231
2	6.14	209571.516	16.277	0.208

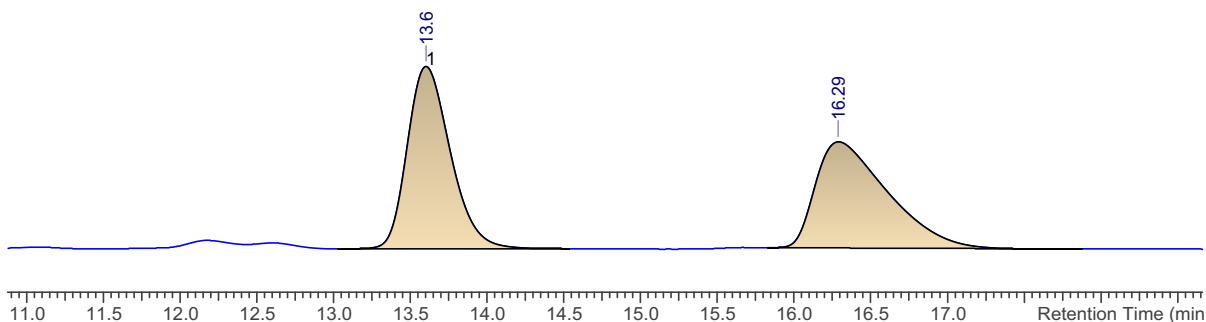
5.6.1 The enantio-inversion of 3,3'-spiro THP



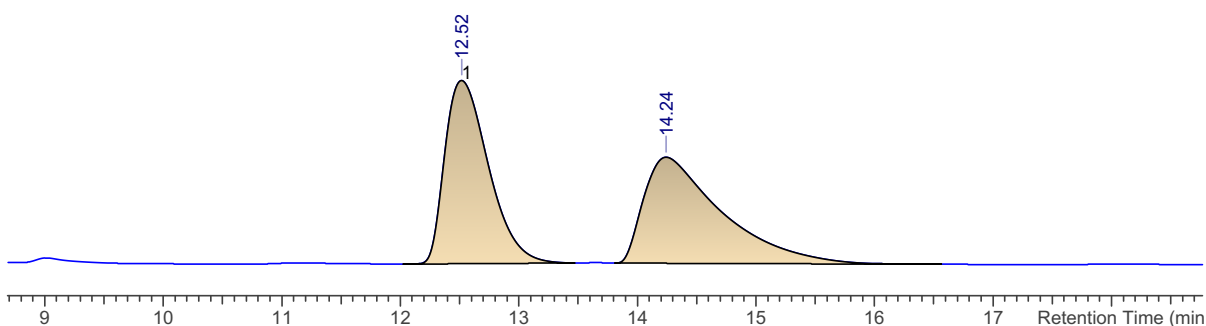
(S)-S-(2,4,6-Triisopropylphenyl) 2-(2,9-dioxaspiro[5.5]undecan-3-yl)ethanethioate (298)

HPLC separation conditions: CHIRALPAK IA column, hexane/2-propanol (99:1), flow rate: 0.6 ml/min, 40 °C

Racemic:

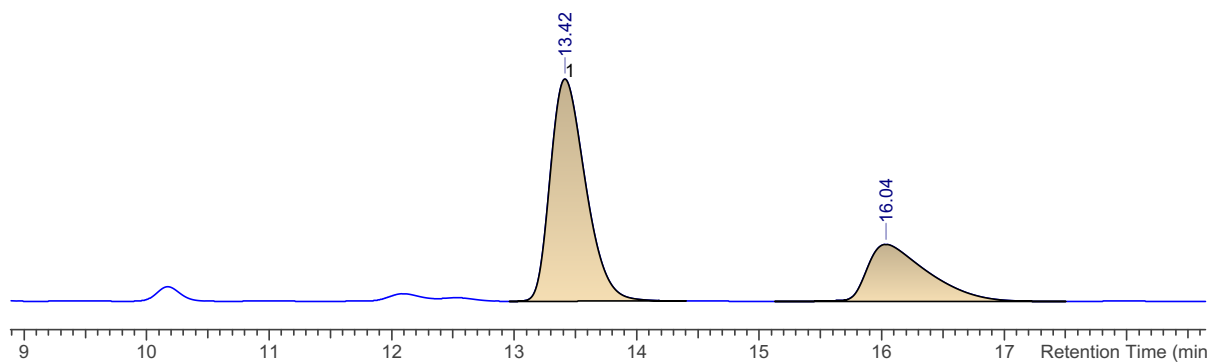


No.	tR	Peak Area (Y units*ms)	Area (%)	Width
1	13.60	3270212.750	50.766	0.510
2	16.29	3171546.500	49.234	0.862

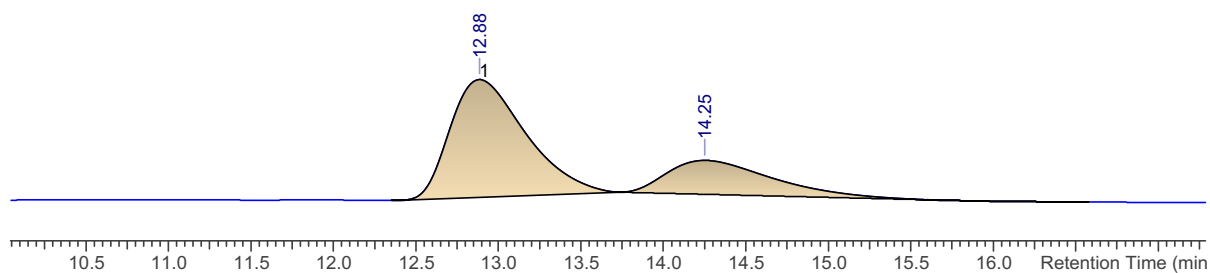


No.	tR	Peak Area (Y units*ms)	Area (%)	Width
1	12.52	35136680.000	49.275	0.679
2	14.24	36170044.000	50.725	1.143

(*R*)-TRIP 20 mol%, at 50 °C; 39% ee

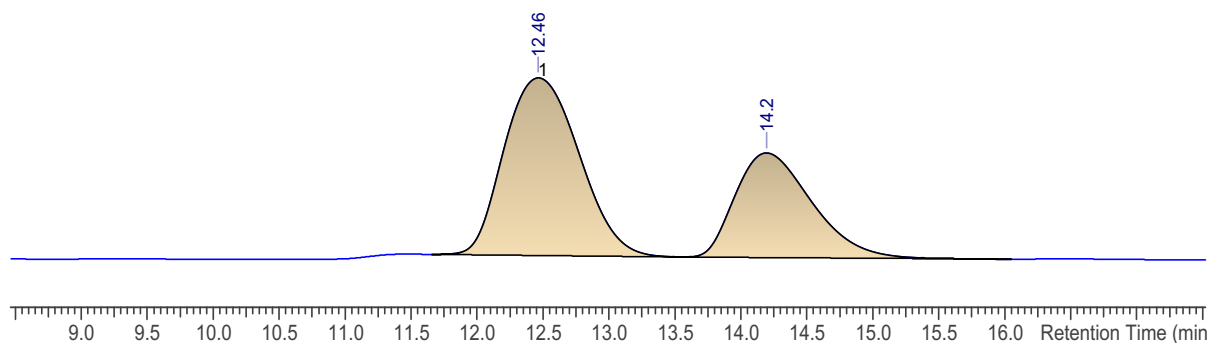


No.	tR	Peak Area (Y units*ms)	Area (%)	Width
1	13.42	9410043.000	69.551	0.524
2	16.04	4119725.250	30.449	0.885



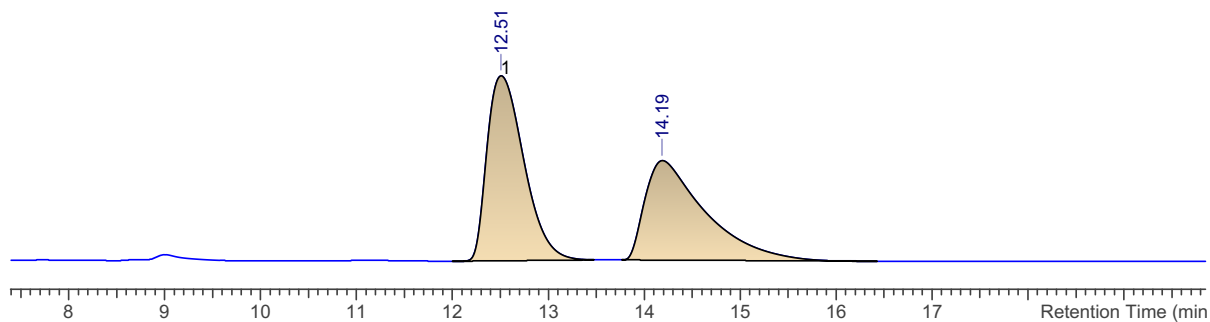
No.	tR	Peak Area (Y units*ms)	Area (%)	Width
1	12.88	4560005.000	69.580	0.821
2	14.25	1993566.500	30.420	1.149

(*R*)-TRIP 20 mol%, at 40 °C; 31% ee



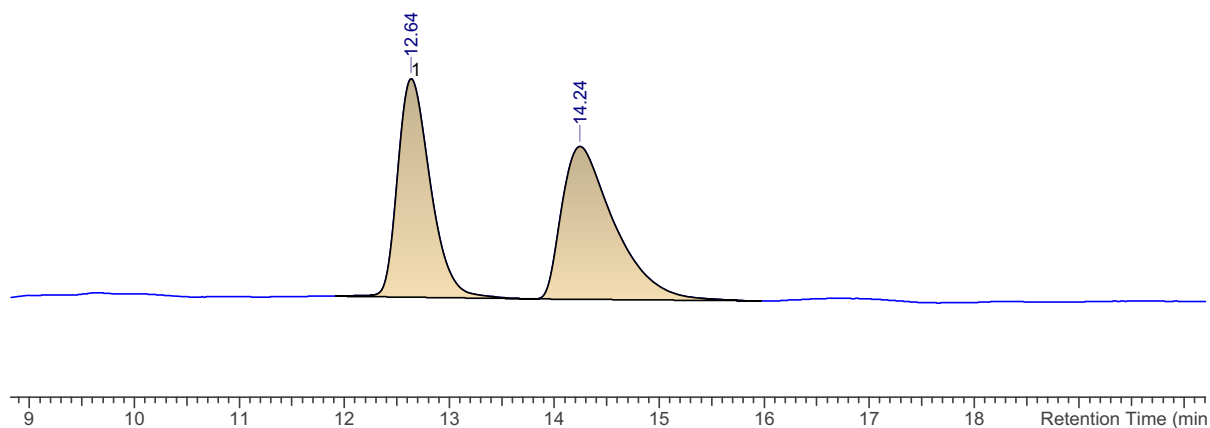
No.	tR	Peak Area (Y units*ms)	Area (%)	Width
1	12.46	9317568.000	65.737	1.085
2	14.20	4856486.000	34.263	1.020

(*R*)-TRIP 20 mol%, at 35 °C; 27% ee



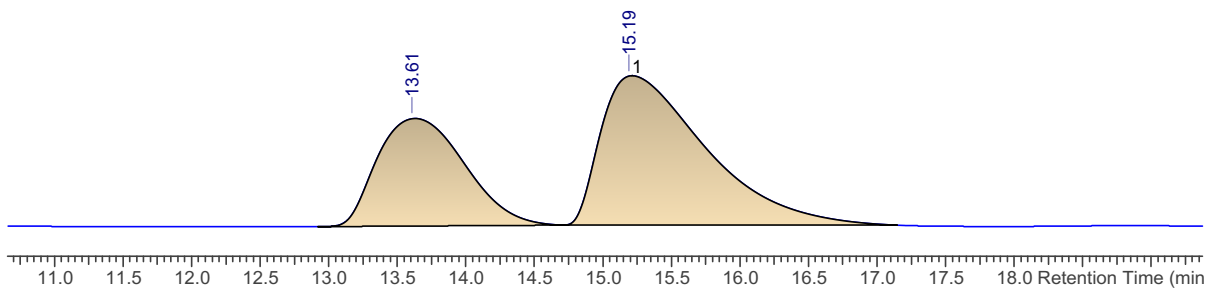
No.	tR	Peak Area (Y units*ms)	Area (%)	Width
1	12.51	40070616.000	63.256	0.712
2	14.19	23276562.000	36.744	0.892

(*R*)-TRIP 20 mol%, at 30 °C; 8% ee



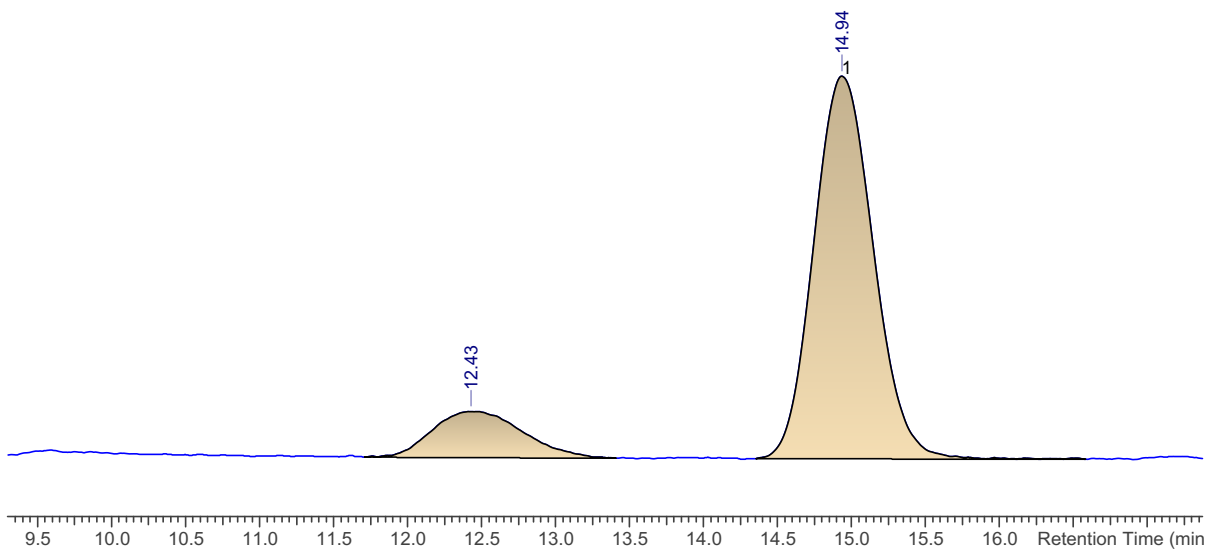
No.	tR	Peak Area (Y units*ms)	Area (%)	Width
1	12.64	1696315.500	45.955	0.554
2	14.24	1994940.625	54.045	0.890

(*R*)-TRIP 20 mol%, at 25 °C; 23% ee



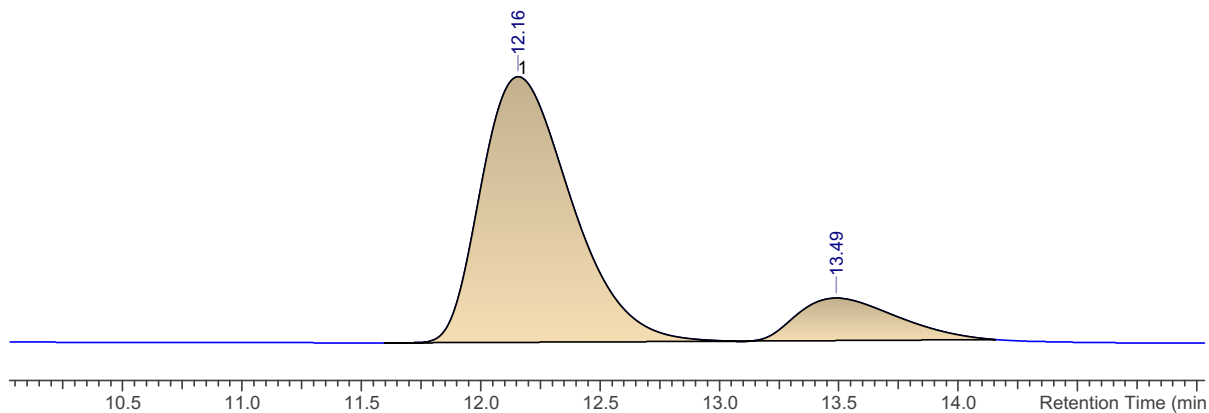
No.	tR	Peak Area (Y units*ms)	Area (%)	Width
1	13.61	43740724.000	38.712	1.230
2	15.19	69249352.000	61.288	1.365

(*R*)-TRIP 20 mol%, at 20 °C; 71 % ee



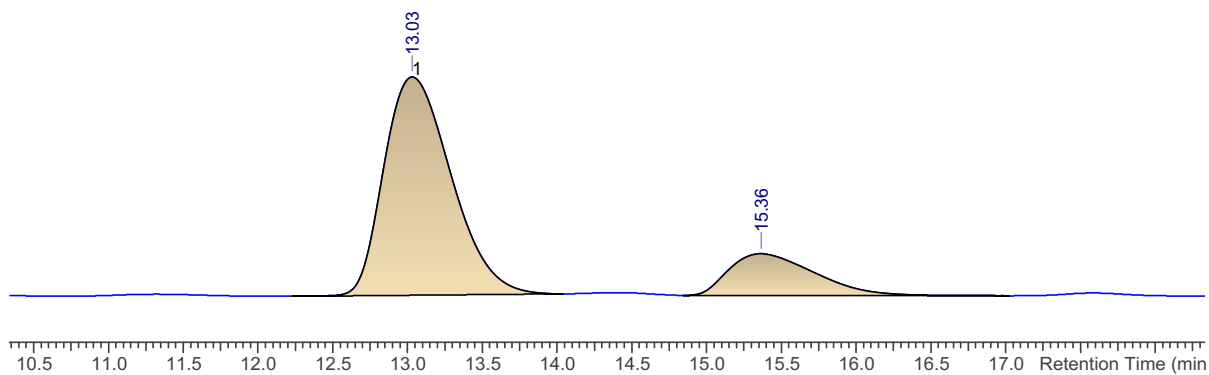
No.	tR	Peak Area (Y units*ms)	Area (%)	Width
1	12.43	94718.234	14.689	1.115
2	14.94	550101.187	85.311	0.736

(*R*)-TRIP 40 mol%, at 50 °C; 66% ee



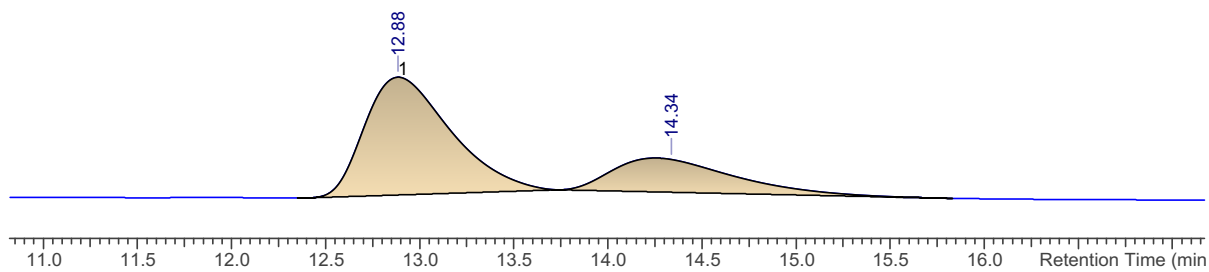
No.	tR	Peak Area (Y units*ms)	Area (%)	Width
1	12.16	24464880.000	83.011	0.667
2	13.49	5007090.000	16.989	0.798

(*R*)-TRIP 30 mol%, at 50 °C; 57% ee



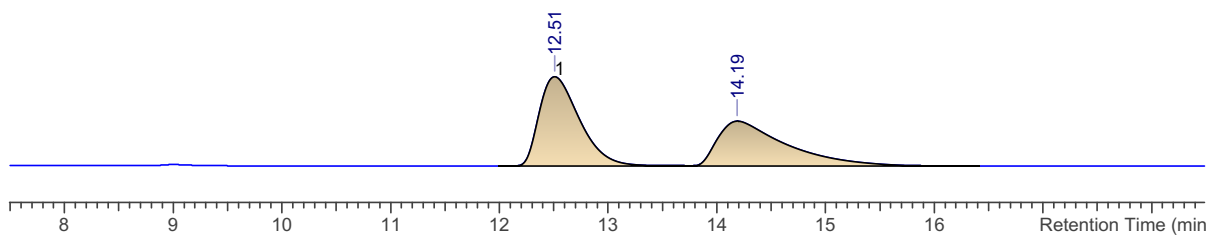
No.	tR	Peak Area (Y units*ms)	Area (%)	Width
1	13.03	12470862.000	78.580	0.809
2	15.36	3399361.500	21.420	1.082

(*R*)-TRIP 10 mol%, at 50 °C; 34% ee



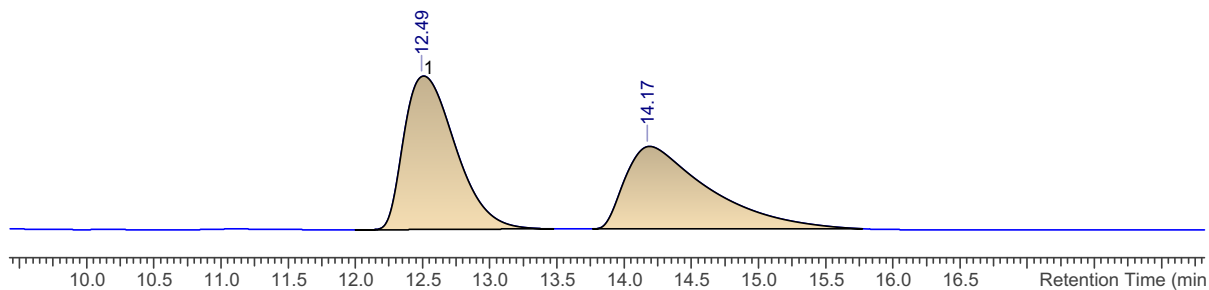
No.	tR	Peak Area (Y units*ms)	Area (%)	Width
1	12.86	4038967.500	66.977	0.769
2	14.34	1991381.625	33.023	1.203

(*R*)-TRIP 5mol%, at 50 °C; 30% ee



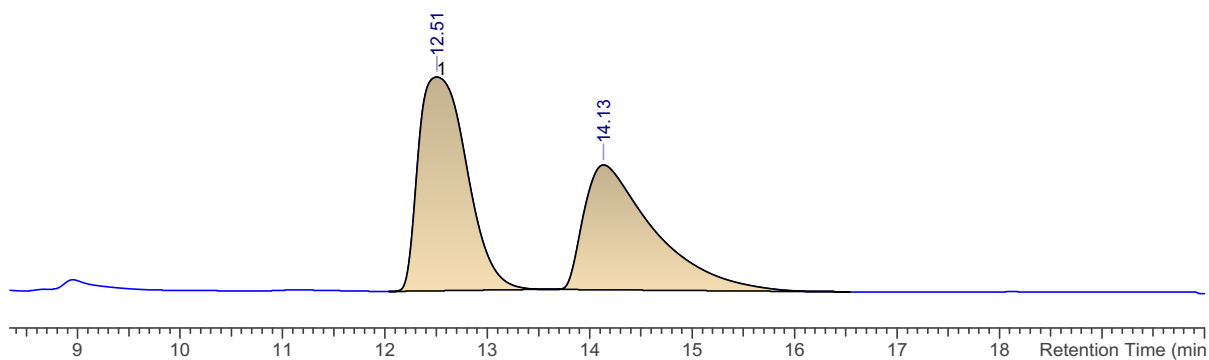
No.	tR	Peak Area (Y units*ms)	Area (%)	Width
1	12.51	12842138.000	64.993	0.676
2	14.19	6917130.000	35.007	0.867

(*R*)-TRIP 50 mol%, at 20 °C; 38% ee



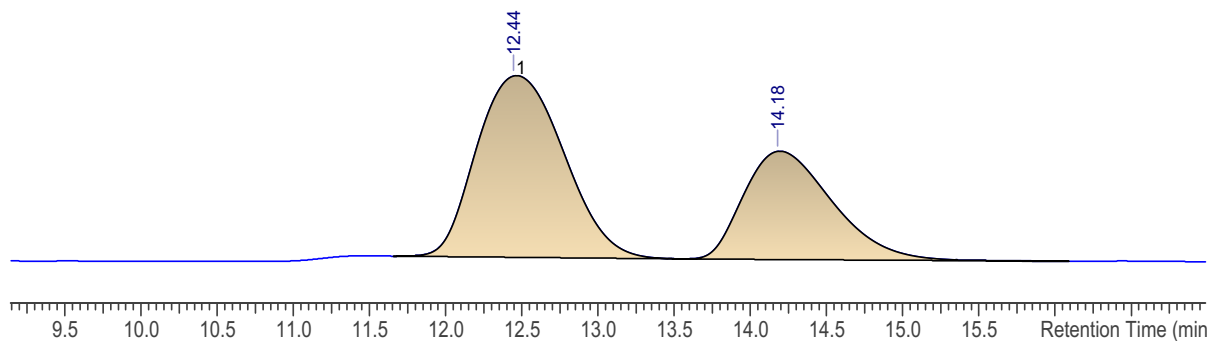
No.	tR	Peak Area (Y units*ms)	Area (%)	Width
1	12.49	40070616.000	68.966	0.714
2	14.17	18031616.000	31.034	0.773

(*R*)-TRIP 40 mol%, at 20 °C; 32% ee



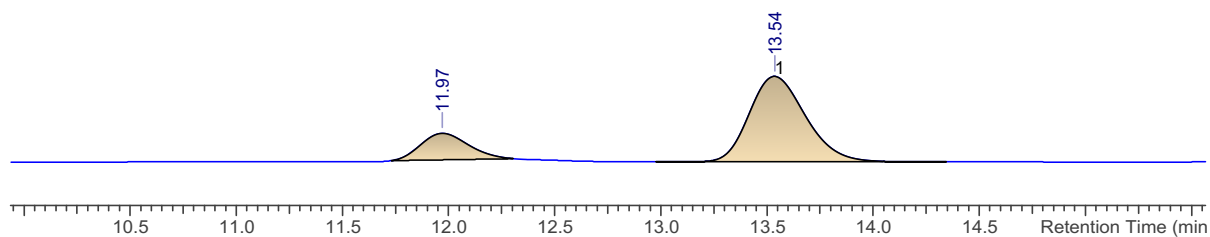
No.	tR	Peak Area (Y units*ms)	Area (%)	Width
1	12.50	60279348.000	65.994	0.894
2	14.13	31060704.000	34.006	0.903

(R)-TRIP 30 mol%, at 20 °C; 21% ee



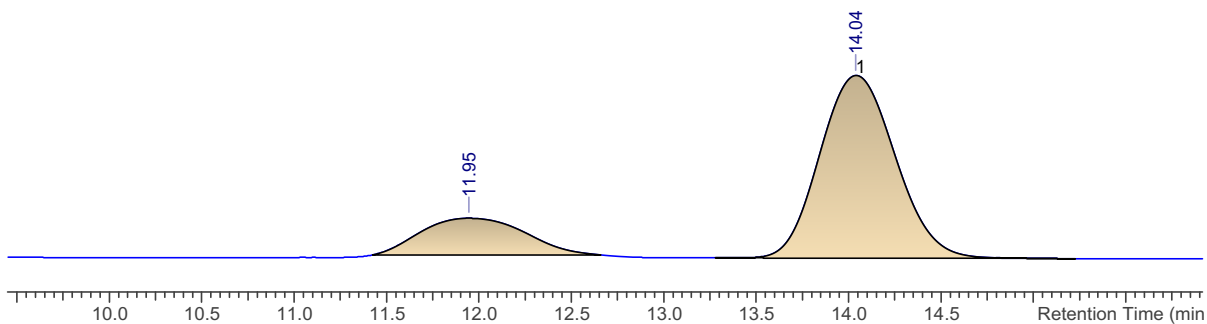
No.	tR	Peak Area (Y units*ms)	Area (%)	Width
1	12.44	15349623.000	60.260	1.065
2	14.18	10122843.000	39.740	1.081

(R)-TRIP 20 mol%, at 20 °C; 71% ee



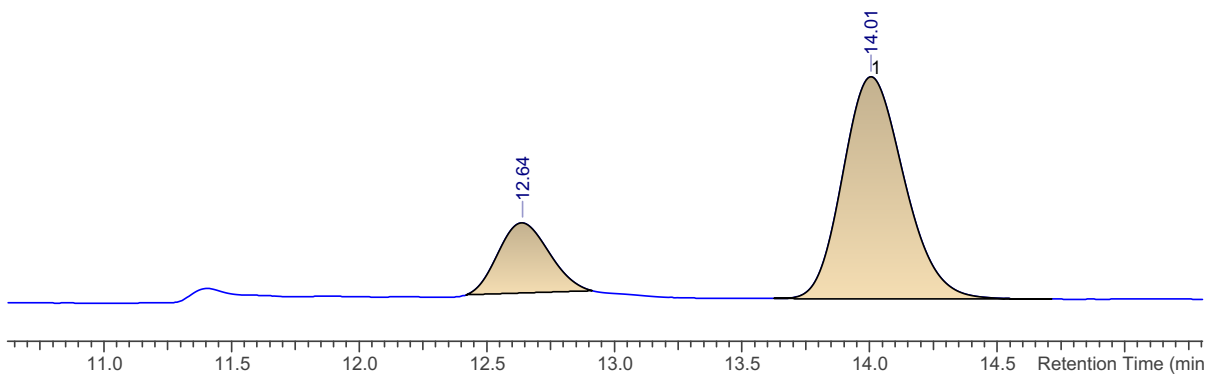
No.	tR	Peak Area (Y units*ms)	Area (%)	Width
1	11.97	553522.563	14.603	0.358
2	13.54	3237027.000	85.397	0.485

(*R*)-TRIP 15 mol%, at 20 °C; 68% ee



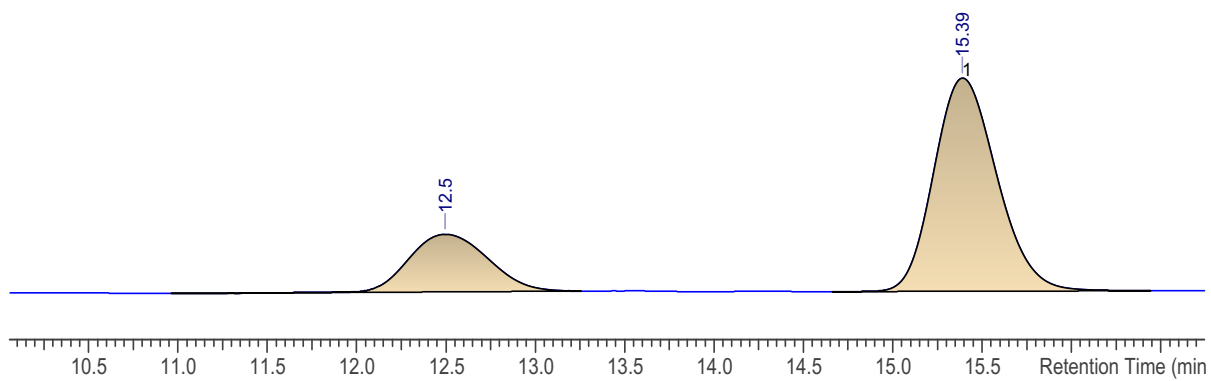
No.	tR	Peak Area (Y units*ms)	Area (%)	Width
1	11.95	474995.375	15.991	0.986
2	14.04	2495334.000	84.009	0.761

(*R*)-TRIP 10 mol%, at 20 °C; 65% ee



No.	tR	Peak Area (Y units*ms)	Area (%)	Width
1	12.64	206023.141	17.411	0.350
2	14.01	977288.875	82.589	0.441

(R)-TRIP 5 mol%, at 20 °C; 48% ee



No.	tR	Peak Area (Y units*ms)	Area (%)	Width
1	12.50	562414.625	25.879	0.830
2	15.39	1610801.875	74.121	0.636

6 Abbreviations

(<i>R</i>)-Anth	(<i>R</i>)-3,3'-Bis(9-anthracenyl)-1,1'-binaphthyl-2,2'-diyl hydrogenphosphate
(<i>R</i>)-Phenanth	(<i>R</i>)-3,3'-Bis(9-phenanthryl)-1,1'-binaphthalene-2,2'-diylhydrogen phosphate
(<i>R</i>)-TIPSY	(<i>R</i>)-3,3'-Bis(triphenylsilyl)-1,1'-binaphthyl-2,2'-diyl hydrogenphosphate
(<i>R</i>)-TRIP	(<i>R</i>)-3,3'-Bis(2,4,6-triisopropylphenyl)-1,1'-binaphthyl-2,2'-diyl hydrogenphosphate
(<i>R</i>)-VAPOL	(<i>R</i>)-2,2'-Diphenyl-3,3'-(4-biphenanthrol)
1,2-DCE	1,2-dichloroethane
4 Å MS	4 Ångström molecular sieves
Ac	acetyl
ACP	Acyl carrier protein
AIBN	azobisisobutyronitrile
APCI	atmospheric pressure chemical ionization
aq	aqueous
Ar	aryl
atm	atmospheres
BHT	Butylated hydroxy toluene (2,6-di- <i>t</i> -butyl-4-methylphenol)
BINOL	1,1'-bi-2-naphthol
Bn	benzyl
Boc	tert-butyloxycarbonyl
bp	boiling point
Bz	benzoyl
Cat.	catalyst
Cbz	carboxybenzyl
CM	cross metathesis

conv	conversion
COSY	correlated spectroscopy
CPA	Chiral phosphoric acid
CPME	cyclopentyl methyl ether
CSA	Camphor sulfonic acid
CuTC	copper(I)-thiophene-2-carboxylate
Cy	cyclohexyl
d	doublet
DCE	dichloroethane
DCM	dichloromethane
dd	doublet of doublet
dddd	double doublet
ddt	doublet of doublet of triplet
DFT	Density Function Theory
DAST	diethylaminosulfur trifluoride
DIBAL-H	diisobutylaluminium hydride
DIPT	diisopropyl tartrate
DMAP	4-dimethylaminopyridine
DMF	<i>N,N</i> -dimethylformamide
DMS	dimethyl sulfide
DMSO	dimethylsulfoxide
DPP	diphenyl hydrogen phosphate
DPPA	diphenylphosphoryl azide
dr	diastereomeric ratio
DTBMP	2,6-di- <i>tert</i> -butyl-4-methylpyridine
ee	enantiomeric excess
eq.	equivalents
er	enantiomeric ratio
ESI	electrospray ionisation

FDA	U.S. Food and Drug Administration
Fmoc	fluorenylmethyloxycarbonyl chloride
gem	geminal
HDA	Hetero Diels Alder
HIV	human immunodeficiency virus
HG-II	Hoveyda Grubbs 2 nd generation
HMBC	heteronuclear multiple bond coherence
HMQC	heteronuclear multiple quantum coherence
HOMO	highest occupied molecular orbital
HPLC	high-performance liquid chromatography
HRMS	high-resolution mass spectrometry
Hz	Hertz
h	hours
IBX	2-iodoxybenzoic acid
iDPA	imidodiphosphoric acid
iIDP	iminoimidodiphosphate
IEDHDA	inversion electron demand hetero Diels Alder
<i>i</i> -Pr	isopropyl
IPA	isopropyl alcohol
IR	infrared
<i>J</i>	coupling constant (Hz)
KIE	kinetic isotope effect
KJ	kilo Joule
LC50	median lethal concentration
LDA	lithium diisopropylamide
LiHMDS	lithium bis(trimethylsilyl)amide
LUMO	lowest unoccupied molecular orbital
m	multiplet
<i>m</i> CPBA	<i>m</i> -chloroperoxybenzoic acid

Mes	mesityl (1,3,5-trimethylbenzene)
min	minute
Mp	melting point
mol	molar
MOM	methoxymethyl
MPM	methoxybenzyl
Ms	mesyl
NCI	National Cancer Institute
NLE	non-linear effect
NMR	nuclear magnetic resonance
Ns	<i>p</i> -nitrobenzenesulfonyl
PMI	principal moments inertia
PMP	<i>p</i> -methoxyphenyl
ppm	parts per million
q	quartet
rac-CSA	racemic camphorsulfonic acid
rt	room temperature
s	singlet
sat	saturated
s-Bu	sec-butyl
t	triplet
TBACl	tetrabutylammonium chloride
TBAF	tetrabutylammonium fluoride
TBS	tris-buffered saline
t-Bu	tert-butyl
TES	triethylsilane
Tf	triflate
TFA	trifluoroacetic acid
THF	tetrahydrofuran

THP	tetrahydropyran
TLC	thin layer chromatography
TMS	trimethylsilyl
Ts	<i>p</i> -toluenesulfonyl
μW	microwaves

7 References

- 1 P. A. Clarke and S. Santos, *Eur. J. Org. Chem.*, 2006, 2045–2053.
- 2 N. M. Nasir, K. Ermanis and P. A. Clarke, *Org. Biomol. Chem*, 2014, **12**, 3323.
- 3 J. Yin, K. Kouda, Y. Tezuka, Q. le Tran, T. Miyahara, Y. Chen and S. Kadota, *Planta Med*, 2004, **70**, 54–58.
- 4 P. A. Searle and T. F. Molinski, *J. Am. Chem. Soc*, 1995, **117**, 8126–8131.
- 5 T. F. Molinski, *Tetrahedron Lett*, 1996, **37**, 7879–7880.
- 6 R. H. Cichewicz, A. Frederick A. Valeriote and P. Crews, *Org. Lett.* , 2004, **12**, 1951–1954.
- 7 R. D. Taylor, M. Maccoss and A. D. G. Lawson, *J. Med. Chem.*, 2014, **57**, 5845–5859.
- 8 M. D. Delost, D. T. Smith, B. J. Anderson and J. T. Njardarson, *J. Med. Chem.*, 2018, **61**, 10996–11020.
- 9 H. Fuwa, N. Ichinokawa, K. Noto and M. Sasaki, *J. Org. Chem.*, 2012, **77**, 2588–2607.
- 10 A. M. Martelli, F. Buontempo and J. A. McCubrey, *Clin. Sci.*, 2018, **132**, 543–568.
- 11 A. Budakoti, P. K. Mondal, P. Verma and J. Khamrai, *Beilstein J. Org. Chem.*, 2021, **17**, 932–963.
- 12 H. J. Prins, *Chem. Weekblad.*, 1919, **16**, 1072.
- 13 E. Hanschke, *Chem. Ber.*, 1955, **88**, 1053–1061.
- 14 R. W. Alder, J. N. Harvey and M. T. Oakley, *J. Am. Chem. Soc.*, 2002, **124**, 4960–4961.
- 15 G. C. Tsui, L. Liu and B. List, *Angew. Chem. Int. Ed.*, 2015, **54**, 7703–7706.
- 16 A. Martínez, M. van Gemmeren and B. List, *Synlett*, 2014, **25**, 961–964.
- 17 L. Liu, P. S. J. Kaib, A. Tap and B. List, *J. Am. Chem. Soc.*, 2016, **138**, 10822–10825.
- 18 T. Glachet, F. Fache, B. Pelotier and O. Piva, *Synthesis (Stuttg)*, 2017, **49**, 5197–5202.
- 19 J. S. Yadav, B. V. S. Reddy, S. Aravind, G. G. K. S. N. Kumar, C. Madhavi and A. C. Kunwar, *Tetrahedron*, 2008, **64**, 3025–3031.
- 20 S. R. Crosby, J. R. Harding, C. D. King, G. D. Parker and C. L. Willis, *Org. Lett.*, 2002, **4**, 577–580.

- 21 C. S. J. Barry, S. R. Crosby, J. R. Harding, R. A. Hughes, C. D. King, G. D. Parker and C. L. Willis, *Org. Lett.*, 2003, **5**, 2429–2432.
- 22 S. D. Rychnovsky, S. Marumoto and J. J. Jaber, *Org. Lett.*, 2001, **3**, 3815–3818.
- 23 S. Marumoto, J. J. Jaber, J. P. Vitale and S. D. Rychnovsky, *Org. Lett.*, 2002, **4**, 3919–3922.
- 24 Z. M. Png, H. Zeng, Q. Ye and J. Xu, *Chem. Asian J.*, 2017, **12**, 2142–2159.
- 25 V. Laina-Martín, J. A. Fernández-Salas and J. Alemán, *Chem. Eur. J.*, 2021, **27**, 12509–12520.
- 26 A. K. Ghosh and G. Gong, *Chem. Asian J.*, 2008, **3**, 1811–1823.
- 27 A. G. Dossetter, T. F. Jamison and E. N. Jacobsen, *Angew. Chem.*, 1999, **111**, 2549.
- 28 S. Raghavan and P. K. Samanta, *Org. Lett.*, 2012, **14**, 2346–2349.
- 29 M. L. Shi, G. Zhan, S. L. Zhou, W. Du and Y. C. Chen, *Org. Lett.*, 2016, **18**, 6480–6483.
- 30 M. Xie, L. Lin and X. Feng, *Chem. Rec.*, 2017, **17**, 1184–1202.
- 31 X. Jiang and R. Wang, *Chem. Rev.*, 2013, **113**, 5515–5546.
- 32 Ł. Albrecht, G. Dickmeiss, C. F. Weise, C. Rodríguez-Esrich and K. A. Jørgensen, *Angew. Chem. Int. Ed.*, 2012, **51**, 13109–13113.
- 33 X. K. Guan, G. F. Liu, D. An, H. Zhang and S. Q. Zhang, *Org. Lett.*, 2019, **21**, 5438–5442.
- 34 B. Francis Robert Japp, *J. Chem. Soc.*, 1904, **85**, 1473.
- 35 D. Vorländer and K. Hobohm, *Ber. Dtsch. Chem. Ges.*, 1896, **29**, 1352.
- 36 C. A. R. Baxter, D. A. Whiting, G. C. Forward, J. C. A. R. Baxter, F. Arndt, P. Natchwey, J. Pusch, K. B. Wiberg, B. J. Nist and E. Schauder, *J. Chem. Soc.*, 1968, 1174–1178.
- 37 R. Cornubert and P. Robinet, *Bull. Chem. Soc. Fr.*
- 38 P. A. Clarke and W. H. C. Martin, *Org. Lett.*, 2002, **4**, 4527–4529.
- 39 S. N. Huckin and L. Weiler, *Can. J. Chem.*, 1974, **52**, 2157–2164.
- 40 T. H. Chan and P. Brownbridge, *J. Am. Chem. Soc.*, 1980, **102**, 3534.
- 41 P. A. Clarke, W. H. C. Martin, J. M. Hargreaves, C. Wilson and A. J. Blake, *Chem. Commun.*, 2005, **0**, 1061–1063.
- 42 P. A. Clarke, W. H. C. Martin, J. M. Hargreaves, C. Wilson and A. J. Biake, *Org. Bio. Chem.*, 2005, **3**, 3551–3563.

- 43 P. A. Clarke and W. H. C. Martin, *Tetrahedron Lett.*, 2004, **45**, 9061–9063.
- 44 P. A. Clarke and W. H. C. Martin, *Tetrahedron*, 2005, **61**, 5433–5438.
- 45 P. A. Clarke, S. Santos and W. H. C. Martin, *Green Chem.*, 2007, **9**, 438–440.
- 46 P. A. Clarke, S. Santos, N. Mistry, L. Burroughs and A. C. Humphries, *Org. Lett.*, 2011, **13**, 624–627.
- 47 P. A. Clarke, S. Santos, N. Mistry, L. Burroughs and A. C. Humphries, *Org. Lett.*, 2011, **13**, 624–627.
- 48 C. F. Nising and S. Brase, *Chem. Soc. Rev.*, 2012, **41**, 988–999.
- 49 F. Loydl, *Justus Liebigs Ann. Chem.*, 1878, **192**, 80–89.
- 50 Y. Tang, J. Oppenheimer, Z. Song, L. You, X. Zhang and R. P. Hsung, *Tetrahedron*, 2009, **62**, 10785–10813.
- 51 H. Fuwa, H. Yamaguchi and M. Sasaki, *Org. Lett.*, 2010, **12**, 1848–1851.
- 52 B. M. Trost and M. J. Bartlett, *Org. Lett.*, 2012, **14**, 1322–1325.
- 53 H. Fuwa, K. Noto and M. Sasaki, *Org. Lett.*, 2010, **12**, 1636–1639.
- 54 H. Irschik, M. Kopp, K. J. Weissman, K. Buntin, J. Piel and R. Müller, *Chem. Bio. Chem.*, 2010, **11**, 1840–1849.
- 55 H. Fuwa, N. Ichinokawa, K. Noto and M. Sasaki, *J. Org. Chem.*, 2012, **77**, 2588–2607.
- 56 K. Asano and S. Matsubara, *J. Am. Chem. Soc.*, 2011, **133**, 16711–16713.
- 57 Y. Fukata, R. Miyaji, T. Okamura, K. Asano and S. Matsubara, *Synthesis (Stuttg)*, 2013, **45**, 1627–1634.
- 58 Y. Lu, G. Zou and G. Zhao, *ACS Catal.*, 2013, **3**, 1356–1359.
- 59 B. Mondal, M. Balha and S. C. Pan, *Asian J. Org. Chem.*, 2018, **7**, 1788–1792.
- 60 P. K. Mykhailiuk, K. Fominova, T. Diachuk, D. Granat, T. Savchuk, V. Vilchynskyi, O. Svitlychnyi, V. Meliantsev, I. Kovalchuk, E. Litskan, V. v Levterov, V. R. Badlo, R. I. Vaskevych, A. I. Vaskevych, A. v Bolbut, V. v Semeno, R. Iminov, K. Shvydenko, A. S. Kuznetsova, Y. v Dmytriv, D. Vysochyn, V. Ripenko, A. A. Tolmachev, O. Pavlova, H. Kuznietsova, I. Pishel and P. Borysko, *Chem. Sci.*, 2021, **12**, 11239–11606.
- 61 F. Lovering, J. Bikker and C. Humblet, *J. Med. Chem.*, 2009, **52**, 6752–6756.
- 62 F. Lovering, *RSC Med. Chem.*, 2013, **4**, 515–519.

- 63 W. H. B. Sauer and M. K. Schwarz, *J. Chem. Inf. Model.*, 2003, **43**, 987–1003.
- 64 J. Meyers, M. Carter, N. Y. Mok and N. Brown, *Futur. Med. Chem.*, 2016, **8**, 1753–1767.
- 65 R. R. Reddy, S. S. Gudup and P. Ghorai, *Angew. Chem. Int. Ed.*, 2016, **55**, 15115–15119.
- 66 P. A. Clarke, S. Santos, N. Mistry, L. Burroughs and A. C. Humphries, *Org. Lett.*, 2011, **13**, 624–627.
- 67 P. A. Clarke and K. Ermanis, *Org. Lett.*, 2012, **14**, 5550–5553.
- 68 K. Ermanis, Y. T. Hsiao, U. Kaya, A. Jeuken and P. A. Clarke, *Chem. Sci.*, 2016, **8**, 482–490.
- 69 J. F. Carpentier, Z. Wu, C. W. Lee, S. Strömberg, J. N. Christopher and R. F. Jordan, *J. Am. Chem. Soc.*, 2000, **122**, 7750–7767.
- 70 C. J. Maddocks, K. Ermanis and P. A. Clarke, *Org. Lett.*, 2022, **22**, 8116–8121.
- 71 A. K. Chatterjee, T. L. Choi, D. P. Sanders and R. H. Grubbs, *J. Am. Chem. Soc.*, 2003, **125**, 11360–11370.
- 72 J. S. Kingsbury, J. P. A. Harrity, P. J. Bonitatebus and A. H. Hoveyda, *J. Am. Chem. Soc.*, 1999, **121**, 791–799.
- 73 K. Voigtritter, S. Ghorai and B. H. Lipshutz, *J. Org. Chem.*, 2011, **76**, 4697–4702.
- 74 P. J.-L. Hérisson and Y. Chauvin, *Makromol. Chem.*, 1971, **141**, 161–176.
- 75 N. Bahri-Laleh, R. Credendino and L. Cavallo, *Beilstein J. Org. Chem.*, 2011, **7**, 40–45.
- 76 F. Lovering, J. Bikker and C. Humblet, *J. Med. Chem.*, 2009, **52**, 6752–6756.
- 77 S. D. Griggs, N. Thompson, D. T. Tape, M. Fabre and P. A. Clarke, *Chem. Eur. J.*, 2017, **23**, 9262–9265.
- 78 C. J. Maddocks, K. Ermanis and P. A. Clarke, *Org. Lett.*, 2020, **22**, 8116–8121.
- 79 S. Hanessian, A. Tehim and P. Chen, *J. Org. Chem.*, 1993, **58**, 29.
- 80 E. Marotta, E. Foresti, T. Marcelli, F. Peri, P. Righi, N. Scardovi and G. Rosini, *Org. Lett.*, 2002, **4**, 4451–4453.
- 81 C. J. Maddocks, K. Ermanis and P. A. Clarke, *Org. Lett.*, 2020, **22**, 8116–8121.
- 82 M. E. Jung and G. Piizzi, *Chem. Rev.*, 2005, **105**, 1735–1766.

- 83 C. Ingold, *J. Chem. Soc.*, 1921, **305**, 119.
- 84 R. M. Beesley, C. K. Ingold and J. F. Thorpe, *J. Chem. Soc.*, 1915, **107**, 1080–1106.
- 85 P. T. Franke, R. L. Johansen, S. Bertelsen and K. A. Jørgensen, *Chem. Asian. J.*, 2008, **3**, 216–224.
- 86 K. Alomari, N. Sai Pavan Chakravarthy, B. Duchadeau, K. Ermanis and P. A. Clarke, *Org. Bio. Chem.*, 2022, **20**, 1181–1185.
- 87 V. Ashokkumar, K. Duraimurugan and A. Siva, *New J. Chem.*, 2016, **40**, 7148–7156.
- 88 R. Monaco, G. Pupo and B. List, *Synlett*, 2016, **27**, 1027–1040.
- 89 M. R. Monaco, D. Fazzi, N. Tsuji, M. Leutzsch, S. Liao, W. Thiel and B. List, *J. Am. Chem. Soc.*, 2016, **138**, 14740–14749.
- 90 N. Li, X. H. Chen, S. M. Zhou, S. W. Luo, J. Song, L. Ren and L. Z. Gong, *Angew. Chem. Int. Ed.*, 2010, **49**, 6378–6381.
- 91 D. Jansen, J. Gramüller, F. Niemeyer, T. Schaller, M. C. Letzel, S. Grimme, H. Zhu, R. M. Gschwind and J. Niemeyer, *Chem. Sci.*, 2020, **11**, 4381–4390.
- 92 Y. Geiger, T. Achard, A. Maise-François and S. Bellemin-Laponnaz, *Chem. Sci.*, 2020, **11**, 12453–12463.
- 93 C. Puchot, C. Agami, O. Samuel, E. Dunach, S. Zhao and H. B. Kagan, *J. Am. Chem. Soc.*, 1986, **108**, 2353–2357.
- 94 H. B. Kagan, *Oil Gas Sci. Technol.*, 2007, **62**, 731–738.
- 95 J. Burés, *Angew. Chem. Int. Ed.*, 2016, **55**, 2028–2031.